SYNTHESIS, CHARACTERISATION AND BIOLOGICAL PROPERTIES OF SOME METAL(II) COMPLEXES OF VARIOUS PYRIMIDINE SCHIFF BASES AND THEIR ANALOGUES

BY

CHIOMA FESTUS

B.Ed Chemistry Education (Port Harcourt), M. Sc. Inorganic Chemistry (Ibadan)

MATRIC NO.: 146986

A Thesis in the Department of Chemistry,
Submitted to the Faculty of Science
in partial fulfilment of the requirements for the Degree of

DOCTOR OF PHILOSOPHY

of the

UNIVERSITY OF IBADAN

MARCH, 2019

ABSTRACT

Metal complexes are important precursors of antimalarial, antimicrobial and anticancer agents. Although pyrimidinyl ligands are known to exhibit biological acivity, studies on metal(II) complexes of some pyrimidines have focused on the non-amino substituted derivatives with no information on ligands of 2-aminopyrimidine derivatives with 2-hydroxy-1-naphthaldehyde and 2-hydroxy-1,4-naphthoquinone. Therefore, the aim of this study was to synthesise and characterise metal(II) complexes of aminopyrimidinyl ligands of 2-hydroxy-1-napthaldehyde/2-hydroxy-1,4-naphthoquinone and evaluate their biological properties.

The pyrimidinyl ligands were synthesised from 2-amino-pyrimidine derivatives with 2-hydroxyl-1-napthaldehyde or 2-hydroxy-1,4-naphthoquinone in methanol under reflux at 55-60^{o}C. The ligands were separately reacted with $Mn(CH_3CO_2)_2.4H_2O$, $FeSO_4.7H_2O$, $Co(CH_3CO_2)_2.4H_2O$, $Ni(CH_3CO_2)_2.4H_2O$, $Cu(CH_3CO_2)_2.H_2O$ and $Zn(CH_3CO_2)_2.2H_2O$, after which the products were further reacted with 2,2$^{'}$-bipyridine. The compounds were characterised using nuclear magnetic resonance (NMR), infrared (IR) and electronic (UV/Vis) spectroscopy, elemental analysis (CHN), mass spectrometry (EIMS), conductivity and magnetic susceptibility measurements. Antimicrobial activities were evaluated at 10 mg/mL (and inocula suspension of 10^6 CFU/mL), using agar diffusion methods against *Staphylococcus aureus* (ATCC 25923), *Escherichia coli* (ATCC-25922), *Pseudomonas aeruginosa* (ATCC-27853), *Proteus mirabilis* (ATCC-12459), *Bacillus cereus* (ATCC-8035), *Klebsilla oxytoca* (ATCC-70603), *Aspergillus niger, Aspergillus flevus* and *Rhizopus Stolonifer.* Antioxidant properties were assessed at 50, 100, 200 µg/mL using 2,2'-diphenyl-1-picryl-hydrazyl (DPPH) radical scavenging and ferrous ion chelating assays and compared with standard ascorbic acid.

The synthesised ligands were 3-{[-(pyrimidin-2-yl)imino]methyl}napthalen-2-ol, 3-{[(4,6-dihydroxypyrimidin-2-yl)imino]methyl}napthalen-2-ol, 3-{[(4,6-dimethylpyrimidin-2-yl)imino]methyl}napthalen-2-ol, 2-(pyrimidin-2-ylamino)naphthalene-1,4-dione, 2-(4,6-dihydroxypyrimidin-2-ylamino)naphthalene-1,4-dione and 2-(4,6-dimethylpyrimidin-2-ylamino)naphthalene-1,4-dione. The ligands and complexes were obtained in 59-86 and 46-96% yields, respectively. The ^{1}HNMR spectra displayed HC=N and N-H signals at 8.22-9.55 and 3.38-4.95 ppm, respectively,

while ^{13}CNMR spectra showed C=N signal at 163.98-168.7 ppm. These corroborate the formation of ligands. Infrared spectra confirmed ligands' bidentate nature and coordination with metal(II) ions through imine/deprotonated amide nitrogen and through the deprotonated naptho/ketonic oxygen atoms. Intra-ligand ($\pi^* \leftarrow n$, $\pi^* \leftarrow \pi$) bands observed at 22182-29019 and 30030-39361 cm^{-1} shifted to lower wave numbers in the complexes confirming coordination of the ligands with metal ions. The *d-d* transitions of the complexes were consistent with tetrahedral/square planar and octahedral geometries. The CHN data suggest 2:1 (L:M) and 1:1:1 (Ligand:Metal:Bipyridine) stoichiometry for the symmetrical and heteroleptic complexes. The complexes were non-electrolytes with conductivity values of 4.72-16.09 $Ohm^{-1}mol^{-1}cm^2$ in dimethylsulphoxide. Manganese(II) and iron(II) complexes exhibited magnetic moments of 5.54-6.02 and 4.97-5.25 B.M indicative of high spin geometries. $[Mn(L^1)_2].H_2O$, however, gave 4.39 B.M suggesting tetrahedral geometry. Cobalt(II) and nickel(II) complexes displayed moments of 4.65-5.14 and 2.77-3.59 B.M (symmetrical complexes), 4.29-4.53 and 3.49-3.80 B.M (heteroleptic complexes), respectively, corroborating octahedral and tetrahedral geometries. Copper(II) and zinc(II) complexes had moments of 1.75-2.21 and 0.09-0.43 B.M, indicating square planar, tetrahedral and octahedral geometries for the complexes. The ligands and complexes had antimicrobial activities against tested organisms, with inhibitory zones of 5.5-20.0 and 6.5-34.0 mm, respectively. The antioxidant potentials with ferrous ion chelating assay showed 89.74-92.10% (IC_{50} of 92–154 µg/mL), while DPPH radical scavenging ability of 69.74-85.10% (IC_{50} of 79-118 µg/mL) were obtained.

Spectral and magnetic data of the metal(II) pyrimidinyl derivatives indicated tetrahedral, square planar and octahedral geometries and the complexes showed potentials for biological application.

Keywords: Aminopyrimidine, hydroxylnapthaldehyde, hydroxy-1,4-naphthoquinone, magnetic properties and antimicrobial activities

Word counts: 497

ACKNOWLEDGEMENTS

Without the special grace of "God Personified", this work would have not seen the light of the day. So I return all thanks, adoration and praises to Him for the gift of life and sound health, safety on roads and favour throughout the period of this program.

I sincerely acknowledge with thanks the efforts of the Head of the Department of Chemistry, University of Ibadan, Professor Timothy I. Odiaka. Prof. your invaluable advice made the completion of this research work a reality. May God bless you! I wish to express my appreciation to the Department of Chemistry, University of Ibadan for affording me the opportunity to study and carry out this research work.

My special appreciation goes to my late supervisor Professor Aderoju Amoke Osowole, whose intellectual guide, moral advice and professional supervision encouraged me to success in this research work. Ma, as I often call you, 'thank you and rest in peace'

I am very grateful to my supervisor Professor Dr. Helen O. Omoregie who in spite of her tight commitments, through consistent and unconditional reading and corrections made this write up a presentable thesis. May God bless you Ma.

I humbly acknowledge the fatherly advice and guidance of Professor J. A. O. Woods towards the completion this program. He brought me close and ensured that I graduate from this program, may God keep and strengthen you; thank you Sir.

The scholarly advice, encouragements and motivation of Prof. A. A. Adesomoju, Dr Ibrahim Adebayo Oladosu, Prof. G. O. Adewuyi, Dr N. O. Obi-Egbedi, Dr Tunmise T. Eugene-Osoikhia and Dr T. E. Olalekan all of Chemistry Department, University of Ibadan towards the success of my graduation cannot been forgotten in a hurry; God bless you all.

My immense and profound gratitude goes to my family members, Bishop-Elect Anele, Festus Onyeche, a man of excellence, who shines as the brightest light and motivator behind this effort; Blessed Mother-Designate Festus Benadeth Chika, a mother like no other; Charity Nkoo, my Kids:- Ikenna Chinedu, Ngozichukwu, Ugochi, and Chidubem; my siblings:- Chinyere, Eberechukwu, Uloaku, Chiehgura, Udochukwu,

and Nnamdi; my nephews and nices:- Ugochuchwu, Princess, Rejoice, Osinachi, Chinturu, Nnamdi, Nnadozi, God-desire, and others for their prayers, encouragement and above all for their understanding

Healthfully, I say a big thanks to Hon. Prof. Lady Ozioma A. Ekpete; a mother, an academic mentor and a role model, for her prayers and all-round assistance before and during the program. Even after this program, I known your support and love will not seize. God Almighty will keep you to reap the fruits of your labour. My academic friends and colleagues: Mr. Edori, Onisogen Simeon, Dr Blessing Ikiroma, Dr. Joshua Konne, Engr. Alison Sodienye, Miss Excellent Portable Nwokoji, Mr Goodluck Anele, Bishop-Elect Glory M. Ufuoma, and Brother Temple Ojika are deeply acknowledged for their individual and collective impacts in my personal life. Dr Nna-Joe Prince-a friend turned brother, thank you for being there for me.

The technical staff of the Department of Chemistry, University of Ibadan are highly appreciated for their corporations and assistance at different stages of this research work.

This acknowledgement cannot be complete without mentioning the academic and moral encouragements and prayers of my colleagues: Anthony, C. Ekennia and Mrs B. Adewusin, for their understanding and cooperation during the course of our study and research.

Dr. Demain of Northwest University, South Africa is highly appreciated for his assistance and contributions towards the characterization of all my samples.

TetFund (Tertiary Education Trust Fund) is deeply acknowledged for the research sponsorship of this program.

Above all, thanks to Almighty God for His inspiration and sustenance throughout the course of my study.

CERTIFICATION

I certify that this research work was carried out by Chioma Festus in the Department of Chemistry, University of Ibadan.

Supervisor
Helen O. Omoregie
B.Sc, M.Sc, Ph.D (Ibadan)
Department of Chemistry
University of Ibadan, Ibadan Nigeria

DEDICATION

This work is dedicated to the glory of **"ALMIGHTY JEHOVAH GOD**

and

HIS CHRIST"

ABBREVIATIONS

ε	Molar absorptivity
μ_{eff}	Effective magnetic moment
χ_A	Susceptibility per gram atom
χ_m	Molar Susceptibility
χ_L	Diamagnetic corrections
λ_{max}	Wavelength of maximum absorption
Λ_m	Molar conductance
B.M	Bohr magneton
Bipy/B	2,2'-Bipyridine
CH_2Cl_2	Dichloridemethane
Cl	Chloro
Co	Cobalt
Cu	Copper
DMF	Dimethylformamide
DMSO	Dimethylsulphoxide
DSC	Differential scanning calorimetry
DTA	Differential thermal analysis
EtOH	Ethanol
Fe	Iron
G	gyromagnetic ratio
h	Planck.s constant
H	magnetic field
HL^1	3-{[-(pyrimidin-2-yl)imino]methyl} napthalen-2-ol
HL^2	3-{[(4,6-dihydroxypyrimidin-2-yl)imino]methyl}napthalen-2-ol
HL^3	3-{[(4,6-dimethylpyrimidin-2-yl)imino]methyl}napthalen-2-ol
HL^4	2-(pyrimidin-2-ylamino)naphthalene-1,4-dione
HL^5	2-(4,6-dihydroxypyrimidin-2-ylamino)naphthalene-1,4-dione
HL^6	2-(4,6-dimethylpyrimidin-2-ylamino)naphthalene-1,4-dione
OAc	Acetate
O-	Ortho
M-	Meta

Ni	Nickel
NMR	Nuclear Magnetic Resonance
Nm	Nanometre
Mn	Manganese
MeOH	Methanol
M	Molarity or metal ion
Zn	Zinc

TABLE OF CONTENTS

CHAPTER FIVE: DISCUSSIONS OF RESULTS

LIST OF FIGURES

LIST OF EQUATIONS/SCHEMES

Page

LIST OF TABLES

CHAPTER ONE
INTRODUCTION

1.0 Introduction

The chemistry of pyrimidine and its by-products has drawn substantial research interests in recent times due to their similarity with natural products/core constituents of nucleic acids and their ability to form Schiff bases with carbonyl (aromatic and non-aromatic) compounds. The basic structural feature of the latter is the imine moiety/group, $RHC=NR^{I}$. Furthermore, pyrimidine Schiff base ligands are good coordinating compounds forming stable metal-based compounds and exhibiting vital potentials as new pathways for the design and isolation of active metal-based therapeutic agents. However, desired research attention has not yet been given to the use of pyrimidine compounds as agents for pharmacology. Hence, appropriateness of evaluating the pharmacological (antimicrobial and antioxidant) properties of pyrimidine derivatives and their corresponding metal(II) compounds.

1.1 Concept of Schiff bases

Condensation reaction of primary amines (aromatic or aliphatic) and ketone/aldehyde typically results into compounds with the formula $R_1R_2C=N-R_3$, and are called Schiff bases (Abdullah and Salman, 2010). The R_1 and R_3 may be either an aryl or alkyl assemblage, whereas R_2 represents a hydrogen atom. Schiff bases in which 'R_1 and R_3' represents aryl moieties are extensively unchanging and easily synthesised when compared to their counterparts where 'R_1 and R_3' stands for alkyl substituents (Kolawole, 1979). The carbonyl group can be from aldehyde giving aldimines or the ketones to give ketoimines.

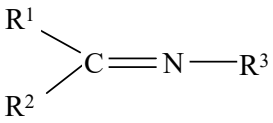

Figure 1.1. General structure of Schiff bases

Nejo *et al.,* (2009) reported that Schiff bases of aldehyde origin are better and easier synthesised, compared to their ketone counterparts, due to sterically less hindered reaction centres of aldehydes. The extra carbon atom of ketones in ketoimines releases an electron density to the imine carbon, hence making the ketoimine less electron loving. Consequently, Schiff base formation and stability is greatly enhanced by the nature of substituents close to the carbonyl carbon. While electron withdrawing substituents near the carbonyl carbon makes it more electrophilic and the formed Schiff base more stable. Electron releasing/donating substituents near the carbonyl carbon makes the carbon atom less electrophilic and foil azomethine formation (Nejo *et al.,* 2009). Generally, the development of Schiff base compounds using a carbonyl group is a rescindable process, which occurs in the presences of an acid or a base catalyst and finally completed when water molecule is removed as shown in equation 1.1 (Elzahany *et al.,* 2008) below.

Schiff base synthetic mechanism forms alternative pathway to theconcept of nucleophilic addition to C=O moiety of a carbonyl compound. Nitrogen containing compounds which acts as nucleophile combines with carbonyl compounds to offer an unsteady product, 'carbinolamine'. The carbinolamine dehydration through catalyzation forms rate formative stage for Schiff base preparation (Abdul, 2005).

$$R_1R_2C{=}O + R{-}NH_2 \leftrightarrow R_1R_2{-}C(OH)NHR \leftrightarrow R_1R_2\text{-}C{=}NR + H_2O$$

Equation 1.1. Formation of carbinolamine before Schiff base

Hugo Schiff in 1864, prepared, studied and reported the first imine compound called Schiff base. Since after Schiff adopted the classical method in his synthesis, several synthetic methods for Schiff bases generally anchored on the removal of water molecule(s) from the intermediate (carbinolamine) Hformed between an amine and a carbonyl have emerged. For example, use of molecular sieves (Taguchi and Westheimer, 1971), application of dehydrating solvents (tetramethyl orthosilicate or trimethyl orthoformate) to the reaction process (Love and Ren, 1993; Look *et al.,* 1995) and the use of Lowry-Brønsted or Lewis acids (H_2SO_4, $NaHCO_3$, $MgSO_4$, $Mg(ClO_4)_2$, CH_3COOH, etc) to catalyze and dehydrate reaction(s) (Chakraborty *et al.,* 2004). However, the last one and half decade has witnessed solvent-less synthetic methods i.e. microwave irradiation, solid-state synthesis, solvent free infrared irradiation, etc, which are considered simple, more environmentally safe and faster synthetic processes for

Schiff bases (Schmeyers *et al.,*1998; Vazquez *et al.,* 2004 and Gopalakrishnan *et al.,* 2007).

Schiff bases are more adequate chelating ligands only when they have ligating moieties, commonly a hydroxyl assemblage, close to the position of coordination, to enhance the formation of a five or six membered coordinate ring on reaction with a positively charged ion (Kolawole, 1979). Schiff bases could be aromatic, aliphatic or mixed. They could also be bidentate, tridentate or polydentate as shown in Figure 1.2 (Owolabi, 2005).

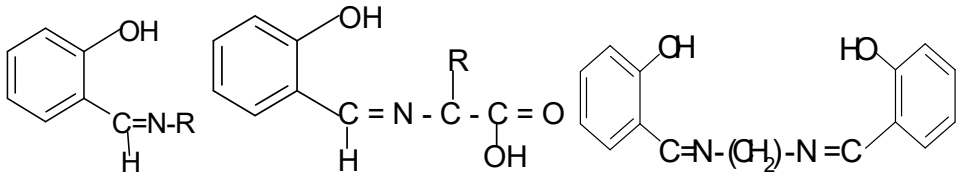

Bidendate Tridendate Tetradendate

Figure 1.2. Classification of Schiff base ligands according to donor atoms

Schiff bases have remained extensively described as indispensable assemblage of compounds, owing to their preparative litheness, structural resemblances with living organic matters, selectivity and sensitivity to core transition elements, also owing to the existence of imine moiety (C=N-R) (Abou-Melha and Faruk, 2008; Spinu and Kriza, 2000). Though, attention in metallic compounds of Schiff bases has intensely improved in recent times owing to their exploration for medications with greater pharmacological properties in combination with reduced poisonousness (Zhaohua *et al.,* 2001). Similarly, it has been documented that drugs of metallic compounds comprising heterocyclic ring plus imine (C=N–R) group displayed improved bio-potent actions in the therapeutic and medicinal arenas, as anti-bacterial (Panneerselvam *et al.,* 2010) and anti-tumor agents (Liu and Yang, 2009, Abdullah and Salman, 2010), etc as a result of their excellent anti-proliferation actions, decreased toxicity and improved stability in the living system.

1.1.1 Pyrimidine and its Schiff bases

Pyrimidine whose ring systematic study started in 1884 with Pinner (Pinner, 1884) when he coined the term (pyrimidine) from a combination of two words ‘pyridine and

amidine' due to its structural similarity to those compounds, is an aromatic colourless heterocyclic organic compound. It is analogous to benzene with two nitrogen atoms at positions 1 and 3 having the condensed formula $C_4H_4N_2$. Pyrimidine, a water-soluble hygroscopic compound is one of the known diazines, with the others being pyrazine and pyridazine shown below. Pyrimidine which exhibits a melting point of 22°C is also called *m*-diazine, a weak base (with a p*K*a = 1.23) that possess basic pyridine-like odour (Patel *et al.,* 2012).

Figure 1.3. Types of Diazines

Pyrimidine is electron deficient due to the electronegative nature of the *N*-atom. The electron densities at positions 2, 4 and 6 are depleted making these positions strongly electrophilic, hence are referred to as electrophilic positions. The electron density at 5-position becomes slightly depleted as the pyrimidine ring retains its benzenoid properties as shown below by the canonical forms.

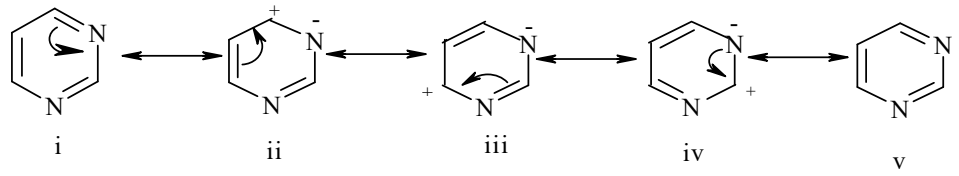

Figure 1.4. Canonical forms of Pyrimidine

Pyrimidine constitutes major nucleotides of deoxyribonucleic acid (DNA) and ribonucleic acid (RNA). However, derivatives of pyrimidine are widely distributed in nature (Kumar *et al.,* 2011; Pinner, 1884; Vachala *et al.,* 2012) e.g. thiamine, riboflavin (vitamin B_2), barbitone, isoalloxazine, folic acid and olloxan (Singh and Chouhan, 2014; Eussell, 1945). Synthetic pyrimidine compounds are also well known i.e. barbiturates, zidovudine (HIV drug), cytostaticum fluorouracil, pyrimethamine, trimethoprim, sulfadiazine, minoxidil, etc (Rakesh and Anuja, 2014).

Pyrimidine can be synthesised through cyclization of β-dicarbonyl compounds bearing N-C-N atoms, through displacement reactions or by direct ring creation, i.e. reaction of

acetamidine with ethylacetoacetate affords a hydroxyl-methyl-pyrimidine (Xue-Qiang*et al.,* 2017)

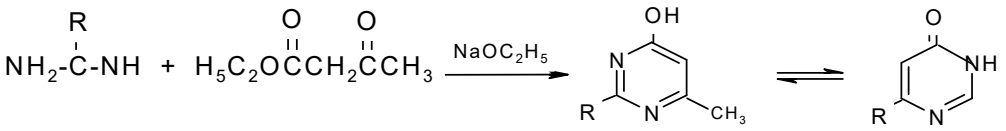

Equation 1.2. Formation of position 2-substituted hydroxyl-methyl-pyrimidine

Reaction of acetyl acetone with an R-substituted acetamidine (where R=CH_3, SH, OH, $HNC_6H_4CH_3$ or $NHNO_3$) gave a position 2-substituted 4,6-dimethyl pyrimidine derivative (Nasser, 2003).

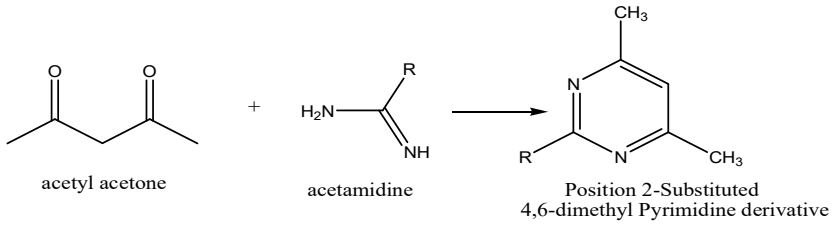

Equation 1.3. Formation of position 2-substituted 4,6-dimethyl-pyrimidine

However, 2-amino-4,6-dimethylpyrimidine have been directly synthesised by reacting guanidine nitrate with acetylacetone in the presence of potassium carbonate (Olugbade *et al.,* 1990).

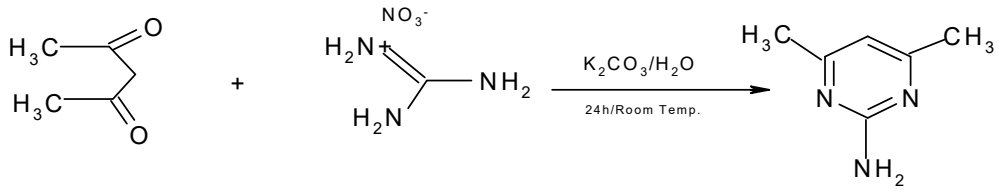

Equation 1.4. Position 2-substituted4,6-dimethylpyrimidine formation

Consequently, 4-aminopent-3-en-2-one reacts with cyanamide in an aqueous solution to afford high yield substituted 2-aminopyrimidine (Alherola *et al.,* 1987).

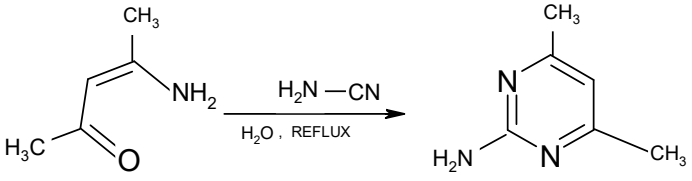

Equation 1.5 Synthesis of 2-amino-4,6-dimethylpyrimidine

Reaction of (*E*)-3-(dimethylamino)acryaladehyde with guanidine in a simple process gave 2-aminopyrimidine (Jachak *et al.,*1993).

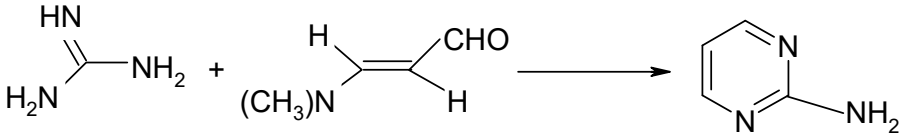

Equation 1.6 preparation of 2-aminopyrimidine

Furthermore, 2,4-diamine pyrimidine has been synthesised through a simple reaction process of guanidine with nitrile (Smal *et al.,* 1986).

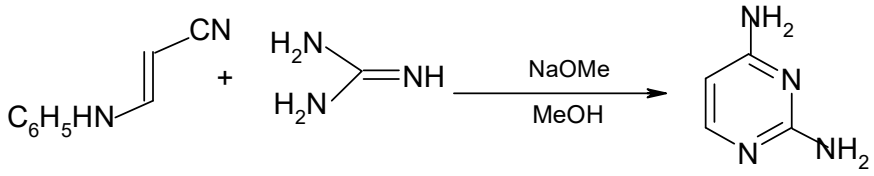

Equation 1.7 Preparation of 2,4-diaminopyrimidine

Researches have also shown that reactions of formamides with amidines yields 2-substituted pyrimidines, formamides with guanidines affords 2-aminopyrimidines (compounds of our interest) while 4- and 6-aminopyrimidines derivatives are synthesised from nitriles, etc (Brown *et al.,* 1990; 1994).

Pyrimidine and its derivatives have been widely synthesised and reported to possess various range of therapeutic uses and pharmacological activities, i.e. β-enaminoester prepared via Michael addition of α-cyano chalcone to ethylcyanoacetate, was further combined with phenylisothiocyanate, ethylcyanoacetate and trichloro acetonitrite affording pyranopyrimidines. The later was screened and found to possess antibacterial activities (El-Hossini *et al.,* 1991).

With aromatization oxidative of ethyl-2-amino-4-methyl-4,5,6,7-tetrahydro-1-benzothiophene-3-carboxylate, first-rate anti-folates bearing tricyclic benzo{4,5}thieno{2,3*d*} pyrimidine framework was synthesised as a two-way thymidylate synthase and dihydro-folate reductase (DHFR) hinderance and screened for anticancer activities. Ibrahim *et al.,(* 2011) screened and reported high cytotoxicity activity of pyrazolo{3,4*d*}pyrimidines against breast cancer cell lines {MCF7}.

These bases possesses vast biological applications which include but not limited to DNA repair research with implications in cancer and epigenetics, replication and transcription of new DNA and RNA, regulation of enzymes and cell signing, production of starches and proteins, temporary vigour storage with the greatest shared form of liveliness in living-cells been adenosine triphosphate (ATP). DNA plus RNA constitutes major elements of every living cell and constitute the genes inside the nucleus which disports essential role in the ascertainment of genetic features through regulation of protein production in cells (Houghton, 2009).

The pyrimidines' derivatives of benzothieno{2,3*d*}pyrimidines isolated from 2-amino-3-carboxoamido/cyano-5-styryl-7,7-dimethyl-6,7-dihydrobenzo{b}thiophenes in the presence of sodiumethoxide with formamide have been reported. The compounds `were verified for antimicrobial activity against various strains of bacteria and fungi and were reported to exhibit moderate to good antifungal activity and comparable activity against *A. awamori* (Desai and Shah, 1997).

Reactions of 1,2,3,4-tetrahydropyrimidine-2-thiones and chloroacetic acid with appropriate benzaldehydes gave different 2,3-dihydro-5*H*-thiazolo{3,2-a}pyrimidine-6-carboxylic acid methyl ester. The synthesised pyrimidines with R=4-Br, R^{I}=4-CH_3/OCH_3 and R=2-F, R^{I}=H/4-OCH_3 showed moderate anti-inflammatory activity when evaluated. Birsen *et al.,* (1999) affirms that the activities were comparable to Indomethacin.

Compounds with pyrimidine moiety in their structures have also been reported to possess wide range of applications in medicine due to their pronounced biological activities. Such compounds have proved to be active inhibitor of bovine liver dihydrofolate reductase (Taylor and Flood, 1983), antiviral (El-Bendary and Badria, 2000), anticancer and antitumour (Zhohua *et al.,* 2001) and as tyrosine kinase inhibitor (Smaill *et al.,* 2000).

Aminopyrimdines, which are crystalline solids, constitutes biologically most efficient class of pyrimidine derivatives, i.e. 2-aminopyrimidine-, 4-amino-, 6-amino-, 2,4-diaminopyrimidine-, 2,6-diamino-, 2,4,6-triaminopyrimidines, etc (Tozkoparan *et*

*al.,*1999; Clark *et al.,* 1993). Pyrimidines with amino groups at position two have been reported widely in the synthesis of Schiff bases mostly with fused aromatic carbonyl compounds. Hetero-aromatic compounds bearing the pyrimidine moiety and its compounds occupy distinct and unique place in our lives with great biological and medicinal significance, hence their choice for this study (Marjan *et al.,* 2015).

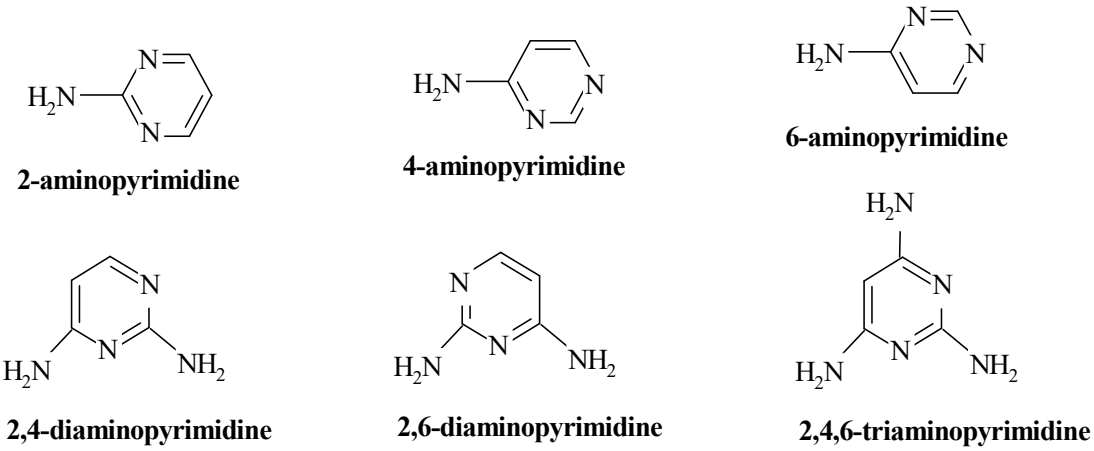

Figure 1.5 Classes of Aminopyrimidine

1.1.2 Hydroxyl naphthaldehydes and their Schiff bases`

2-Hydroxy-1-naphthaldehyde Schiff bases with different amines mostly aromatic amines have been widely studied (Iniama *et al.,* 2015; Rabab *et al.,* 2015) and reported for their ability in chelate formations (Zoeb *et al.,* 2008; Grace *et al.,* 2015). The reversible colour characteristic of 2-hydroxy-1-naphthaldehyde Schiff base complexes caused by thermochromism and photochromism has been largely attributed to the *ortho*-hydroxyl substituent (Rontoyianni *et al.,* 1994), an important element favouring the existence of intramolecular hydrogen bonding and also accounts for development of either enol- (O–H...N) or keto- (O...H–N) amine tautomers in 2-hydroxy-1-naphthaldehyde Schiff base compounds as shown in Figure 1.6 (Abdullah and Badahdah, 2007). Generally, intermolecular hydrogen bond formation in hydroxyl Schiff bases contributes to planarity of formed molecules (Julija *et al.,* 2006)

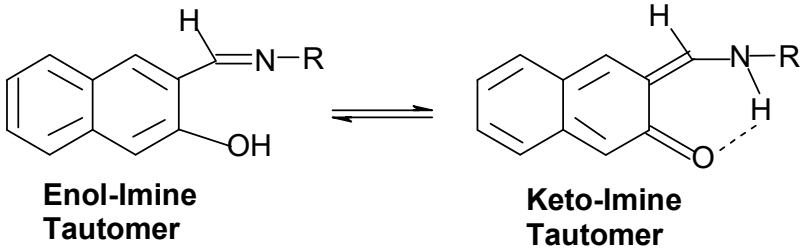

Figure 1.6. Tautomers of enol- and keto-amines

Tautomerism studies of 2-hydroxy-1-naphthaldehyde Schiff bases carried out in solution and in the solid states have been evaluated with different spectroscopic (IR and UV-Vis) techniques in polar and non-polar solvents. While the IR data established that such Schiff bases exist in enol form (Antonov *et al.,* 2000), keto form (Salman *et al.,* 1991), or enol -keto forms (Salman *et al.,*1993 and Abbas *et al.,* 1996), the UV-visible results indicate that enol-structured Schiff bases exhibits absorption bands below 25000 cm^{-1} while bands above 25000 cm^{-1} were assigned to either keto- or enol-keto-structured (Salman and Saleh, 1998) Schiff base compounds.

Schiff bases of 2-hydroxy-1-naphthaldehyde and their metal complexes have recently raised considerable interest in synthesis due to their analytical, industrial and biological applications (Cheng *et al.,* 2010; Rabab *et al.,* 2015).

Al-Masoudi *et al.,* (2015) reported the synthesis of biologically active Schiff base derivative of amoxicillin derived from 2-hydroxyl-1-naphthaldehyde and 4-thia-1-aza bicyclo[3:2:0] heptane-2-carboxylicacid / 6[[amino (-4-hydroxyl phenyl)acetyl] amino]3,3-dimethyl-7-oxo-trihydrate in a 1:1 molar ratio. The ligand exhibited moderate toxicity at LD_{50} and good antimicrobial activities against micro-organisms.

Similarly, a series of four novel Schiff bases condensed from 2-hydroxy-1-naphthaldehyde with 2-hydroxy benzaldhyde and diamino propane have been reported. The ligands were evaluated for antioxidant activity using scavenger technique. The results showed that the ligands were very effective as radical scavengers compared to the standard ascorbic acid. The feasible antioxidant activity of the ligands could be credited to the promotion of hydrogen particles from azomethine as well as OH moieties (Zugir *et al.,* 2015)

Iniama *et al.,* (2015) documented the preparation of Zn(II) compounds from the Schiff bases (L-arginine-2-hydroxynaphthaldehyde as well as glycine-2-hydroxynaphthaldehyde). The synthesised compounds which were characterized via spectroscopic techniques were also screen against*E.coli, S.aureus, S.typhi* and *C.albicans* microbes for antimicrobial activity. Obtained results indicate that all

synthesised compounds exhibited promising antimicrobial properties, with the Zn(II) complexes having more enhanced activity which is attributed to chelation.

Consequently, Osowole *et al.,* (2012) reported the preparation, spectral, thermal, in-vitroanti-bacterial and anti-cancer actions of the Schiff base, 3-(-1-(4-methoxy-6-methyl)-2-pyrimidinylimino)methyl-2-napthol and its Mn(II), Co(II), Ni(II), Cu(II), Zn(II) and Pd(II) compounds. While the in-vitroanti-bacterial andcytotoxic investigations indicates that the ligand was in-active against the microbes (*E. cloacae*, *E. coli, S. liquefaciens*, *S. aureus*, *C. violaceum,Bacillus sp* and *Klebsiella sp*)and HL-60 (Leukaemia) cells nonetheless was toxic toward 518A2 (melanoma) cells having IC_{50} of ±70.00 μM, the metal complexes exhibited moderate activities in all cases. However, the Cu(II) complex displayed excellent antibacterial action towards every tested micro-organisms, and the Pd (II) compound showed fantastic in-vitro anti-cancer actions towards 518A2 (melanoma), also HL-60 (Leukaemia) carcinomas at IC_{50} standards with ±1.34 and 1.85 μM, exceeding the activities of cisplatin with 35.0 and 3.5 μM values in the same assay.

Furthermore, Gomathi *et al.,* (2013) synthesised and reported metallic compounds with $[M(L\text{-}H)_n(X)_n]$ (M = Mn(II) and Zn(II); L=Schiff base obtained with the mixture of 2-hydroxynaphthaldehyde and *para*-toluide; X=H_2O, and n=2). The metallic compounds with the Schiff base remained characterized using CHN examination, magnetic susceptibility and conductivity measurements, electronic, IR plus cyclic voltammetry evaluation. Spectroscopic studies confirmed the ligand bidendate, while the metallic compounds assumed six coordinate stereo-chemistries owing to magnetic and spectral results. The complexes generally exhibited considerable therapeutic activity compared to the ligand.

1.1.3 Naphthoquinones and its Schiff base compounds

Naphthoquinones are largely found in nature (fungi, plants, animals, etc) and have been studied for decades due to their biological activities (Touraire *et al.,* 1996 and Riffel *et al.,* 2002). Naphthoquinone which exist in the isomeric forms of1,4-naphtho-quinone, 1,2-naphtho-quinone, 2,3-naphtho-quinone and 2,6-naphtho-quinone is

immiscible in icy aqua solvent, somewhat miscible in petroleum ether with additional miscibility in dipole carbon-based solvents (DMSO, DMF, etc). It is an oxidation product of a variety of naphthalene compounds. Generally, naphthoquinone and its derivatives have been widely used as colorants/dyes in fabrics, cosmetics and foods, also in radiation modulators of artificial lipid peroxidation in iron compounds of numerous hydroxyl napthouinone (Kumbhar *et al.,* 1997). Their medicinal applications as antibacterial, antitumor, antifungal, anti-inflammatory and anticancer agents and for larvicidal and insecticidal activities are also reported (Masuda, 1987; Papageorgiou *et al.,* 1999; Ngoc-Chau *et al.,* 2009; Lopes *et al.,* 1977; Lucimi *et al.,* 2010).

Napthoquinones exist as precursors in the syntheses of biological active compounds such as imidazoles, phthiocols and benzophenothiazinols (Agarwal and Mital, 1976; Efimova and Efros, 1967; Srivastava *et al.,* 1987). However, hydroxyl derivatives of 1,4 naphtho-quinones (2-hydroxy-1,4-naphtho-quinone (lawsone), 5-hydroxy-1,4-naphtho-quinone (juglone), 6-hydroxy-1,4-naphtho-quinone) constitute a special class of ligands with vital chelating ability. 2-hydroxy-1,4-naphtho-quinone, a natural product extract of henna (*Lawsonia inermis or Lawsonia alba*) which has also been synthesised in the laboratory (César*et al.,* 2009) will only be discussed for the purpose of this review.

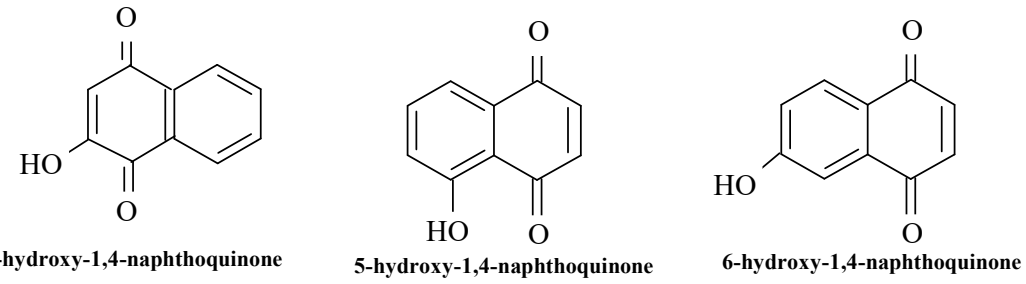

Figure 1.7. Classes of 1,4 naphthoquinones

Dekkers *et al.,* (1996) first analysed the structure of 2-hydroxy-1,4-naphthoquinone by X-ray crystallography and confirmed its tautomeric forms (Figure 1.8) to be more stable over the other isomeric forms of naphthoquinone. The stability is attributed to the cancellation of the dipole moments of the carbonyl groups, combined with an intramolecular hydrogen bond in the 1,4-isomer. 2-hydroxy-1,4-naphthoquinone (Figure 1.7) has a molecular formula of $C_{10}H_6O_3$ with a melting point of 126^0C (259^0F,

399K). For over five decades, hydroxyl-naphthoquinones have been extensively evaluated for their various excellent pharmacological actions which includes anti-malarial, anti-bacterial, anti-fungal, anti-viral, anti-tumor as well as anti-parasitic activities (Desiree *et al.,* 2013). For instance, atovaquone, a drug derivative of hydroxyl-naphthoquinone displayed outstanding antimalarial action, nonetheless showed very low pharmacological qualities including poor bio-availability with high plasma protein binding (Dressman and Reppas, 2000). 2- methyl-heptyl/2-methyl-heptyl-trifluoro-methyl-2-hydroxy-1,4-naphtho-quinones which were synthesised by modifying the side chains (alkyl) on atovaquone recorded highly effective anti-malarial activity against atovaquone-resistant *P. falciparum* (Hughes *et al.,* 2010).

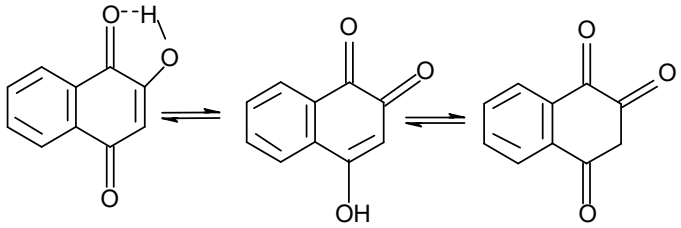

Figure 1.8 Tautomeric forms of 2-Hydroxy-1,4-Naphthoquinone

Synthetic 2-hydroxy-3-chloro-1,4-naphtho quinone has been reported to exhibit potent antifungal activity against *C. albicans* ATCC-10231 and drug-resistant *C. albicans* 955 with MIC=1.0 μg/mL and 0.25 μg/mL even better than the activity of clinically anti-fungal medicine, clotrimazole (MIC=8.0 μg/ml and 16.0 μg/ml) respectively (Ngoc-Chau *et al.,* 2009).

2-hydroxy-1,4-naphthoquinone forms stable compounds mostly with chelating ligands which can interact with most of the metals forming a huge number of metal chelates. A search through literature shows few reports on Schiff base compounds derived from 2-hydroxy-1,4-naphtho quinone, hence its choice for this research work.

Divalent manganese, cobalt, nickel, copper, zinc and palladium complexes of the 3-hydroxy-4-{[4-(methylsulfanyl)phenyl]imino}-3,4-dihydroxynaphthalen-1(2*H*)-one derived from 4-methylthioaniline and 2-hydroxy-1,4-napthoquinone have been synthesised and characterized. The spectroscopic data revealed that the ligand was bidendate, exhibited ketoimine tautomer in chloroform, while the solid state unveiled its enolimine form. The compounds were assessed for antibacterial and anticancer

activities. While Co(II) complex with its Cu(II) counterpart had better biopotent actions, the antiproliferative studies revealed the Zn(II) complex to exhibit the greatest in-vitro anti-cancer action towards MCF-7 (human breast) adeno-carcinoma and HT-29 (colon) carcinoma by 3.19 μm and 6.46 μm values at IC_{50} higher than the activity of cis-platin by 63 % and 8 % respectively (Osowole, 2012).

1.1.4 2,2'-bipyridine and its related compounds

2,2'-bipyridine, a colourless solid which belongs to the family of bipyridine is often soluble in polar and non-polar organic solvents but slightly soluble in aquo-solvent. 2,2'-bipyridine is considered a bidendate donor group owing to the presences of the two nitrogeneous atoms in its ring system as shown in Figure 1.9.

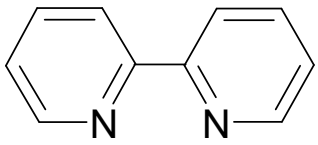

Figure 1.9: 2, 2^{I}-Bipyridine Structure

It is usually synthesised by the dehydrogenation of pyridine (Sasse, 1966) to give the formula ($C_{10}H_8N_2$).

$$2C_5H_5N \longrightarrow (C_5H_4N)_2 + H_2$$

Equation 1.8 Synthesis of 2,2^{I}-Bipyridine

Research evidence (Ju´lio *et al.,* 2014) has shown that 2,2'-bipyridine chelates combine with metal ions to form complexes. However, heteroleptic metal complexes of 2,2'-bipyridine have also been reported for their distinctive properties (Joshi *et al.,* 2014).

Osowole *et al.,* (2013) reported mixed ligand bivalent manganese, iron, cobalt, nickel, copper and zinc complexes of riboflavin with 2,2'-bipyridine. All synthesised compounds stood analysed with spectroscopic techniques (infrared and electronic), melting points, magnetic moments and electrolytic conductance measurements and screened for antibacterial activities. All relevant data confirmed that the metal complexes exhibited high-low spin octahedral equilibrium. The synthesised

compounds (ligand and complexes) showed no activity towards *B. cereus, P. mirabilis, E. coli, K. oxytoca, P. aeruginosa* and *S. aureus* with the exception of bivalent copper complex with 13.0 mm activity against *Proteus mirabilis*.2,2'-bipyridine was sensitive against all the micro-organisms with greater activity ranged between 24.0 mm and 47.0 mm verifying its potential as an excellent anti-bacterial agent.

Divalent cobalt, nickel, copper and zinc mixed ligand compounds of quinoline-2-carboxylic acid and 4,4'-dimethyl-2,2'-bipyridine were synthesized and characterized by infrared and electronic spectroscopy, CHN, FAA, TGA, magnetic moment and molar conductance measurements. In all the complexes studied, quinoline-2–carboxylic acid and bipyridine acted as bidentate ligands. The former chaleted with metal ions through the 'nitrogen and oxygen' atoms while the latter was reported to chelate with the metal ions through its two nitrogen atoms (Mahasin *et al.,* 2015).

Furthermore, mixed ligand complexes of bivalent manganese, cobalt, nickel, copper and zinc of 4-amino-6-hydroxy-2-mercaptopyrimidine and 2,2'-bipyridine were synthesised and characterized. The spectral results confirmed bidentate NN binding of the ligands bearing nitrogeneous centres with metal ions. For effective examination of the influence resulting from the anti-microbial actions of the ligands and their metal-ions upon chelation, all compounds synthesised afresh were screened for anti-bacterial activities against *B. cereus, P. mirabilis, E. coli, P. aeruginosa, S. aureus*and *K. oxytoca*. The anti-microbial evaluation data indicated that all metal(II) compounds synthesised afresh displayed moderate to very good activity when likened to that of the uncoordinated ligand (Osowole *et al.,* 2014).

1.2 Transition metal ions and their relevance in biological systems

The normal and effective functioning of the living organisms is quit inconceivable without certain metallo transition elements, i.e. V, Cr, Mn, Fe, Co, Cu and Zn. Out of these, five are also considered 'trace elements' (Mn, Fe, Co, Cu and Zn) due to their nuclei magnitude and negatively charged ions' accessibility to combine with organic species in biological schemes (Cesar, 2005). However, these elements, when existent at trace and ultra-trace amounts, exact significant roles at the molecular stages in living systems; e.g. deficiencies of these elements at trace quantities in living systems results into premature aging and cell breakdown. Generally, without metal ions, vitamins may

have little or no effect in the body (Satyl *et al.,* 2004). Metal ions, in enzyme-catalytic processes, form enzyme active sites, stabilize tertiary/quaternary structures of enzymes and act as catalysts which trigger enzymatic reactions and vitamins to function in the body.

Enzymes activities are completely dependent on metal ions, i.e. the human body systems contains about two (2) grams of zinc, since about one-hundred (100) enzymes function in the presences of zinc (i.e. carbonic anhydrase which is present in red blood cells and is involved in respiration, speeds up absorption of CO_2 in muscles and tissues, helps in release of CO_2 in the lungs and regulates pH in the blood and body of humans, dehydrogenases and aldolases are involved in blood and body sugar metabolism, etc) (Satyl *et al.,* 2004 and Lee, 1999). Zinc is efficiently regulated by major proteins in cell signaling and also regulates several proteins by shifting its concentration. The metallic ion in the central nervous system is given out from the synaptic vesicles at some glutamatergic nerve terminals to activate signaling paths that affects physiological activities which include synaptic plasticity, potentiation and cell loss. Zinc influences the productivity of nitric acid (HNO_3), and changing of the immune system. Zinc deficiency is widely attributed to the high phytic acid content of diets which gives rise to low growth rate, immunity impairment, as well as accelerates morbidity from normal diseases, mostly yeast and fungal diseases (Melaku, 2005; Michael,2011).

Daily requirement of copper in human system is about 4-5 mg. Copper is involved in the repair of calcium in the bones and connective tissues. Deficiencies or excess of copper content in the body system leads to osteoporosis, bone spurs and scoliosis likened conditions as well as in the inability of stored iron in the liver to function, leading to anemia (Satyl *et al.,* 2004). Copper is also involved in oxidation of amines (amine oxidase), oxidation of ascorbic acid (ascorbate oxidase), acts as an oxygen carrier in invertebrates and aids photosynthesis in green plants while its imbalance in the reproductive system results into premenstrual syndrome, ovarian cysts, miscarriages plus sexual malfunctions. Copper is essential for pregnancy and fertility (Lee, 1999; Wikipedia, 2013). Copper enhances the immune system, artery strength and reacts with heam as the terminal oxidase step (cytochrome oxidase, etc). Studies have revealed that presence of copper in the nervous system displays vital role in

activating the manufacture of neuro-transmitters, epin-ephrine, norepin-ephrine but dopamine and its deficiency has been associated with psychological, neurological and emotional problems (Wikipedia, 2013).

Enzymes like ribonucleolide reductase and glutamic mutase involved in the biosynthesis of DNA and metabolism of amino acids respectively functions with transition elements (i.e. Co) in trace quantities (Satyl *et al.,* 2004). Cobalt is a major component of vitamin B_{12} (cobalamine) (Kobayashi and Shimizu, 1999) which acts as a coenzyme and serves as a prosthetic group that is tightly bound to many enzymes in the body. Methylcobalamin is vital in metabolism of certain bacteria that produces methane. The methyl group of the methane is transferred to few metals (Pt^{II}, Au^{I} and Hg^{II}) by the bacteria to form highly toxic methyl mercury (CH_3Hg^{+}) or dimethyl mercury [$(CH_3)_2Hg$] (Lee, 1999). Surplus consumption of cobalt results into vomiting, nausea, vision problems, heart problems and thyroid damage. It also blocks pyruvate translation to acetyl Coenzyme (CoA) as well as succinate conversion from α-ketoglutarate.

10-20 milligrams of manganese (Mn) is averagely required by the human body. Mn acts as a co-factor to essential enzymes, i.e. pyruvate carboxylase in conversion of non-carbohydrate substances into glucose in the body (Satyl *et al.,* 2004). Research evidences have proved that enzymes associated with the production of greasy acids as well as cholesterol function better in the presence of manganese. However, deficiencies of manganese in the body leads to creation of irregular cartilage and skeletal tissue, damaged connective tissue, low muscle organisation and reduced glucose acceptance as well as in managing of blood sugar stages (Wikipedia, 2013).

Iron (Fe) which constitutes about 0.35% of the entire haemoglobin (Satyl *et al.,* 2004) is an indispensable trace metal in human system. Fe is involved as oxygen carrier in the body (from lungs to the cells), oxygen storage in the muscle tissue, electron carrier in plants and animals and increases the functions of enzymes such as nitrogenase, succinic dehydrogenase, etc (Lee, 1999). Excess iron content in the human body results into enzymes' dysfunctions, inflammation, production of radical oxygen species and kidney damage.

1.3 Applications of Schiff bases and their metal complexes

The *d*-block elements are extensively acknowledged to form Schiff base compounds; hence Schiff bases partake frequently as coordinating donor groups in coordination chemistry. Schiff base metallic compounds have remained of countless importance for years. Schiff bases comprising *N*, *O* and *S* atoms are known to exhibit vital roles in the chelation of metal ions at the dynamic sites of various metallo-bio-molecules. The latter also demonstrated broad spectrum biological action, since the presence of positively-charged-ions attached to biologically active compounds improve their actions (Yildiz *et al.,* 2004).

Schiff base chelators are involved as intermediates in enzymatic as well as non-enzymatic processes. The latter involves glycosylation processes which starts with attack at the sugar carbonyls or lipid peroxydation fragments on amino groups' proteins, aminophospholipids and nucleic acid producing tissue impairment by various rearrangements involving oxidation but are still considered normal throughout aging and are hastened in pathogeneses triggered by stress, extra metal ions or diseases such as diabetes, atherosclerosis and Alzheimer's disease. The former on the contrary, involves interface of the amino moiety of an enzyme typically that involving lysine residue, with a carbonyl function of the substrate. Stereochemical evaluations revealed that Schiff bases derived from methyl-glyoxal with an amino moiety of the lysine side chains of proteins can turn back in a manner to the *N*-atom of the peptide moieties that a charge transfer may arise among these moieties and the *O*-atoms of the Schiff base.

The *d*-block metals Schiff base complexes remain renowned for various bio-potent uses which include, medicinal (anticancer and antimicrobial agents, anticoagulant, anti-inflammatory analgesic agents, etc) and industrial applications (catalysis).

Cu^{2+}, Zn^{2+} including Co^{2+} Schiff base complexes have remained reported to show different levels of cytotoxicities towards cultured cancer cells (Chew *et al.,* 2004 and Ye *et al.,* 2004). i.e. first row metal(II) complexes of heteroamine chromonyl Schiff bases are reported potent anti-inflammatory agents with their Zn(II) chelates as good inhibitors of tumor associated carbonic anhydrase isozymes (Thangadurai and Natarajan, 2001). The role of Schiff base metal complexes mostly thio and hydrazine derivatives of pyrimidinyl-β-ketoimine are renowned as anti-metabolites impeding the

bio-synthesis of acids with nucleotides, hence causing death of murine leukemina cells (Owolabi, 2005 and Osowole, 2008). Indole-2-carboxaldehyde-based Schiff bases exhibited inhibitor actions towards KB cell lines while diorgano-tin^{4+} complex and its Schiff base showed anti-tumor actionsin-vitro against tumor cell lines (KB HCT-8 and BEL-7402) (Shalin *et al.,* 2009). Similarly amino transition metal Schiff bases formed from aromatic and heterocyclic amine possess high anti-tumor actions against human tumor cell lines.

Schiff base metal complexes serve as prototypes for essential organic molecules with applications in bio-mimetic catalytic processes. Hence, modern developments in catalytic and therapeutic activities of vanadyl complexes have led to interesting discoveries, i.e. vanadium detection in organisms (i.e ascidians and amanita mushrooms), as a component of the cofactor in vanadate-dependent haloperoxides and vanadyl nitroginase. Moreover, vanadyl(IV) and zinc(II) Schiff base complexes have been found to possess utility as insulin mimetic and antiamoebic agent (Mishra and Monika, 2008).

Divalent 3*d*-transition metal ions [nickel, copper, cobalt and zinc] synthesised with the chelator, 4-{[(*E*)-(2-hydroxy-5-bromophenyl) methylidene]amino}-N-(4,6-dimethylpyrimidin-2-yl) benzene sulfonamide have been reported. The in-vitro anti-bacterial, anti-fungal and cytotoxic screening data of the metal complexes and their chelator displayed average to very-significant anti-bacterial actions against one or more microbial strains with moderate anti-fungal actions against numerous fungiform strains (Zahid *et al.,* 2010).

The Schiff base Co^{2+}, Ni^{2+}, and Cu^{2+} complexes have been reported to be active in physiological processes and to have effective therapeutic effects, i.e. vanadium acts as a cofactor in neutron transmitter, blood sugar, lipid and cholesterol metabolism, tooth and bone development, helps fertility thyroid function and has antidiabetic properties. Ni(II) phenanthroline complexes have been documented to be bactericidal (Temilolu, 2008). Co(II) is used in tetrahydrofolate synthesis, for the survival of bacterial cells and copper(II) is involved in tyrosine and quercetin oxidations in microbes (Osowole and Fagade, 2007).

Schiff bases formed from thiazole showed analgesic alongside anti-inflammatory actions, i.e. chitosan-based Schiff bases showed antioxidant actions which includes super-oxide and hydroxyl scavenging while furan semicarbazone metallic compounds exhibited substantial antihelmintic and analgesic actions. Furthermore, Salicylidene anthranilic acid exhibits antiulcer actions as well as coordination behavior with d^9 ion compounds, showed an upsurge in anti-ulcer actions. Additionally, Cu, Ni, Zn, and Co complexes of the Schiff bases derived from salicylaldehyde-2,4-dihydroxylbenzaldehyde, gylcine and L-alanine showed good antitumor activity (Kumar, 2012).

The Ni(II) Schiff base complexes have been employed as forerunners in formulation of additional non-ring and ring chelators. Schiff base chelators' metallic compounds having structural resemblances to thiolocyanines (N4-macrocycles) and other associated compounds presently are applied in modification of electrodes' active surfaces with the aim to increase their catalytic actions in the careful detection of carbon-based pollutants including entrainment of metals.

Cobalt(II) Schiff base complexes such as Co(II) acetylacetone-ethylenediamine, co(acacen), etc are used as model in metal to oxygen binding in biological systems. Schiff base d^9 complexes are assumed to be important intermediates of pyridoxal reliant enzymes. Series of evaluations on Schiff bases formed from amino-related acids have been documented using pyridoxal as the cocodensent (Owolabi, 2005). Mn^{2+} and Fe^{3+} Schiff base complexes have been applied as magnetic resonance imaging (MRI) agents of the human heart (Troughton *et al.,* 2004), 4-hydroxycoumarin and its derivatives i.e. warfarin and dicoumarol are anticoagulant agents (Renata *et al.,* 2009).

Condensed metal complexes of Schiff base ligands from benzene-related-nitrogen compounds and heterocyclic carbonyls have displayed diversity of uses in numerous fields of chemistry, medicine, etc, i.e. they have been used as analytical devices in optical and elemental devices, and also applied in chromatographic studies using organic solvents/substances as indispensable compounds of determining schemes. They are also applied to enable selective and sensitive detection and imaging (Mohammed and Salah, 2007). Metal complexes of Schiff bases are used also as

fluorescent dyes for synthetic fibers, day-moon fluorescent pigments in laser dyes and solar energy collectors (O' Kennedy and Thornes, 1997).

1.4 Justification of Research

Detailed literature search have shown that Schiff base ligands with their metal complexes are significant in different areas of medicine, chemistry, biology as well as in the industries. Different works on the synthesis, characterization as well as antimicrobial assessments of various Schiff bases namely: aniline Schiff bases (i.e. *N*-(2-hydroxy-1-naphthylidene)-4-chloroaniline, *N*-(2-hydroxy-1-benzylidene)-2,3-dimethylaniline, etc); substituted chromenone Schiff bases (i.e.3-((2-hydroxyphenylimino)methyl)-4H-chromen-4-one, 3-((2-mercaptophenylimino) methyl)-4H-chromen-4-one, etc); benzohydrazide Schiff bases (2-hydroxy-N^1-((Z)-3-(hydroxyimino)-4-oxopentan-2-ylidene)benzohydrazide,); Substituted nitro-phenol/benzene Schiff bases (i.e. 2-((2,4-dimethylphenylimino)methyl)-6-methoxy-4-nitrophenol(E-4-(2-hydrox-3-methoxybenzalideneamino)-N-(pyrididin-2-yl)2-((2,4-imethylphenylimino)methyl-6-methoxy-4-nitrophenol), 1-{3-[(3-hydroxypropyl imino)methyl]-4-hydroxyphenylazo}-4-nitrobenzene-1-{3-[(3-hydroxypropylimino)methyl]-4-hydroxyphenylazo}-2-chloro-4-nitrobenzene, 2-((3,4-difluorophenylimino) methyl)-6-methoxy-5-nitrophenol, 1-{3-[(-3-hydroxypropylimino)methyl]-4-hydroxy phenylazo}-4-chloro-3-nitrobenzene, 1-{3-[(-3-hydroxypropylimino)methyl]-4-hydroxyphenylazo}-4-chloro-3-nitrobenzene2-{4-[(2-hydroxynaphthalen-1-yl)methyleneamino] benzene) and benzoic acid Schiff bases (i.e. 2-((4-oxo-4H-chromen-3-yl) methylneamino)benzoic acid,) have remained documented. Additionally, 2-hydroxy-2-ethyl-(3-carboxylideneamino)-3-(2-(4-methyl-phenyl))-1,2-dihydroquinazolin-4(3H)-one, (*E*-4-(2-hydroxy-3-methoxybenzalideneamino)-N-(pyrimidin-2-yl)benzene sulfonamide, (Z)-1-(1-(1H-indol-3-yl)ethylideneamino)quinolin-2(1H)-one, 5-bromo-3-(((8-hydroxy-2-methylquinolin-7-yl)methylene)hydrazono)indolin-2-one, sulfonamido} quinoxalin, potassium-2-N(4-N,N'-dimethylaminobenzyliden-4-trithiocarbonate-1,3,4-thiadiazole,3-(2-(2-hydroxy-3-methoxybenzylidene)hydrazine)indo line-2-one have also been reported. There are also literature on the syntheses, characterization and antimicrobial studies of some pyrimidinyl Schiff base ligands and their metal complexes (Osowole *et al.,* 2009, 2012 and Osowole and Reuben 2014). However, there is little or no detailed information on Schiff bases of pyrimidine derivatives with

2-hydroxynaphthaldehyde/2-hydroxy-1,4-naphthoquinone, their subsequent metal complexes, as well as their heteroleptic analogues with 2,2'-bipyridine.

1.5 Aims of research

Consequently, the aims of this research work are to synthesise series of novel bidentate ligands from condensation of substituted aminopyrimidines and 2-hydroxy-1-napthaldehyde/2-hydroxy-1,4-naphthoquinone. Secondly, Mn(II), Fe(II), Co(II), Ni(II), Cu(II) and Zn(II) complexes and their heteroleptic analogues with 2,2'-bipyridine will be synthesised and characterized.

1.6 Objectives of the research

The objectives of this research work include:-

1. Synthesis of ligands from various pyrimidines (2-amino-pyrimidine, 2-amino-4,6-dihydroxypyrimidine and 2-amino-4,6-dimethylpyrimidine) and 2-hydroxyl-1-napthaldehyde/2-hydroxy-1,4-naphthoquinone. The ligands synthesised are
   3-{[-(pyrimidin-2-yl)imino]methyl}napthalen-2-ol (HL^1)
   3-{[(4,6-dihydroxypyrimidin-2-yl)imino]methyl}napthalen-2-ol (HL^2)
   3-{[(4,6-dimethylpyrimidin-2-yl)imino]methyl}napthalen-2-ol (HL^3)
   2-(pyrimidin-2-ylamino)naphthalene-1,4-dione (HL^4)
   2-(4,6-dihydroxypyrimidin-2-ylamino)naphthalene-1,4-dione (HL^5)
   2-(4,6-dimethylpyrimidin-2-ylamino)naphthalene-1,4-dione (HL^6)

2 Complexation of the various above named ligands with metal(II) salts to form metal complexes of manganese, iron, cobalt, nickel, copper and zinc respectively. Also the synthesis of heteroleptic Mn(II), Fe(II), Co(II), Ni(II), Cu(II) and Zn(II) complexes of the above synthesised ligands with 2,2'-bipyridine will be carried out

3 All the synthesised compounds will be characterized by FTIR, UV-Vis, ^{1}H NMR and ^{13}C NMR spectroscopies, mass spectrometryandelemental (C,H,N,S) analyses, melting point, room temperature magnetic susceptibilities and molar conductance measurements.

4 The effect of hydroxy and methyl groups substitution on the pyrimidine ring, and consequent replacement of the 2-hydroxy-1-napthaldehyde with 2-hydroxy-1,4-naphthoquinone in HL^4, HL^5 and HL^6 ligands/complexes on the physicochemical and biological properties of various compounds will be investigated.

5 The effectiveness of the synthesised compounds as antimicrobial, antifungal and antioxidant agents will be verified through Agar well diffusion and disc methods; and DPPH scavenging ability and ferrous chelating techniques.

CHAPTER TWO
LITERATURE REVIEW

2.0 Historical background

Schiff bases are generally nitrogen analogy compounds that contain C=NR moiety, drawing much interest in both carbon-based syntheses and metal ion coordination. The study of Schiff bases and their derivatives started in the mid nineteenth century, with the first Schiff base compound (Schiff base copper complex) prepared in 1840 by Ettling (Aliyu*et al.,* 2013a). However, the systematic study of Schiff base derivatives began in 1931 with the synthetic work of Pfeiffer and his co-workers (Pfeiffer *et al.,* 1931). The formation of the intermediate product, carbinolamine which loses water molecule during Schiff base synthesis to a Schiff base ligand was reported by Jencks (Jencks, 1964).

Schiff bases have been synthesised through different pathways, i.e. Mourea and Mignonac in 1801 synthesised Schiff bases by direct combination of Grignard's reagent and aryl cyanide with cautious addition of water molecule across the intermediate yield to give the desired Schiff base ligand. Similarly, Vukadin (2005) reports the reaction of metal salt(s) with synthesised Schiff base in aqueous alcoholic solvents, i.e. ethanol, methanol through refluxing process. The direct reaction of primary amines with synthesised salicyaldehyde to give a metal complex is another synthetic method for Schiff base metal complexes formation. In this method, the two reactants are heated in a solvent (alcoholic solvents miscible with water), and the product is usually in high yields and are allowed to crystallize using organic solvents i.e. chloroform or benzene (Otunla, 2008). Additionally, Schiff bases and their derivatives have been synthesised through solventless method with the assistance of microwave irradiation. The solventless reactions are reported to proceed faster and efficiently giving raise to higher experimental yields. The products are usually crystallized by re-purification in a suitable solvent or a blend of solvents (Yang *et al.,* 2002).

2.1 Review of properties of Schiff bases and their metal complexes

2.1.1 Infrared spectroscopy

Characterization of coordination compounds involves different physical measurements and methods which provide detailed assignments of bond types and metal ligand attachment points (Steward, 1970). Among these physical measurements is the infrared spectroscopy (Nakamoto, 1986).

Infrared spectroscopy studies produce absorption frequency for vibration of bonds in a molecule (Wade, 1999). It has been applied in the study of Schiff base ligands as well as their metallic complexes. Research reports reveal that Schiff bases coordinate to metallic ions through their imine nitrogen and phenolic oxygen atoms. Hence, It is anticipated that chelation of nitrogen to the metallic atom would decrease the electron density of the imine bond and thus lower the C=N moiety absorption in the metal complexes. The infrared spectrum also offers valuable data regarding the nature of other functional moieties (i.e. C=C, C=N, etc) present in a molecule and that are attached to the metal atoms of a complex (M-N, M-O, M-S and M-Cl) (Raman *et al.,* 2007 and Sonmez *et al.,* 2004).

In the evaluation of mixed ligand Ni^{2+}, Co^{2+}, Cu^{2+} and Zn^{2+} complexes of N-(2-hydroxy-1-naphthylidene)-4-chloroaniline (L^1H) and *N*-(2-hydroxy-1-benzylidene)-2,3-dimethylaniline (L^2H) Schiff bases, the bands at 3440 and 3447 cm^{-1} were due to *v*OH bonds of the free ligands. The non-appearance of *υ*(OH) broad bands in the spectra of the metallic compounds indicates coordination of the phenolic oxygen atom to metal atoms. However, diffused broad bands, strong bands and very weak bands detected in the spectra of the metallic compounds around 3100-3700 cm^{-1}, 1535-1538 cm^{-1} and 814-833 cm^{-1} were assigned to *v*(OH), *δ*(OH) and *Pr*(OH) vibrations of chelated aqua molecules. The strong *v*(C-O) and *v*(C=N) bands at 1327-1279 cm^{-1} and 1620-1613 cm^{-1} in the ligands moved to upper/lesser regions in the spectra of the metallic compounds around 1385-1366 cm^{-1} and 1616-1599 cm^{-1}. The latter indicated participation of phenolic oxygen and azomethine nitrogen atoms in complex formation. This was additionally proved by the presence of non-ligand bands between 497-545

cm^{-1} and 417-465 cm^{-1} in the complexes' spectra owing to M-O and M-N bands respectively (Atmaram and Kiran, 2011).

The infrared study of the Schiff base chelator, 2-[(4-oxo-4H-chromen-3yl) methyleneamino]benzoic acid with its bivalent cobalt, copper, nickel, manganese, and zinc complexes have been documented. The ligand spectrum exhibited a characteristic band at 1606 cm^{-1} owing to C=N group vibration which moved to lower wave numbers (1627-1619 cm^{-1}) in the spectra of metal(II) complexes. The shift indicated complexation of metal ions through nitrogen atom of azomethine group. A band at 1692 cm^{-1} in the ligand spectrum attributed to *ν*C=O shifted to a lower frequency (1614–1651) in the spectra of its metallic compounds confirming the involvement of the C=O group oxygen atom in coordination. Two new non-ligand bands observed at 521-533 and 421-437 cm^{-1} range in the spectra of metal complexes were attributed to the M-O and M-N vibrations respectively. The appearance of these bands corroborates the participation of *O* and *N* atoms in coordination with metal (II) ions (Mendu *et al.,* 2011).

In addition, the infrared spectra data of the ligand prepared from salicylic acid hydrazide and 2,4-dihydroxyacetophone and its divalent and trivalent iron complexes have been reported. The ligand spectrum exhibited feeble to average bands around 3577-3320 cm^{-1} which were ascribed to stretching vibrations of H-bond, while the band at 1707 cm^{-1} was owing to coupled ν(C=N) and ν(C=C) moieties. The bands observed at 3260 and 1610 cm^{-1} corroborates ν(N=H) and H-bonded amide carbonyl groups respectively. The ν(C-O) and ν(N-N) bands were observed at 1240 cm^{-1} and 1100 cm^{-1}, while the complexation evidences were noticed in a shift of ν(C=N) and ν(N-H) to lower frequencies with ± 50 cm^{-1} and ± 35 cm^{-1} respectively, a shift to higher frequency of ν(N-N) to ± 45 cm^{-1} and the observation of novel bands in the range 490-510 cm^{-1} and 420-422 cm^{-1} attributed to ν(Fe-O) and ν(Fe-N) (Ramana *et al.,* 2012)

The infrared spectra data of bivalent metallic compounds of a Schiff base chelator comprising benzofuran function displayed bands at 3354 cm^{-1} and 3185 cm^{-1} attributable to secondary amide ν_{asy}(NH) and ν_{sy}(NH) stretching vibrations of the ligand. These bands remained un-shifted to lower frequency (Halli *et al.,* 2004) signifying non-involvement of NH atom in coordination with the metallic atoms. The

shift of ν(C=O) band in the metal complexes with ±15-40 cm^{-1} to lower frequencies from that of the ligand (1670 cm^{-1}) confirmed complexation of the carbonyl oxygen atom to the metal ions. The free Schiff base ligand showed ν(C=N) and ν(N-N) bands at 1606 cm^{-1} and 942 cm^{-1} which shifted to lower/higher regions with 20-52 cm^{-1} and 21-43 cm^{-1} in the spectra of the metallic compounds. The latter confirmed involvement of the azomethine nitrogen and *N*-atom of N-N in dative bonding with the atoms. The spectra of the metal complexes exhibited weak free ligand bands in the regions 515-575 cm^{-1}, 425-475 cm^{-1} and 376-410 cm^{-1} attributed to ν(M-O), ν(M-N) and ν(M-Cl) stretching vibrations respectively (Reddy *et al.,* 2013).

Infrared spectral studies of the Schiff base ligands 3-((2-hydroxyphenylimino) methyl)-4*H*-chromen-4-one (HL_1), 2-((4-oxo-4H-chromen-3-yl)methylneamino)benzoic acid (HL_2), 3-((3-hydroxypyridin-2-ylimino)methyl)-4*H*-chromen-4-one and 3-((2-mercaptophenylimino)methyl)-4*H*-chromen-4-one (HL_3) condensed from various 3-formyl chromones with their divalent zinc and nickel complexes exhibited υ(C=N) and high intensity υ(C-O) vibrations at 1605-1563 cm^{-1} and 1365 cm^{-1} correspondingly. The former suggested the formation of the Schiff base which moved to a lower frequency in the metallic compounds (±25-45 cm^{-1}) and corroborated the complexation of metallic ion(s) with imine group. However, the latter band observed only in HL_2 ligand disappeared on complexation, with a new medium intensity band observed at the range 1412-1383 cm^{-1}, supportive of coordination of enolic *O*-atom to the metallic ions via removal of hydrogen atom. The appearance of two strong bands at 599-500 cm^{-1} and 488-419 cm^{-1} assignable to υ(M-O) and υ(M-N) vibrations further supports complexation. Hence, the bands at the range 1650-1620 cm^{-1} in the ligands which upon complexation shifted to lower wavenumber by 20–35 cm^{-1} were assigned υ(C=O) of the chromone system (Palakuri and Reddy, 2014).

Furthermore, studies on bivalent manganese, nickel, cobalt, copper and zinc complexes of the ligand; (E-4-(2-hydroxy-3-methoxybenzalideneamino)-N-(pyrimidin-2-yl)benzene sulfonamide have been reported. The infrared data revealed a broad band around 3423 cm^{-1} (which conspicuously was absent in the spectra of the metallic compounds) corroborating *OH* stretching frequency of the ligand. Non-appearance of this band in the metallic compounds shows deprotonation and participation of the enol *O* in chelation. The uncoordinated νC=N band of the ligand occurred at 1582 cm^{-1} but

shifted to higher frequencies in the spectra of the bivalent metallic compounds with 10-23 cm^{-1} and corroborates coordination of azomethine *N*-atom to the metallic ions. Further confirmation of the enol *O* and imine *N* atoms coordination to the metallic ions were proved by the presence of new bands at 420-464 cm^{-1} and 512-578 cm^{-1} apportioned to ν(M-O) and ν(M-N) in the spectra of the metallic compounds (Valarmathy and Subbalakshmi, 2014).

Infrared spectra of Mn(II), Co(II), Ni(II) Cu(II) and Zn(II) complexes with a Schiff base chelator formed from 2-hydroxybenzophenone with aniline have been reported. The uncoordinated ligand exhibited νC=N and νOH bands at 1602 cm^{-1} and 1250 cm^{-1} respectively. These bands had significant shifts to lower/higher frequencies (1585-1578 cm^{-1} and 1265-1275 cm^{-1}) in the spectra of the metal(II) complexes and indicated coordination of the Schiff base ligand to the metal(II) ions/atoms via azomethine nitrogen and phenolic oxygen atoms. Free-ligand bands in the spectra of the metal complexes at the ranges 425-500 cm^{-1} and 570-585 cm^{-1} attributed to νM-O and νM-N modes further confirmed chelation between the ligand and metal atoms (Subbaraj *et al.,* 2015).

2.1.2 Electronic properties of Schiff bases and their metal complexes

Metallic compounds of Schiff bases have been synthesised with characterisation using electronic studies. The complexes (Co^{2+}, Cu^{2+} and Ni^{2+}) of amino acid (Alanine, Glycine and Tyrosine) derived Schiff bases have been synthesised with their electronic studies reported. The bands between 29100-31000, 17550-18220 and 8250-9850 cm^{-1}regions in the Co(II) complexes were attributed to the transitions $^4T_{1g}\rightarrow{}^4T_{2g}$ (υ_1), $^4T_{1g}\rightarrow{}^4A_{2g}(\upsilon_2)$ and $^4T_{1g}\rightarrow{}^4T_{ig}(P)(\upsilon_3)$ of a six coordinate geometry; while the Cu(II) complexes showed three broad bands within the regions 30270-31500 cm^{-1}, 22550-23170 cm^{-1} and 12500-13750 cm^{-1}. The latter (12500-13750 cm^{-1}) band was assigned as 10Dq band for a distorted six coordinate configuration conforming to $^2E_g\rightarrow{}^2T_{2g}$ transition while the 22550-23170 cm^{-1} band is attributed to intra-ligand charge transfer with the highest energy band allotted to charge transfer transitions. The electronic spectra of Ni^{2+} complexes displayed three bands assigned to $^3A_{2g}\rightarrow{}^3T_{2g}(\upsilon_1)$ (28350-28950 cm^{-1}), $^3A_{2g}\rightarrow{}^3T_{1g}(\upsilon_2)$ (16250-17500 cm^{-1}) and $^3A_{2g}\rightarrow{}^3T_{2g}(P)(\upsilon_3)$ (9550-10220 cm^{-1}) respectively of the octahedral geometry (Zahid *et al.,* 1997).

The Schiff base ligand obtained from ninhydrin and α,L-alanine (indane-1,3-dione-2-imine-N-2-propionate) and its complexes of Mn(II), Fe(III), Co(II), Ni(II) and Zn(II) have been synthesised and reported. The visible spectrum of the Co(II) complex showed two *d-d* absorption bands at 14840 cm^{-1} and 12690-12550 cm^{-1} attributable to $^4T_{1g}\rightarrow{}^4A_{2g}$and $^4T_{1g}\rightarrow{}^4T_{2g}$ transitions consistent of an octahedral geometry. The 3rd *d-d* band predictable close to 20000 cm^{-1} ($^4T_{1g}\rightarrow{}^4T_{2g}$ (P)) was obscured by strong ν(C=N) band due to azomethine function observed around 20120 cm^{-1}. The visible spectrum of the bivalent nickel compound exhibited three absorption bands at 27170 cm^{-1}, 15390 cm^{-1} and 10460 cm^{-1} attributed to $^3A_{2g}\rightarrow{}^3T_{1g}$ (P), $^3A_{2g}\rightarrow{}^3T_{1g}$ (F) and $^3A_{2g}\rightarrow{}^3T_{2g}$ correspondingly complementary of six coordinate geometry. The complexes of Mn(II) and Fe(III) displayed numerous weak *d-d* bands which often corresponds to high spin d^5 six coordinate systems. The Zn(II) complex likewise assumed a six coordinate geometry (Mehabaw *et al.,* 2002).

The electronic studies of divalent iron, nickel, cobalt, copper and zinc complexes of the Schiff base formed from 2-thiophenecarboxaldehyde with 2-aminopyridine and N-(2-thienylmethylidene)-2-aminopyridine have been documented. The spectrum of Fe(II) complex displayed a pair of truncated intensity bands at 12800 and 11200 cm^{-1} assigned to $^5T_{2g}\rightarrow{}^5E_g$ transition complementary of a distorted six coordinate geometry. The doublet was due to Jahn Teller distortion in the excited state. The Co(II) complex revealed five absorption bands at 21270-19.040 cm^{-1}, 15600 cm^{-1} and 9210-8330 cm^{-1} attributed to $^4T_{1g}\rightarrow{}^4T_{1g}$(P), $^4T_{1g}\rightarrow{}^4A_{2g}$ and $^4T_{1g}\rightarrow{}^4T_{2g}$ transitions consistent of a distorted octahedral geometry. The observed split with the first transition is usually associated to D_4h symmetry complexes. However, a pseudo octahedral stereochemistry was assigned to the Ni(II) complex with transitions from $^3A_{2g}$ to $^3T_{2g}$, $^3T_{ig}$ and $^3T_{ig}$(P) but the low intensity split-broad bands observed at 10000 cm^{-1} and 9150 cm^{-1} corroborates tetragonal distortion. The divalent copper and zinc compounds exhibited one absorption band each at 16500 cm^{-1} and 26000 cm^{-1} respectively indicative of a distorted six coordinate geometry for the divalent copper complex and a ligand-metal-charge transfer transition for the divalent zinc complex (Cesar *et al.,* 2008).

Schiff base complexes of the sort $[M^{2+}L].XH_2O$, where M=Mn, Ni, Co, Cu, and Zn; L=$[(C_6H_5)C{:}OCH{:}C(CH_3)NH(C_6H_7N_2)]$ have been prepared, characterized and reported. The Ni^{2+} complexes have remained known for their coordination numbers of

six (octahedral) to four (square planar/tetrahedral) with the studied nickel complex exhibiting absorption bands at 15700 cm^{-1} and 20300 cm^{-1} assigned to $^3T_1(F) \rightarrow {}^3T_2$ and $^3T_1(F) \rightarrow {}^3A_2$ transitions. The Mn^{2+} complexes gave weak bands at 14000 cm^{-1} and 20000 cm^{-1} typical of tetrahedral geometry and are assigned to the forbidden transitions $^6A_1 \rightarrow {}^4E_1$ and $^6A_1 \rightarrow {}^4A_1$ respectively, while Co^{2+} complex gave bands at 11500 cm^{-1}, 15700 cm^{-1} and 23800 cm^{-1} assigned to $^4T_{1g} \rightarrow {}^4T_{2g}$, $^4T_{1g} \rightarrow {}^4A_{2g}$, and $^4T_{1g} \rightarrow {}^4T_{1g}(P)$ transitions of octahedral geometry. However, the bands for the Cu^{2+} complex were detected at 15200 cm^{-1} and 23800 cm^{-1} apportioned to $^2B_{1g} \rightarrow {}^2A_{1g}$ and $^2B_{1g} \rightarrow {}^2e_{1g}$ transitions of square planar geometry (Osowole, 2008).

The divalent cobalt, nickel and copper complexes ofSchiff bases obtained from substituted aminobenzothiazole with dimethylbezaldehyde have been evaluated.The electronic spectra of the Schiff bases showed strong bands at 33200-33400 cm^{-1} and 41150-42200 cm^{-1} ranges accredited to $\pi \rightarrow \pi^*$ as well as charge transfer transitions respectively. The Co(II) Schiff base complexes displayed two bands at 15250-15730 cm^{-1} and 23230-23470 cm^{-1} assigned to $^4T_{1g} \rightarrow {}^4A_{2g}$ (ν_2) and $^4T_{1g} \rightarrow {}^4T_{1g}(P)$($\nu_3$) transitions characteristic of a six coordinate stereochemistry. The visible spectra of the divalent nickel complexes revealed bands around 15230-15440 cm^{-1} and 21110-21290 cm^{-1} attributed to $^3A_{2g} \rightarrow {}^3T_{1g}(\nu_2)$ and $^3A_{2g} \rightarrow {}^3T_{1g}(P)(\nu_3)$ transitions of a six coordinate configuration. Electronic spectra of divalent copper complexes showed one broad band at 14890-15320 cm^{-1} apportioned to two or three transitions of $^2B_{1g} \rightarrow {}^2A_{1g}$, $^2B_{1g} \rightarrow {}^2B_{2g}$ and $^2E_{2g} \rightarrow {}^2T_{2g}$ and corroborates a distorted six coordinate geometry for the Cu(II) complexes (Saleh *et al.,* 2009).

Schiff base dye ligands (1-{3-[(3-hydroxypropylimino)methyl]-4-hydroxyphenylazo}-4-nitrobenzene, 1-{3-[(3-hydroxypropylimino)methyl]-4-hdroxyphenyl azo}-2-chloro-4-nitrobenzene and 1-{3-[(-3-hydroxypropylimino)methyl]-4-hydroxyphenyl azo}-4-chloro-3-nitrobenzene) and their bivalent copper and cobalt coordinate compounds have been reported for electronic studies. The bivalent cobalt complexes exhibited high spin tetrahedral geometries with three spin-allowed crystal-field-bands at the ranges 18940-16077 cm^{-1}, 22830-19682 cm^{-1} and 18200 cm^{-1} assigned to $^4A_2 \rightarrow {}^4T_2$, $^4A_2 \rightarrow {}^4T_1$ and $^4A_2 \rightarrow {}^4T_1(P)$ transitions. The visible spectra of the bivalent copper complexes showed absorption bands at 16393-21880 cm^{-1} and 22674-27770 cm^{-1}. The first absorption bands were attributed to ligand field transition, while the latter were

allocated to charge-transfer transitions arising from the antibonding orbital of the Cu-O (oxygen atoms) (Raziyeh and Saeid, 2012).

The electronic studies of 2-[2-amino-5-(3,4,5-trimethoxybenzyl)pyrimidinyl-4-azo]4-bromophenol with bivalent nickel, iron, copper, cobalt and zinc complexes showed two bands at the ranges 39060-36130 cm^{-1} and 29410-27620 cm^{-1} attributed to π - $\pi*$ and n - $\pi*$transitions. The bivalent iron complex assumed octahedral geometry with a distinctive absorption band at 36130 cm^{-1} apportioned to LMCT. Two visible bands were observed in the spectrum of the bivalent cobalt complex at 15820 cm^{-1} and 23750 cm^{-1} due to $^4A_{2g}\rightarrow{}^4T_{2g}$ and $^4A_{2g}\rightarrow{}^4T_{1g}(P)$ transitions attributed to octahedral geometry. The bivalent nickel complex exhibited three bands at 11130 cm^{-1} and 18200-23200 cm^{-1} allocated to $^3A_{2g}\rightarrow{}^4T_{1g}$, $^3A_{2g}\rightarrow{}^3T_{1g}(P)$ transitions and corroborates octahedral geometry. However, the spectrum of bivalent copper complex had a broad band at 16230 cm^{-1} assigned to $^2B_{1g}\rightarrow{}^2E_g$ and $^2B_{1g}\rightarrow{}^2E_{2g}$ transitions around a distorted six coordinate environment (Saadiyah *et al.,* 2012).

In addition, Schiff base complexes of the categories $[M(L)(H_2O)_n]$ and $[M_4(L)(H_2O)_n]$, where M=Ni(II), Co(II) and Cu(II) for the mononuclear complexes and Ni(II) and Cu(II) for tetranuclear complexes; L=salicilydene-cefotaxime ligand and n=6, have been studied and reported. The metal (II) complexes in all cases exhibited two visible spectral prominent bands at 17543-14933 cm^{-1} (ε=148-180 $Lmol^{-1}cm^{-1}$) and 23800-22732 cm^{-1} (ε=1.16-3.65 L $mol^{-1}cm^{-1}$) ranges consistent of four coordinate tetrahedral geometry. The first band was assigned to the transitions $^4A_2\rightarrow{}^4T_1(P)$, for [Co(L)], $^3A_2\rightarrow{}^4T_2(F)$ for [Ni(L)] and $^2T_2\rightarrow{}^4E_2(G)$ for [Cu(L)] complexes. However, the second band was attributed to charger transfer transition of tetrahedral geometry. The extra band observed in the spectra of the tetranuclear complexes around 23250 cm^{-1} was accredited to *d-d* transition of the metal in a tetrahedral field (Anacona, 2013).

The UV-Vis studies involving cobalt, nickel, copper and zinc complexes of the Schiff bases formed from ethylene-1,2-diamine and 5-methyl Furfural/2-anisaldehyde and 2-hydroxybenzaldehyde in their divalent states have been reported. Generally, the spectra of d^7 cobalt complexes displayed three strong bands at the ranges 8520–8690, 17510–17970 and 29540–29980 cm^{-1} and were assigned to $^4T_{1g}\rightarrow{}^4T_{2g}$, $^4T_{1g}\rightarrow{}^4A_{2g}$, and $^4T_{1g}\rightarrow{}^4T_{1g}(P)$ transitions separately, corroborative of six coordinate stereochemistry

around the d^7 cobalt ion. Similarly, the visible spectra of d^8 nickel complexes exhibited absorption bands at 8590–8760, 17620–17850, and 25660–25890 cm^{-1} ascribed to $^3A_{2g}\rightarrow{}^3T_{2g}$ and $^3A_{2g}\rightarrow{}^3T_{1g}$*d-d* transitions. However, the strong band at 29670–29890 cm^{-1} was owing to metal to ligand charge transfer. The d^9 copper complexes displayed absorption bands at 8520–8740 and 17220–17670 cm^{-1}apportioned to the transition $^2E_g\rightarrow{}^2T_{2g}$ of a six coordinate geometry. The band observed at 29530–29980 cm^{-1} was attributed to 'ligand to metal' charge transfer transition. The d^{10} zinc complexes did not exhibit any *d-d* transitions however displayed only charge transfer bands at 28380–28650 cm^{-1} **(**Sajjad *et al.,* 2014)

The synthesis and characterization of d^7-cobalt, d^8-nickel, d^9-copper and d^{10}-zinc complexes of the tetradentate Schiff base [(4*E*)-4-[(2-{(*E*)-[1-(2,4-dihydroxyphenyl) ethylidene]amino}ethyl)imino]pentan-2-one] have been studied. The ligand UV-spectrum showed double bands at 31550 and 26250 cm^{-1} attributed to π - $\pi*$transition of the conjugated cyclic ring and n - $\pi*$transition of the -C=N moiety. The π - $\pi*$ and n - $\pi*$transitions of the ligand moved to longer wavelengths in the spectra of the metal complexes indicating coordination of the ligand to metal atoms. The d^7-cobalt complex exhibited a less intensity *d-d* absorption at 18120 cm^{-1} consistent of a distorted tetrahedral geometry assigned to $^4A_2(F)\rightarrow{}^4T_1(P)$ transition. The visible spectrum of d^8-nickel complex exhibited two absorption bands at 22940 and 17730 cm^{-1} attributed to spin allowed transitions $^1A_{1g}\rightarrow{}^1A_{2g}$ and $^1A_{1g}\rightarrow{}^1B_{1g}$ typical of square-planar stereochemistry around d^8-nickel ion. Observed reddish-brown colour further confirmed square-planar geometry for the d^8-nickel complex (Abd-Elzar, 2001). Divalent copper (d^9) complex displayed a single band at 17990 cm^{-1} creditable to $^2B_{1g}\rightarrow{}^2A_{1g}$ transition complementary of a square planar geometry. The band at 24330 cm^{-1a} in the d^{10}-zinc complex was attributed to L→M charge-transfer transition (LMCT) as no *d-d* transition was expected (Ikechukwu and Peter, 2015).

2.1.3 Structural properties of Schiff bases and their related metal complexes

The isolated cobalt (d^7), nickel (d^8) and copper (d^9) complexes of the Schiff bases formed from (2-aminobenzothiazole, 6-nitro-2-aminobenzothiazole, 4,6-dibromo-2-aminobenzothiazole) and 4-*N*-dimethylbezaldehyde have been documented. The complexes adopted the general formula $[ML_2Cl_2]$ and they were characterized using atomic absorption, infrared and electronic spectra, molar conductance and magnetic

moment measurements. All measurements supported octahedral structures for the metal complexes (Ahmed *et al.,* 2009).

The synthesised complexes of bivalent copper and manganese of coumarin-6,7-dioxyacetic acid ($cdoaH_2$) and 4-methyl coumarin-6,7-dioxyacetic acid ($4\text{-}MecdoaH_2$) were analysed using microanalysis, molar conductance in aqueous-free solvents, electronic, infrared and proton spectra. The X-ray crystal structure of $[Cu(cdoa)(phen)_2].8H_2O$ and $[Cu(4\text{-}MecdoaH_2)\ (phen)_2].13H_2O$; (phen =1,10-phenanthroline) suggested trigonal bipyramidal geometries with metals bonded to the 4-nitrogen atoms of the two chelating phenanthroline molecules as well as to a single carboxylate oxygen of the dicarboxylate ligand (Bernadette *et al.,* 2007).

Ketan *et al.,* (2012) prepared the Schiff base 6-bromo-3-(3-(4-chlorophenyl)acryloyl)-2H- chromen-2-one. Their ciprofloxacin d^7-cobalt, d^8-nickel, d^9-copper and d^5-manganese complexes were synthesised and investigated on the basis of various spectral techniques such as ^{1}H-NMR, ^{13}C-NMR, FT-IR and ESI-MS and elemental analyses. The geometry of complexes were confirmed octahedral by electronic spectra and thermogravimetric analyses data.

The complexes of first row d^5, d^7, d^8, d^9 and d^{10} ions with the Schiff base ligand obtained from *p*-nitroaniline and benzoyl trifluoroacetone (HL^1) / theonyltrifluoroacetone have been synthesised and characterized with various physico-chemical techniques (FT-IR and electronic, etc). The spectroscopic analyses showed the formation of the complexes and they assumed 4-coordinate square planar/ tetrahedral stereochemistry (Osowole *et al.,* 2013).

The compounds [Cu(L)(acacc)], $[(Cu(L)_2)_2]$, [Zn(L)(acacc)] and $[(Zn(L)_2)_2]$, where L is the Schiff base condensed from 2-hydroxy-1-naphthaldehyde and 7-amino-4-methylcoumarin were synthesised and characterized by numerous spectral methods such as microanalysis, UV–Vis, FT-IR, and NMR. The single crystal X-ray structures indicated 5-coordinate geometry for the latter, while the former exhibited square planar geometry (Elham, 2010).

The synthesised bivalent cobalt, copper, nickel and zinc complexes of 2-hydroxy-2-ethyl-(3-carboxylideneamino)-3-(2-(4-methyl-phenyl))-1,2-dihydroquinazolin-4(3H)-one (HECMDQ) have been characterized through several physico-chemical (analytical, infrared, nuclear magnetic resonance, Electron Paramagnetic Resonance, mass spectrometry and Thermo-gravimetric Analysis) processes. Infrared spectral analyses revealed that the ligand coordinated using the deprotonated *–O---H* function, azomethine nitrogen as well as carbonyl oxygen. However, four coordinate geometries were apportioned to all the metallic compounds on the basis of spectral data (Rekha *et al.,* 2010).

Novel Mn(II), Fe(II), Co(II), Ni(II), Cu(II), Cd(II), Hg(II) and Zn(II) complexes of 2-hydroxy-N^1-((Z)-3-(hydroxyimino)-4-oxopentan-2-ylidene)benzohydrazide were prepared and characterized by elemental and thermal analyses (DTA and TGA); IR, UV-VIS, 1H-NMR, ESR spectroscopy; and mass spectrometry; magnetic susceptibilities and conductivities measurements. All the available data showed that the complexes assumed distorted six coordinate geometry (Abdou *et al.,* 2015).

2.1.4 Conductance measurements of Schiff base metal complexes

Electrolytic conductivity is the extent to which a solution has the capacity to transmit an electric current. Solutions of electrolytes conduct electric current by the movement of charged-ions under the influence of a gradient. The ions move at the rate dependent on their charge and most metals display good electricity and heat conduction. Conductivity measurement gives an idea of the degree to which a substance is dissociated in solution and consequently the number of species present in the solution. The conductivity of a sample is often expressed as molar conductivity and usually obtained by dividing the measured conductivity by the concentration of added electrolyte. So the electrical conductivity of a particular sample is dependent on several factors including temperature, concentration, etc. A good electrical conductivity of a metal results from orbitals partly filled with electrons as well as very close-spaced energy levels within the subshells. Schiff base metal complexes have been studied with molar conductivity measurements.

The molar conductivity of the complex [CoL], (where L=N,N'-bis(4-benzeneazoscliylidene) -*o*-phenylenediimindo derived from *o*-phenylenediamine and

4-(benzeneazo) salicylaldehyde) in 10^{-3} DMSO at 293K was 4.6 $Ohm^{-1}cm^2mol^{-1}$. A molar conductivity in the range 0-45 $Ohm^{-1}cm^2mol^{-1}$ is accepted for ion free compounds. Thus, the Co(II) complex was non-electrolyte (Aliyu, 2013). Similarly, ML_2Cl_2 type of Schiff base complexes (where M=Mn, Co, Ni, Cu and Cd; L=2-[(4-methylphenylimino) methyl]-6-methoxyphenol) have been studied for conductance in methanol (1.0 x $10^{-3}mol.L^{-1}$). The reported values were in the range 11-18 $Ohm^{-1}cm^2.mol^{-1}$ indicative of electrolyte-free state for the metallic compounds (Yu-Ye *et al.,* 2009).

The conductance measurement of the complexes $[M(L)_2(L^I)(L^{II})].X$,(where M= Mn, Fe, Co, Ni, Cu and Cd; L=sclicylidene-4-chorophenyl-2-aminothiazole;$L^i=H_2O$;L^{ii}=Cl) in DMF showed the complexes were non-ionic with molar conductivity value in the range 7.12-10.20 $ohm^{-1}cm^2mol^{-1}$(Abdel-Nasser et al.,2013). Similarly, the molar conductance of the complexes $[M(L)_2X]$, where M=Co, Ni and Cu(II), X = Cl, L = (Z)-1-(1-(1H-indol-3-yl)ethylideneamino)quinolin-2(1H)-one or (E)-1-(2-hydroxybenylidene amino)quinolin-2(IH)-one formed from coumarin and N-aminoquinoline-2-one/hydrazine hydrate in DMF were within 11.00-19.11$ohm^{-1}cm^2mol^{-1}$ as non-electrolytes (Redha *et al.,* 2010)

The conductance measurement of d^5-manganese, d^6-iron, d^7-cobalt and d^8-nickel complexes of a Schiff base derived from pyridine-3-carboxaldehyde and *o*-phenylenediamine in DMF have been studied. The values obtained were in the range 7-17 $Ohm^{-1}cm^2mol^{-1}$ indicative of non-electrolytes for the octahedral complexes, while the square planar complexes exhibited molar conductivity values in the range 110-115 $ohm^{-1}mol^{-1}cm^2$ consistent with 1:2 electrolytes (Kumar and Arabinda, 1994). Similarly, the molar conductance of mixed ligand complexes of the kind $[M(L^I)_2(L^{II})/L^{III})]X$, (where L^I = benzyidenethiourea obtained from benzaldehyde and thiourea, L^{II} = acetamide or thioacetamide, M=Cu(II), ZnII); X=Cl) in DMSO were in the range 105-119 $\Omega M/scm^2Mol^{-1}$ indicative of their electrolytic nature (Omar, 2012)

In addition, bivalent metallic compounds of the Schiff base (HL) obtained from 2-sulphanilamido pyimidine and 2-hydroxy-3-methoxybenzaldelyde with the formula $[ML_{2\text{-}2}H(X)_2]$, (where M=Mn (d^5), Co(d^7) Ni(d^8), Cu(d^9), and Zn(d^{10}); $L_{2\text{-}2}H$ = Schiff base; X=H_2O have been studied. The electrical conductance in 10^{-3} DMF was in the

range 2.9-16.7 $Ohm^{-1}mol^{-1}cm^2$ due to non-electrolytic nature of all complexes (Valarmathy and Subbalakshmi, 2014).

Schiff base ligands of the type 3-((2-hydroxybenzylidene)amin-3-*p*-tolylpropanioc acid formed from 2-hydrobenzaldehyde and 3-amino-3-*p*-tolylpropanoic acid with its divalent cobalt, copper, nickel and zinc complexes have been reported. The molar conductivity of the complexes obtained in DMF were between 90-120 $Ohm^{-1}mol^{-1}cm^2$. Molar conductivity values higher than 70 $Ohm^{-1}mol^{-1}cm^2$ were usually reported ionic. Thus, the complexes were electrolytes (Crystal, 2015).

2.1.5 Magnetic properties of Schiff base metal complexes

The room temperature magnetic moment of pyridine-3-carboxaldehyle Mn(II), Fe(II), Co(II), and Ni(II) complexes with L^I (*o*-phenylenediamine) and L^{II} (*m*-phenylenediamine) have been reported. The Mn(II) complexes had subnormal moments within 2.70-2.74 B.M corroborative of π-type antiferro- and ferromagnetic interactions operating through the metal atoms in bimetallic structure and suggestive of octahedral geometry. Magnetic moment values of 5.21-5.24 B.M. obtained for the divalent iron complexes were suggestive of high spin octahedral geometry. The subnormal magnetic moments of 2.0 and 2.2 B.M. displayed by $[Co_2(L^I)_4(L^{III})_2]$ and $[Co_2(L^{II})_4(L^{III})_2]$,(where $L^{III}=NO_3$) were indicative of partial quenching of paramagnetism arising from Co-Co interaction. On the other hand, the acetate derivatives of the divalent cobalt complexes exhibited moments within 5.7-5.8 B.M. suggestive of high spin octahedral structure. The complexes $[Ni(L^I)_2]X$ and $[Ni(L^{II})_2]X$, (where X=Cl) were diamagnetic, while $[Ni(L^I)_2.2H_2O]Y$ and $[Ni(L^I)(Z)]$, where $Y=SO_4$; $Z=CH_3CO_2)_2$) exhibited moment values within 3.10-3.43 B.M; which corroborates high-spin six coordinate divalent nickel complexes. Consequently, $[Ni_2(L^I)_4(L^{II})_2]$ complexes had subnormal moment of 2.08-2.12 B.M. attributable to partial quenching of paramagnetic between the Ni-atoms (Kumar and Arabinda, 1994).

Divalent Mn, Ni, Cu and Zn complexes of the Schiff base obtained by the combination of o-phenylenediamine and acetoactanilide have been studied and documented. The copper, nickel and zinc complexes exhibited magnetic susceptibility values of 1.72, 0.0 and 0.0 B.M. which were consistent with square planar geometry. Mn(II) and VO(II)

complexes showed octahedral and square pyramidral geometries with 5.62 and 1.71 B.M. values around the metal ions (Raman *et al.,* 2001).

The cobalt(II) complex of N-methylsalicylaldimine had moment value of 4.62 B.M. and represented the first example of five–coordinate high spin complex whose structure has been established by X-ray analysis. The obtained magnetic susceptibility value for its Cu(II) derivative was 1.79 B.M. which was almost a spin only value. However, Cu(II) tridentate Schiff base complex ion had magnetic moment value of 1.30 B.M. per copper ion at 303 K which decreased to 1.0 B.M. at 77K due to ferromagnetism operating between the two metal centres (Sobola, 2005).

The magnetic evaluation of the 3*d* metallic complexes of 1, 4(2'-hydroxyphenyl-1-yl) di-imino azine {1,4(2'HPDA)} have been described. The Mn(II) complex exhibited a 5.25 BM magnetic moment value, which was within the range expected for sextet ground term manganese(II) ion. The Fe(III) complex had observed magnetic value of 5.67 B.M characteristic of a d^5 system. The paramagnetic d^7-cobalt complex displayed a moment value of 4.65 BM and corroborates high spin d^7 system. A 3.23 BM magnetic moment value was obtained for the divalent nickel complex and indicated high spin Ni(II) ion. The experimental magnetic moment value for copper (d^9) complex was 1.86 BM. This value agreed to spin only value (Revanasiddappa *et al.,* 2008).

In the reported studies on the magnetic moments of Schiff base complexes of Mn(II), Co(II), Ni(II) and Cu(II) derived from 2-amino-4,6-dimethylpyrimidine and phenylbutane 1,3-dione, it was shown that Mn(II), Co(II), Ni(II) and Cu(II) complexes had normal moments of 5.92, 4.62, 3.40 and 1.20 B.M. respectively. However their adducts had magnetic moments in the range 6.15-6.20, 5.10–5.50, 3.50–3.60 and 2.30–2.40 B.M. respectively, indicative of some ferromagnetism functioning through a dimeric structure (Osowole *et al.,* 2009).

The magnetic moment of the mixed binuclear complexes $[M(L^I)(L^{II})(X)_2]$ (where M = Co, Ni, Cu and Zn); L^I = N-(2-hydroxy-1-naphthylidene)-4-chloroaniline, L^{II} = N-(2-hydroxybenzylidene)-2,3-dimethylaniline; X=H_2O) at 27^oC have been reported. Moment values of 5.10, 3.20, 1.81, and 0.0 B.M were observed for the Co(d^7), Ni(d^8),

Cu(d^9) and Zn(d^{10}) complexes. Moment values of 4.7-5.2, 2.8-3.2 and 1.9-2.2 B.M were described for high spin six coordinate Co(d^7), Ni(d^8) and Cu(d^9) complexes. Thus, the complexes assumed six coordinate geometries with high spin configurations except the Zn(d^{10}) complexes that was low spin and consequently diamagnetic (Atmaram and Kirian,2011).

In the study of Co(d^7), Ni(d^8),Cu(d^9) and Zn(d^{10}) complexes of 5-bromo-3-(((8-hydroxy-2-methylquinolin-7-yl)methylene)hydrazono)indolin-2-one Schiff base ligand, the Co(II) Ni(d^8) and Cu(d^9) complexes exhibited magnetic values of 4.88, 3.00 and 1.94 B.M. which were within the expected ranges of 4.46–5.53, 2.7–3.3 and 1.75–2.20 B.M. consistent of mononuclear Co(d^7), Ni(d^8) and Cu(d^9) complexes (Kuruba and Nabiya, 2014).

The synthesised divalent Co(d^7), Ni(d^8), Mn(d^7) and Cu(d^9) complexes of the mixed Schiff base ligands obtained from 5-chloro-2-hydroxyacethophenone with 1-amino-5-benzoyl-4-phenyl-1H-pyrimidine-2-one/thione have been reported. The magnetic moment of the mixed ligand mononuclear Cu(II) complex was 1.72 (1.80) B.M. corresponding to spin-only value of 1.77 B.M. for S=0.5, observed for bivalent copper complexes. The d^7-cobalt complex had a magnetic moment of 3.69 B.M. corroborative of octahedral geometry. Similarly, the d^5-manganese complex displayed a magnetic moment of 5.44 B.M. predictable for high spin distorted six coordinate stereochemistry. However, a magnetic moment of 0.52 B.M. was obtained for the d^8-nickel complex suggestive of square planar geometry (Hatice *et al.,* 2015).

In the study of some 3*d*-series transition elements of 3-(2-(2-hydroxy-3-methoxybenzylidene)hydrazine) indoline-2-one Schiff base ligand, the Co^{2+}, Ni^{2+} and Cu^{2+} complexes were paramagnetic and expectedly the Zn^{2+} complex was diamagnetic (Zahid *et al.,* 2015).

2.1.6 ^{1}H and ^{13}C-nmr studies of Schiff bases and their metal complexes

Spectroscopy is the study of quantized interaction of energy characteristically electromagnetic energy with matter. However, the study of matter is better achieved with molecular type of spectroscopy i.e. spectroscopy of atoms that are bound together in molecules. Hence, nuclear magnetic resonance (NMR) is an important spectroscopic

technique employed to study the behaviour of magnetically distinct type of atoms in a molecule. NMR studies various nuclei, $^{1}_{1}H$, $^{1}_{2}H$, $^{13}_{6}C$, $^{14}_{7}N$, $^{17}_{8}O$, $^{19}_{9}F$, $^{31}_{15}P$ and $^{35}_{17}Cl$ but hydrogen and carbon are commonly studied since they mostly exhibit the atomic nuclei property called 'spin', i.e. the ability of the nucleus of atom to spin when it absorbs electromagnetic emission in the presence of an applied magnetic field. Atomic nuclei with either un-even mass, un-even atomic number or both possessing quantized 'spin angular momentum as well as a magnetic moment' (Pavia *et al.,* 2001). NMR spectroscopies have been applied in the study of atomic nuclei in Schiff bases.

The NMR studies of the Schiff base ligand synthesised from 4-aminoantipyrine, 3-hydroxy-4-nitrobenzaldehyde and *o*-phenylenediamine with its metal(II) complexes in $CDCl_3$ were reported. The spectrum of the ligand displayed peaks at 2.5(*s*, 3H), 3.3(*s*, 3H), 7.2-7.8(*m*, 8H), 9.7(*s*, H) and 13.3(*s*, H) attributed to protons of =C-CH_3, N-CH_3, phenyl ring, -CH=N (imine moiety) and phenolic OH group. The observation of a phenolic OH peak in the spectrum of the divalent zinc complexes indicated non-participation of the OH proton in chelation-(Raman *et al.,* 2007).

The ^{1}H and $^{13}CNMR$ spectral data of the ligands 1-{3-[(3-hydroxypropylimino)methyl]-4-hydroxyphenylazo}-4-nitrobenzene,1-{3-[(3-hydroxypropylimino)methyl]-4-hdroxy phenylazo}-2-chloro-4-nitrobenzene and 1-{3-[(-3-hydroxypropylimino)methyl]-4-hydroxyphenyl azo}-4-chloro-3-nitrobenzene were studied. The HNMR spectra of the ligands exhibited singlet peaks at 14-13.21 ppm and 4.7-4.79 ppm ranges assigned to phenolic and alcoholic proton respectively. The singlet and multiplet peaks due to azomethine group and aliphatic protons were observed at 8.2-8.76 and 3.7-1.83 ppm ranges in all the ligands. The $^{13}CNMR$ spectra of the ligands displayed signals at the ranges 32.8-58.2 and 115.3-166.79 ppm consistent of noncyclic and cyclic carbon atoms. The signal around 176-178 ppm in the ligands' spectra were attributed to C=N carbon (Raziyeh and Saeid, 2012).

The $^{1}HNMR$ studies of the ligand N,N'-1,4-phenylenebis(2,4-dihdroxylacetophenonylidene imine (derived from 2,4-dihydroxyacetophenone and p-phenylenediamine) and its Mn(II), Co(II), Ni(II) Cu(II) and Zn(II) complexes in DMSO-d_6 at 400 MHz displayed a peak (*s*, H) at δ = 126 ppm in the spectrum of the ligand typical of phenolic OH, with no corresponding peak(s) in the spectra of the

complexes. This corroborated removal of H-atom and coordination through the phenolic oxygen to the metallic ions. The multiplet peaks of the cyclic compound were reported within 6.3-7.5 ppm in both spectra of the ligand and the metal complexes (Shubhangi, 2013)

Schiff base ligands of the type 2-((2,4-dimethylphenylimino)methyl-6-methoxy-4-nitrophenol and 2-((3,4-difluorophenylimino)methyl)-6-methoxyl-4-nitrobenzaldehyde (condensed from 2-hydroxy-3-methoxy-5-nitrobenzaldehyde and 2,4-dimethylaniline or 3,4-difluoroaniline) have been studied in $CDCl_3$. The ^{1}HNMR spectra of the Schiff base ligands showed lone signals at the ranges δ2.37-2.44 ppm and δ4.01-4.03 ppm attributable to methyl and methoxyl protons respectively. Overlapping multiplet signals were observed at the ranges 7.12-8.08 ppm consistent with aryl protons of the benzene ring. The –CH=N- and OH protons' signals appeared as singlets at 8.65 ppm and 14.43-15.98 ppm range (Joshi *et al.,* 2014)

The preparation and analytical investigation of d^5-manganese, d^7-cobalt, d^8-nickel, d^9-copper and d^{10}-zinc complexes of the Schiff base prepared from 2-sulphanilamidopyrimidine and 2-hydroxy-3-methoxy benzaldehyde have been reported. The studied HNMR spectra in DMSO-d_6 revealed a peak at δ = 8.5 ppm assigned to azomethine proton of the ligand but shifted downfield in the M(II) complexes. This confirmed chelation of the "-CH=N" N-atom to the metal ions. The aromatic peaks appeared around 6.8-8.1 ppm in the spectrum of the ligand and around 6.5-8.5 ppm in the spectra of the metallic complexes. The phenolic OH proton signal observed at δ = 12.2 ppm in the ligand's spectrum disappeared in the spectra of the metallic compounds corroborating removal of hydrogen atom from the phenolic OH on complexation to the metallic ions. The ^{13}CNMR spectra displayed signals at δ = 160, 119.1 and 157.9 ppm credited to the carbon atoms of the imine moiety aromatic C-OH and pyrimidine CH of the ligand and peaks at 158.04 (-CH=N), 129.4 (aromatic C-OH) and 158.0 ppm (pyrimidine-CH) for the metal complexes (Valarmathy and Subbalakshmi, 2014).

The Schiff base resulting from 2-hydroxy-4-methoxy-phenyl)phenylmethanone and aniline with its divalent Mn, Co, Ni, Cu and Zn compounds have been reported. The NMR spectrum of the bidendate Schiff base ligand showed a singlet peak around 12.1

ppm, consistent with phenolic OH group. This peak was absent in the spectrum of the divalent zinc compound and indicated hydrogen atom removal from the phenolic *O*-atom on coordination. The spectra of the ligand and divalent zinc compound displayed peaks around 6.5-7.7 ppm (multiplets) and 3.8ppm (singlet) attributed to protons of the aromatic ring and methoxy moiety respectively. No peaks were observed around 4.69-4.82 ppm in the spectra of the compounds studied, which corroborated absence of coordinated water molecules (Subbaraj *et al .,* 2015).

Furthermore, studies on the HNMR spectra of the Schiff base ligand (formed from sulphaquinoxaline with naphthaldehyde) and its Zn(II) compound revealed a signal at 8.41(*s*, H) attributed to –N=CH proton of the ligands but shifted downfield (8.65, *s*, H) in the spectrum of the Zn(II) complexes. The latter corroborated complexation of the N-atom of the –N=CH group with the metallic ion. The peaks around 12.11-12.47 ppm observed in the free ligand spectrum were consistent with OH proton which was completely absent in the Zn(II) compound spectrum and supported bonding through hydroxy O-atom. The broad-singlet peak at 8.9-9.6 (*s*, H) ppm, which was assigned to N-H group in the spectra of both the ligand and Zn(II) complex indicated non-participation of N-H group in chelation (Tarek *et al.,* 2015).

2.1.7 Mass spectrometry

Mass spectrometry as an analytical tool, is one of the oldest instrumental techniques developed. It can provide both quantitative (molecular mass or concentration) and qualitative (structure) information about a molecule or compound after its conversion to ions. The mass spectrometry provides the researcher with vital information about the molecular mass/accurate mass of a compound which in turn aids in molecular formula determination. Mass spectrometry finds strong applications (Pavia *et al.,* 2001) in

1. Characterization of a compound (mostly new synthesized compounds)
2. Structural information involving functional groups and connectivity
3. Chemical and biological mechanistic studies especially in evaluation of isotope labeling experiments.
4. Identification of ion kinetics and mechanisms
5. Detailed analyses of complex compounds when inter-paced with other analytical techniques.

Mass spectrometry utilizes mass spectrometer, a device used to provide and measure the mass of ions which result into a spectrum. The modern mass spectrometer is made up of the inlet system, ion source, ion detector, mass analyser/ion separator and recorder/computer interface as components (Pavia *et al.,* 2001).

The basic functions often carried out by every mass spectrometer include the following

1. It vaporizes sample molecules
2. It bombards molecules with stream of high energy electrons to generate ions
3. It separates accelerated ions of the molecules under bombardment according to their mass-to-charge ratio in a magnetic or electric field, and
4. It detects ions with the same mass-to-charge ratio through its compartment which counts the number of ions striking it (Pavia *et al.,* 2001).
5. It records the ions in form of graphical chart.

2.1.8 Biological activities

2.1.8.1 Microbial activity

The improved biological actions of metallic compounds over Schiff base ligands can be clarified on the basis of the chelation theory (Osowole *et al.,* 2008). Chelation which refers to the formation of cyclic compound by complexation of a metallic ion with a poly-dentate ligand has the cyclic compound formed known as a chelate. The formation of complex leads to precipitation of the metallic or development of a stable and a soluble compound (Tripathi *et al.,* 2007). Chelation decreases the polarity of the metallic ion significantly, principally because of the unequal sharing of its positive charge with donor moieties and possible π-electron delocalization on the whole chelate ring. The cell walls with its membranes have the lipid and polysaccharides as their important constituents which are preferred for metallic ion interaction. However, the cell wall likewise contains amino phosphates, carbonyl and cysteinyl ligands, which stabilizes the integrity of the membrane by acting as a diffusion barrier and provides appropriate site for bonding. Research has also shown that chelation can lessen not only the polarity of the metallic ion, but rises the lipophilic quality of the chelate favouring the interaction amongst the metallic ion and the lipid (Singh *et al.,* 2001). This may lead to permeability obstruction of the cell, which results in the interference of functional cell processes. If the streochemistry and charge dissemination about the

molecule are mismatched with the streochemistry and charge dissemination about the pores of the bacteria cell wall, permeation through the wall by the poisonous agent may not occur and this will inhibit the poisonous reaction within the pores.

Consequently, chelation is not the only criteria for antimicrobial actions, but some other influences such as nature of the metallic-ion, nature of the ligand, chelating positions, hydrophilicity, lipophilicity and presence of co-ligands have substantial impact on antimicrobial actions. Certainly, steric and pharmacokinetic influences also play a pivotal part in determining the strength of an antimicrobial agent. The higher toxicity of the metallic complex can be credited to the influence of metallic ion on the normal cell process. The widespread of interface between metallic ions and cellular compounds may be due to the fact that all these structures contain a variety of functional moieties that can act as metallic binding agents. The problem has remained how to get such interfaces in cells as well as organisms where non-polar membrane exist to prevent the circulation of charged metallic ions into the cell, where myriad of the metallic binding positions exist as to compete for the metallic ion, and where specificity of cellular interface must take-place in order to obtain desired therapeutic value. The existence of lipophilic with polar substituents is estimated to boost antibacterial actions. Heterocyclic ligands with multi-functionality have a better chance of interface either with nucleoside bases (even after coordination with metallic ion) or with biologically indispensable metallic ions present in the biosystem. These compounds are promising candidates as bactericides since they always tend to interact especially with some enzymatic functional moieties, in order to attain greater complexation numbers. Thus the antimicrobial actions of metallic compounds cannot be credited only to chelation, nonetheless it is an intricate mixture of all the above influences (Raman *et al.,* 2008).

2.1.8.2 Antioxidant activity

The system of every living organism undergoes several metabolic processes which involve and utilizes oxygen. Oxygen is essential to the effective and normal function of all bodily activities. When oxygen containing species interacts with certain bodily molecules, oxidation occurs and reactive byproducts with unpaired electrons (electrons not attached to an atom) results. These reactive byproducts are called free radicals and once formed in the body, initiate chain reactions with potential damaging molecules

that impacts damage on important cellular components i.e. proteins, cell membrane, nucleic acid, etc. Presence of free radicals in the body system have been implicated in the following

1. Decline of the immune system
2. Decline in brain function
3. Deterioration of bones and connective joints
4. Wearing out of organs
5. Advance irritation of the visible effects of aging
6. Attack on healthy bodily cells
7. Oxidative damage to DNA, proteins and macromolecules, etc.

These free radicals are highly reactive oxygen containing species (ROS), reactive oxygen molecules (ROM) or reactive oxygen compounds (ROC) i.e. singlet oxygen, hydroxyl, hydrogen peroxide, hypochlorite, superoxide anion, nitric oxide, lipid peroxides, etc. The resultant activities of these molecules with membrane lipids, nucleic acids, proteins and enzymes brings about oxidative metabolism – an imbalance between bodily internal antioxidant mechanism and pro-oxidants.

Additionally, the activities of free radicals have been linked to pathogenesis of over fifty human-lives limiting chronic diseases i.e. diabetes, cancer, cell ageing, arteriosclerosis, liver injury, (Aruoma, 1998 and Apak *et al.,* 2008)

Research evidences (Mohana and Kumar, 2013) have shown that the effects/activities of ROS as well as reactive nitrogen species (RNS) can be controlled or eliminated with substances/molecules (whether natural or synthetic) which possess the potentials to interact, trap, reduce, prevent or neutralize the induced damage of free radicals. Substances which exhibit such activities aforementioned or even stop/terminate initiated chain reactions of ROS/RNS averting free radical damage on essential molecules in living organisms are generally termed antioxidants (Ames *et al.,* 1993). The best antioxidants are reported to be those bearing hydroxyl substituents which have proven key groups in enhancement of their host compounds antioxidant activities through hydrogen atom transfer mechanism (Lahsasni *et al.,* 2014 and Babasaheb *et al.,* 2010).

Demand for compounds with improved lipophilic antioxidant potentials that exhibits health protective factor roles has become imperative as such compounds act as

1. a route of resistance against the danger of evolving terminal aliments, hence paving way for healthier and better living of humans
2. insurance against obvious ageing visible effects
3. weapons in our contest to make our average life expectation to more carefully look like our ultimate lifecycle.

Subsequently, Schiff bases have been proven significant antioxidants and vital scavengers of free radicals, mostly those bearing OH, NH or SH groups as substituents (Anouar *et al.,* 2009 and Mohammed *et al.,* 2012). The Schiff bases scavenge free radicals of ROS through transfer of hydrogen atoms and adduct formation mechanisms (Leopoldini *et al.,* 2011). Similarly, metallic compounds of Schiff bases have received research attention owing to their potentials in binding reversibly oxygen redox systems in biological systems; oxidation of DNA and generally in protection of living organisms and cells from oxidative stress impairment caused by free radicals (Yang *et al.,* 2007; Berners, 2007; Ejidike and Ajibade, 2015).

2.1.8.3 Biological studies of Schiff bases and their metal complexes

The biological activities of metal ions in biological systems are today obvious and have become a subject of great interest amongst researchers. Research reports (Patel *et al.,* 2000; Chohan, 2001) have shown that biologically non-functional compounds become functional and less biologically functional becomes more functional upon coordination with metallic ions. The important role of metal ions in the enhancement of inactive and less active compounds' (ligands/organic compounds) activities in biological systems is certain but still a matter to be completely overhauled. However, the imine moiety (C=N) of Schiff base ligands has been an attractive feature that makes them essential compounds for biological activities especially when coordinated with metal ions. The interaction between metal ions and biologically active ligands helps in designing new metal-based active antibacterial, antifungal, anticancer, etc (Huang, 1998).

The antimicrobial activity of 2-aminomethylthiophenyl-4-bromosalicylaldehyde Schiff base and its metallic complexes using the disc diffusion technique has been reported. The experimental data indicated that the metallic complexes presented increased

inhibitory actions compared to the free ligand, and was clarified on the grounds of chelation theory. The results also revealed that the complexes were exceptionally sensitive against gram-positive organisms than the gram-negative counter-parts (El-Sherif and Eldebss, 2011).

The antimicrobial evaluation on divalent Co, Ni, Cu, and Zn complexes of the Schiff base formed from Isatin monohydrazone and 2-hydroxy-6-methoxybenzaldehyde; acetylacetone and various amino acids; and 4-amino-3-mercapto-6-methyl-5-oxo-1,2,4-triazine and 5-bromothiophene-2-carboxaldehyde against *B. subtilis, E. coli, S. aureus, S. flexeneri, P. aeruginosa, S. typhi, A. niger, A. flavus, T. viride, T. longifusus, C. albicans, C. glaberata, M. caris* and *F. solani* were reported. The data revealed that the metallic complexes were more microbial toxic in all cases than the free Schiff bases. The enhanced antimicrobial actions of the divalent metal complexes were attributed to chelation and nature of binding sites on the ligands (Zahid *et al.,* 2015; Kiran *et al.,* 2012 and Zahid *et al.,* 2006).

Furthermore, Nair *et al.,* (2012) documented the antibacterial activity ofCo(II), Ni(II), Cu(II) and Zn(II) complexes of a Schiff base incorporating indole-3-carboxaldehyde and m-aminobenzoic acid screened against several gram positive and gram negative bacteria by disc diffusion method. The antibacterial activity were recorded in order of the complexes and ligand as follows: Cu(II) > Co(II) > Ni(II) > Zn(II) > Ligand. The higher actions of the metallic complexes when compared to the ligands could be due to the influence of metallic ions on the functional cell membrane of the bacteria. Metallic chelates bear polar plus non-polar properties together; this makes them appropriate for penetration into the cells and tissues. Furthermore, chelation could heighten or subdue the biochemical potency of bioactive organic species.

Divalent cobalt, nickel and copper complexes of the Schiff base formed from *o*-hydroxybenzaldehyde and *m*-aminophenol have been screened in-vitro for their antimicrobial and toxicological activities against *S. aureus, B. megatrium, S. dysentery, Salmonella, Colletotrichum Sp; Aspergillus niulans, Botryodiplodia Sp; Bipolaris sorokiniana* and *Treponemap aledium.* The results revealed the complexes as microbial toxic agents than the free ligands. The complexes containing 2-aminopyridine and *o*-phenylenediamine as secondary ligands are much more microbial active than the other

complexes. The antibacterial result revealed that all the complexes had antibacterial effect with the exemption of divalent nickel complex which displayed less antibacterial actions against the screened organisms. Antifungal actions of the complexes revealed that all the complexes had significant activity toward *Treponemap aledium* except Cu(II) complex with the highest antifungal action (Saidul *et al.,* 2001)

The antimicrobial actions of the Schiff base ligands derived from 3-substituted-4-amino-5-mercapto-1,2,4-triazole and 8-formyl-7-hydroxy-4-methyl coumarin and its Zn(II) complexes against *E. coli, S. aureus, S. pyogenes, P. aeuginosa, S. typhi, A. flavus, cladosporium* and *A. niger* have been studied and reported. The bacteriological studies indicated that the ligands showed high actions towards *E. coli, S. typhi* and *S. pyogenes*and moderate activity towards *P. aeruginosa* and *S. aureus.* The complexes $Zn(C_{14}H_{10}N_4O_3S).2H_2O$ and $Zn(C_{16}H_{14}N_4O_3S).2H_2O$ exhibited extensive high activity towards *E. coli, S. aureus,* and *S. pyogenes* than the other complexes when likened to the standard. However, the antifungal data revealed that the Schiff base had reasonable activities against *A. flavus, A. niger* and high activity against *cladosporium sp*. The metal complexes $Zn(C_{14}H_{10}N_4O_3S).2H_2O$ and $Zn(C_{16}H_{14}N_4O_3S).2H_2O$ exhibited high antifungal actions against *A. niger, cladosporium* and *A. flavus* than the other complexes (Bagihalli *et al.,* 2009).

Ampicillin and ciprofloxacin, and nystatin were respectively used as standard drugs in the biological studies of synthesised Mn(II), Co(II), Ni(II) Cu(II) and Zn(II) complexes of Schiff bases types HL(E-4-(2-hydrox-3-methoxybenzalideneamino)-N-(pyrididin-2-yl) benzene sulfonamide; HL^1B(HL=o-vanillidene-2-aminobenzothiazole, B=1,10-phenanthroline) and HL^{11}(o-vanillidene-2-amino-N-(2pyridyl)-benzenesulfonamide). The synthesised compounds were screened against bacterial organisms (*Escherichia coli*, *Pseudomanas aeruginosa, Staphylococcus typhi,Staphylococcus aureus, Vibrio parhaemolyticus and K.aerogenes), fungi (Aspergillus niger, Mucor, Penicillium, Trichoderma and Virida)* and yeast. The results proved all metal complexes to exhibit remarkable biological activities compared to their parent ligands. The enhanced inhibitory actions of the complexes was attributed to delocalization of π-electrons over the chelate ring due to chelation and disturbance of the cells' respiration processes by the metal complexes, which in-turn blocks protein synthesis and restricts further

growth of the organisms (Neelakantan *et al.,* 2010; Valarmathy and Subbalakshmi, 2014).

Mixed ligand divalent complexes of the types $ML^{I}B$, ML^{II}_2 and M_2L^{III} (where M = Mn, Co, Ni, Cu and Zn; L^{I} = o-vanillidene-2-aminobenzothiazole (derived from o-vanillin and 2-aminobenzothiazole); B = 1,10-phenanthroline; L^{II}_2 = *o*-vanillidene-2-amino-N-(2-pyridylbenzene sulfonamide (derived from *o*-vanillino and 2-amino-N-(2-pyridyl)-benzene sulfonamide)) have been reported. The metal complexes exhibited higher biological activities against *Escherichia coli, Pseudomonas aeruginosa, Salmonella typhi, Vibrio parahaemolyticus, Aspergillus niger, Penicillium, Trichoderma viride and Saccharomyces cerevisiae* than the free Schiff base ligands. The increased activity of the complexes was attributed to chelation. Chelation decreases the polarity of the metallic ions owing to overlap of the ligand's orbitals and un-even sharing of the positive charges on the metallic ion with the donor groups of the ligand. It also enhances the delocalization of π-electrons over the whole complex ring structure (Neelakantan *et al.,* 2010)

Metal complexes of the Schiff base ligand prepared from 1,4-dicarbonyl-phenyl-dihydrazide and chromene-2,3-dione was screened against *Aspergillus sp* and *Rhizoctonia sp.* for inhibition potentials. The antifungal results obtained for the synthesised compounds were likened to the standard antifungal drug, Miconazole. The metallic compounds showed better antifungal actions against *Aspergillussp.* but they had somewhat lesser actions against *Rhizoctoniasp.* when likened to Miconazole. It was also detected that the actions of the metallic compounds depends mainly upon the type of metallic ion and varied in the following order Cr > Fe > Mn based on the experimental data (Kumar*,* 2012)

Several metal complexes have been reported to possess antitumor activities. The most extensively applied complex in cancer-treatment is *cis*-dichlorodiamine platinum. Many rhodium and iridium complexes and the analogues of platinum complexes i.e. $[(Pt(dmgly)_2Cl_2)]$, $[(Pt(Sar)_2Br_2)]$ and $[(Pt(dmgly)_2Br_2)]$ showed anticancer actions. Literature related to anti-cancer actions of metallic complexes has been summarized as:-

1. Metals employed in the syntheses of such complexes must fit into periodic group of VII, i.e. Pd, Pt, Ru and Rd.
2. Chelating agent(s) should be lipid-loving and must look like a nutrient to simplify its permeation into malignant cells through the cell membrane.
3. The metallic complexes must possess the cis configuration.
4. It ought to be adequately kinetically unchanging, so that it remains unaffected throughout circulation over the body fluids (Huhery *et al.,* 2009).

4-(3-coumarinyl)-3-benzyl-4-thiazolin-2-one benzylidenehydrazones were assessed for in-vitro antituberculous actions against mycobacterium tuberculosis H_37Rv with BACTEC 460 radiometric system using Rifampin as standard drug for the test. The results showed that only R_1=Br, R_2=2-OH and 5-NO_2 substituted compounds exhibited at least 11% inhibition in the primary screening at 6.25µg/ml (Aysel and Nilgun, 2003).

The anticancer evaluation of $Cu(C_{18}H_{16}N_3O_2)_2 \cdot 2CH_3OH$, $Zn(C_{18}H_{16}N_3O_2)_2 \cdot 2CH_3CH_2OH$ and $Cd(C_{18}H_{16}N_3O_2)_2 \cdot 2CH_3OH$ complexes of the Schiff base $HL(C_{18}H_{16}N_3O_2)$ formed from 2-acetylpyridine and l-tryptophan were studied. The compounds prepared were screened against MDA-MB-231 breast tumour cells. The complexes inhibited the cellular proliferation, with the cadmium complex exhibiting the best activity proving its potency to impede proteasomal chymotrypsin like action and likewise may induce apoptosis on human breast tumour MDA-MB-231 cells (Zhang *et al.,* 2012).

Alam and Lee, (2012) synthesised and reported anti-inflammatory actions of a Schiff base obtained from 4-aminoantipyrine (4-amino-1,5-dimethyl-2-phenylpyrazole-3-one) and benzaldehyde. The results indicated enhanced anti-inflammatory activity confirming their potential use for the treatment of inflammatory related illness. Obtained results for this study raised promising lead for the development of better therapeutic agents, combating ailments triggered by inflammation and oxidative stress

Li and Liu, (2011) reported the antioxidive properties of ferrocenyl Schiff base ligands *o*-(1-ferrocenylethylideneamino)phenol, *m*-(1-ferrocenylethylideneamino)phenol, and *p*-(1-ferrocenylethylideneamino)phenol appraised in 2,2′-azobis(2-amidinopropane

hydrochloride), Cu^{2+}/glutathione, and hydroxyl radical (OH^{-}) prompted oxidation of DNA, and in trapping 2,2′-diphenyl-1-picrylhydrazyl (DPPH) and 2,2′-azinobis (3-ethylbenzothia-zoline-6-sulfonate)cationic radical ($ABTS_{\bullet}^{+}$) correspondingly. The ligands exhibited comparable actions to trap DPPH and $ABTS_{\bullet}^{+}$. The ferrocenyl Schiff base ligands exhibited perooxidant activities in Cu^{2+}/GSH^{-} and $_{\bullet}OH^{-}$ induced oxidation of DNA excluding *o*-(1-ferrocenylethylideneamino)phenol which showed weak antioxidant action in $_{\bullet}OH^{-}$ induced oxidation of DNA. The enhanced antioxidant activity of the synthesised ligands compared to the benzene-related Schiff bases was greatly attributed to the introduction of ferrocenyl group to azomethine structure.

2.1.9 Other applications of Schiff base ligands and their related metal Complexes

In catalysis, metal complexes of aromatic Schiff bases have remained widely documented to catalyse reactions on hydrolysis, oxygenation and decomposition (Sreekala *et al.,* 1999; Chakraborty *et al.,* 1994; Xi *et al.,* 1987). Divalent cobalt Schiff base complexes have been used to calatyze the oxidation of styrene in the presence of excess oxygen and pyridine (Ali *et al.,* 2005) and also reported to find applications as catalyst in the oxygenation of alkenes on the basis of ketonisation mechanism (Nishinaga *et al.,* 1988). Consequently, Schiff base by-products have efficiently been applied in inhibition corrosion of mild steel, aluminium, copper, and zinc in acidic solution. The effective corrosion inhibitor ability of Schiff bases is credited to the electron cloud of the aromatic ring, electronegative heteroatoms and the presence of the azomethine moiety. Photochemical deprivation of natural rubber yield amine ended liquid natural rubber (ATNR) when carried out in solution, in the presence of ethylenediammine. ATNR on combination with glyoxal yield a poly Schiff base, which increases aging resistance while organocobalt compounds with tridentate Schiff base act as originator of emulsion polymerization and copolymerization of dienyl with vinyl monomers (Kumar *et al.,* 2009).

In the paint and dye industries, symmetrical and unsymmetrical chromium and cobalt Schiff base complexes impacted brilliant shades to leathers, cloths, food packages and wools (Mennicke and Westphal, 1986 and Befta, 1983). Heteroleptic divalent metallic compounds of various Schiff bases obtained from p-/o-toludine and o-hydroxy-4-

methoxybenzonapthone/2-amino-5-chlorobenzophenone have been reported as good pigments in paint production.

Similarly, cobalt complex of a Schiff base prepared from salicylaldehyde and diamine exhibited an outstanding package property, good storage potentials and high light resistance which does not degrade even in acidic medium (Kumar *et al.,* 2009).

CHAPTER THREE

MATERIALS AND METHODS

3.1 Reagents and solvents

Nickel(II) acetate tetrahydrate, cobalt(II) acetate tetrahydrate, copper(II) acetate hydrate, iron(II) sulphate heptahydrate, manganese(II) acetate tetrahydrate, Zinc(II) sulphate, zinc(II) acetate dehydrate, 2-hydroxy-1-naphthaldehyde, 2-hydroxy-1,4-naphthoquinone, 2,2'-bipyridine, 2-aminopyrimidine, 2-amino-4,6-dihydroxypyrimidine, 2-amino-4,6-dimethylpyrimidine, acetic acid, hydrochloric acid, triethylamine, methanol (methyl alcohol), ethanol, anhydrous calcium chloride, distilled water, dichloromethane, dimethylformamide, nitromethane, dimethylsulphoxide, ethylenediamine tetraacetic acid (EDTA), nitric acid, perchloric acid, concentrated ammonia, ammonium chloride, solochrome T-black and murexide.

The above reagents and solvents were obtained from Aldrich and British Drug Houses (BDH) Ltd. The organic solvents were purified using standard methods.

3.2 Syntheses of the ligands

3.2.1.1 Synthesis of 3-{[-(pyrimidin-2-yl)imino]methyl} napthalen-2-ol (HL^1)

2-hydroxy-1-naphthaldehyde (2.0 g, 0.000012 mmols) dissolved in methyl alcohol (10 mL) was refluxed with a methyl alcoholic solution (20 mL) of 2-aminopyrimidine (1.11 g, 0.000012mmols) in the presence of glacial acetic acid (6 drops). A yellow-shade mixture was obtained. The reflux for the reaction mixture was maintained for 6 hr at 60 ^{o}C on a magnetic stirrer hot plate. The solid products formed (bright yellow) on cooling in ice to a temperature of 27 ^{o}C, were suction filtered, washed with methyl alcohol and dried over silica gel in a desiccator. The analytical data are presented in Tables 4.1.1 and 4.1.2

3.2.1.2 Synthesis of 3-{[(4,6-dihydroxypyrimidin-2-yl)imino]methyl}napthalen-2-ol (HL^2)

To a methyl alcoholic solution (20 mL) of 2-hydroxy-1-naphthaaldehyde (2.0 g, 0.000012 mmols), a pre-dissolved 2-amino-4,6-dihydroxylpyrimidine (1.47 g, 0.000012 mmols) in sodium carbonate (Na_2CO_3) (40 mL) solution was added neatly in bits. The reaction mixture was then refluxed on a magnetic stirrer for six (6) hours with minimum heat (40^{o}C). The brown shade products obtained were then filtered under pressure, washed with methyl alcohol and dried over silica gel in a vacuum-desiccator. The analytical data are contained in Tables 4.1.3 and 4.1.4

3.2.1.3 Synthesis of 3-{[(4,6-dimethylpyrimidin-2-yl)imino]methyl}napthalen-2-ol (HL^3)

2-hydroxy-1-naphthaldehyde (3.0 g, 0.000012 mmols) in a 10 mL warm-dry methyl alcoholic solution was mixed with 20 mL methyl alcoholic solution of 2-amino-4,6-dimethypyrimidine (2.146 g, 0.000012 mmols). The mixture was catalysed with six drops of glacial acid and refluxed for six (6) hours on a magnetic stirrer hot plate. The resulting yellow precipitates formed on cooling to 29 ^{o}C temperature in ice were suction filtered, recrystallized from methyl alcohol and dried in desiccator over silica gel. The analytical data are presented in Table 4.1.5

3.2.1.4 Synthesis of 2-(pyrimidin-2-ylamino)naphthalene-1,4-dione (HL^4)

2-amino pyrimidine (2.297 g, 0.000028mmols) was drop wisely added to a methyl alcoholic solution (30 mL) having 2-hydroxy-1-napthoquinone (5.0 g, 0.000028mmols). The resulting reaction mixture was refluxed with stirring for six (6) hours on a magnetic stirrer hot plate. The orange product, obtained on cooling to 30 ^oC temperature, was filtered under pressure and repurified from methyl alcohol and dried *in vacuo* in a vacuum desiccator over silica gel. The analytical data are contained in Tables 4.1.6 and 4.1.7

3.2.1.5 Synthesis of 2-(4,6-dihydroxypyrimidin-2-ylamino)naphthalene-1,4-dione (HL^5)

To a methyl alcoholic solution (20 mL) of 2-hydroxy-1,4-naphthoquinone (5.0 g, 0.000028 mmols), 2-amino-4,6-dihydroxylpyrimidine (3.648 g, 0.000028mmols) pre-dissolved in aqueous sodium carbonate (Na_2CO_3) was added. The reaction mixture was then refluxed on a magnetic stirrer for six (6) hours. The orange coloured solid products obtained on cooling in ice were collected over by filtration under suction. The products were cleansed with dry methyl alcohol and dried in *vacuo* over silica gel in a desiccator. The analytical data are contained in Tables 4.1.8 and 4.1.9

3.2.1.6 Synthesis of 2-(4,6-dimethylpyrimidin-2-ylamino)naphthalene-1,4-dione (HL^6)

The ligand HL^6, was synthesised by drop wise addition of equimolar amounts of 2-hydroxy-1,4-naphthoquinone (3.0 g, 0.000017mmols) pre-dissolved 10 mL of dry methyl alcohol into a 20 mL methanolic solution of 2-amino-4,6-dimethypyrimidine (2.121 g, 0.000017mmols). The mixture was refluxed six (6) hours at 50 ^oC. A brown product obtained on cooling in ice, was filtered by suction, cleansed with methyl alcohol and dried over silica gel. The investigative data of the HL^6 ligand are described Table 4.1.10

3.3 Synthesis of metal(II) complexes

3.3.1.1 Synthesis of M(II) complexes (M(II) = Mn, Fe, Co, Ni, Cu and Zn) of HL^I

The Mn(II) complex was synthesised by the addition of $Mn(CH_3COO)_2.4H_2O$ (0.149 g, $6.1x10^{-5}$mmols) into a hot stirring methyl alcohol solution of the HL^1 ligand (0.3 g, $6.1x10^{-5}$mmols). The resulting coloured homogenous solution was buffered with 0.3 mL of triethyl amine and further refluxed for six (6) hours. The precipitates obtained

were filtered under pressure, cleansed with 20 mL of methyl alcohol and dried over water-free calcium chloride.

Bivalent copper, cobalt, nickel, iron and zinc complexes of HL^I were synthesised using similar method with metal salts of $Cu(CH_3COO)_2.H_2O$ (0.121 g, $6.1x10^{-5}$mmols), $Co(CH_3COO)_2.4H_2O$ (0.151 g, $6.1x10^{-5}$mmols), $Ni(CH_3COO)_2.4H_2O$ (0.151 g, $6.1x10^{-5}$mmols), $FeSO_4.7H_2O$(0.168 g, $6.1x10^{-5}$mmols)and $Zn(CH_3COO)_2.2H_2O$ (0.133g, $6.1x10^{-5}$mmols) respectively. Metal complexes of HL^2, HL^3, HL^4, HL^5 and HL^6 ligands were all synthesised employing the procedure above. All the metal(II) complexes synthesised had different shades of colour from their starting materials. However, the reactions of the metal(II) ions with ligands (HL^1–HL^6) were in the ratio 1:2.

3.3.2 Synthesis of M(II) mixed ligands complexes

The metal(II) mixed ligands (M = Mn, Fe, Co, Ni, Cu and Zn) complexes of 'HL^1-HL^6'were synthesised by mixing the equimolar quantities of the pyrimidinyl ligands (HL^1-HL^6), 2,2'-bipyridine and the metal salts in each case. A 10 mL methyl alcoholic solution of HL^1 ligand (0.4 g, $1.6x10^{-5}$mmols) was stirred for 5 mins, with a clear solution obtained, Mn(II) acetate salt [$Mn((CH_3COO)_2.4H_2O$,0.395 g, $1.6x10^{-5}$mmols)] was gradually added and stirred with slight heating (55^oC) to establish a homogeneous mixture. To the above mixture, a 5 mL methyl alcoholic solution of 2,2'-bipyridine was introduced in bits, buffered with few drops of triethylamine and the entire mixture was allowed to reflux for 6 h. The obtained precipitates were allowed to cool to a temperature of 29 ^oC, filtered under suction, washed with MeOH and dried over anhydrous calcium chloride.

Fe(II), Co(II), Ni(II), Cu(II), and Zn(II) mixed 'HL^1' ligand complexes and the metal(II) mixed 'HL^2 –HL^6' ligands' complexes were all synthesised using the same method from their $FeSO_4.7H_2O$ (0.447 g, $1.6x10^{-5}$mmols), $Co(CH_3COO)_2.H_2O$ (0.401 g, $1.6x10^{-5}$mmols), $Ni(CH_3COO)_2.4H_2O$ (0.400 g, $1.6x10^{-5}$mmols), $Cu(CH_3COO)_2.3H_2O$ (0.322 g, $1.6x10^{-5}$mmols) and $Zn(CH_3COO)_2.2H_2O$ (0.354 g, $1.6x10^{-5}$mmols) salts. The reactions of the metal(II) ions with the ligands (HL^1- HL^6 and 2,2'-bipyridine) were in the molar ratio of 1:1:1.

Table 3.1. Summary of stoichiometry for the preparation of metal(II) complexes

S/N	Molecular Formular	Metal Salt	Stiochiometry (M-L)	Organic Solvent	Colour	Yield (g)	Percentage (%) Yield
1	$[Mn(L^1)_2].H_2O$	Acetate	1:2	Methanol	Brown	0.15	51.4
2	$[Fe(L^1)_2(H_2O)_2]$	Sulphate	1:2	Methanol	Brown	0.17	50.0
3	$[Co(L^1)_2].2H_2O$	Acetate	1:2	Methanol	Red	0.15	37.5
4	$[Ni(L^1)_2].H_2O$	Acetate	1:2	Methanol	Green	0.15	45.6
5	$[Cu(L^1)_2]$	Acetate	1:2	Methanol	Brown	0.12	38.0
6	$[Zn(L^1)_2]$	Acetate	1:2	Methanol	Green	0.13	44.0
7	$[Mn(L^1)(Bipy)(OAc)]$	Acetate	1:1:1	Methanol	Orange	0.39	73.4
8	$[Fe(L^1)(Bipy)(SO_4)]$	Sulphate	1:1:1	Methanol	Brown	0.44	69.8
9	$[Co(L^1)(Bipy)(OAc)].H_2O$	Acetate	1:1:1	Methanol	Red	0.40	47.5
10	$[Ni(L^1)(Bipy)(OAc)].H_2O$	Acetate	1:1:1	Methanol	Brown	0.40	65.0

11	$[Cu(L^1)(Bipy)(OAc)]$	Acetate	1:1:1	Methanol	Green	0.32	73.2
12	$[Zn(L^1)(Bipy)(OAc)].2H_2O$	Acetate	1:1:1	Methanol	Coffee	0.35	79.1
13	$[Mn(L^2)_2].2H_2O$	Acetate	1:2	Methanol	Gray	0.13	86.7
14	$[Fe(L^2)_2].2H_2O$	Sulphate	1:2	Methanol	Brown		50.0
15	$[Co(L^2)_2].H_2O$	Acetate	1:2	Methanol	Brown	0.13	69.6
16	$[Ni(L^2)_2].H_2O$	Acetate	1:2	Methanol	Brown	0.13	64.2
17	$[Cu(L^2)_2]$	Acetate	1:2	Methanol	Brown	0.11	60.9
18	$[Zn(L^2)_2]$	Acetate	1:2	Methanol	Gray	0.11	64.2
19	$[Mn(L^2)(Bipy)(OAc)]H_2O$	Acetate	1:1:1	Methanol	Brown	0.35	86.1
20	$[Fe(L^2)(Bipy)(SO_4)].H_2O$	Sulphate	1:1:1	Methanol	Brown	0.40	62.9
21	$[Co(L^2)(Bipy)(OAc)]$	Acetate	1:1:1	Methanol	Brown	0.36	71.4
22	$[Ni(L^2)(Bipy)(OAc)].H_2O$	Acetate	1:1:1	Methanol	Brown	0.35	91.0
23	$[Cu(L^2)(Bipy)(OAc)].H_2O$	Acetate	1:1:1	Methanol	Brown	0.29	64.8
24	$[Zn(L^2)(Bipy)(OAc)]$	Acetate	1:1:1	Methanol	Gray	0.31	73.0
25	$[Mn(L^3)(Bipy)(OAc)]$	Acetate	1:1:1	Methanol	Brown	0.44	75.2
26	$[Fe(L^3)(Bipy)(SO_4)].H_2O$	Sulphate	1:1:1	Methanol	Brown	0.50	46.0
27	$[Co(L^3)(Bipy)(OAc)]$	Acetate	1:1:1	Methanol	Pink	0.45	55.9
28	$[Ni(L^3)(Bipy)(OAc)]$	Acetate	1:1:1	Methanol	Brown	0.45	46.7

Table 3.1. Summary of stoichiometry for the preparation of metal(II) complexes (Contd)

S/N	Molecular Formular	Metal Salt	Stiochiometry (M-L)	Organic Solvent	Colour	Yield (g)	Percentage (%) Yield
29	$[Cu(L^3)(Bipy)(OAc)]$	Acetate	1:1:1	Methanol	Brown	0.36	47.2
30	$[Zn(L^3)(Bipy)(OAc)].H_2O$	Acetate	1:1:1	Methanol	Yellow	0.39	51.3
31	$[Mn(L^4)_2].H_2O$	Acetate	1:2	Methanol	Brown	0.25	87.5
32	$[Fe(L^4)_2].2H_2O$	Sulphate	1:2	Methanol	Brown	0.28	96.4
33	$[Co(L^4)_2].H_2O$	Acetate	1:2	Methanol	Red	0.25	71.1
34	$[Ni(L^4)_2].H_2O$	Acetate	1:2	Methanol	Brown	0.25	48.4
35	$[Cu(L^4)_2]$	Acetate	1:2	Methanol	Red	0.19	79.6
36	$[Zn(L^4)_2].H_2O$	Acetate	1:2	Methanol	Red	0.21	63.9
37	$[Mn(L^4)(Bipy)(OAc)].H_2O$	Acetate	1:1:1	Methanol	Red	0.48	85.9

38	$[Fe(L^4)(Bipy)(SO_4)].H_2O$	Sulphate	1:1:1	Methanol	Brown	0.55	41.4
39	$[Co(L^4)(Bipy)(OAc)]$	Acetate	1:1:1	Methanol	Brown	0.49	93.8
40	$[Ni(L^4)(Bipy)(OAc)].H_2O$	Acetate	1:1:1	Methanol	Red	0.49	84.2
41	$[Cu(L^4)(Bipy)(OAc)].H_2O$	Acetate	1:1:1	Methanol	Brown	0.39	60.5
42	$[Zn(L^4)(Bipy)(OAc)]$	Acetate	1:1:1	Methanol	Red	0.44	82.6
43	$[Mn(L^5)_2].H_2O$	Acetate	1:2	Methanol	Brown	0.22	44.3
44	$[Fe(L^5)_2].2H_2O$	Sulphate	1:2	Methanol	Brown	0.25	54.9
45	$[Co(L^5)_2].2H_2O$	Acetate	1:2	Methanol	Orange	0.22	84.6
46	$[Ni(L^5)_2(H_2O)_2]$	Acetate	1:2	Methanol	Brown	0.22	45.0
47	$[Cu(L^5)_2]$	Acetate	1:2	Methanol	Red	0.18	32.2
48	$[Zn(L^5)_2].H_2O$	Acetate	1:2	Methanol	Red	0.19	38.2
49	$[Mn(L^5)(Bipy)(OAc)].H_2O$	Acetate	1:1:1	Methanol	Brown	0.43	73.4
50	$[Fe(L^5)(Bipy)(SO_4)]$	Sulphate	1:1:1	Methanol	Red	0.49	96.5
51	$[Co(L^5)(Bipy)(OAc)].2H_2O$	Acetate	1:1:1	Methanol	Brown	0.44	98.0
52	$[Ni(L^5)(Bipy)(OAc)].H_2O$	Acetate	1:1:1	Methanol	Red	0.44	99.8
53	$[Cu(L^5)(Bipy)(OAc)]$	Acetate	1:1:1	Methanol	Coffee	0.35	63.0
54	$[Zn(L^5)(Bipy)(OAc)].H_2O$	Acetate	1:1:1	Methanol	Pink	0.38	63.6
55	$[Mn(L^6)(Bipy)(OAc)]$	Acetate	1:1:1	Methanol	Black	0.44	80.0

Table 3.1. Summary of stoichiometry for the preparation of metal(II) complexes (Contd)

S/N	Molecular Formular	Metal Salt	Stiochiometry (M-L)	Organic Solvent	Colour	Yield (g)	Percentage (%) Yield
56	$[Fe(L^6)(Bipy)(SO_4)]$	Sulphate	1:1:1	Methanol	Brown	0.49	52.1
57	$[Co(L^6)(Bipy)(OAc)]$	Acetate	1:1:1	Methanol	Red	0.45	84.3
58	$[Ni(L^6)(Bipy)(OAc)]$	Acetate	1:1:1	Methanol	Red	0.45	76.9
59	$[Cu(L^6)(Bipy)(OAc)].H_2O$	Acetate	1:1:1	Methanol	Brown	0.35	73.3
60	$[Zn(L^6)(Bipy)(OAc)]$	Acetate	1:1:1	Methanol	Red	0.39	74.3

3.4 Physical Measurements

3.4.1 Melting point measurement

The melting point and decomposition temperatures of the synthesised ligands with their corresponding metal(II) complexes were determined using Electro-thermal Temp-Mel melting point apparatus. The results are shown in Tables 4.1.1 - 4.1.10

3.4.2 Solubility

The solubility tests of the synthesised compounds were evaluated in seven different solvents, namely; water, methyl alcohol, ethyl alcohol, dichloromethane, dimethylsulphuroxide, nitromethane and dimethylformamide. Results are described in Tables 4.2.1 - 4.2.10

3.4.3 Infrared spectra

The infrared spectra of the ligands and their metallic complexes were obtained on a PERKIN ELMER FT-IR SPECTRUM BX spectrophotometer by means of KBr disc in the range 4000–350 cm^{-1} at the Department of Chemistry, University of Ibadan, Ibadan, Nigeria. The pertinent band positions and their interpretations are highlighted in Tables 4.3.1 - 4.3.10.

3.4.4 Electronic spectra

The ultraviolet (UV) and visible (Vis) spectra of the ligands with their metallic compounds were determined using PERKIN ELMER LAMBDA 25 UV/VISIBLE spectrophotometer within the ranges 190–400 nm and 400–900 nm at the "Department of Chemistry, University of Ibadan" Ibadan. The UV-Vis spectral information of the synthesised compounds are contained in Tables 4.4.1- 4.4.10.

3.4.5 Microanalysis

The elemental (CHN) analysis were evaluated on an Elementar, Vario EL Cube setup at the Nelson Mandela Metropolitan University, South Africa. The results are presented in Tables 4.1.1- 4.1.10

3.4.6 Mass spectra studies

The Electrospray Ionization Mass Spectra (ESI-MS) of the Schiff base ligands were recorded on microTOF-Q II 10390 at North-West University, South Africa. The results are presented in Table 4.6

3.4.7 ^{1}HNMR and ^{13}CNMR spectra

The ^{1}H and ^{13}C nuclear magnetic resonance (NMR) spectra of the synthesised Schiff bases were recorded in DMSO-d_6 on 600 MHz Bruker Advance III NMR spectrometers using tetramethylsalane (TMS) as internal standard. The analysis was carried out at the Nelson Mandela Metropolitan University, South Africa. The obtained NMR spectra are presented as results in Figures 4.3.1-4.3.6 and Figures 4.4.1-4.4.6 and the derived data are contained in Tables 4.5.1–4.5.2

3.4.8 Conductance measurement

The molar conductivity measurements were obtained in dimethylsulphuroxide (DMSO) using the electrolytic conducting measuring set; HANNA HI 991300 conductivity meter of 1.0 cell constant. A $1x10^{-3}$ mol/dm^3 solution of the metal(II) complexes were prepared and allowed to equilibrate with the room temperature before measuring their respective conductivities. The results are shown in Tables 4.1.1–4.1.10

3.4.9 Magnetic moment measurement

Magnetic susceptibilities of the synthesised complexes were evaluated at the Inorganic Chemistry Laboratory, Department of Chemistry, University of Ibadan, on a Johnson Mathey magnetic balance at 27-32^oC temperature range, while diamagnetic corrections were evaluated using Pascal's constants. The magnetic susceptibility calculation with diamagnetic corrections for $[Fe(L^1)(H_2O)_2]$complexis shown in appendice 1 as an example while other results are presented in Tables 4.1.1-4.1.10

3.5 Metal analysis

3.5.1.1 Preparation of 0.01M EDTA

14.89 g of disodium salt of ethylenediamine tetraacetic acid was transferred into a one litre flask and 500 mL of distilled water was added, the suspension was shaken till it dissolved and made up to the expected mark with distilled water.

3.5.1.2 Preparation of 0.005M zinc (II) sulphate

0.14 g of $ZnSO_4.7H_2O$ slowly was put into a 100 mL standard flask using a short necked funnel and then made up to the mark with distilled water accompanied by shaking to ensure complete dissolution.

3.5.1.3 Preparation of NH_3/NH_4Cl buffer (pH=10)

35.6 g of NH_4Cl was gradually put into a 500 mL standard flask and washed down with 286 mL of concentrated ammonia. The mixture was shaken together and distilled water was used to make it up to the required mark.

3.5.1.4 Preparation of $HNO_3/HClO_4$ mixture (1:1)

This was prepared by mixing 100 mL of concentrated nitric acid (HNO_3) with 100mL of concentrated perchloric acid ($HClO_4$) in 200 mL brown bottle.

3.5.1.5 Standardization of 0.01 M EDTA

25 mL of standard zinc sulphate was pipetted into a conical flask and 3-5 drops of ammonia/ammonium chloride buffer was added. 3 drops of solchrome black T indicator was added to the zinc sulphate solution and titrated against the 0.01 M EDTA solution. The colour change was from purple to light blue as observed.

$$Zn^{2+} + EDTA^{4-} \rightarrow ZnEDTA^{2-}$$

The molarity of the standardized solution was obtained by the use of the relationship shown in appendice II.

3.5.1.6 Digestion of metal complexes

Between 0.010–0.020 g of each metal complex was weighed into a sample bottle, four (4) drops of 1:1 ratio mixture of $HNO_3/HClO_4$ were dropped into each sample bottle containing the weighed complex and the mixtures heated to near dryness. The near dry mixtures were allowed to cool to room temperature. Two drops of $HNO_3/HClO_4$ were added to the non-clear mixtures and reheated to obtain a clear mixture. The reheated mixtures which were allowed to cool down, had four(4) drops of distilled water introduced into each sample bottle containing the clear mixture and reheated to near dryness to ensure complete digestion. The digested complexes were allowed to cool, then transferred into a 100 mL standard flask and distilled water was used to make it up to the required mark, hence ready to be analyzed for the percentage metal composition.

3.5.1.7 Determination of percentage metal composition

The divalent manganese, cobalt, iron, copper, nickel and zinc complexes were analyzed for percentage metal composition using complexometric titration method with EDTA. With NH_4/NH_3Cl mixture used as a buffer, a purple end point with murexide indicator was obtained in all the metallic compounds with exemption of divalent zinc complex whose indicator was solochrome black T which exhibited a blue end point. The experimental data acquired were matched with that of the calculated percentages of the metals. The values obtained which are in good agreement are contained in Table 4.1.1-4.1.10. The equation for the reaction is given as:

$M^{2+} + EDTA^{4-} \rightarrow [M(EDTA)]^{2-}$

The calculation steps for the metal analysis of the metal complexesare shown in appendice III using NiL^1 complex as an example with a weighed weight of 0.012 g.

3.6 Biological studies

3.6.1 Antimicrobial studies

Identified laboratory strains of *Staphylococcus aureus, Pseudomonas aeruginosa, Escherichia coli, Bacillus cereus, Proteus mirabisis* and *Klebsillaoxytoca;* and *Aspergillus niger, Aspergillus flevus* and *R. Stolonifer* were used for microbial screening. The antimicrobial investigations were determined at the Department of Microbiology, School of Biological Sciences, North-West University, Private Bag X2046, Mmabacho-South Africa.

3.6.1.1 Preparation of agar plates/samples

Antimicrobial susceptibility tests were achieved by means of agar well diffusion procedure (Reddy *et al.,* 2007). The surface of Muller Hinton's agar in petri dish was homogeneously inoculated with 10^6 CFU/mL of 18-24 hr old standard test bacteria cultures. Using a sterilized cork borer, 9 mm wells were bored into the agar. Then 0.06 mL of the 10 mg/mL solution of a particular compound in dimethysulphoxide (DMSO) was introduced into the 9 mm well bored unto the agar. The plates were allowed to stand on the bench for 30 min. before incubation at 30^{o}C for 24 hr after which inhibitory zones were observed in mm as an extent of antimicrobial activity. The investigations were carried out in duplicates using ciprofloxacin as the reference drug.

3.6.1.2 Antifungal activity (in-vitro)

A disc technique was employed in vitroto determine the antifungal activities of the synthesised compounds. Unpeeled but washed-sliced potatoes (250 g), dextrose (25 g), and agar (25 g) in 1250 mL distilled water were used to prepare the 'potato dextrose agar (PDA) media' adopted for the antifungal screening. The antifungal screening (in vitro) was carried out against *Aspergillus niger, Aspergillus flevus* and *Rhizopus Stolonifer*. The pure cultures of *Aspergillus niger, Aspergillus flevus* and *R. Stolonifer* were uniformly inoculated on the surface of the PDA solution petri dish. 15 μg of the stock solutions of a paticular test sample (1 mg/mL) prepared by dissolving 10 mg of the synthesised compounds in 10 mL of dimethyl sulphoxide (DMSO) solvent was

poured into a 6 mm well bored on the PDA with a 6 mm sterile metallic cork borer. All the plates inoculated were incubated at 35^{o}C for 48 h after which inhibition zone growth in diameter (mm) was measured as antifungal activity with antibiogram zone scale. All antifungal activities were determined as mean of three replicates. The drug, fluconazole was used as standard

3.6.2 Antioxidant studies

Antioxidants are vital substances which prevent the free radical damage of reactive oxygen species (ROS) and other unstable molecules (generally called free radicals) in the cells of living organisms. Free radicals (hydroxy ion, superoxide anion and hydrogen peroxide) formed during bodily biochemical processes are very reactive and damaging to living cells causing various aliments cancer, heart disease, atherosclerosis and even aging (Indira, 2005 and Resat *et al.,* 2008). The antioxidant properties of the ligands, 2.2'- bipyridine and their metal (II) complexes were evaluated using both DPPH radical scavenging and the ferrous chelating ability methods.

3.6.2.1 Ferrous ion-chelating ability

The chelating potentials of ferrous ion was evaluated by a colorimetric method. To a 2 mL of DMSO, 1 mL of $FeSO_4.7H_2O$ (400 μM in DMSO), 1 mL of 1,10-phenantroline (50 mg in 100 mL of DMSO) and 1 mL of each ligand test sample solution (1.0 mg/mL) were added to form the reaction mixture used. After about 15 min of incubation at 301 K temperature, absorbance of the mixture was obtained spectrophotometrically at 546 nm. Ascorbic acid was used as standard, while the blank contained the reaction mixture with the exception of the test sample solution. Triplicate measurements were obtained for all test samples. The activity of the test samples were likened to that of ascorbic acid, a standard antioxidant. The percentage scavenging inhibition of ferrous ion-chelating ability was calculated as:

% scavenging inhibition= $(Ac–As)/Ac \times 100$

i.e. *Ac* is the absorbance of blank; As is the absorbance of test sample solution or absorbance of ascorbic acid respectively. The results are presented in Table4.9

3.6.2.2 DPPH radical scavenging studies

The *in-vitro* free radical scavenging actions of the ligands with their corresponding metal (II) complexes were evaluated by DPPH assay technique. A blank containing 2.9 mL of DMSO was prepared and the initial absorbance was determined. Each synthesised test sample/compound or the standard (ascorbic acid) (0.1mL) diluted to different concentrations (50, 100, 200 µg/mL) in DMSO were mixed with 2.9 mL of DPPH (0.025µg/mL) solution in DMSO. The entire reaction mixture was vigorously shaken and allowed to equilibrate in the dark for 30 mins at 300 K temperature. The absorbance of the mixture was recorded at 515 nm against the blank. The experimentation was carried out in triplicate. The percentage reduction in absorbance was calculated from the initial and final absorbance of each mixture. Consequently, percentage scavenging ability of DPPH radical was evaluated using the expression

$$\% \text{ DPPH scavenging effect } (\%) = \frac{(Ac - As)}{Ac} \times 100$$

Where *Ac* = Absorbance of blank and *As* = Absorbance of test sample/compound or the standard antioxidant (ascorbic acid). The results are presented in Table 4.8

CHAPTER FOUR

RESULTS

4.1 Physical and analytical data

The physical and analytical data:- melting point, molar conductance, elemental, colour, formula weight (g/mol) and percentage yield (%) of the synthesised ligands, their corresponding Mn(II), Fe(II), Co(II), Ni(II), Cu(II) and Zn(II) complexes and heteroleptic metal(II) complexes are presented in Tables 4.1.1-4.1.10. The summary

of the methods, solvents and stoichiometryof reactants used for the synthesis of the complexes are given in Table 3.1

4.2 Solubility data

The solubility tests of the ligands, metal(II) complexes and the heteroleptic complexes in both polar and non-polar organic solvents have been summarized and presented in Tables 4.2.1-4.2.10

4.3 Infrared (IR) spectra data

The infrared spectral data of the ligands (HL^1-HL^6) and their metal(II) complexes (symmetrical and non-symmetrical) are shown in Figures 4.1.1-4.1.16. The vibrational frequencies observed and the tentative assignments of relevant bands in the different spectra are given in Tables 4.3.1-4.3.10

4.4 Electronic spectra data

The solid reflectance UV-Vis spectra of the ligands, the corresponding Mn(II), Fe(II), Co(II), Ni(II), Cu(II) and Zn(II) complexes and their heteroleptic metal(II) analogues are shown in Figures 4.2.1-4.2.2. The electronic absorption spectra data; and their assignments and the proposed geometries are listed in Tables 4.4.1-4.4.10.

4.5 ^{1}Hnmr and ^{13}cnmr spectra data

The NMR (^{1}H- and ^{13}C-) spectra of the ligands (HL^1-HL^6) obtained in DMSO-*d*6 on a Bruker Avance III 300 MHz spectrophotometer with reference to tetramethylsilane (TMS) as internal standard are given in Figures 4.3.1-4.3.6 and 4.4.1-4.4.6 respectively.The chemical shifts were documented in parts per million (ppm) downfield after the standard (TMS) and presented in Tables 4.5.1 and 4.5.2.

4.6 Electrospray ionization mass spectra (ESI-MS) data

The electrospray ionization mass spectra studies (ESI-MS) carried out to obtain the molecular weight and the fragmentation patterns of the ligands (HL^1-HL^6)are given as Figures 4.5.1-4.5.6. The m/e and m/z data are listed in Table 4.6.

4.7 Biological studies

4.7.1.1 Antibacterial activities

The antibacterial actions of the synthesised ligands (HL^1-HL^6) and their corresponding metal(II) complexes at 10 mg/mL against *Staphylococcus aureus, Pseudomonas aeruginosa, Escherichia coli, Bacillus cereus, Proteus mirabilis* and *Klebsillaoxytoca* to assess their potentials as antibacterial agents are summarized in Tables 4.8.1-4.8.10. Additionally, a comparison of the data generated was carried out and presented as Figures 4.7.1-4.7.10, while samples of the petri dishes used for the screening are shown in appendice IV.

4.7.1.2 Antifungal studies

The antifungal activities of HL^1, HL^2, HL^3 HL^4, HL^5 and HL^6 ligands, and their symmetrical and non-symmetrical divalent metal complexes against *A. niger, A. flevus and R. Stolonifer*in 10 mL DMSO have been obtained. Using the zone of growthinhibition diameter as criteria for measurement, the antifungal activities were determined and presented in Tables 4.9.1-4.9.10 and Figures 4.8.1-4.8.10.

4.7.2 Antioxidant studies

4.7.2.1 Ferrous ion-chelating ability

The antioxidant capacities of the synthesised ligands were evaluated using ferrous ion-chelating assay (FICA). Obtained FICA values were generally documented comparable to that of the standard antioxidant agent (ascorbic acid). The values are listed in Table 4.11.

4.7.2.2DPPH radical scavenging studies

The ligands and their divalent metallic compounds were investigated for free radical scavenging properties with DPPH radical at different concentrations (50, 100 and 200μg/mL) in 1 mL dimethylsulphuroxide. The values of the DPPH radical scavenging actions for the compounds on the basis of percent inhibition are contained in Tables 4.10.1-4.10.10.

TABLE 4.1.1. Analytical data for HL^1 ligand and its metal(II) complexes

Molecular Formula	Formula Weight (g/mol)	Colour	Melting Point (^oC)	Yeild (%)	μ_{eff} (B.M)	Molar Conductance ($Ohm^{-1}Mol^{-1}cm^2$)	Analytical/Found (Calculated) %			
							C	H	N	M
HL^1		Bright					72.40	4.61	17.03	-
$C_{15}H_{11}N_3O$	249.268	Yellow	110-112	58.50	-	-	(72.27)	(4.45)	(16.86)	-
$[Mn(L^1)_2].H_2O$							63.30	4.02	14.11	9.73
$[MnC_{30}H_{20}N_6O_2].H_2O$	569.496	Brown	308-310	51.43	4.39	16.09	(63.26)	(3.89)	(14.76)	(9.64)
$[Fe(L^1)_2(H_2O)_2]$							61.28	4.42	14.33	9.73
$[FeC_{30}H_{24}N_6O_4]$	588.412	Brown	252-254	50.00	5.25	5.69	(61.23)	4.11)	(14.29)	(9.49)
$[Co(L^1)_2].2H_2O$							60.99	4.18	14.26	10.03
$[CoC_{30}H_{24}N_6O_2].2H_2O$	591.482	Red	290-292	37.50	4.41	7.91	(60.91)	(4.09)	(14.21)	(9.96)
$[Ni(L^1)_2].H_2O$			(Dec)				63.07	3.92	14.84	10.26
$[NiC_{30}H_{20}N_6O_2].H_2O$	573.246	Green	250-252	45.60	3.49	5.25	(60.94)	(4.09)	(14.22)	(9.92)
$[Cu(L^1)_2]$							64.39	3.71	15.04	11.41
$[CuC_{30}H_{20}N_6O_2]$	560.06	Brown	234-236	38.00	1.88	5.01	(64.33)	(3.59)	(15.01)	(11.34)
$[Zn(L^1)_2]$							64.20	3.63	14.99	11.66
$[ZnC_{30}H_{20}N_6O_2]$	561.89	Green	288-290	44.00	0.29	11.13	(64.12)	(3.59)	(14.96)	(11.63)

Key: μ_{eff} = Effective Magnetic Moment Value; B.M = Bohr Magneton

Table 4.1.2. Analytical data for HL^1 ligand and its heteroleptic metal(II) complexes

Molecular Formula	Formula Weight (g/mol)	Colour	Melting Point (^oC)	Yeild (%)	μ_{eff} (B.M)	Molar Conductance ($Ohm^{-1}Mol^{-1}cm^2$)	Analytical/Found (Calculated) %				
							C	H	N	S	M
HL^1		Bright					72.40	4.61	17.03	-	-
$C_{15}H_{11}N_3O$	249.268	Yellow	110-112	58.50	-	-	(72.27)	(4.45)	(16.86)	-	-
Bipy, $[C_{10}H_8N_2]$	156.18	White	63-66	-	-	-	-	-	-	-	-
$[Mn(L^1)(Bipy)(OAc)]$							62.97	4.11	13.68	-	10.77
$[MnC_{27}H_{21}N_5O_3]$	518.37	Orange	238-240	73.40	5.80	15.03	(62.55)	(4.08)	(13.50)	-	(10.59)
$[Fe(L^1)(Bipy)(SO_4)]$							54.07	3.48	12.68	5.84	10.12
$[FeC_{25}H_{18}N_5O_5S]$	556.304	Brown	244-246	69.80	5.16	10.31	(53.95)	(3.26)	(12.59)	(5.75)	10.04)
$[Co(L^1)(Bipy)(OAc)].H_2O$							60.03	4.29	13.04	-	12.05
$[CoC_{27}H_{21}N_5O_3].H_2O$	540.41	Red	278-280	47.50	4.92	12.14	(60.00)	(4.26)	(12.96)	-	10.90)
$[Ni(L^1)(Bipy)(OAc)].H_2O$							60.08	4.32	13.01	-	10.88
$[NiC_{27}H_{24}N_5O_4].H_2O$	540.166	Brown	266-268	65.00	3.39	10.05	(60.03)	(4.29)	(12.97)	-	(10.86)
$[Cu(L^1)(Bipy)(OAc)]$							61.38	4.29	13.65	-	12.47
$[CuC_{27}H_{21}N_5O_3]$	527.004	Green	240-242	73.20	2.16	10.78	(61.15)	(4.02)	(13.29)	-	(12.06)
$[Zn(L^1)(Bipy)(OAc)].2H_2O$			(Dec)				57.60	4.79	12.79	-	11.95
$[ZnC_{27}H_{25}N_5O_5].2H_2O$	564.862	Coffee	156-158	79.10	0.43	7.88	(57.41)	(4.46)	(12.40)	-	(11.57)

Key: Bipy = 2,2'-Bipyridine; OAc = Acetate; μ_{eff}= Effective Magnetic Moment Value; B.M = Bohr Magneton

Table 4.1.3. Analytical data for HL^2 ligand and its metal(II) complexes

Molecular Formula	Formula Weight (g/mol)	Colour	Melting Point (^oC)	Yeild (%)	μ_{eff} (B.M)	Molar Conductance ($Ohm^{-1}Mol^{-1}cm^2$)	Analytical/Found (Calculated) %			
							C	H	N	M
HL^2							64.04	4.13	17.03	-
$C_{15}H_{11}N_3O_3$	281.268	Brown	220-222	86.70	-	-	(64.15)	(3.94)	(14.94)	-
$[Mn(L^2)_2].2H_2O$							55.51	4.02	13.11	8.78
$[MnC_{30}H_{20}N_6O_6].2H_2O$	651.482	Silver	308-310	50.00	5.79	8.23	(55.30)	(3.71)	(12.90)	(8.43)
$[Fe(L^2)_2].2H_2O$							55.28	3.82	13.13	8.93
$[FeC_{30}H_{20}N_6O_6].2H_2O$	652.412	Brown	346-348	69.60	5.19	6.98	(55.23)	(3.71)	(12.88)	(8.56)
$[Co(L^2)_2].H_2O$		Light					56.61	3.49	13.26	9.24
$[CoC_{30}H_{20}N_6O_6].H_2O$	637.486	Brown	312-314	64.20	2.51	9.01	(56.52)	(3.47)	(13.18)	(9.24)
$[Ni(L^2)_2].H_2O$		Yellowish					56.57	3.52	13.24	9.29
$[NiC_{30}H_{20}N_6O_6].H_2O$	637.086	Brown	298-280	60.90	3.59	6.54	(56.55)	(3.48)	(13.19)	(9.21)
$[Cu(L^2)_2]$		Greenish					58.07	3.37	13.56	10.26
$[CuC_{30}H_{20}N_6O_6]$	623.09	Brown	307-309	76.40	1.75	7.05	(57.73)	(3.23)	(13.47)	(10.18)
$[Zn(L^2)_2]$		Dark					57.93	3.42	13.61	11.54
$[ZnC_{30}H_{20}N_6O_6]$	625.73	Gray	287-289	64.20	0.36	11.53	(57.57)	(3.22)	(13.43)	(10.44)

Key: μ_{eff}= Effective Magnetic Moment Value; B.M = Bohr Magneton

Table 4.1.4. Analytical data for HL^2 ligand and its heteroleptic metal(II) complexes

Molecular Formula	Formula Weight (g/mol)	Colour	Melting Point (^oC)	Yeild (%)	μ_{eff} (B.M)	Molar Conductance ($Ohm^{-1}Mol^{-1}cm^2$)	Analytical/Found (Calculated) %				
							C	H	N	S	M
HL^2							64.04	4.13	17.03	-	-
$C_{15}H_{11}N_3O_3$	281.268	Brown	220-222	86.70	-	-	(64.15)	(3.94)	(16.94)	-	-
Bipy, $[C_{10}H_8N_2]$	156.18	White	63-66	-	-	-	-	-	-	-	-
$[Mn(L^2)(Bipy)(OAc)].H_2O$		Redish					57.09	4.11	12.38	-	9.69
$[MnC_{27}H_{21}N_5O_5].H_2O$	568.308	Brown	293.295	86.10	5.72	13.4	(57.05)	(4.07)	(12.32)	-	(9.66)
$[Fe(L^2)(Bipy)(SO_4)].H_2O$							52.81	3. 64	12.36	5.66	9.89
$[FeC_{25}H_{18}N_5O_7S].H_2O$	569.336	Brown	320-322	62.90	3.91	9.02	(52.74)	(3.54)	(12.30)	(5.63)	(9.81)
$[Co(L^2)(Bipy)(OAc)].$		Light					58.64	3.89	12.71	-	10.69
$[CoC_{27}H_{21}N_5O_5]$	554.292	Brown	334-336	71.40	3.92	14.05	(58.50)	(3.85)	(12.64)	-	(10.63)
$[Ni(L^2)(Bipy)(OAc)].H_2O$							57.01	4.46	12.35	-	10.29
$[NiC_{27}H_{21}N_5O_5].H_2O$	572.088	Brown	301-303	91.00	3.10	13.35	(56.67)	(4.41)	(12.24)	-	(10.26)
$[Cu(L^2)(Bipy)(OAc)].H_2O$		Yellowish					56.26	4.42	12.18	-	11.11
$[CuC_{27}H_{21}N_5O_5].H_2O$	577.02	Brown	298-300	64.80	1.76	14.51	(56.19)	(4.37)	(12.14)	-	(11.01)
$[Zn(L^2)(Bipy)(OAc)]$							57.92	3.85	12.52	-	11.85
$[ZnC_{27}H_{21}N_5O_5]$	560.732	Gray	312-314	73.00	0.11	7.15	(57.83)	(3.78)	(12.49)	-	(11.66)

Key: Bipy = 2,2'-Bipyridine; OAc = Acetate; μ_{eff}= Effective Magnetic Moment Value; B.M = Bohr Magneton

Table 4.1.5. Analytical data for HL^3 ligand and its heteroleptic metal(II) complexes

Molecular Formula	Formula Weight (g/mol)	Colour	Melting Point (^oC)	Yeild (%)	μ_{eff} (B.M)	Molar Conductance ($Ohm^{-1}Mol^{-1}cm^2$)	Analytical/Found (Calculated) %				
							C	H	N	S	M
HL^3							73.94	5.53	15.41	-	-
$C_{17}H_{15}N_3O$	278.86	Yellow	194-196	59.30	-	-	(73.89)	(5.47)	(15.23)	-	-
Bipy, $[C_{10}H_8N_2]$	156.18	White	63-66	-	-	-	-	-	-	-	-
$[Mn(L^3)(Bipy)(OAc)]$		Yellowish					6390	4.62	12.85	-	10.23
$[MnC_{29}H_{25}N_5O_3]$	546.45	Brown	216-218	75.20	5.52	4.72	(63.74)	(4.57)	(12.82)	-	(10.05)
$[Fe(L^3)(Bipy)(SO_4)].H_2O$		Redish					53.99	4. 05	11.68	5.52	9.56
$[FeC_{27}H_{22}N_5O_5S].H_2O$	602.368	Brown	319-321	46.00	4.97	12.08	(53.83)	(4.02)	(11.63)	(5.32)	(9.27)
$[Co(L^3)(Bipy)(OAc)]$							63.40	4.62	12.88	-	10.37
$[CoC_{29}H_{25}N_5O_3]$	550.45	Pink	310-312	55.90	4.81	8.96	(63.27)	(4.55)	(12.73)	-	(10.71)
$[Ni(L^3)(Bipy)(OAc)]$							63.47	4.69	12.82	-	10.81
$[Ni\ C_{29}H_{25}N_5O_3]$	550.0	Brown	314-316	46.70	3.16	5.63	(63.33)	(4.54)	(12.74)	-	(10.67)
$[Cu(L^3)(Bipy)(OAc)]$		Dark					62.95	4.81	12.77	-	11.84
$[Cu\ C_{29}H_{25}N_5O_3]$	554.83	Brown	229-231	47.20	2.04	13.10	(62.77)	(4.51)	(12.63)	-	(11.45)
$[Zn(L^3)(Bipy)(OAc)].H_2O$		Bright					60.64	4.83	12.22	-	11.44
$[Zn\ C_{29}H_{25}N_5O_3].H_2O$	574.676	Yellow	289-291	51.30	0.24	9.71	(60.60)	(4.74)	(12.19)	-	(11.38)

Key: Bipy = 2,2'-Bipyridine; OAc = Acetate; μ_{eff}= Effective Magnetic Moment Value; B.M = Bohr Magneton

Table 4.1.6. Analytical data for HL^4 ligand and its metal(II) complexes

Molecular Formula	Formula Weight (g/mol)	Colour	Melting Point (^oC)	Yeild (%)	μ_{eff} (B.M)	Molar Conductance ($Ohm^{-1}Mol^{-1}cm^2$)	Analytical/Found (Calculated) %			
							C	H	N	M
HL^4							66.96	6.92	16.81	-
$C_{14}H_9N_3O_2$	251.242	Orange	168-170	71.20	--	-	(66.92)	(6.61)	(16.73)	-
$[Mn(L^4)_2].H_2O$							58.65	3.63	14.74	9.76
$[MnC_{28}H_{16}N_6O_4].H_2O$	573.414	Brown	244-246	87.50	5.94	8.35	(58.64)	(3.52)	(14.66)	(9.58)
$[Fe(L^4)_2].2H_2O$							56.82	3.78	14.22	9.46
$[FeC_{28}H_{16}N_6O_2].2H_2O$	592.77	Brown	285-287	96.40	5.05	14.6	(56.77)	(3.74)	(14.19)	(9.43)
$[Co(L^4)_2].H_2O$		Redish					58.32	3.49	14.64	10.27
$[Co\ C_{28}H_{16}N_6O_2].H_2O$	577.414	Pink	231-233	71.10	2.62	15.2	(58.24)	(3.54)	(14.55)	(10.21)
$[Ni(L^4)_2].H_2O$		Greenish					58.37	3.55	14.59	10.25
$[Ni\ C_{28}H_{16}N_6O_4].H_2O$	577.194	Brown	234-236	48.40	3.80	14.2	(58.35)	(3.49)	(14.56)	(10.17)
$[Cu(L^4)_2]$		Redish					59.99	3.27	14.95	11.30
$[Cu\ C_{28}H_{16}N_6O_2]$	564.008	Brown	201-203	79.60	2.02	6.24	(59.62)	(3.22)	(14.90)	(11.27)
$[Zn(L^4)_2].H_2O$		Dark					57.66	3.51	14.45	11.24

$[ZnC_{28}H_{20}N_6O_6].H_2O$	583.854	Red	209-211	63.90	0.21	10.9	(57.59)	(3.45)	(14.39)	(11.19)

Key: μ_{eff} = Effective Magnetic Moment Value; B.M = Bohr Magneton

Table 4.1.7. Analytical data for HL^4 ligand and its heteroleptic metal(II) complexes

Molecular Formula	Formula Weight (g/mol)	Colour	Melting Point (^oC)	Yeild (%)	μ_{eff} (B.M)	Molar Conductance ($Ohm^{-1}Mol^{-1}cm^2$)	Analytical/Found (Calculated) %				
							C	H	N	S	M
HL^4							66.96	6.92	16.81	-	-
$C_{14}H_9N_3O_2$	251.242	Orange	168-170	71.20	--	-	(66.92)	(6.61)	(16.73)	-	-
Bipy, $[C_{10}H_8N_2]$	156.18	White	63-66	-	-	-	-	-	-	-	-
$[Mn(L^4)(Bipy)(OAc)].H_2O$		Brownis					58.04	3.97	13.09	-	10.24
$[MnC_{26}H_{19}N_5O_4].H_2O$	538.384	h	258-260	85.90	5.85	9.88	(57.99)	(3.94)	(13.01)	-	(10.20)
		Red									
$[Fe(L^4)(Bipy)(SO_4)].H_2O$							50.09	3. 22	12.31	5.64	9.87
$[FeC_{24}H_{16}N_5O_6S].H_2O$	576.294	Brown	294-296	41.40	5.18	7.94	(50.02)	(3.15)	(12.16)	(5.55)	(9.69)
$[Co(L^4)(Bipy)(OAc)]$							59.62	3.81	13.47	-	11.20
$[CoC_{26}H_{19}N_5O_4]$	524.368	Brown	251-253	93.80	4.83	13.9	(59.55)	(3.66)	(13.36)	-	(11.24)
$[Ni(L^4)(Bipy)(OAc)].H_2O$		Redish					57.74	3.98	13.04	-	11.01
$[Ni\ C_{26}H_{19}N_5O_4].H_2O$	542.164	Brown	269-271	84.20	3.17	6.73	(57.60)	(3.91)	(12.92)	-	(10.83)
$[Cu(L^4)(Bipy)(OAc)].H_2O$		Dark					57.13	3.97	12.85	-	12.14
$[Cu\ C_{26}H_{19}N_5O_4].H_2O$	546.994	Peach	227-229	60.50	1.78	12.5	(57.09)	(3.87)	(12.81)	-	(12.01)

$[Zn(L^{4o})(Bipy)(OAc)]$							58.96	3.77	13.24	-	12.14
$[Zn\ C_{26}H_{19}N_5O_4]$	530.800	Red	197-199	82.60	0.28	9.83	(58.83)	(3.61)	(13.19)	-	(11.91)

Key: Bipy = 2,2'-Bipyridine; OAc = Acetate; μ_{eff}= Effective Magnetic Moment Value; B.M = Bohr Magneton

Table 4.1.8. Analytical data for HL^5ligand and its metal(II) complexes

Molecular Formula	**Formula Weight (g/mol)**	**Colour**	**Melting Point (^oC)**	**Yeild (%)**	**μ_{eff} (B.M)**	**Molar Conductance ($Ohm^{-1}Mol^{-1}cm^2$)**	**Analytical/Found (Calculated) %**			
							C	**H**	**N**	**M**
HL^5							59.42	3.29	15.02	-
$C_{14}H_9N_3O_4$	283.242	Orange	232-234	63.40	--	-	(59.36)	(3.21)	(14.84)	-
$[Mn(L^5)_2].H_2O$							50.07	3.64	12.52	8.36
$[MnC_{24}H_{20}N_6O_8].H_2O$	673.446	Brown	288-290	44.30	5.54	11.9	(49.93)	(3.59)	(12.48)	(8.16)
$[Fe(L^5)_2].2H_2O$							51.39	3.53	12.94	8.68
$[FeC_{26}H_{20}N_6O_8].2H_2O$	656.36	Brown	316-318	54.90	3.17	14.7	(51.23)	(3.38)	(12.81)	(8.51)
$[Co(L^5)_2].2H_2O$							52.51	3.22	13.19	9.28
$[Co\ C_{28}H_{20}N_6O_{10}].2H_2O$	659.43	Orange	282-284	84.60	2.41	9.06	(52.43)	(3.14)	(13.11)	(9.19)
$[Ni(L^5)_2(H_2O)_2]$		Redish					51.14	3.42	12.94	8.99
$[NiC_{28}H_{20}N_6O_{10}]$	659.21	Brown	301-303	45.00	2.95	15.7	(51.01)	(3.36)	(12.75)	(8.91)
$[Cu(L^5)_2]$		Brownis					53.62	3.09	13.44	10.24
$[Cu\ C_{28}H_{16}N_6O_8]$	628.008	h	296-298	32.20	1.91	8.35	(53.55)	(2.89)	(13.39)	(10.12)

		Red								
$[Zn(L^5)_2].H_2O$							52.07	3.25	13.11	10.21
$[ZnC_{24}H_{20}N_6O_8]$	665.87	Red	291-293	38.20	0.33	5.72	(51.91)	(3.11)	(12.98)	(10.09)

Key: μ_{eff}= Effective Magnetic Moment Value; B.M = Bohr Magneton

Table 4.1.9. Analytical data for HL^5ligand and its heteroleptic metal(II) complexes

Molecular Formula	**Formula Weight (g/mol)**	**Colour**	**Melting Point (^oC)**	**Yeild (%)**	**μ_{eff} (B.M)**	**Molar Conductance ($Ohm^{-1}Mol^{-1}cm^2$)**	**Analytical/Found (Calculated) %**				
							C	**H**	**N**	**S**	**M**
HL^5							54.32	3.29	15.02	-	-
$C_{14}H_9N_3O_4$	283.242	Orange	232-235	63.40	-	-	(54.29)	(3.21)	(14.84)	-	-
Bipy, $[C_{10}H_8N_2]$	156.18	White	63-66	-	-	-	-	-	-	-	-
$[Mn(L^5)(Bipy)(OAc)].H_2O$		Yellowish					55.01	3.72	12.40	-	9.54
$[MnC_{26}H_{19}N_5O_6].H_2O$	569.778	Brown	296.298	73.40	5.59	12.7	(54.80)	(3.68)	(12.29)	-	(9.46)
$[Fe(L^5)(Bipy)(SO_4)]$							48.99	2. 82	12.04	5. 49	9.54
$[FeC_{24}H_{16}N_5O_8S]$	590.302	Red	319-321	96.50	3.74	10.6	(48.83)	(2.75)	(11.87)	(5.42)	(9.46)
$[Co(L^5)(Bipy)(OAc)].2H_2O$							53.05	4.11	12.00	-	9.97
$[CoC_{26}H_{19}N_5O_6].2H_2O$	592.424	Brown	314-316	98.00	3.81	8.17	(52.71)	(3.92)	(11.83)	-	(9.95)
$[Ni(L^5)(Bipy)(OAc)].H_2O$							51.34	4.28	11.64	-	9.74
$[Ni\ C_{26}H_{19}N_5O_6].H_2O$	610.22	Red	310-312	100.0	2.77	6.82	(51.17)	(4.13)	(11.48)	-	(9.62)
$[Cu(L^5)(Bipy)(OAc)]$							55.81	3.60	12.62	-	11.50

[Cu $C_{26}H_{19}N_5O_6$]	561.002	Coffee	286-288	63.00	1.68	13.0	(55.66)	(3.41)	(12.49)	-	(11.33)
[Zn(L^5)(Bipy)(OAc)].H_2O							52.19	3.91	11.77	-	11.03
[Zn $C_{26}H_{19}N_5O_6$].H_2O	598.864	Pink	321-323	63.60	0.09	7.92	(52.14)	(3.88)	(11.69)	-	(10.92)

Key: Bipy = 2,2'-Bipyridine; OAc = Acetate; μ_{eff}= Effective Magnetic Moment Value; B.M = Bohr Magneton

Table 4.1.10. Analytical data for HL^6 ligand and its heteroleptic metal(II) complexes

Molecular Formula	**Formula Weight (g/mol)**	**Colour**	**Melting Point (^oC)**	**Yeild (%)**	**μ_{eff} (B.M)**	**Molar Conductance ($Ohm^{-1}Mol^{-1}cm^2$)**	**Analytical/Found (Calculated) %**				
							C	**H**	**N**	**S**	**M**
HL^6		Yellowish		68.15			69.03	4.77	15.12	-	-
$C_{16}H_{13}N_3O_2$	279.294	Brown	214-216		-	-	(68.80)	(4.69)	(15.05)	-	-
Bipy, [$C_{10}H_8N_2$]	156.18	White	63-66	-	-	-	-	-	-	-	-
[Mn(L^6)(Bipy)(OAc)]							70.55	4.31	12.83	-	10.29
[$MnC_{28}H_{23}N_5O_4$]	548.444	Black	230-232	80.0	6.02	5.62	(70.43)	(4.23)	(12.77)	-	(10.02)
[Fe(L^6)(Bipy)(SO_4)]							53.31	3. 52	12.04	5. 49	9.75
[$FeC_{26}H_{20}N_5O_6S$]	586.354	Brown	298-300	52.10	5.71	9.38	(53.25)	(3.44)	(11.95)	(5.46)	(9.53)
[Co(L^6)(Bipy)(OAc)]		Wine Red					70.09	4.22	12.73	-	10.88
[$CoC_{28}H_{23}N_5O_4$]	552.442		302-304	84.30	4.99	6.89	(69.92)	(4.19)	(12.68)	-	(10.67)
[Ni(L^6)(Bipy)(OAc)]		Maroon					69.99	4.23	12.70	-	10.85
[Ni $C_{28}H_{23}N_5O_4$]	552.224	Red	321-323	76.90	3.16	8.32	(69.95)	(4.19)	(12.67)	-	(10.63)

$[Cu(L^6)(Bipy)(OAc)].H_2O$		Dark					64.09	4.51	12.24	-	11.19
$[Cu\ C_{28}H_{23}N_5O_4].H_2O$	575.07	Brown	272-274	73.30	1.82	15.2	(64.04)	(4.39)	(12.18)	-	(11.04)
$[Zn(L^6)(Bipy)(OAc)]$							66.03	4.29	12.60	-	11.82
$[Zn\ C_{28}H_{23}N_5O_4]$	558.884	Red	295-297	74.30	0.21	12.9	(65.89)	(4.15)	(12.53)	-	(11.69)

Key: Bipy = 2,2'-Bipyridine; OAc = Acetate; μ_{eff}= Effective Magnetic Moment Value; B.M = Bohr Magneton

Table 4.2.1. Solubility results of HL^1 ligand and its metal(II) complexes in various Solvents

Compound	Distilled H_2O	MeOH	EtOH	CH_2Cl_2	$CHCl_3$	DMSO	DMF	CH_3NO_2
HL^1	SS	SS	S	S	S	S	S	SS
$[Mn(L^1)_2].H_2O$	SS	S	S	S	SS	S	S	S
$[Fe(L^1)_2(H_2O)_2]$	NS	S	S	S	S	S	S	SS
$[Co(L^1)_2].2H_2O$	NS	SS	SS	SS	SS	S	SS	NS
$[Ni(L^1)_2].H_2O$	SS	SS	SS	SS	SS	S	S	SS
$[Cu(L^1)_2]$	NS	NS	SS	S	S	S	S	SS
$[Zn(L^1)_2]$	SS	SS	SS	SS	S	S	SS	SS

Key: *S=Soluble; SS=Slightly Soluble; NS=Not Soluble; H_2O=Water;; MeOH=Methanol; EtOH=Ethanol; CH_2Cl_2=Dichloromethane, $CHCl_3$=Trichloromethane; DMSO=Dimethylsuphoxide, DMF=Dimethylformamide, CH_3NO_2=Dinitromethane*

Table 4.2.2. Solubility results of HL^1 ligand and its Hetroleptic Metal(II) Complexes in various Solvents

Compound	Distilled H_2O	MeOH	EtOH	CH_2Cl_2	$CHCl_3$	DMSO	DMF	CH_3NO_2
HL^1	SS	SS	S	S	S	S	S	SS
$[Mn(L^1)(Bipy)(OAc)]$	SS	S	S	SS	SS	S	S	S
$[Fe(L^1)(Bipy)(SO_4)]$	NS	NS	SS	SS	S	SS	S	SS
$[Co(L^1)(Bipy)(OAc)].H_2O$	SS	S	S	S	SS	S	S	S
$[Ni(L^1)(Bipy)(OAc)].H_2O$	NS	NS	SS	SS	S	S	S	SS
$[Cu(L^1)(Bipy)(OAc)]$	SS	S	S	S	S	S	S	NS
$[Zn(L^1)(Bipy)(OAc)].2H_2O$	NS	NS	SS	SS	SS	S	SS	NS

Key: *S=Soluble; SS=Slightly Soluble; NS=Not Soluble; H_2O=Water; MeOH=Methanol; EtOH=Ethanol; CH_2Cl_2 = Dichloromethane, $CHCl_3$=Trichloromethane; DMSO=Dimethylsuphoxide, DMF=Dimethylformamide; CH_3NO_2=Dinitromethane; Bipy=2,2'-Bipyridine, OAc= Acetate*

Table 4.2.3. Solubility results of HL^2 ligand and its metal(II) complexes in various Solvents

Compound	Distilled H_2O	MeOH	EtOH	CH_2Cl_2	$CHCl_3$	DMSO	DMF	CH_3NO_2
HL^2	NS	SS	SS	SS	SS	S	S	NS
$[Mn(L^2)_2].2H_2O$	NS	NS	SS	SS	SS	S	SS	NS
$[Fe(L^2)_2(H_2O)].H_2O$	NS	NS	SS	SS	S	S	SS	NS
$[Co(L^2)_2].H_2O$	NS	NS	SS	SS	S	S	S	SS
$[Ni(L^2)_2].H_2O$	NS	SS	SS	SS	SS	S	SS	SS
$[Cu(L^2)_2]$	NS	NS	SS	SS	SS	S	SS	NS
$[Zn(L^2)_2]$	NS	NS	SS	SS	S	SS	SS	NS

Key: *S=Soluble; SS=Slightly Soluble; NS=Not Soluble; H_2O=Water;; MeOH=Methanol; EtOH=Ethanol; CH_2Cl_2 = Dichloromethane, $CHCl_3$=Trichloromethane; DMSO=Dimethylsuphoxide, DMF=Dimethylformamide, CH_3NO_2=Dinitromethane*

Table 4.2.4. Solubility results of HL^2 ligand and its heteroleptic metal(II) complexes in various Solvents

Compound	Distilled H_2O	MeOH	EtOH	CH_2Cl_2	$CHCl_3$	DMSO	DMF	CH_3NO_2
HL^2	NS	SS	SS	SS	SS	S	S	NS
$[Mn(L^2)(Bipy)(OAc)]H_2O$	NS	S	S	SS	S	S	SS	SS
$[Fe(L^2)(Bipy)(SO_4)].H_2O$	NS	SS	S	SS	SS	SS	SS	SS
$[Co(L^2)(Bipy)(OAc)]$	SS	SS	S	SS	S	S	S	SS
$[Ni(L^2)(Bipy)(OAc)].H_2O$	NS	NS	SS	SS	S	S	S	SS
$[Cu(L^2)(Bipy)(OAc)].H_2O$	SS	SS	SS	S	S	S	S	SS
$[Zn(L^2)(Bipy)(OAc)]$	NS	SS	SS	SS	SS	SS	S	SS

Key: *S=Soluble; SS=Slightly Soluble; NS=Not Soluble; H_2O=Water;; MeOH=Methanol; EtOH=Ethanol; CH_2Cl_2 = Dichloromethane, $CHCl_3$=Trichloromethane; DMSO=Dimethylsuphoxide, DMF=Dimethylformamide; CH_3NO_2=Dinitromethane; Bipy=2,2'-Bipyridine, OAc= Acetate*

Table 4.2.5. Solubility results of HL^3 ligand and its heteroleptic metal(II) complexes in various Solvents

Compound	Distilled H_2O	MeOH	EtOH	CH_2Cl_2	$CHCl_3$	DMSO	DMF	CH_3NO_2
HL^3	SS	SS	S	SS	S	S	S	SS
$[Mn(L^3)(Bipy)(OAc)]$	NS	SS	SS	SS	S	S	S	SS
$[Fe(L^3)(Bipy)(SO_4)].H_2O$	SS	S	S	SS	S	S	SS	SS
$[Co(L^3)(Bipy)(OAc)]$	SS	S	S	S	S	S	S	S
$[Ni(L^3)(Bipy)(OAc)]$	NS	S	S	SS	SS	S	S	SS
$[Cu(L^3)(Bipy)(OAc)]$	SS	SS	S	S	SS	S	SS	SS
$[Zn(L^3)(Bipy)(OAc)].H_2O$	SS	SS	SS	SS	SS	SS	SS	SS

Key: *S=Soluble; SS=Slightly Soluble; NS=Not Soluble; H_2O=Water;; MeOH=Methanol; EtOH=Ethanol; CH_2Cl_2 = Dichloromethane, $CHCl_3$=Trichloromethane; DMSO=Dimethylsuphoxide, DMF=Dimethylformamide; CH_3NO_2=Dinitromethane; Bipy=2,2'-Bipyridine, OAc= Acetate*

Table 4.2.6. Solubility results of HL^4 ligand and its metal(II) complexes in various Solvents

Compound	Distilled H_2O	MeOH	EtOH	CH_2Cl_2	$CHCl_3$	DMSO	DMF	CH_3NO_2
HL^4	**SS**	**S**	**S**	**S**	**S**	**S**	**S**	**SS**
$[Mn(L^4)_2].H_2O$	**NS**	**SS**	**S**	**SS**	**SS**	**S**	**SS**	**SS**
$[Fe(L^4)_2].2H_2O$	**NS**	**SS**	**SS**	**SS**	**S**	**S**	**S**	**S**
$[Co(L^4)_2].H_2O$	**SS**	**SS**	**SS**	**S**	**S**	**S**	**SS**	**SS**
$[Ni(L^4)_2].H_2O$	**SS**	**SS**	**S**	**SS**	**SS**	**SS**	**S**	**NS**
$[Cu(L^4)_2]$	**NS**	**SS**	**SS**	**SS**	**SS**	**SS**	**SS**	**NS**
$[Zn(L^4)_2].H_2O$	**SS**	**SS**	**S**	**S**	**S**	**S**	**SS**	**SS**

Key: *S=Soluble; SS=Slightly Soluble; NS=Not Soluble; H_2O=Water;; MeOH=Methanol; EtOH=Ethanol; CH_2Cl_2=Dichloromethane, $CHCl_3$=Trichloromethane; DMSO=Dimethylsuphoxide, DMF=Dimethylformamide, CH_3NO_2=Dinitromethane*

Table 4.2.7. Solubility results of HL^4 ligand and its heteroleptic metal(II) complexes in various Solvents

Compound	Distilled H_2O	MeOH	EtOH	CH_2Cl_2	$CHCl_3$	DMSO	DMF	CH_3NO_2
HL^4	**SS**	**S**	**S**	**S**	**S**	**S**	**S**	**SS**
$[Mn(L^4)(Bipy)(OAc)].H_2O$	**SS**	**S**	**S**	**S**	**S**	**S**	**S**	**S**
$[Fe(L^4)(Bipy)(SO_4)].H_2O$	**SS**	**S**	**S**	**S**	**S**	**S**	**S**	**SS**
$[Co(L^4)(Bipy)(OAc)]$	**NS**	**SS**	**SS**	**SS**	**SS**	**S**	**SS**	**SS**
$[Ni(L^4)(Bipy)(OAc)].H_2O$	**SS**	**S**	**S**	**SS**	**SS**	**SS**	**SS**	**S**
$[Cu(L^4)(Bipy)(OAc)].H_2O$	**NS**	**SS**	**S**	**S**	**S**	**S**	**S**	**SS**
$[Zn(L^4)(Bipy)(OAc)]$	**NS**	**SS**	**SS**	**SS**	**SS**	**SS**	**SS**	**SS**

Key: *S=Soluble; SS=Slightly Soluble; NS=Not Soluble; H_2O=Water;; MeOH=Methanol; EtOH=Ethanol; CH_2Cl_2 = Dichloromethane, $CHCl_3$=Trichloromethane; DMSO=Dimethylsuphoxide, DMF=Dimethylformamide; CH_3NO_2=Dinitromethane; Bipy=2,2'-Bipyridine, OAc= Acetate*

Table 4.2.8. Solubility results of HL^5 ligand and its metal(II) complexes in various Solvents

Compound	Distilled H_2O	MeOH	EtOH	CH_2Cl_2	$CHCl_3$	DMSO	DMF	CH_3NO_2
HL^5	SS	S	S	SS	SS	S	S	S
$[Mn(L^5)_2].H_2O$	NS	SS	SS	SS	SS	S	S	NS
$[Fe(L^5)_2(H_2O)].H_2O$	NS	SS	SS	SS	SS	SS	SS	NS
$[Co(L^5)_2].2H_2O$	SS	SS	SS	SS	SS	S	SS	SS
$[Ni(L^5)_2(H_2O)_2]$	NS	SS	S	SS	SS	S	S	NS
$[Cu(L^5)_2]$	NS	S	S	S	S	SS	S	S
$[Zn(L^5)_2].H_2O$	SS	S	SS	S	SS	S	S	S

Key: *S=Soluble; SS=Slightly Soluble; NS=Not Soluble; H_2O=Water;; MeOH=Methanol; EtOH=Ethanol; CH_2Cl_2 = Dichloromethane, $CHCl_3$=Trichloromethane; DMSO=Dimethylsuphoxide, DMF=Dimethylformamide, CH_3NO_2=Dinitromethane*

Table 4.2.9. Solubility results of HL^5 ligand and its heteroleptic metal(II) complexes in various Solvents

Compound	Distilled H_2O	MeOH	EtOH	CH_2Cl_2	$CHCl_3$	DMSO	DMF	CH_3NO_2
HL^5	SS	S	S	SS	SS	S	S	S
$[Mn(L^5)(Bipy)(OAc)].H_2O$	SS	S	SS	S	SS	S	S	S
$[Fe(L^5)(Bipy)(SO_4)]$	SS	SS	SS	SS	S	S	S	SS
$[Co(L^5)(Bipy)(OAc)].2H_2O$	NS	SS	SS	S	S	SS	SS	NS
$[Ni(L^5)(Bipy)(OAc)].H_2O$	NS	S	SS	S	S	S	S	SS
$[Cu(L^5)(Bipy)(OAc)]$	NS	SS	SS	SS	SS	SS	SS	NS
$[Zn(L^5)(Bipy)(OAc)].H_2O$	NS	S	S	S	S	S	SS	SS

Key: *S=Soluble; SS=Slightly Soluble; NS=Not Soluble; H_2O=Water;; MeOH=Methanol; EtOH=Ethanol; CH_2Cl_2 = Dichloromethane, $CHCl_3$=Trichloromethane; DMSO=Dimethylsuphoxide, DMF=Dimethylformamide; CH_3NO_2=Dinitromethane; Bipy=2,2'-Bipyridine, OAc= Acetate*

Table 4.2.10. Solubility results of HL^6 ligand and its heteroleptic metal(II) complexes in various Solvents

Compound	Distilled H_2O	MeOH	EtOH	CH_2Cl_2	$CHCl_3$	DMSO	DMF	CH_3NO_2
HL^6	SS	S	S	S	S	S	S	S
$[Mn(L^6)(Bipy)(OAc)]$	NS	S	S	S	SS	S	S	SS
$[Fe(L^6)(Bipy)(SO_4)]$	NS	NS	SS	SS	SS	S	S	NS
$[Co(L^6)(Bipy)(OAc)]$	NS	SS	SS	S	SS	S	SS	NS
$[Ni(L^6)(Bipy)(OAc)]$	SS	S	S	S	S	S	SS	S
$[Cu(L^6)(Bipy)(OAc)].H_2O$	NS	SS	SS	S	SS	S	S	SS
$[Zn(L^6)(Bipy)(OAc)]$	SS	S	S	S	S	S	SS	S

Key: *S=Soluble; SS=Slightly Soluble; NS=Not Soluble; H_2O=Water; MeOH=Methanol; EtOH=Ethanol; CH_2Cl_2 = Dichloromethane, $CHCl_3$=Trichloromethane; DMSO=Dimethylsuphoxide, DMF=Dimethylformamide; CH_3NO_2=Dinitromethane; Bipy=2,2'-Bipyridine, OAc= Acetate*

Table 4.3.1. Infrared spectral (cm^{-1}) data of HL^1 ligand and its metal(II) complexes

Compound	*ν*(OH)	*ν*(C=N)	*ν*(C=C)	*ν*(C-N)	*ν*(C-C)	*ν*(C-O)	δC-H	M-N	M-O
HL^1	3389_b	1669_s	1625_s	1567_s	1393_s	1161_s	990_m	-	-
$[Mn(L^1)_2].H_2O$	3390_s	1644_s	1538_s	1425_s	1391_s	1183_s	976_s	655_s	496_s
$[Fe(L^1)_2(H_2O)_2]$	3435_b	1616_s	1538_s	1423_s	1388_s	1188_s	979_s	551_s	458_s
$[Co(L^1)_2].2H_2O$	3384_b	1643_s	1536_s	1431_s	1352_s	1189_s	997_s	584_s	497_s
$[Ni(L^1)_2].H_2O$	3395_b	1619_s	1536_s	1430_s	1385_s	1190_s	987_s	577_m	496_m
$[Cu(L^1)_2]$	-	1612_b	1538_m	1429_s	1397_s	1183_s	981_s	529_s	469_s
$[Zn(L^1)_2]$	-	1619_s	1539_s	1461_s	1352_s	1191_s	998_s	585_s	497_s

Key*: b = broad, s = sharp, d = doublet and m = medium*

Table 4.3.2. Infrared spectral (cm^{-1}) data of HL^1 ligand and its heteroleptic metal(II) complexes

Compound	*ν*(OH)	*ν*(C=N)	*ν*(C=C)	*ν*(C-N)	*ν*(C-C)	*ν*(C-O)	δC-H	M-N	M-O
HL^1	3389_b	1669_s	1625_s	1567_s	1393_s	1161_s	990_m	-	-
Bipy, $[C_{10}H_8N_2]$	-	1639_s	1580_s	1453_s	1349_s	-	991_s	-	-
$[Mn(L^1)(Bipy)(OAc)]$	3426_m	1614_s	1538_s	1461_s	1362_s	1178_s	976_s	540_s	446_s
$[Fe(L^1)(Bipy)(SO_4)]$	-	1616_s	1538_s	1423_s	1386_s	1189_s	979_s	551_s	458_s
$[Co(L^1)(Bipy)(OAc)].H_2O$	3416_b	1615_s	1536_s	1431_s	1352_s	1190_s	997_s	547_s	448_s
$[Ni(L^1)(Bipy)(OAc)].H_2O$	3356_m	1619_s	1538_s	1423_s	1366_s	1181_s	977_s	519_s	476_s
$[Cu(L^1)(Bipy)(OAc)]$	-	1615_s	1536_s	1431_s	1352_s	1190_s	997_s	585_s	448_s
$[Zn(L^1)(Bipy)(OAc)].2H_2O$	3434_m	1663_s	1587_s	1499_m	1384_s	1288_s	1022_s	507_s	481_s

Key*: b = broad, s = sharp, d = doublet and m = medium*

Table 4.3.3. Infrared spectral (cm^{-1}) data of HL^2 ligand and its metal(II) complexes

Compounds	*v*(OH)	*v*(C=N)	*v*(C=C)	*v*(C-N)	*v*(C-C)	*v*(C-O)	δC-H	M-N	M-O
HL^2	3341_b	1688_b	1650_b	1550_b	1366_b	1268_s	991_s	-	-
$[Mn(L^2)_2].2H_2O$	3348_b	1656_b	1560_b	1517_m	1364_m	1267_s	991_s	560_s	482_s
$[Fe(L^2)_2(H_2O)].H_2O$	3348_b	1667_s	1580_s	1539_s	1366_s	1267_s	991_s	552_s	482_s
$[Co(L^2)_2].H_2O$	3349_b	1642_s	1543_s	1459_m	1368_s	1268_s	991_s	564_s	459_s
$[Ni(L^2)_2].H_2O$	3330_b	1620_b	1485_b	1459_b	1362_b	1266_s	991_m	530_s	455_s
$[Cu(L^2)_2]$	-	1633_m	1582_s	1541_s	1373_s	1268_s	991_m	529_s	481_s
$[Zn(L^2)_2]$	-	1645_b	1511_m	1461_m	1361_m	1266_s	990_s	558_s	482_s

Key*: b = broad, s = sharp, d = doublet and m = medium*

Table 4.3.4. Infrared spectral (cm^{-1}) data of HL^2 ligand and its heteroleptic metal(II) complexes

Compounds	*ν*(OH)	*ν*(C=N)	*ν*(C=C)	*ν*(C-N)	*ν*(C-C)	*ν*(C-O)	δC-H	M-N	M-O
HL^2	3341_b	1688_b	1650_b	1550_b	1366_b	1268_s	991_s	-	-
Bipy, $[C_{10}H_8N_2]$	-	1639_s	1580_s	1453_s	1349_s	-	991_s	-	-
$[Mn(L^2)(Bipy)(OAc)].H_2O$	3342_s	1667_s	1524_m	1466_m	1364_s	1267_s	990_s	530_s	446_s
$[Fe(L^2)(Bipy)(SO_4)].H_2O$	3416_b	1640_b	1566_m	1466_s	1315_m	1113_s	875_m	546_s	474_s
$[Co(L^2)(Bipy)(OAc)].$	-	1634_s	1562_m	1443_m	1366_s	1269_s	991_s	563_s	446_s
$[Ni(L^2)(Bipy)(OAc)].H_2O$	3436_b	1642_s	1543_s	1436_m	1367_s	1267_m	991_s	564_s	449_m
$[Cu(L^2)(Bipy)(OAc)].H_2O$	3342_s	1620_s	1579_m	1448_s	1384_s	1267_m	991_s	561_s	462_m
$[Zn(L^2)(Bipy)(OAc)]$	-	1638_s	1528_m	1456_m	1384_s	1268_m	983_m	559_m	486_m

Key*: b = broad, s = sharp, d = doublet and m = medium*

Table 4.3.5. Infrared spectral (cm^{-1}) data of HL^3 ligand and its heteroleptic metal(II) complexes

Compounds	*ν*(OH)	*ν*(C=N)	*ν*(C=C)	*ν*(C-N)	*ν*(C-C)	*ν*(C-O)	δC-H	M-N	M-O
HL^3	3441_b	1628_s	1593_s	1537_s	1432_s	1290_s	981_s	-	-
Bipy, $[C_{10}H_8N_2]$	-	1639_s	1580_s	1453_s	1349_s	-	991_s	-	-
$[Mn(L^3)(Bipy)(OAc)]$	-	1615_s	1571_s	1538_s	1362_s	1178_s	977_s	540_s	497_s
$[Fe(L^3)(Bipy)(SO_4)].H_2O$	3439_b	1614_s	1574_s	1529_s	1345_m	1185_m	985_s	547_m	451_m
$[Co(L^3)(Bipy)(OAc)]$	-	1616_s	1568_s	1528_s	1335_s	1183_m	830_s	556_s	499_s
$[Ni(L^3)(Bipy)(OAc)]$	-	1616_s	1586_s	1527_s	1334_s	1186_s	837_s	539_m	457_m
$[Cu(L^3)(Bipy)(OAc)]$	3427_m	1615_s	1594_m	1530_s	1334_s	1186_s	833_s	533_m	454_m
$[Zn(L^3)(Bipy)(OAc)].H_2O$	3434_b	1619_s	1589_m	1532_s	1334_m	1188_s	835_m	594_m	452_m

Key*: b = broad, s = sharp, d = doublet and m = medium*

Table 4.3.6. Infrared spectral (cm^{-1}) data of HL^4 ligand and its metal(II) complexes

Compounds	*ν*NH	*ν*(OH)	*ν*(C=O)	*ν*(C=N)	*ν*(C=C)	*ν*(C-N)	*ν*(C-C)	*ν*(C-O)	δC-H	M-N	M-O
HL^4	3494_b	3389_b	$1672_{s,}\ 1651_s$	1630_s	1592_s	1554_s	1491_s	1224_s	982_s	-	-
$[Mn(L^4)_2].H_2O$	-	3434_b	1644_s	1589_s	1570_m	1537_s	1480_s	1268_s	994_s	539_s	486_s
$[Fe(L^4)_2].2H_2O$	-	3375_b	1641_s	1584_m	1562_s	1561_s	1405_s	1259_s	986_s	547_s	463_s
$[Co(L^4)_2].H_2O$	-	3304_b	1639_s	1613_m	1586_s	1563_s	1376_s	1251_s	994_s	507_s	459_s
$[Ni(L^4)_2].H_2O$	-	3378_b	1637_s	1583_s	1559_s	1497_m	1382_s	1279_s	996_s	513_s	467_s
$[Cu(L^4)_2]$	-	-	1658_s	1586_s	1568_s	1478_s	1385_s	1272_s	987_s	559_s	454_s
$[Zn(L^4)_2].H_2O$	-	3348_b	1651_s	1594_s	1547_s	1477_s	1393_s	1285_s	991_s	501_s	451_s

Key*: b = broad, s = sharp, d = doublet and m = medium*

Table 4.3.7. Infrared spectral (cm^{-1}) data of HL^4 ligand and its heteroleptic metal(II) complexes

Compounds	*ν*NH	*ν*(OH)	*ν*(C=O)	*ν*(C=N)	*ν*(C=C)	*ν*(C-N)	*ν*(C-C)	*ν*(C-O)	δC-H	M-N	M-O
HL^4	3494_b	3389_b	1672_s1651_s	1630_s	1592_s	1554_s	1491_s	1224_s	982_s	-	-
Bipy, $[C_{10}H_8N_2]$	-	-	-	1639_s	1580_s	1453_s	1349_s	-	991_s	-	-
$[Mn(L^4)(Bipy)(OAc)].H_2O$	-	3443_b	1683_s	1628_s	1588_s	1545_s	1329_s	1267_s	993_s	494_s	423_s
$[Fe(L^4)(Bipy)(SO_4)].H_2O$	-	3416_b	1667_m	1631_s	1591_s	1563_s	1371_s	1273_s	939_m	502_s	
$[Co(L^4)(Bipy)(OAc)]$	-	3430_b	-	1628_s	1586_s	1561_s	1371_s	1278_s	993_s	542_s	454_s
$[Ni(L^4)(Bipy)(OAc)].H_2O$	-	3194_b	-	1626_s	1586_s	1558_s	1443_m	1279_s	994_s	502_s	422_s
$[Cu(L^4)(Bipy)(OAc)].H_2O$	-	3430_m	1656_s	1627_s	1593_s	1560_s	1443_s	1259_s	984_s	527_m	440_m
$[Zn(L^4)(Bipy)(OAc)]$	-	-	-	1631_s	1584_s	1560_s	1476_m	1269_s	992_s	503_m	446_m

Key*: b = broad, s = sharp, d = doublet and m = medium*

Table 4.3.8. Infrared spectral (cm^{-1}) dataof HL^5 ligand and its metal(II) complexes

Compounds	*ν*NH	*ν*(OH)	*ν*(C=O)	*ν*(C=N)	*ν*(C=C)	*ν*(C-N)	*ν*(C-C)	*ν*(C-O)	δC-H	M-N	M-O
HL^5	3584_b	3336_b	1682_b	1651_b	1592_s	1556_s	1359_b	1268_s	982_s	-	-
$[Mn(L^5)_2].H_2O$	-	3415_b	1688_s	1655_s	1589_s	1544_s	1347_m	1270_s	988_s	564_s	459_s
$[Fe(L^5)_2(H_2O)].H_2O$	-	3422_b	1689_s	1633_b	1593_s	1563_s	1367_s	1269_s	991_s	563_s	482_s
$[Co(L^5)_2].2H_2O$	-	3335_b	1688_s	1640_m	1586_s	1562_s	1367_s	1269_s	992_s	562_s	482_s
$[Ni(L^5)_2(H_2O)_2]$	-	3330_b	1689_s	1634_m	1583_s	1557_s	1371_b	1272_s	991_s	530_s	483_s
$[Cu(L^5)_2]$	-	-	1688_s	1658_s	1586_s	1568_s	1376_s	1270_s	989_s	560_s	484_s
$[Zn(L^5)_2].H_2O$	-	3340_b	1689_s	1657_s	1593_s	1547_s	1351_s	1268_s	991_s	557_s	483_s

Key*: b = broad, s = sharp, d = doublet and m = medium*

Table 4.3.9. Infrared spectral (cm^{-1}) data of HL^5 ligand and its heteroleptic metal(II) complexes

Compounds	*ν*NH	*ν*(OH)	*ν*(C=O)	*ν*(C=N)	*ν*(C=C)	*ν*(C-N)	*ν*(C-C)	*ν*(C-O)	δC-H	M-N	M-O
HL^5	3584_b	3336_b	1682_b	1651_b	1592_s	1556_s	1359_b	1268_s	982_s	-	-
Bipy, $[C_{10}H_8N_2]$	-	-	-	1639_s	1580_s	1453_s	1349_s	-	991_s	-	-
$[Mn(L^5)(Bipy)(OAc)].H_2O$	-	3346_b	1685_s	1641_s	1588_s	1565_s	1364_s	1267_s	992_s	561_s	482_s
$[Fe(L^5)(Bipy)(SO_4)]$	-	-	1688_s	1638_s	1579_s	1557_s	1364_s	1268_s	990_s	530_s	445_s
$[Co(L^5)(Bipy)(OAc)].2H_2O$	-	3325_b	1689_s	1627_s	1582_s	1557_s	1364_s	1269_s	992_s	562_s	495_s
$[Ni(L^5)(Bipy)(OAc)].H_2O$	-	3167_b	1688_s	1626_s	1587_s	1558_s	1372_s	1275_s	992_s	562_s	458_s
$[Cu(L^5)(Bipy)(OAc)]$	-	-	1652_s	1627_s	1593_s	1560_s	1369_s	1260_s	984_s	560_s	460_s
$[Zn(L^5)(Bipy)(OAc)].H_2O$	-	3347_b	1688_s	1533_s	1584_s	1562_s	1366_s	1270_s	992_s	563_s	504_s

Key*: b = broad, s = sharp, d = doublet and m = medium*

Table 4.3.10. Infrared spectral (cm^{-1}) data of HL^6 ligand and its heteroleptic metal(II) complexes

Compounds	*ν*NH	*ν*(OH)	*ν*(C=O)	*ν*(C=N)	*ν*(C=C)	*ν*(C-N)	*ν*(C-C)	*ν*(C-O)	δC-H	M-N	M-O
HL^6	3539_b	-	1678_s	1641_s	1652_s	1579_s	1459_s	1384_s	982_s	-	-
Bipy, $[C_{10}H_8N_2]$	-	-	-	1639_s	1580_s	1453_s	1349_s	-	991_s	-	-
$[Mn(L^6)(Bipy)(OAc)]$	-	-	1683_s	1628_s	1583_s	1588_s	1442_s	1329_s	976_s	534_s	493_s
$[Fe(L^6)(Bipy)(SO_4)]$	-	3430_s	1674_s	1629_s	1591_s	1563_s	1475_s	1273_s	1015_s	501	457_s
$[Co(L^6)(Bipy)(OAc)]$	-	-	1669_s	1626_s	1581_s	1558_s	1475_s	1269_s	994_s	539_s	450_s
$[Ni(L^6)(Bipy)(OAc)]$	-	-	1671_s	1625_s	1586_s	1559_s	1476_s	1279_s	994_s	501_s	423_s
$[Cu(L^6)(Bipy)(OAc)].H_2O$	-	3434_b	1642_s	1617_m	1589_s	1542s	1445s	1273_s	976_s	551_s	490_s
$[Zn(L^6)(Bipy)(OAc)]$	-	-	1683_s	1632_s	1584_s	1561_s	1442_s	1270_s	992_s	504_s	421_s

Key*: b = broad, s = sharp, d = doublet and m = medium*

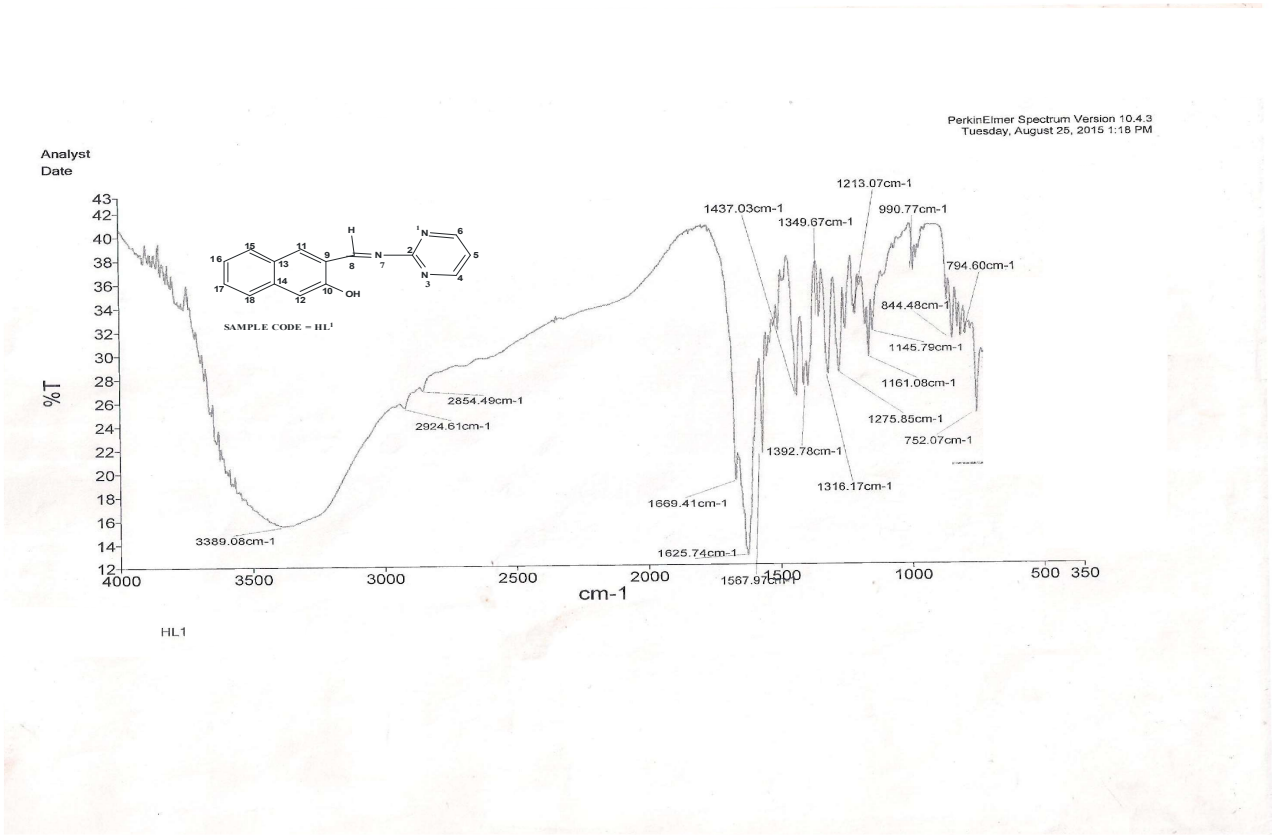

Figure 4.1.1: Infrared spectrum of HL^1 ligand

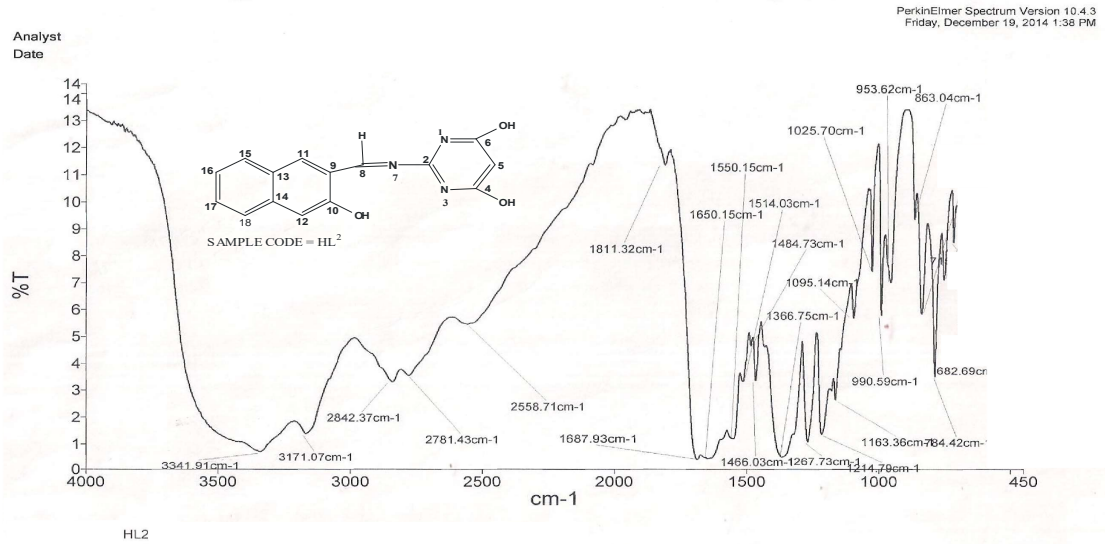

Figure 4.1.2: Infrared spectrum of HL^2 ligand

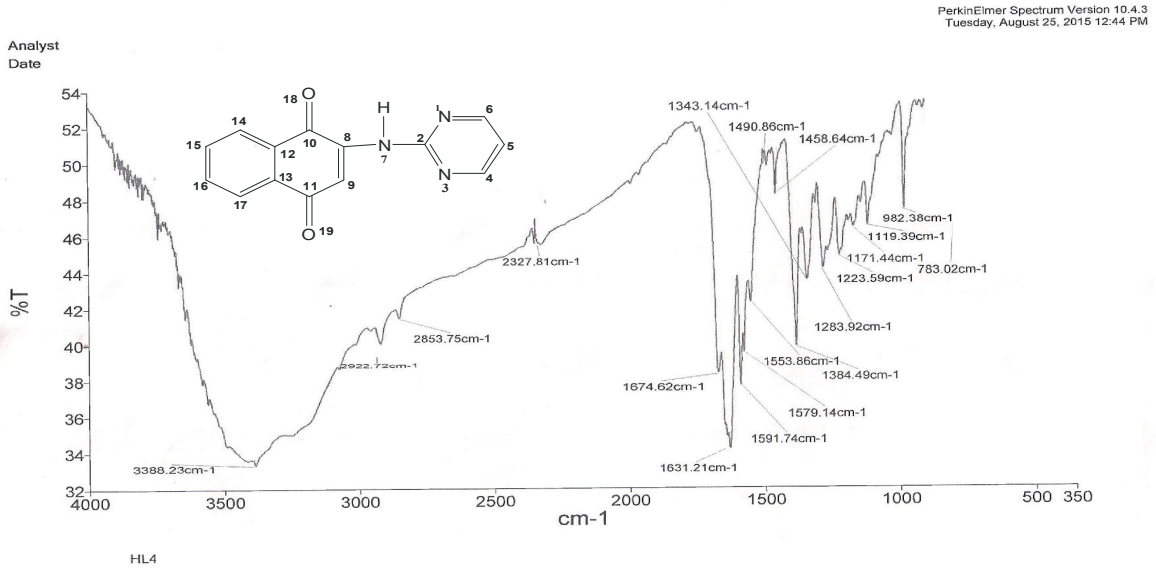

Figure 4.1.3: Infrared spectrum of HL^4 ligand

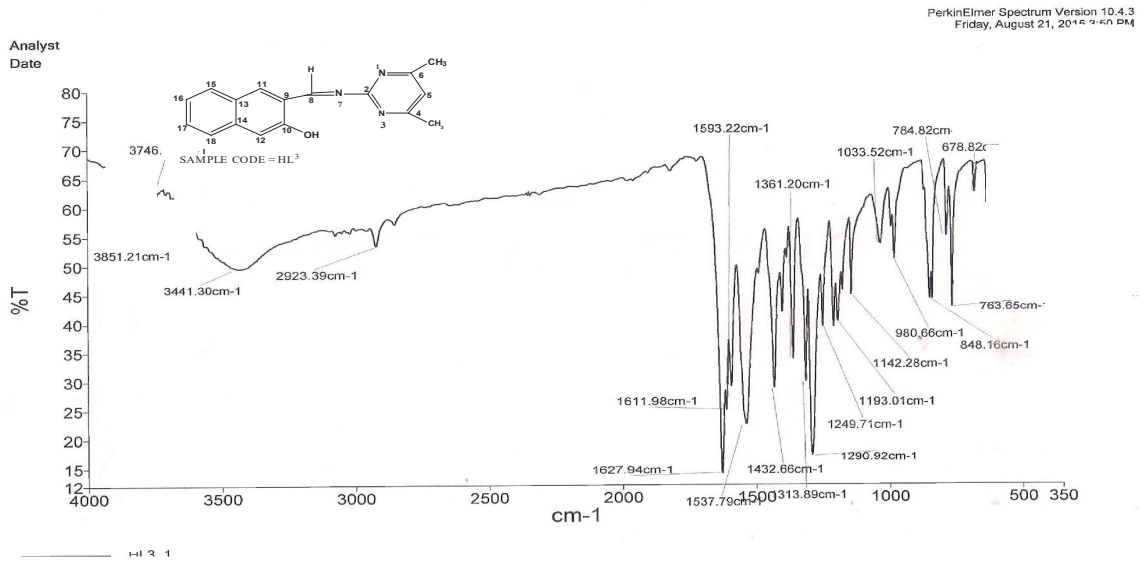

Figure 4.1.4: Infrared spectrum of HL^5 Ligand

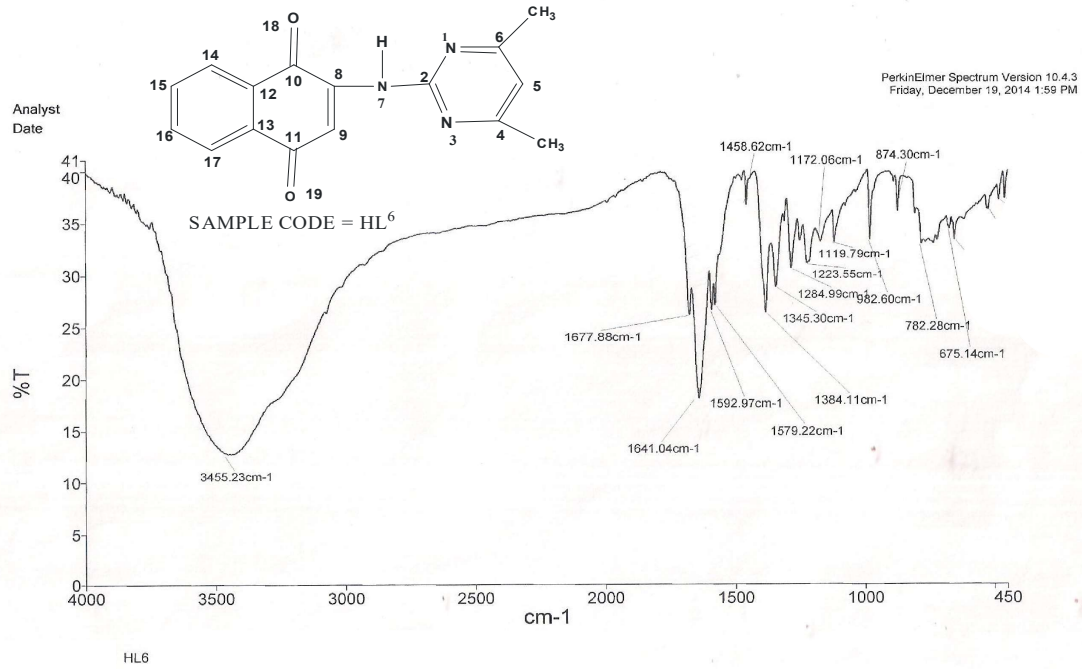

Figure 4.1.5: Infrared spectrum of HL^6ligand

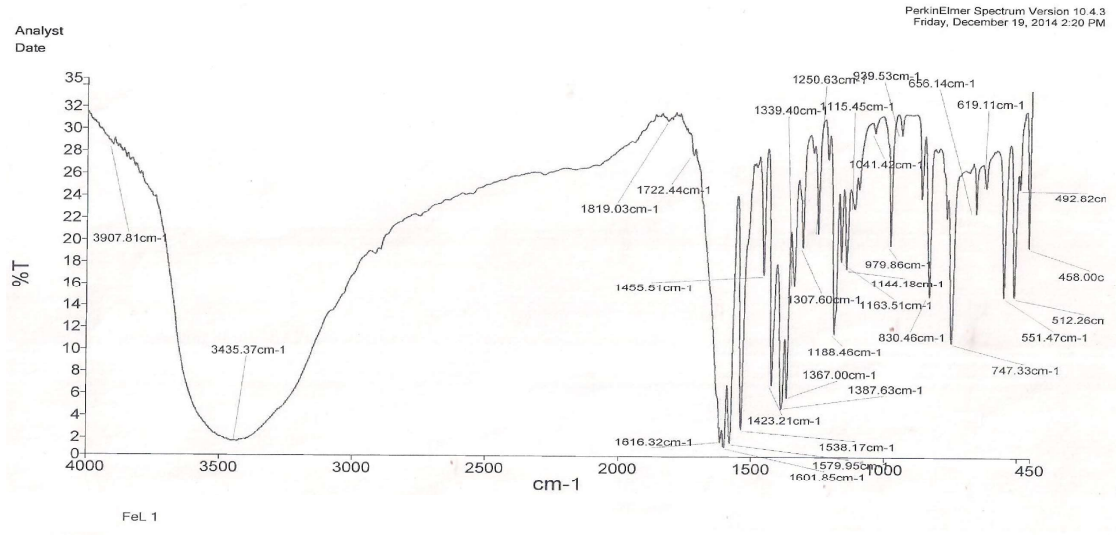

Figure 4.1.6: Infrared spectrum of FeL^1complex

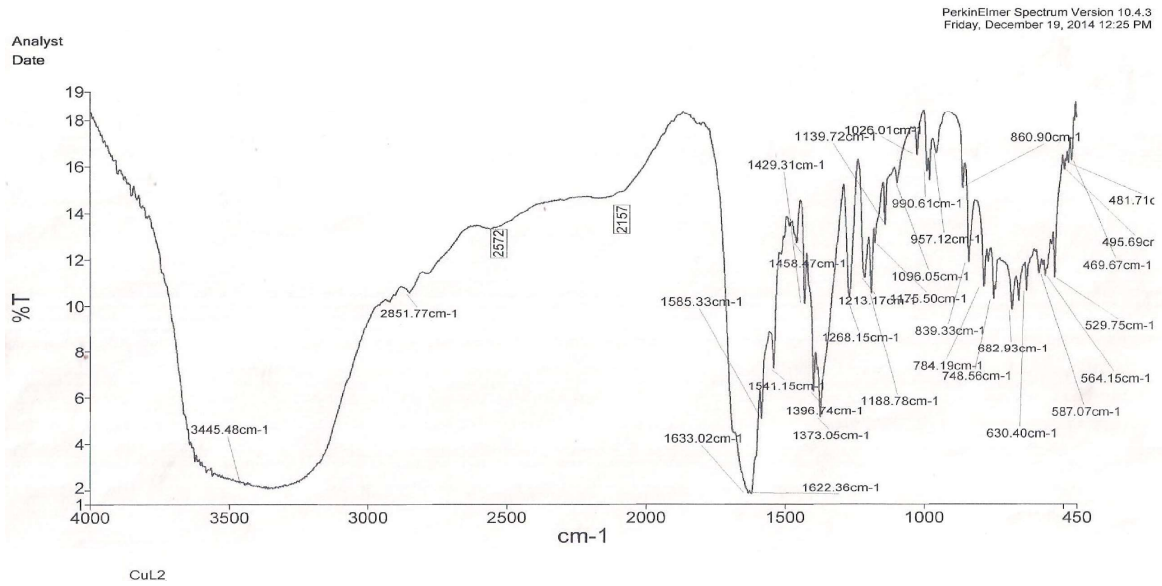

Figure 4.1.7: Infrared spectrum of CuL^2complex

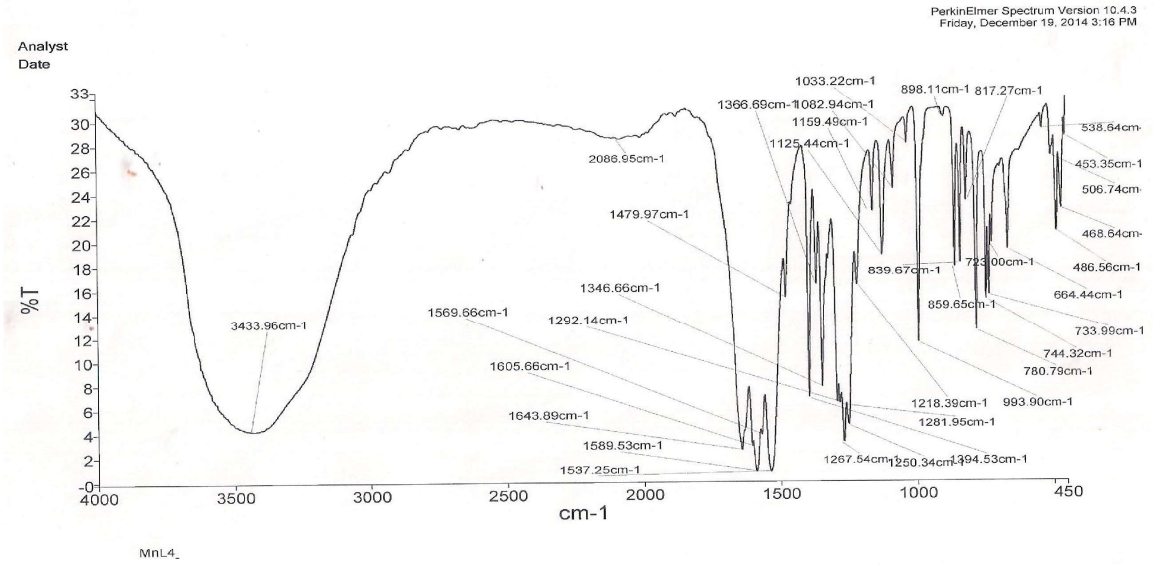

Figure 4.1.8: Infrared spectrum of MnL^4complex

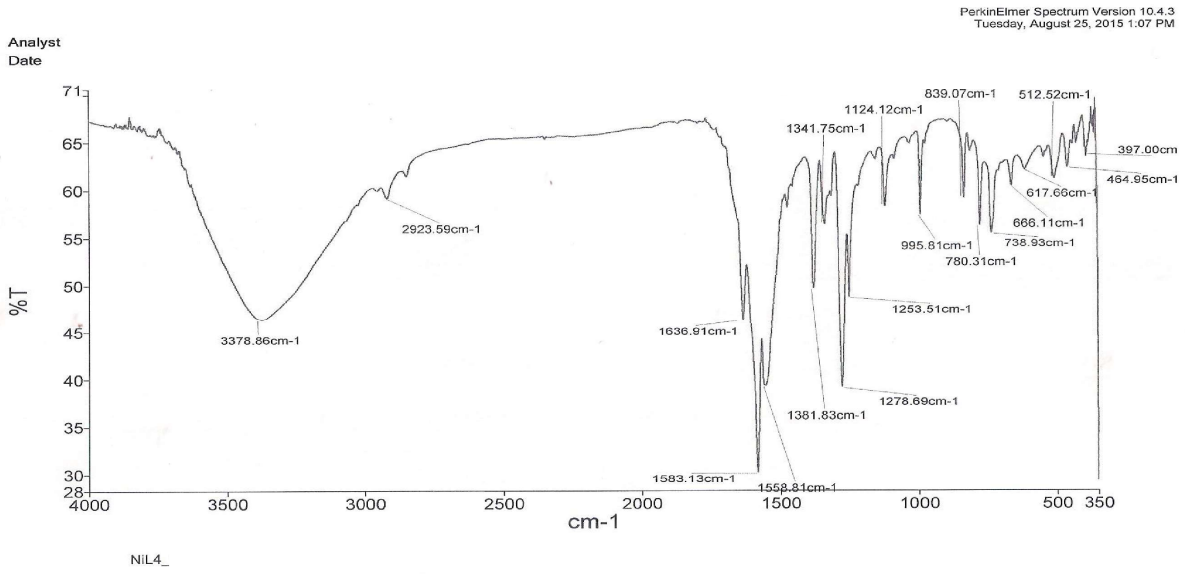

Figure 4.1.9: Infrared spectrum of NiL^4complex

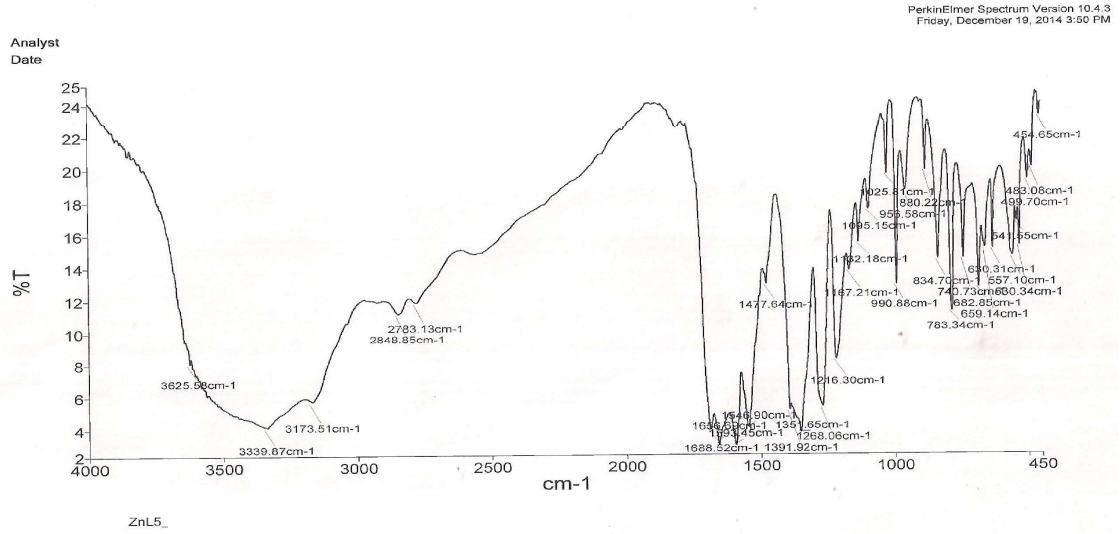

Figure 4.1.10: Infrared spectrum of ZnL^6complex

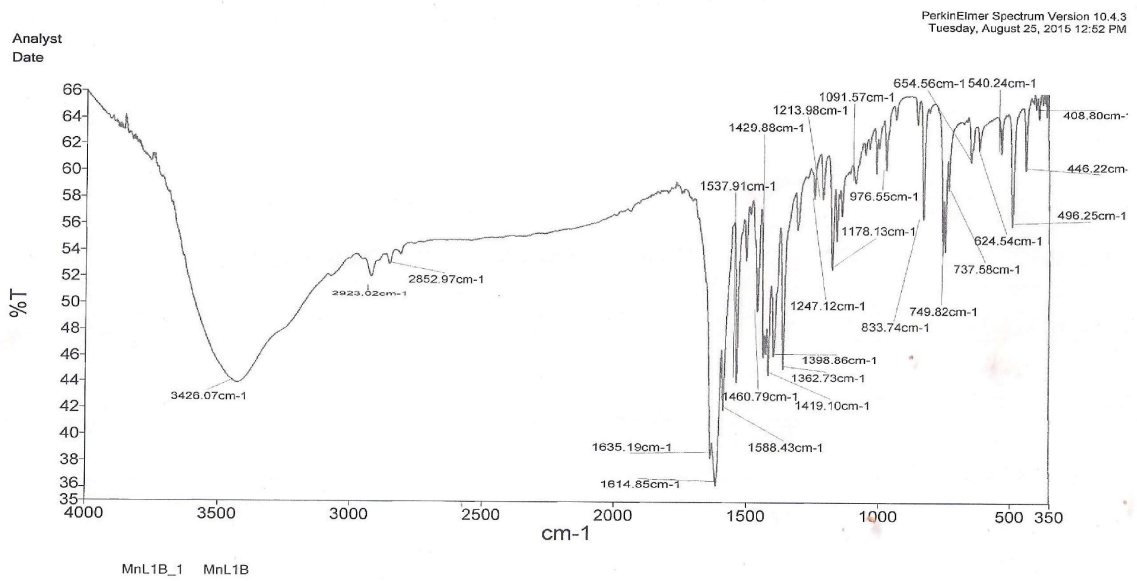

Figure 4.1.11: Infrared spectrum of MnL^1B complex

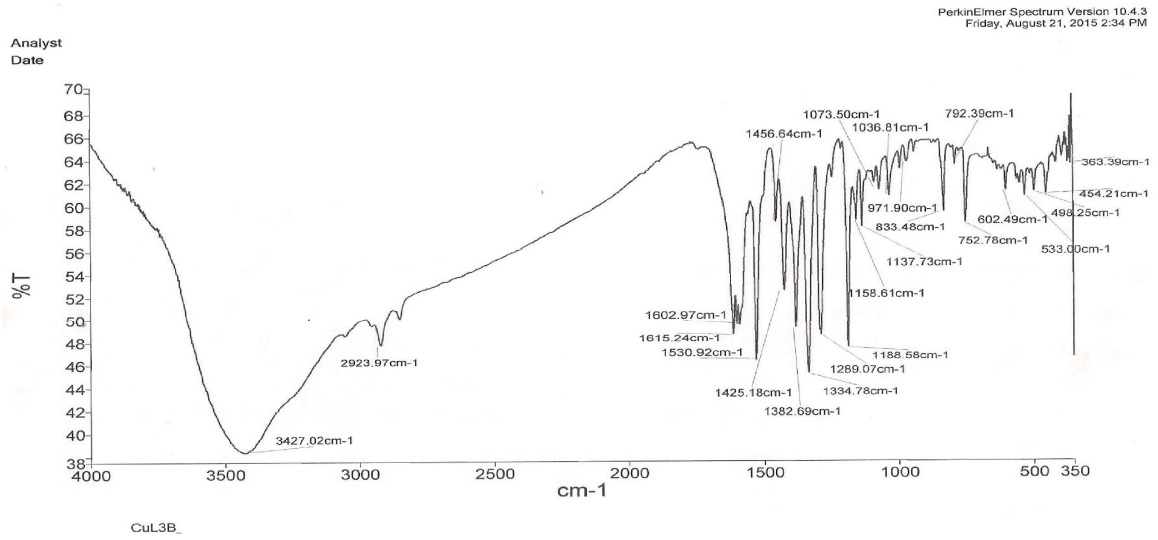

Figure 4.1.12: Infrared spectrum of CuL^3B complex

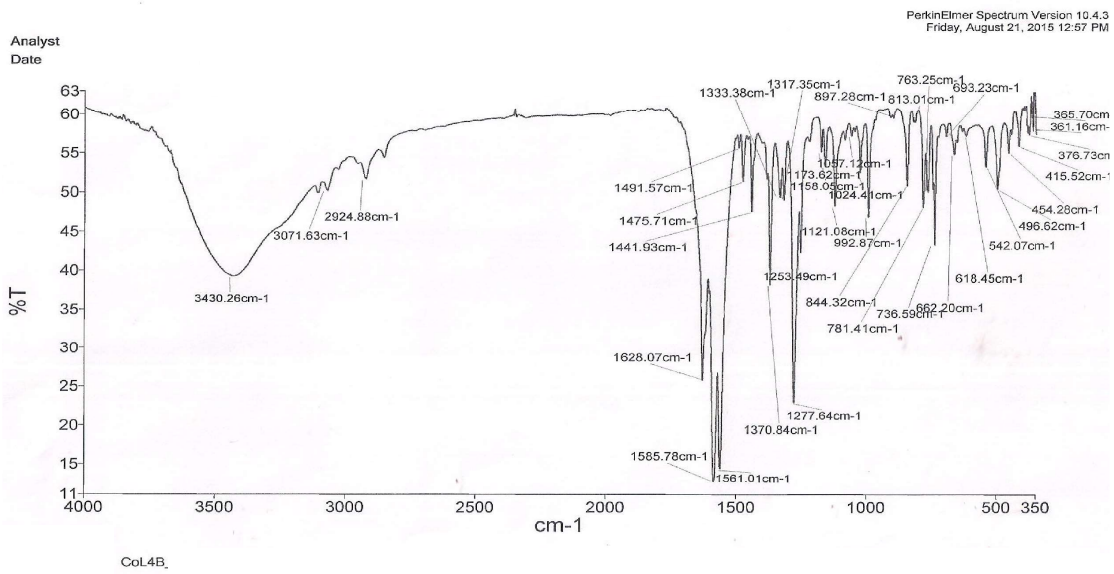

Figure 4.1.13: Infrared spectrum of CoL^4B complex

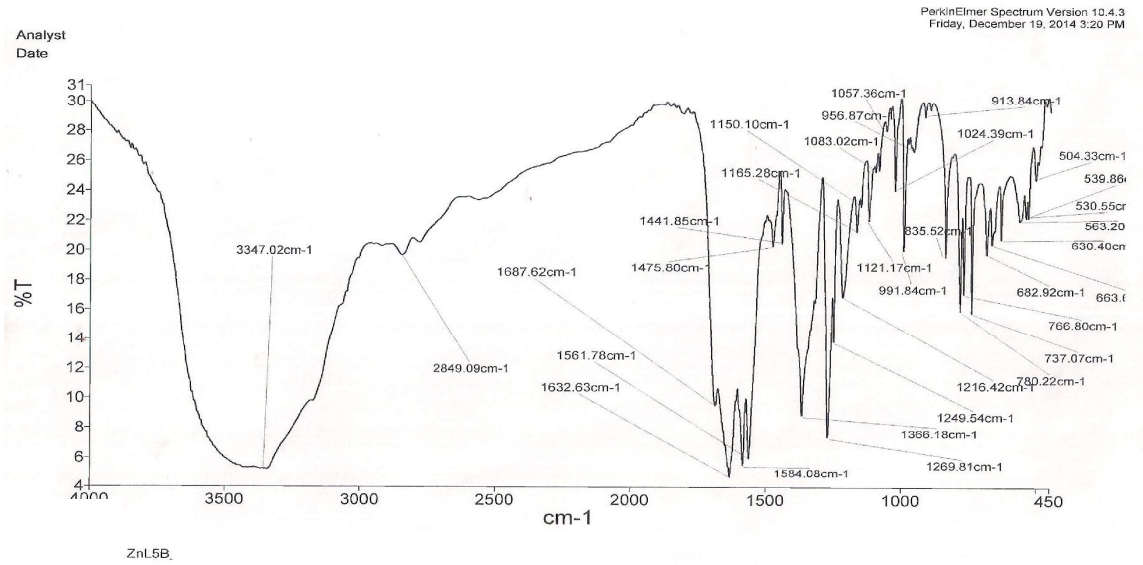

Figure 4.1.14: Infrared spectrum of ZnL^5B complex

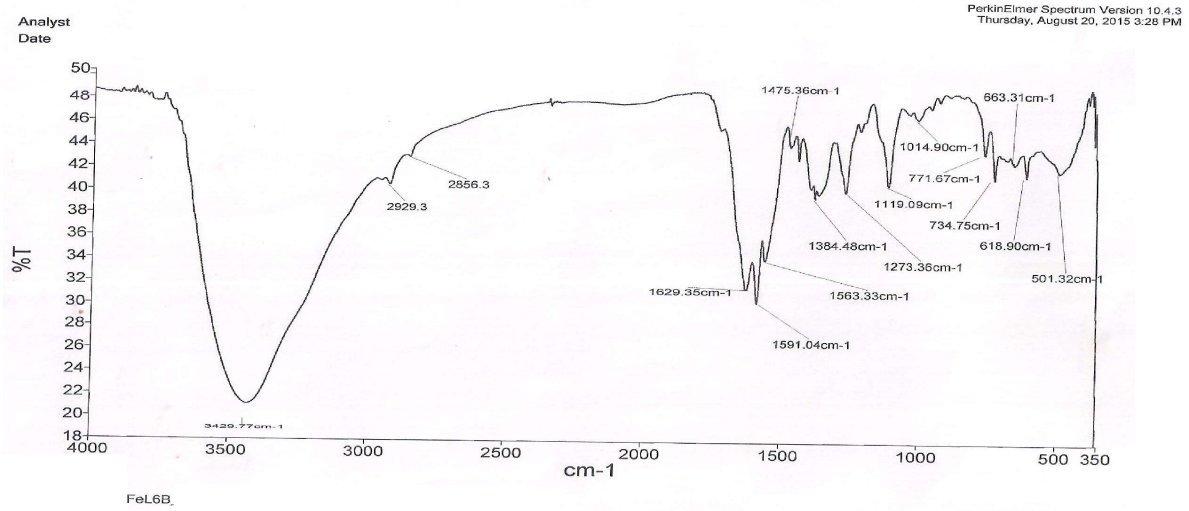

Figure 4.1.15: Infrared spectrum of $FeL^{6}B$ complex

Table 4.4.1. Electronic spectra data for HL^1 ligand and its metal(II) complexes

Compounds	Absorption Bands (cm^{-1})	Bands Assignment	Tentative Geometry
HL^1	33000, 38460	$\pi - \pi^*$	-
	27780	$n - \pi^*$	
	31640, 33330	$\pi - \pi^*$	
	26850	$n - \pi^*$	
$[Mn(L^1)_2].H_2O$	23980	$^6A_1 \rightarrow {}^4E_1(\nu_1)$	Tetrahedral
	12930	$^6A_1 \rightarrow {}^4A_1(\nu_2)$	
	31055	$\pi - \pi^*$	
	26309	$n - \pi^*$	
$[Fe(L^1)_2(H_2O)_2]$	22900, 21367	$^5T_{2g} \rightarrow {}^5A_{1g}$	Octahedral
	17760	$^5T_{2g} \rightarrow {}^5B_{1g}$	
	12770	$^5T_{2g} \rightarrow {}^5B_{2g}$	
	31350	$\pi \rightarrow \pi^*$	
	27397	$n \rightarrow \pi^*$	
$[Co(L^1)_2].2H_2O$	17544	$^4A_2 \rightarrow {}^4T_1(F)$	Tetrahedral
	13423	$^4A_2 \rightarrow {}^4T_1(P)$	
	43668	C.T	
	39215	$\pi \rightarrow \pi^*$	
$[Ni(L^1)_2].H_2O$	26147	$n \rightarrow \pi^*$	Tetrahedral
	23640	$^3T_1(F) \rightarrow {}^3T_2(F)$	
	20920	$^3T_1(F) \rightarrow {}^3A_2(F)$	
	13316	$^3T_1(F) \rightarrow {}^3T_1(P)$	
	37946	$\pi \rightarrow \pi^*$	
$[Cu(L^1)_2]$	28152, 25920	$n \rightarrow \pi^*$	Square Planar
	23585	$^2B_{1g} \rightarrow {}^2A_{1g}$	
	17513	$^2B_{1g} \rightarrow {}^2E_{1g}$	
	30096	$\pi \rightarrow \pi^*$	
$[Zn(L^1)_2]$	23697	$n \rightarrow \pi^*$	
	18083	$M \rightarrow L$	Tetrahedral

Table 4.4.2. Electronic Spectra Data of HL^1 ligand and its Heteroleptic Metal(II) Complexes

Compounds	Absorption Bands (cm^{-1})	Bands Assignment	Tentative Geometry
HL^1	33000, 38460	$\pi - \pi^*$	
	27780	$n - \pi^*$	
	30487	$\pi \rightarrow \pi^*$	-
	28011	$n - \pi^*$	
$[Mn(L^1)(Bipy)(OAc)]$	18018	$^6A_{1g} \rightarrow {}^4T_{1g}$,	Octahedral
	14430	$^6A_{1g} \rightarrow {}^4T_{2g}(G)$,	
	12562	$^6A_{1g} \rightarrow {}^4E_g(G)$	
	45662	C.T	
$[Fe(L^1)(Bipy)(SO_4)]$	34843	$\pi - \pi^*$	
	21978	$^5T_{2g} \rightarrow {}^5A_{1g}$	Octahedral
	17762	$^5T_{2g} \rightarrow {}^5B_{1g}$	
	34843, 32490	$\pi \rightarrow \pi^*$	
	27867, 25052	$n \rightarrow \pi^*$	
$[Co(L^1)(Bipy)(OAc)].H_2O$	23474	$^4T_{1g} \rightarrow {}^4T_{2g}$	
	17699	$^4T_{1g} \rightarrow {}^4A_{2g}$	Octahedral
	12804	$^4T_1 \rightarrow {}^4T_{1g}(P)$	
	37269, 33578	$\pi \rightarrow \pi^*$	
	25010	$n \rightarrow \pi^*$	
$[Ni(L^1)(Bipy)(OAc)].H_2O$	23048	$^3A_{2g} \rightarrow {}^3T_{2g}(F)$	Octahedral
	18083	$^3A_{2g} \rightarrow {}^3T_{1g}(F)$	
	11962	$^3A_{2g} \rightarrow {}^3T_{1g}(P)$	
	47619	C.T.	
$[Cu(L^1)(Bipy)(OAc)]$	32154, 30300	$\pi \rightarrow \pi^*$	
	26510	$n \rightarrow \pi^*$	Octahedral
	16807	$^2E_g \rightarrow {}^2T_{2g}$	
	33003	$\pi \rightarrow \pi^*$	
$[Zn(L^1)(Bipy)(OAc)].2H_2O$	25245	$n \rightarrow \pi^*$	
	23094, 19157	$M \rightarrow L$	Octahedral

Table 4.4.3. Electronic spectra data for HL^2 ligand and its metal(II) complexes

Compounds	Absorption Bands (cm^{-1})	Bands Assignment	Tentative Geometry
HL^2			
	48309, 45248	C.T	
	30487	$\pi - \pi^*$	
$[Mn(L^2)_2].2H_2O$	28335	$n - \pi^*$	Tetrahedral
	17065	$^6A_1 \rightarrow {}^4E_1(\nu_1)$	
	11920	$^6A_1 \rightarrow {}^4A_1(\nu_2)$	
	36231, 31152	$\pi \rightarrow \pi^*$	
$[Fe(L^2)_2].2H_2O$	26525	$n - \pi^*$	Tetrahedral
	18116, 16295	$^5E \rightarrow {}^5T_2$	
	48544, 44843	C.T	
	30675	$\pi \rightarrow \pi^*$	
$[Co(L^2)_2].H_2O$	26455	$n \rightarrow \pi^*$	Tetrahedral
	18519	$^4A_2 \rightarrow {}^4T_1(F)$	
	13298	$^4A_2 \rightarrow {}^4T_1(P)$	
	36828, 30120	$\pi \rightarrow \pi^*$	
	26525	$n \rightarrow \pi^*$	
$[Ni(L^2)_2].H_2O$	23529	$^3T_1(F) \rightarrow {}^3T_2(F)$	Tetrahedral
	18116	$^3T_1(F) \rightarrow {}^3A_2(F)$	
	11723	$^3T_1(F) \rightarrow {}^3T_1(P)$	
	31582	$\pi \rightarrow \pi^*$	
	26512	$n \rightarrow \pi^*$	
$[Cu(L^2)_2]$	23855	$^2B_{1g} \rightarrow {}^2A_{1g}$	Square Planar
	17182	$^2B_{1g} \rightarrow {}^2E_{1g}$	
	36232	$\pi \rightarrow \pi^*$	
$[Zn(L^2)_2]$	20121	$n \rightarrow \pi^*$	Tetrahedral
	13175	M→L	

Table 4.4.4. Electronic spectra data for HL^2 ligand and its heteroleptic metal(II) complexes

Compounds	Absorption Bands (cm^{-1})	Bands Assignment	Tentative Geometry
HL^2	37100, 31646	$\pi - \pi^*$	
	27933	$n - \pi^*$	-
	47393, 42194	C.T	
	37200, 33040	$\pi \rightarrow \pi^*$	
$[Mn(L^2)(Bipy)(OAc)].H_2O$	22990, 21770	$^6A_{1g} \rightarrow {}^4T_{1g}$,	Octahedral
	15660	$^6A_{1g} \rightarrow {}^4T_{2g}(G)$,	
	12450	$^6A_{1g} \rightarrow {}^4E_g(G)$	
	37910	$\pi - \pi^*$	
$[Fe(L^2)(Bipy)(SO_4)].H_2O$	26018	$n - \pi^*$	
	18080, 18975	$^5T_{2g} \rightarrow {}^5A_{1g}$	Octahedral
	15723	$^5T_{2g} \rightarrow {}^5B_{1g}$	
	31348	$\pi \rightarrow \pi^*$	
$[Co(L^2)(Bipy)(OAc)]$	26497	$n \rightarrow \pi^*$	Octahedral
	17182	$^4T_{1g} \rightarrow {}^4A_{2g}$	
	12903	$^4T_1 \rightarrow {}^4T_{1g}(P)$	
	41629	C.T.	
	34076	$\pi \rightarrow \pi^*$	
$[Ni(L^2)(Bipy)(OAc)].H_2O$	25507	$n \rightarrow \pi^*$	Octahedral
	23364	$^3A_{2g} \rightarrow {}^3T_{2g}(F)$	
	16019	$^3A_{2g} \rightarrow {}^3T_{1g}(F)$	
	12766	$^3A_{2g} \rightarrow {}^3T_{1g}(P)$	
	44843	C.T.	
$[Cu(L^2)(Bipy)(OAc)].H_2O$	32809	$\pi \rightarrow \pi^*$	
	25100	$n \rightarrow \pi^*$	Octahedral
	21739, 17271	$^2E_g \rightarrow {}^2T_{2g}$	
	39525, 30487	$\pi \rightarrow \pi^*$	
$[Zn(L^2)(Bipy)(OAc)]$	25356	$n \rightarrow \pi^*$	Octahedral
	17452, 13072	M→L	

Table 4.4.5. Electronic spectra data for HL^3 ligand and its heteroleptic metal(II) complexes

Compounds	Absorption Bands (cm^{-1})	Bands Assignment	Tentative Geometry
HL^3	32362	$\pi - \pi^*$	-
	29019	$n - \pi^*$	
	35087, 31545	$\pi \rightarrow \pi^*$	
	27100	$n - \pi^*$	
$[Mn(L^3)(Bipy)(OAc)]$	23809	$^6A_{1g} \rightarrow {}^4T_{1g}$,	Octahedral
	14970	$^6A_{1g} \rightarrow {}^4T_{2g}(G)$,	
	12840	$^6A_{1g} \rightarrow {}^4E_g(G)$	
	44052	C.T	
	39682, 30769	$\pi - \pi^*$	
$[Fe(L^3)(Bipy)(SO_4)].H_2O$	26607	$n - \pi^*$	Octahedral
	22727	$^5T_{2g} \rightarrow {}^5A_{1g}$	
	18904	$^5T_{2g} \rightarrow {}^5B_{1g}$	
	31518	$\pi \rightarrow \pi^*$	
$[Co(L^3)(Bipy)(OAc)]$	29219	$n \rightarrow \pi^*$	Octahedral
	22422	$^4T_{1g} \rightarrow {}^4A_{2g}$	
	15015	$^4T_1 \rightarrow {}^4T_{1g}(P)$	
	31830	$\pi \rightarrow \pi^*$	
$[Ni(L^3)(Bipy)(OAc)]$	26018	$n \rightarrow \pi^*$	
	22220	$^3A_{2g} \rightarrow {}^3T_{2g}(F)$	Octahedral
	18915	$^3A_{2g} \rightarrow {}^3T_{1g}(F)$	
	13280	$^3A_{2g} \rightarrow {}^3T_{1g}(P)$	
	36190	$\pi \rightarrow \pi^*$	
$[Cu(L^3)(Bipy)(OAc)]$	25216	$n \rightarrow \pi^*$	
	22371, 17065	$^2E_g \rightarrow {}^2T_{2g}$	Octahedral
	31949	$\pi \rightarrow \pi^*$	
$[Zn(L^3)(Bipy)(OAc)].H_2O$	26290	$n \rightarrow \pi^*$	Octahedral
	23419	$M \rightarrow L$	

Table 4.4.6. Electronic spectra data for HL^4 ligand and its metal(II) complexes

Compounds	Absorption Bands (cm^{-1})	Bands Assignment	Tentative Geometry
HL^4	39361, 36765	$\pi - \pi^*$	-
	28653, 25356	$n - \pi$	
	30485	$\pi - \pi^*$	
$[Mn(L^4)_2].H_2O$	25864	$n - \pi$	
	17793	$^6A_1 \rightarrow {}^4E_1(\nu_1)$	Tetrahedral
	41813	C.T	
$[Fe(L^4)_2].2H_2O$	30000	$\pi \rightarrow \pi^*$	Tetrahedral
	26195	$n - \pi^*$	
	20161	$^5E \rightarrow {}^5T_2$	
	37174, 30488	$\pi \rightarrow \pi^*$	
$[Co(L^4)_2].H_2O$	26316	$n \rightarrow \pi^*$	
	19417	$^4A_2 \rightarrow {}^4T_1(F)$	Tetrahedral
	13263	$^4A_2 \rightarrow {}^4T_1(P)$	
	34484	$\pi \rightarrow \pi^*$	
$[Ni(L^4)_2].H_2O$	28096, 25109	$n \rightarrow \pi^*$	
	20195	$^3T_1(F) \rightarrow {}^3T_2(F)$	Tetrahedral
	18183	$^3T_1(F) \rightarrow {}^3A_2(F)$	
	12771	$^3T_1(F) \rightarrow {}^3T_1(P)$	
	35087	$\pi \rightarrow \pi^*$	
$[Cu(L^4)_2]$	25356	$n \rightarrow \pi^*$	
	19493	$B_{1g} \rightarrow {}^2A_{1g}$	Square Planar
	13158	$^2B_{1g} \rightarrow {}^2E_{1g}$	
	32845	$\pi \rightarrow \pi^*$	
$[Zn(L^4)_2].H_2O$	277920	$n \rightarrow \pi^*$	Tetrahedral
	17575, 12970	$M \rightarrow L$	

Table 4.4.7. Electronic spectra data for HL^4 ligand and its Heteroleptic metal(II) complexes

Compounds	Absorption Bands (cm^{-1})	Bands Assignment	Tentative Geometry
HL^4	39361, 36765	$\pi - \pi^*$	-
	28653, 25356	$n - \pi$	
	36101, 30674	$\pi \rightarrow \pi^*$	
	27846	$n - \pi$	
$[Mn(L^4)(Bipy)(OAc)].H_2O$	23585	$^6A_{1g} \rightarrow {}^4T_{1g}$,	Octahedral
	14577	$^6A_{1g} \rightarrow {}^4T_{2g}(G)$,	
	11480	$^6A_{1g} \rightarrow {}^4E_g(G)$	
	46948, 44843	C.T	
	35971, 31545	$\pi - \pi^*$	
$[Fe(L^4)(Bipy)(SO_4)].H_2O$	25924	$n - \pi^*$	Octahedral
	18832	$^5T_{2g} \rightarrow {}^5A_{1g}$	
	12578	$^5T_{2g} \rightarrow {}^5B_{1g}$	
	42918	C.T	
$[Co(L^4)(Bipy)(OAc)]$	35762	$\pi \rightarrow \pi^*$	
	28276, 25057	$n \rightarrow \pi^*$	Octahedral
	17241	$^4T_{1g} \rightarrow {}^4A_{2g}$	
	12820	$^4T_1 \rightarrow {}^4T_{1g}(P)$	
	46948	C.T.	
	34843, 30429	$\pi \rightarrow \pi^*$	
$[Ni(L^4)(Bipy)(OAc)].H_2O$	26491	$n \rightarrow \pi^*$	Octahedral
	18382	$^3A_{2g} \rightarrow {}^3T_{2g}(F)$	
	14598	$^3A_{2g} \rightarrow {}^3T_{1g}(F)$	
	12315	$^3A_{2g} \rightarrow {}^3T_{1g}(P)$	
	35564	$\pi \rightarrow \pi^*$	
$[Cu(L^4)(Bipy)(OAc)].H_2O$	28736, 26455	$n \rightarrow \pi^*$	Octahedral
	21786, 17123	$^2E_g \rightarrow {}^2T_{2g}$	
	34793	$\pi \rightarrow \pi^*$	
$[Zn(L^4)(Bipy)(OAc)]$	27247	$n \rightarrow \pi^*$	Octahedral
	20450	$M \rightarrow L$	

Table 4.4.8: Electronic spectra data for HL^5 ligand and its metal(II) complexes

Compounds	Absorption Bands (cm^{-1})	Bands Assignment	Tentative Geometry
HL^5	37394, 30919	$\pi - \pi^*$	-
	28859, 25182	$n - \pi^*$	
	38910, 35348	$\pi - \pi^*$	
$[Mn(L^5)_2].H_2O$	26719, 25051	$n - \pi^*$	
	19685	$^6A_1 \rightarrow {}^4E_1(\nu_1)$	Tetrahedral
	13550	$^6A_1 \rightarrow {}^4A_1(\nu_2)$	
$[Fe(L^5)_2].2H_2O$	48076	C.T	
	35914	$\pi \rightarrow \pi^*$	Tetrahedral
	20325	$^5E \rightarrow {}^5T_2$	
	33626	$\pi \rightarrow \pi^*$	
$[Co(L^5)_2].2H_2O$	28653, 25182	$n \rightarrow \pi^*$	
	19841	$^4A_2 \rightarrow {}^4T_1(F)$	Tetrahedral
	11952	$^4A_2 \rightarrow {}^4T_1(P)$	
	46948	C.T.	
$[Ni(L^5)_2(H_2O)_2]$	34965	$\pi \rightarrow \pi^*$	
	25051	$n \rightarrow \pi^*$	Octahedral
	19493	$^3A_{2g} \rightarrow {}^3T_{2g}(F)$	
	14030	$^3A_{2g} \rightarrow {}^3T_{1g}(F)$	
	12987	$^3A_{2g} \rightarrow {}^3T_{1g}(P)$	
	32928	$\pi \rightarrow \pi^*$	
$[Cu(L^5)_2]$	26316, 25596	$\pi \rightarrow \pi^*$	Square Planar
	19342	$B_{1g} \rightarrow {}^2A_{1g}$	
	12095	$^2B_{1g} \rightarrow {}^2E_{1g}$	
	33405	$\pi \rightarrow \pi^*$	
$[Zn(L^5)_2].H_2O$	24900	$n \rightarrow \pi^*$	Tetrahedral
	19880	$M \rightarrow L$	

Table 4.4.9. Electronic spectra data for HL^5 ligand and its heteroleptic metal(II) complexes

Compounds	Absorption Bands (cm^{-1})	Bands Assignment	Tentative Geometry
HL^5	37394, 30919	$\pi - \pi^*$	
	28859, 25182	$n - \pi^*$	-
	34943, 30487	$\pi - \pi^*$	
	26315	$n - \pi^*$	
$[Mn(L^5)(Bipy)(OAc)].H_2O$	18552, 17629	$^6A_{1g} \rightarrow {}^4T_{1g}$,	Octahedral
	15650	$^6A_{1g} \rightarrow {}^4T_{2g}(G)$,	
	12610	$^6A_{1g} \rightarrow {}^4E_g(G)$	
	31220, 30581	$\pi - \pi^*$	
	28743, 25015	$n - \pi^*$	
$[Fe(L^5)(Bipy)(SO_4)]$	24252	$^5T_{2g} \rightarrow {}^5A_{1g}$	Octahedral
	18904	$^5T_{2g} \rightarrow {}^5B_{1g}$	
	37037, 30000	$\pi \rightarrow \pi^*$	
$[Co(L^5)(Bipy)(OAc)].2H_2O$	26303	$\pi \rightarrow \pi^*$	Octahedral
	19841	$^4T_{1g} \rightarrow {}^4A_{2g}$	
	12195	$^4T_1 \rightarrow {}^4T_{1g}(P)$	
	45248, 41841	C.T.	
$[Ni(L^5)(Bipy)(OAc)].H_2O$	34809	$\pi \rightarrow \pi^*$	
	29850, 26385	$n \rightarrow \pi^*$	Octahedral
	19268	$^3A_{2g} \rightarrow {}^3T_{2g}(F)$	
	16030	$^3A_{2g} \rightarrow {}^3T_{1g}(F)$	
	13004	$^3A_{2g} \rightarrow {}^3T_{1g}(P)$	
	43290	C.T.	
$[Cu(L^5)(Bipy)(OAc)]$	30211	$\pi \rightarrow \pi^*$	
	26455	$n \rightarrow \pi^*$	Octahedral
	21505, 17668	$^2E_g \rightarrow {}^2T_{2g}$	
	30864	$\pi \rightarrow \pi^*$	
$[Zn(L^5)(Bipy)(OAc)].H_2O$	26455	$n \rightarrow \pi^*$	Octahedral
	19960	$M \rightarrow L$	

Table 4.4.10. Electronic spectra data for HL^6 ligand and its heteroleptic metal(II) complexes

Compounds	Absorption Bands (cm^{-1})	Bands Assignment	Tentative Geometry
HL^6	33578, 30030	$\pi - \pi^*$	-
	26247, 22182	$n - \pi^*$	
	46082	C.T	
	38167, 32719	$\pi - \pi^*$	
$[Mn(L^6)(Bipy)(OAc)]$	25761	$n - \pi^*$	Octahedral
	21368	$^6A_{1g} \rightarrow {}^4T_{1g}$,	
	16077	$^6A_{1g} \rightarrow {}^4T_{2g}(G)$,	
	12658	$^6A_{1g} \rightarrow {}^4E_g(G)$	
	36828, 31220	$\pi - \pi^*$	
	26881, 24032	$n - \pi^*$	
$[Fe(L^6)(Bipy)(SO_4)]$	22758	$^5T_{2g} \rightarrow {}^5A_{1g}$	Octahedral
	19157	$^5T_{2g} \rightarrow {}^5B_{1g}$	
	12594	$^5T_{2g} \rightarrow {}^5B_{2g}$	
	38023, 32835	$\pi \rightarrow \pi^*$	
$[Co(L^6)(Bipy)(OAc)]$	42012	$\pi \rightarrow \pi^*$	Octahedral
	18382	$^4T_{1g} \rightarrow {}^4T_{1g}$	
	12642	$^4T_{1g} \rightarrow {}^4A_{2g}$	
	11080	$^4T_1 \rightarrow {}^4T_{1g}(P)$	
	36900	$\pi \rightarrow \pi^*$	
$[Ni(L^6)(Bipy)(OAc)]$	25356	$n \rightarrow \pi^*$	
	18018	$^3A_{2g} \rightarrow {}^3T_{2g}(F)$	Octahedral
	15810	$^3A_{2g} \rightarrow {}^3T_{1g}(F)$	
	12460	$^3A_{2g} \rightarrow {}^3T_{1g}(P)$	
	44642	C.T.	
$[Cu(L^6)(Bipy)(OAc)].H_2O$	33112, 31949	$\pi \rightarrow \pi^*$	
	26296	$n \rightarrow \pi^*$	Octahedral
	21413	$^2E_g \rightarrow {}^2T_{2g}$	
$[Zn(L^6)(Bipy)(OAc)]$	35045	$\pi \rightarrow \pi^*$	
	26880	$n \rightarrow \pi^*$	Octahedral
	20040	M→L	

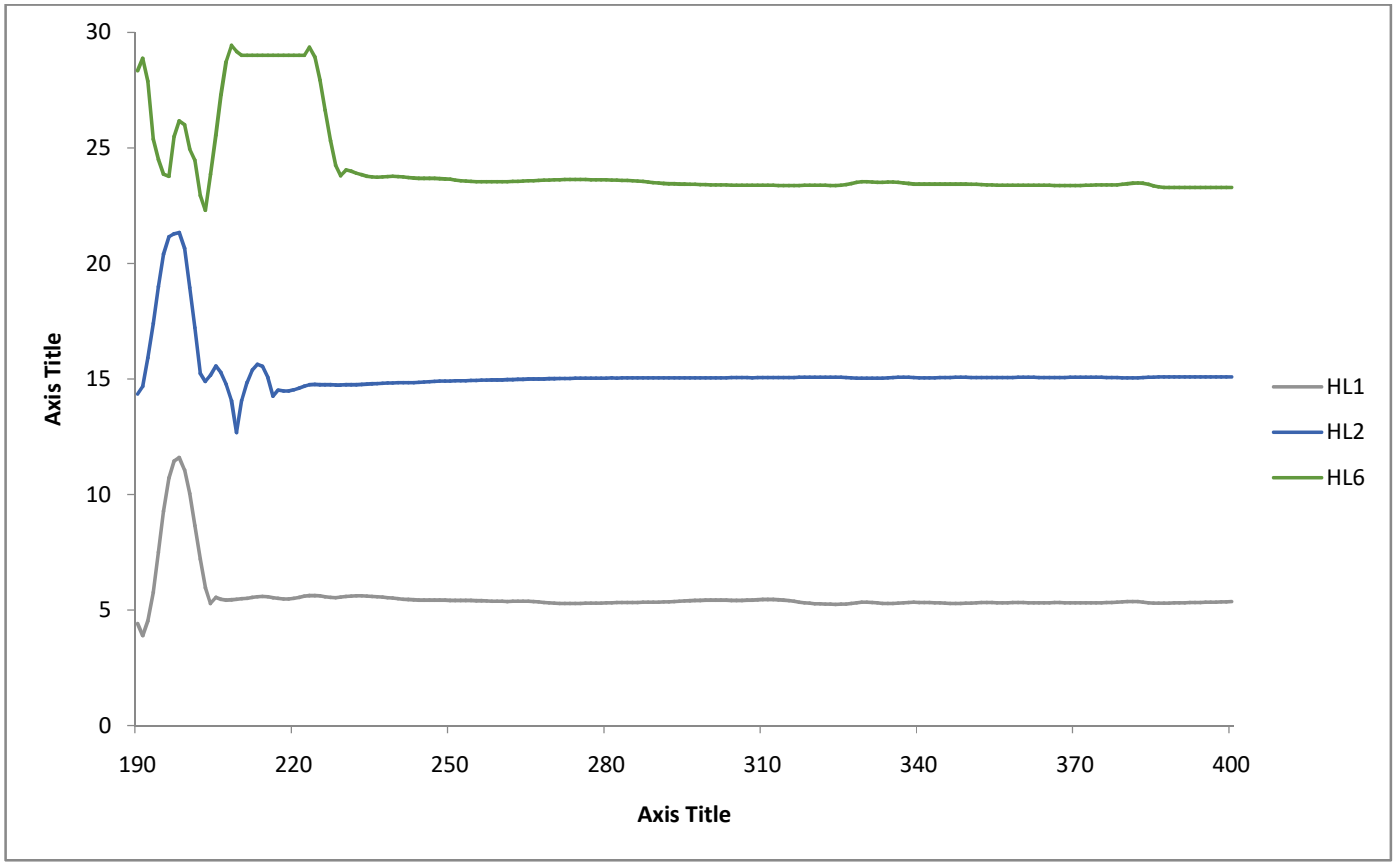

Figure 4.2.1. Ultraviolet spectra of HL^1, HL^2 and HL^6 ligands

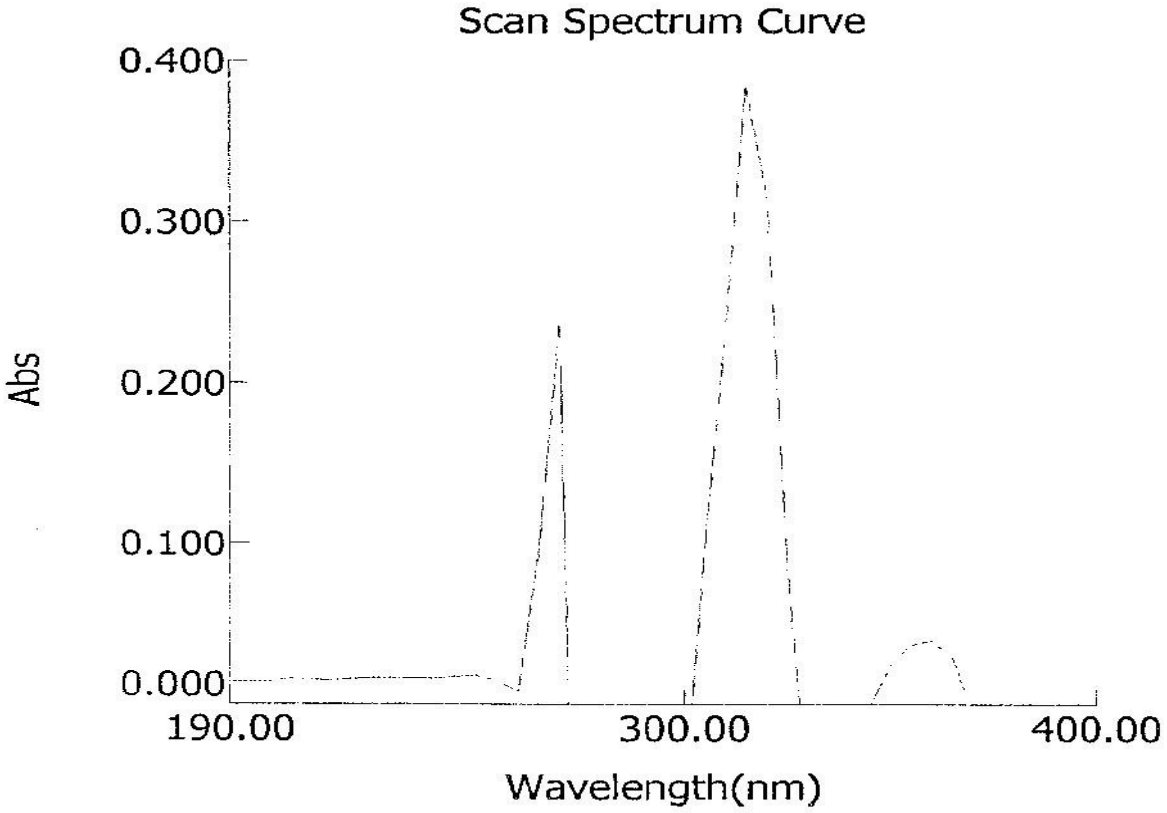

Figure 4.2.2. Ultraviolet spectrum of heteroleptic $[Co(L^1)(Bipy)(OAc)].H_2O$ complex

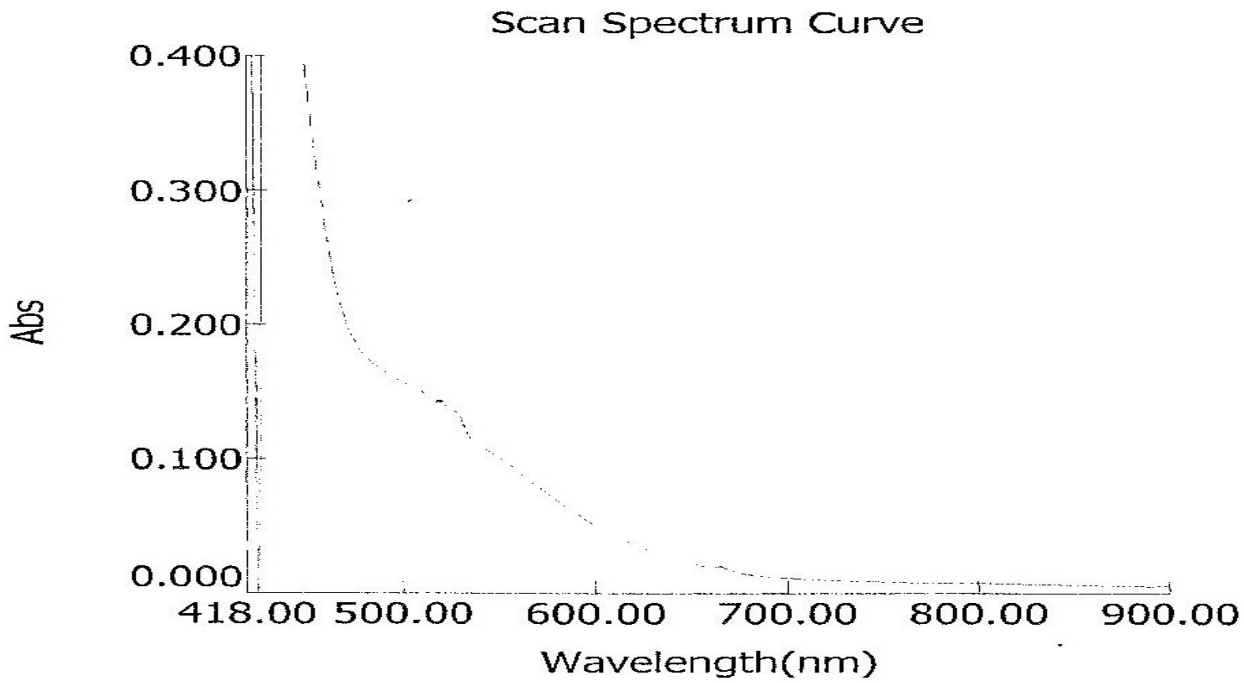

Figure 4.2.3. Visible spectrum of $[Co(L^1)2].{}_2H_2O$complex

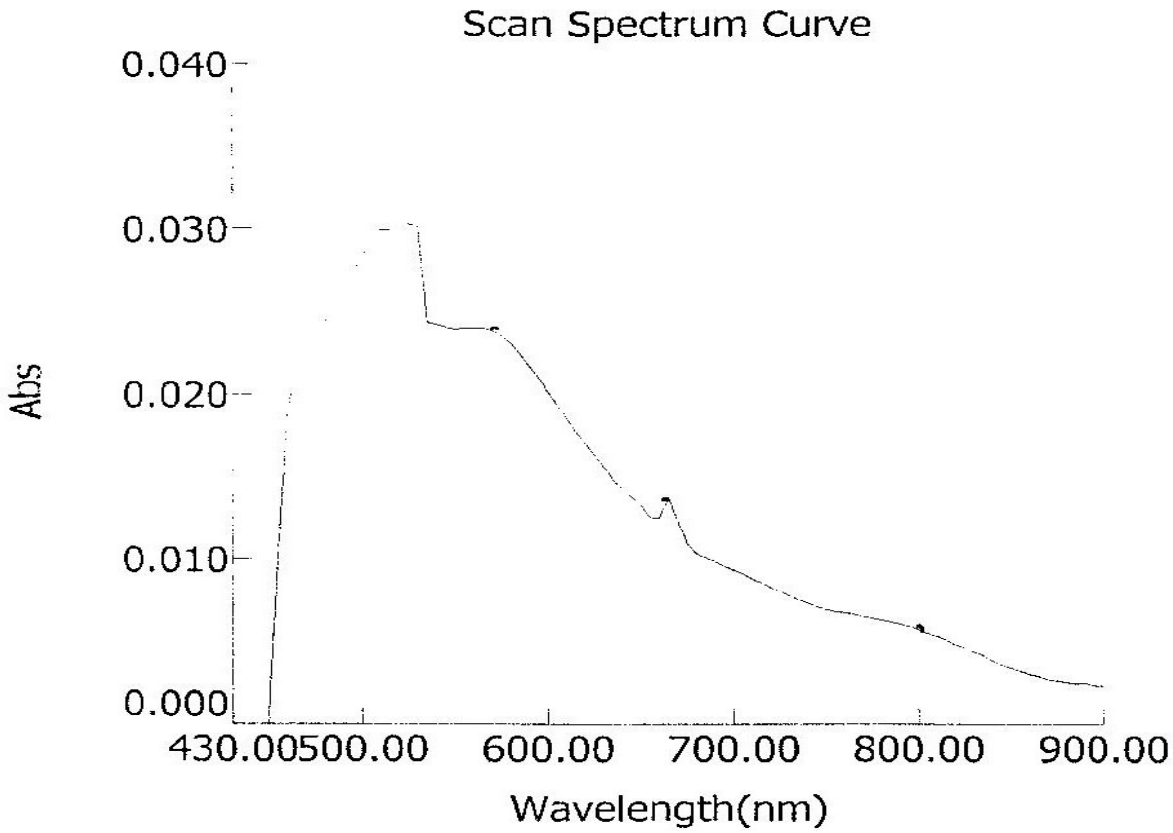

Figure 4.2.4. Visible spectrum of heteroleptic [Co(L^6)(Bipy)(OAc)] complex

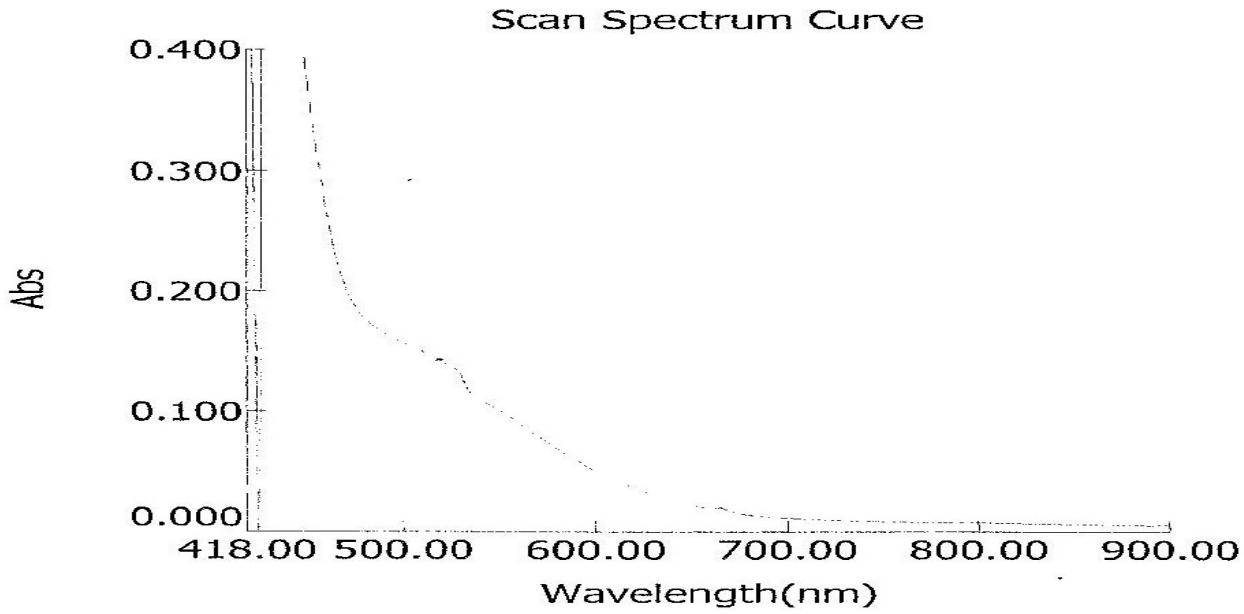

Figure 4.2.5. Visible spectrum of [Ni(L_6)(Bipy)(OAc)] complex

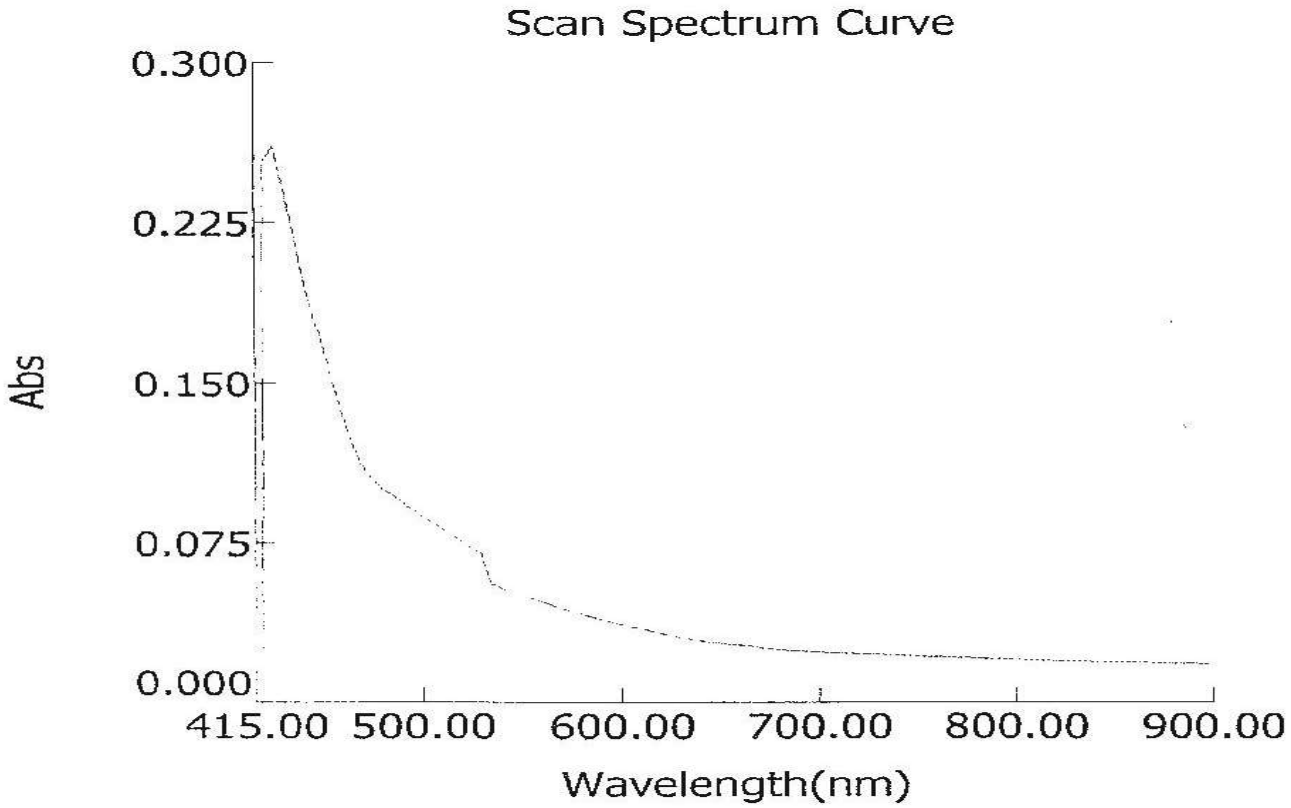

Figure 4.2.6: Visible spectrum of $[Fe(L^2)_2].2H_2O$ complex

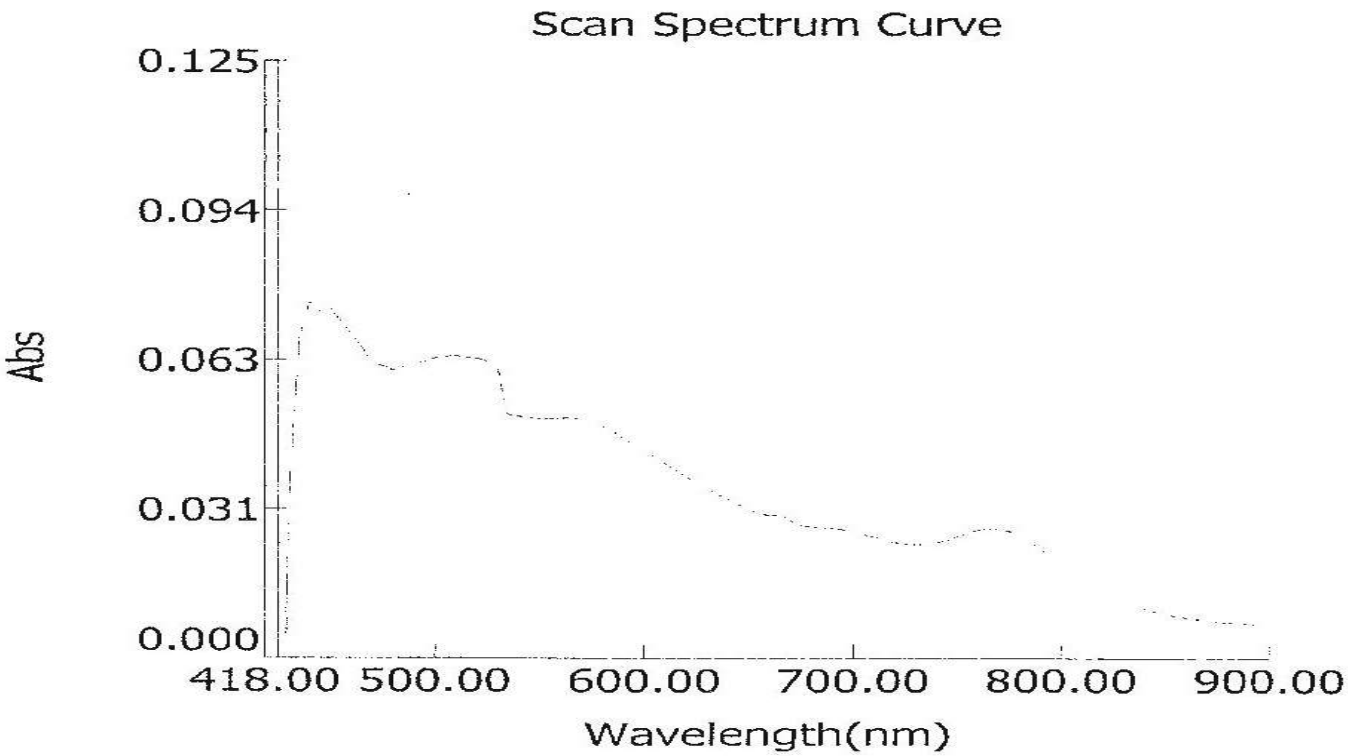

Figure 4.2.7: Visible spectrum of $[Ni(L^5)_2(H_2O)_2]$ complex

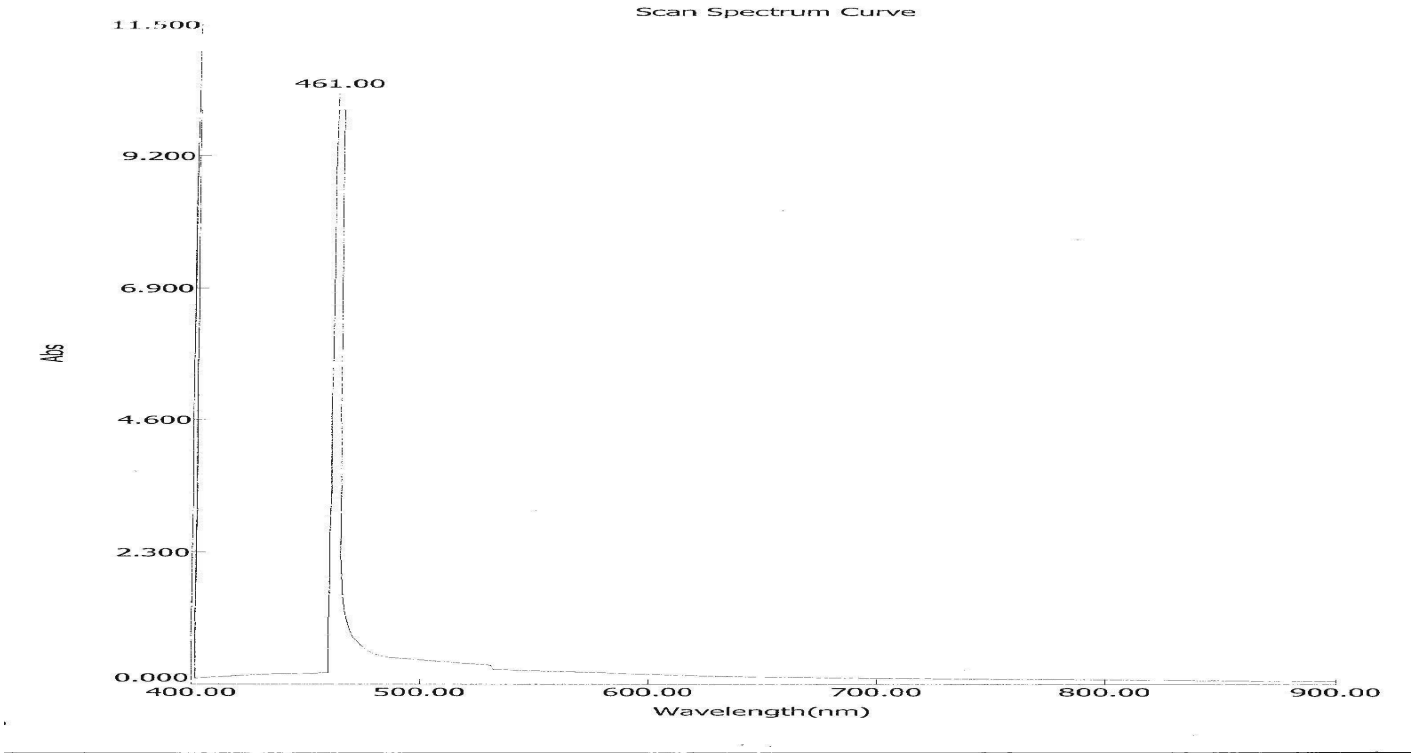

Figure 4.2.8: Ultraviolet spectrum of $[Zn(L^5)_2].H_2O$ complex

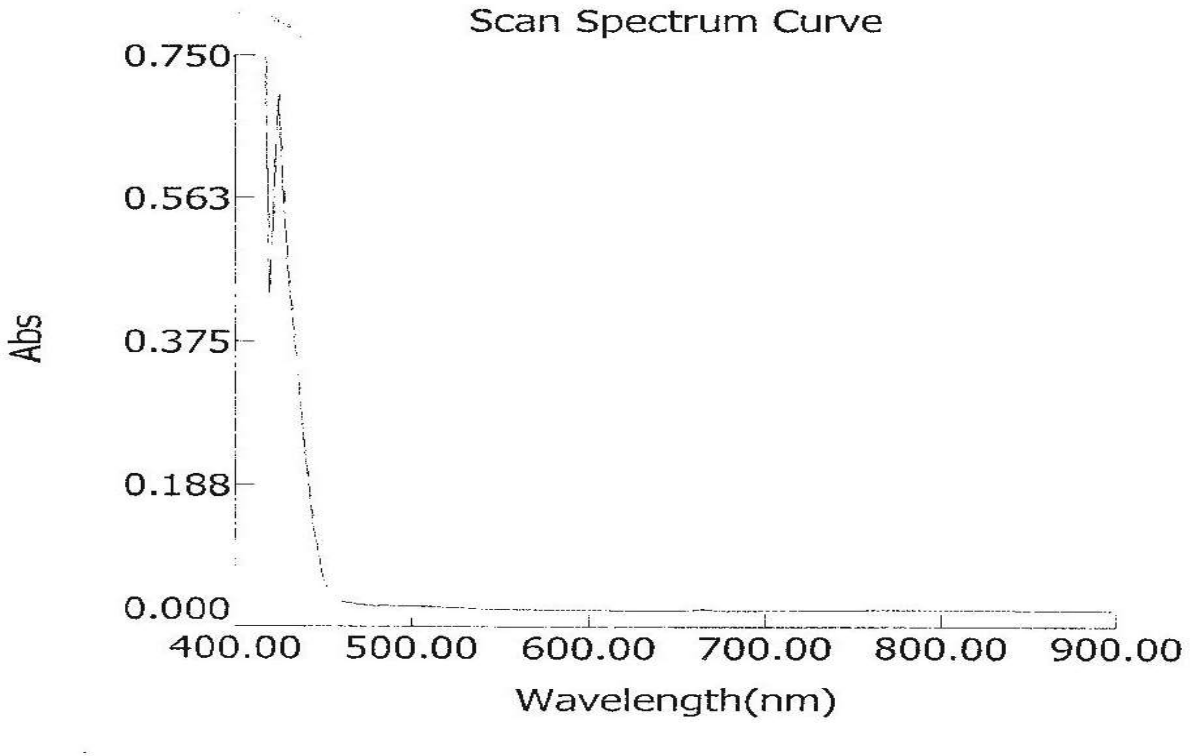

Figure 4.2.9: Visible spectrum of $[Mn(L^4)_2].H_2O$ complex

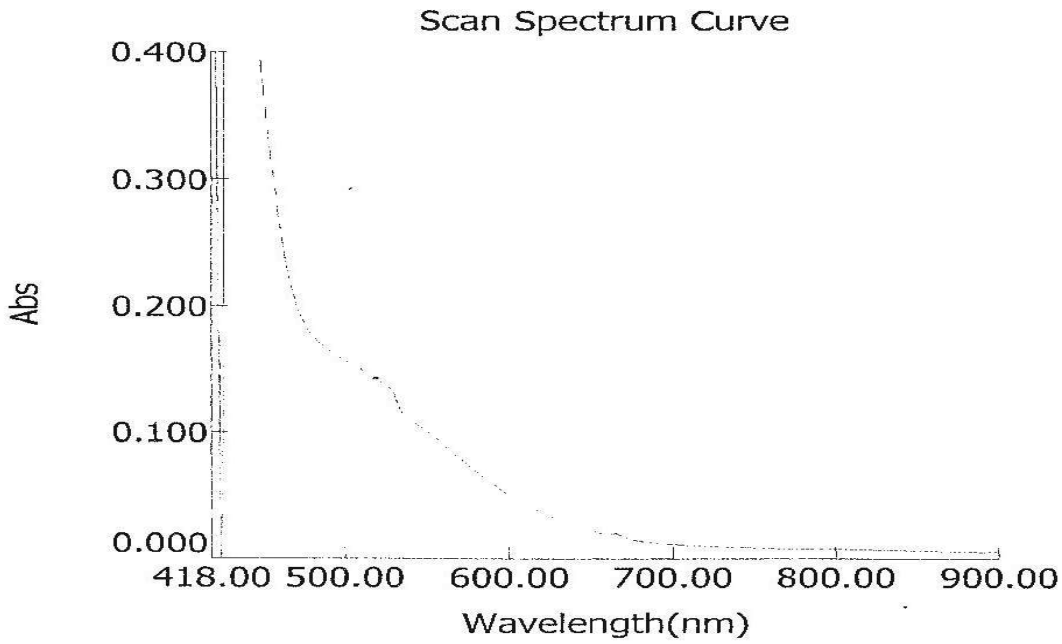

Figure 4.2.10: Visible spectrum of $[Fe(L^6)_2(Bipy)(SO_4)]$ complex

Table 4.5.1. ^{1}Hnmr data of the synthesized ligands (HL^{1}-HL^{6}), in ppm

Ligands	$C_{10}H_6$	C_4H_6-N_2	$C_{10}H_4$-O_2	HC=N	O-H	CH_3	N-H
HL^{1} $C_{15}H_{11}N_3O$	6.51-8.90	7.60-10.77	-	9.49	14.52	-	-
HL^{2} $C_{15}H_{11}N_3O_3$	7.33-8.22	6.40	-	8.92	10.80	-	-
HL^{3} $C_{17}H_{15}N_3O$	7.10-7.84	6.65	-	9.55	14.42	3.34	-
HL^{4} $C_{14}H_9N_3O_2$	-	6.06-7.99	6.52-7.77	-	-	-	4.79
HL^{5} $C_{14}H_9N_3O_4$	-	6.61	6.96-7.95	-	6.04	-	4.95
HL^{6} $C_{16}H_{13}N_3O_2$	-	6.28	7.35-7.98	-	-	2.49	3.38

Table 4.5.2. ^{13}Cnmr data of the synthesized ligands (HL^1-HL^6)

Ligands	$C_{10}H_6/C_8H_5$	C_4H_6-N_2	[-C=O (-one)]$_2$	HC=N	CH_3
HL^1	108.36-157.07	118.07-183.72	-	163.98	-
$C_{15}H_{11}N_3O$					
HL^2	118.8-138.4	98.1-192.8	-	164.1	-
$C_{15}H_{11}N_3O_3$					
HL^3	108.06-133.7	116.8-183.8	-	141.3	23.44
$C_{17}H_{15}N_3O$					
HL^4	125.4-132.1	110.8-153.4	181.5-184.5	-	-
$C_{14}H_9N_3O_2$					
HL^5	110.3-134.31	103.7-161.7	182.2-184.1	-	-
$C_{14}H_9N_3O_4$					
HL^6	111.0-156.9	106.7-159.6	181.3-184.7	-	31.8
$C_{16}H_{13}N_3O_2$					

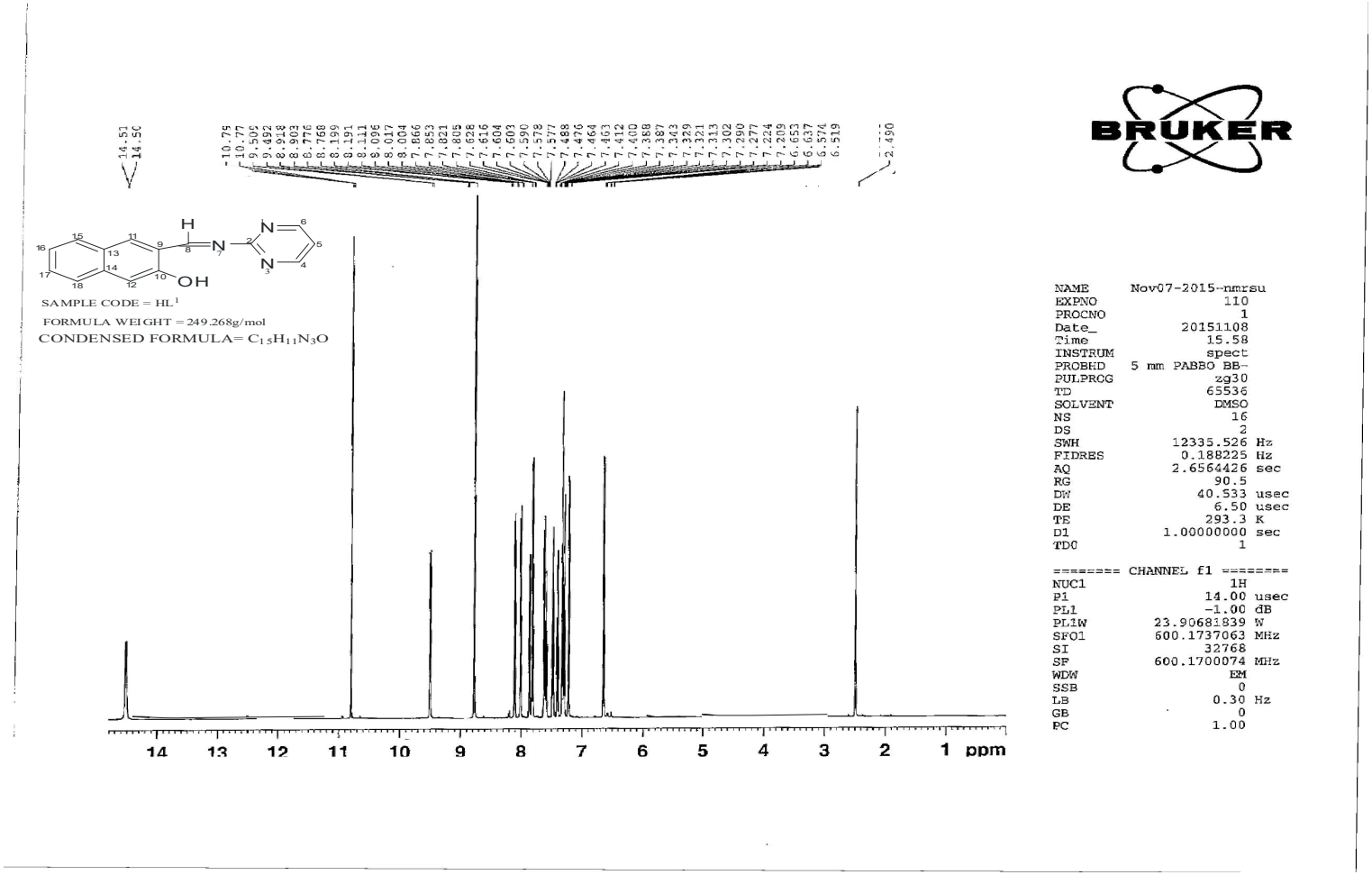

Figure 4.3.1. ^{1}Hnmr spectrum of HL^{1} ligand

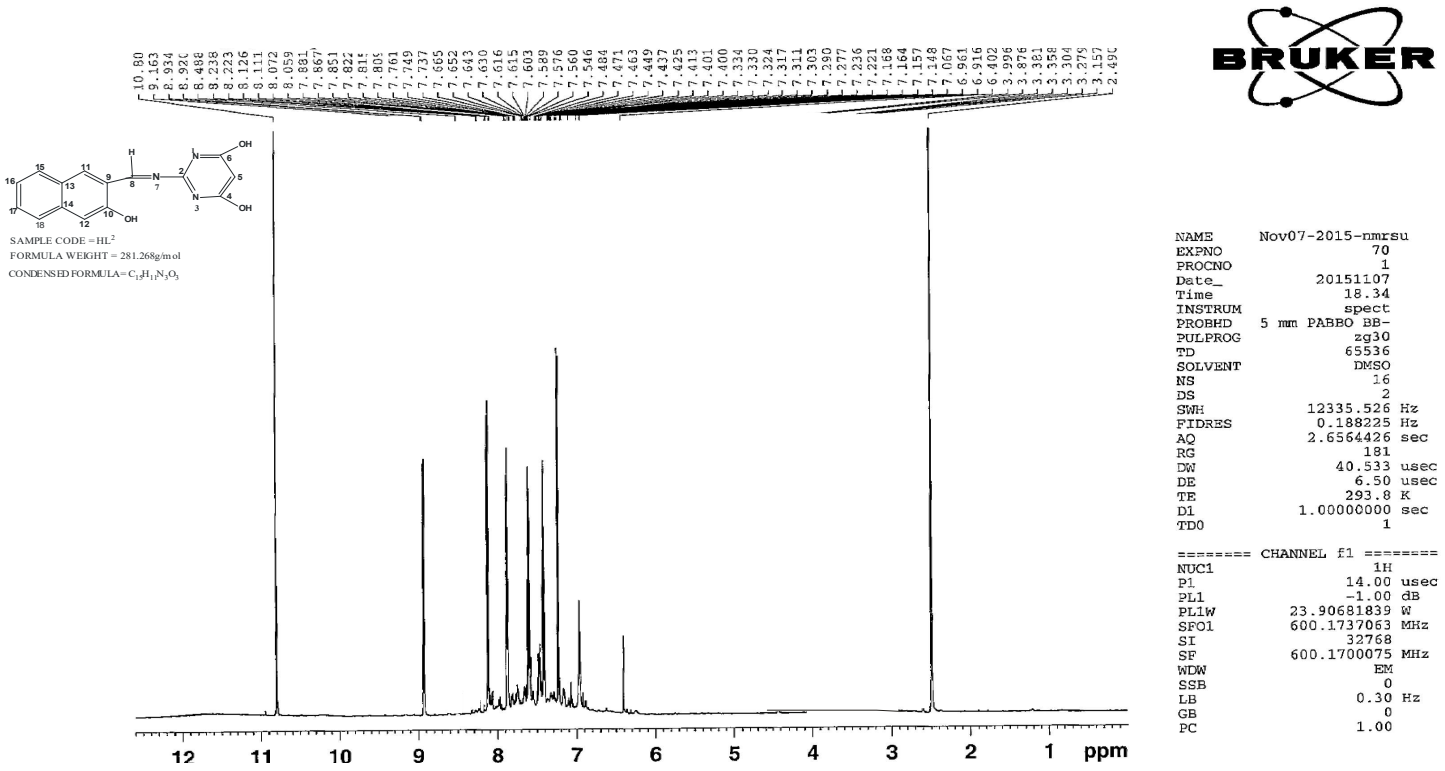

Figure 4.3.2. ^{1}Hnmr spectrum of HL^{2} ligand

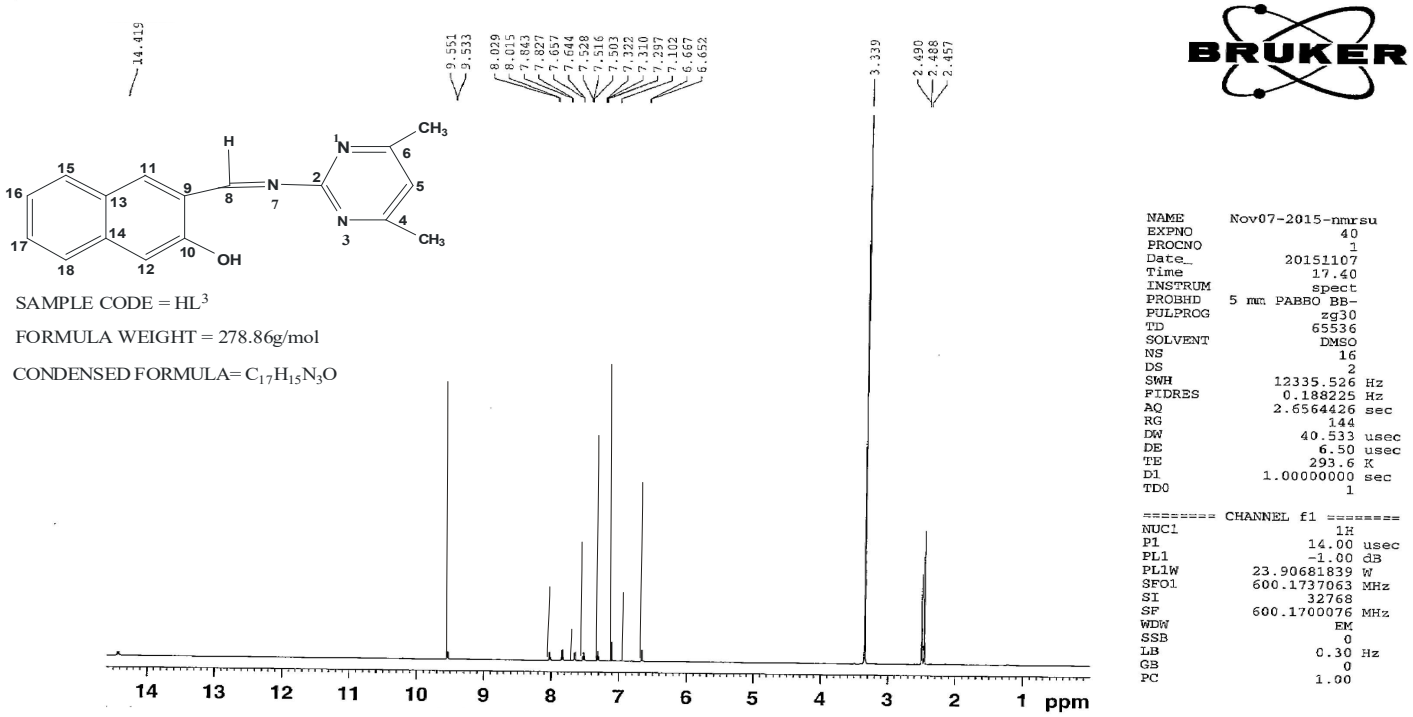

BRUKER

NAME	Nov07-2015-nmrsu
EXPNO	40
PROCNO	1
Date_	20151107
Time	17.40
INSTRUM	spect
PROBHD	5 mm PABBO BB-
PULPROG	zg30
TD	65536
SOLVENT	DMSO
NS	16
DS	2
SWH	12335.526 Hz
FIDRES	0.188225 Hz
AQ	2.6564426 sec
RG	144
DW	40.533 usec
DE	6.50 usec
TE	293.6 K
D1	1.00000000 sec
TD0	1
======== CHANNEL f1 ========	
NUC1	1H
P1	14.00 usec
PL1	-1.00 dB
PL1W	23.90681839 W
SFO1	600.1737063 MHz
SI	32768
SF	600.1700076 MHz
WDW	EM
SSB	0
LB	0.30 Hz
GB	0
PC	1.00

Figure 4.3.3. ^{1}Hnmr spectrum of HL^{3} ligand

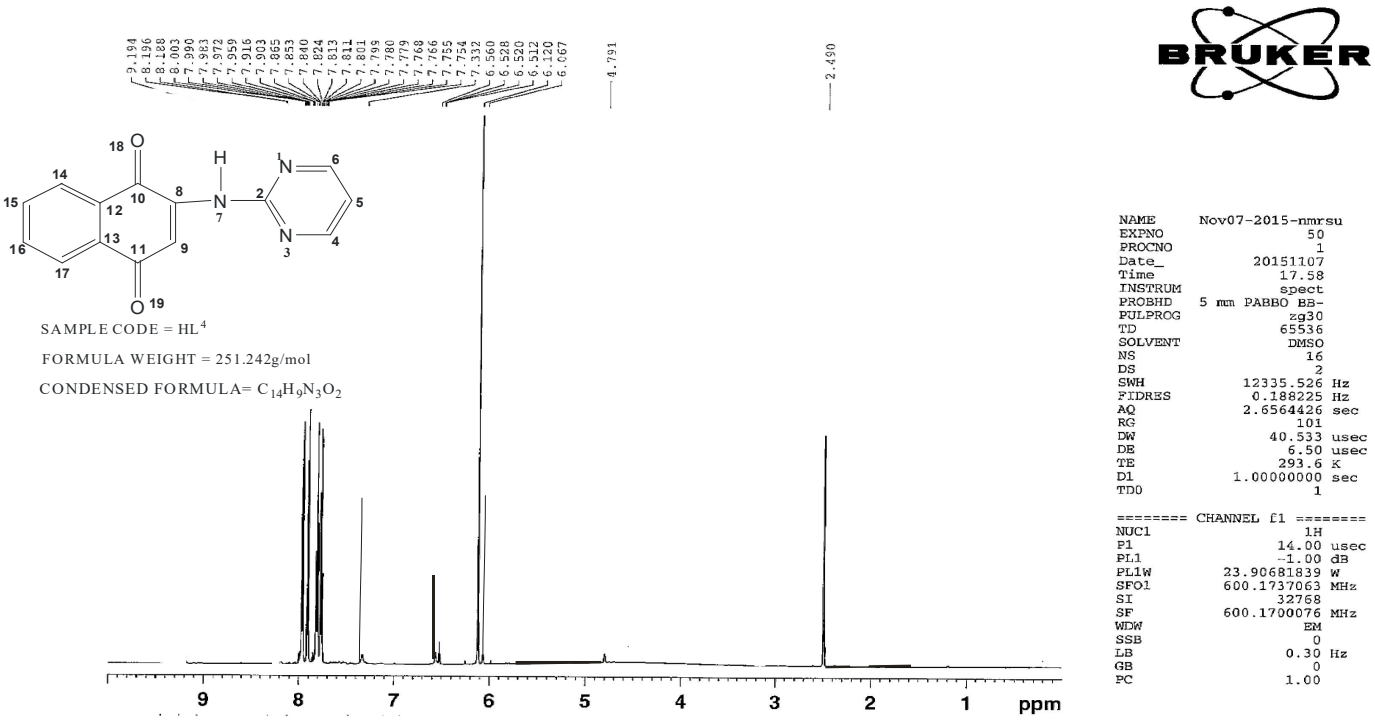

BRUKER

NAME	Nov07-2015-nmrsu
EXPNO	50
PROCNO	1
Date_	20151107
Time	17.58
INSTRUM	spect
PROBHD	5 mm PABBO BB-
PULPROG	zg30
TD	65536
SOLVENT	DMSO
NS	16
DS	2
SWH	12335.526 Hz
FIDRES	0.188225 Hz
AQ	2.6564426 sec
RG	101
DW	40.533 usec
DE	6.50 usec
TE	293.6 K
D1	1.00000000 sec
TD0	1
======== CHANNEL f1 ========	
NUC1	1H
P1	14.00 usec
PL1	-1.00 dB
PL1W	23.90681839 W
SFO1	600.1737063 MHz
SI	32768
SF	600.1700076 MHz
WDW	EM
SSB	0
LB	0.30 Hz
GB	0
PC	1.00

Figure 4.3.4. ^{1}Hnmr spectrum of HL^{4} ligand

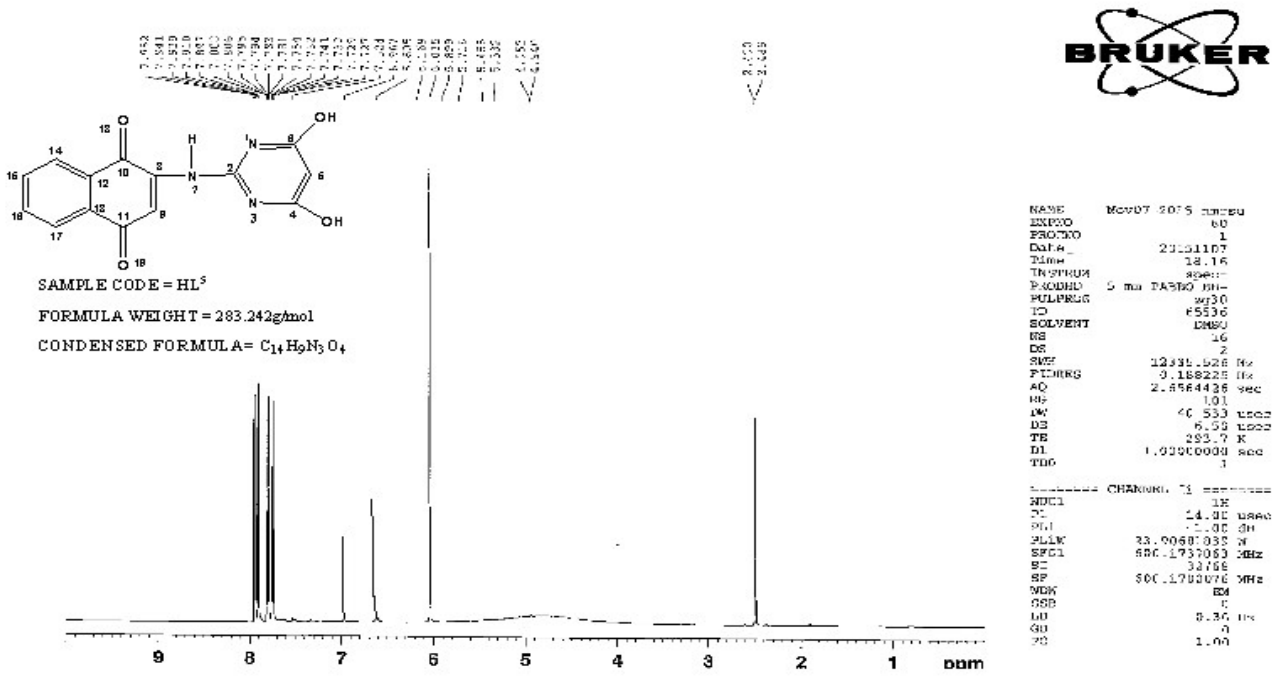

Figure 4.3.5. ^{1}Hnmr spectrum of HL^{5} ligand

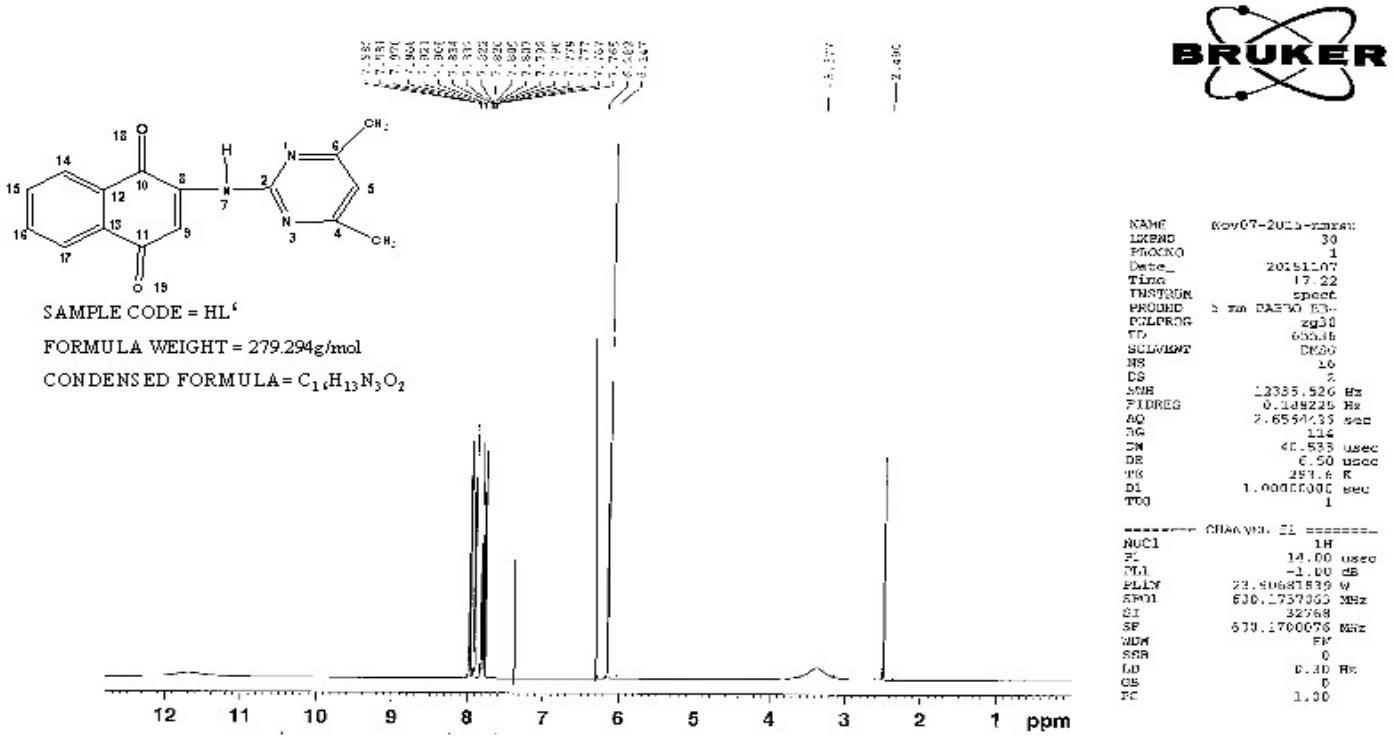

Figure 4.3.6. ^{1}Hnmr spectrum of HL^{6} ligand

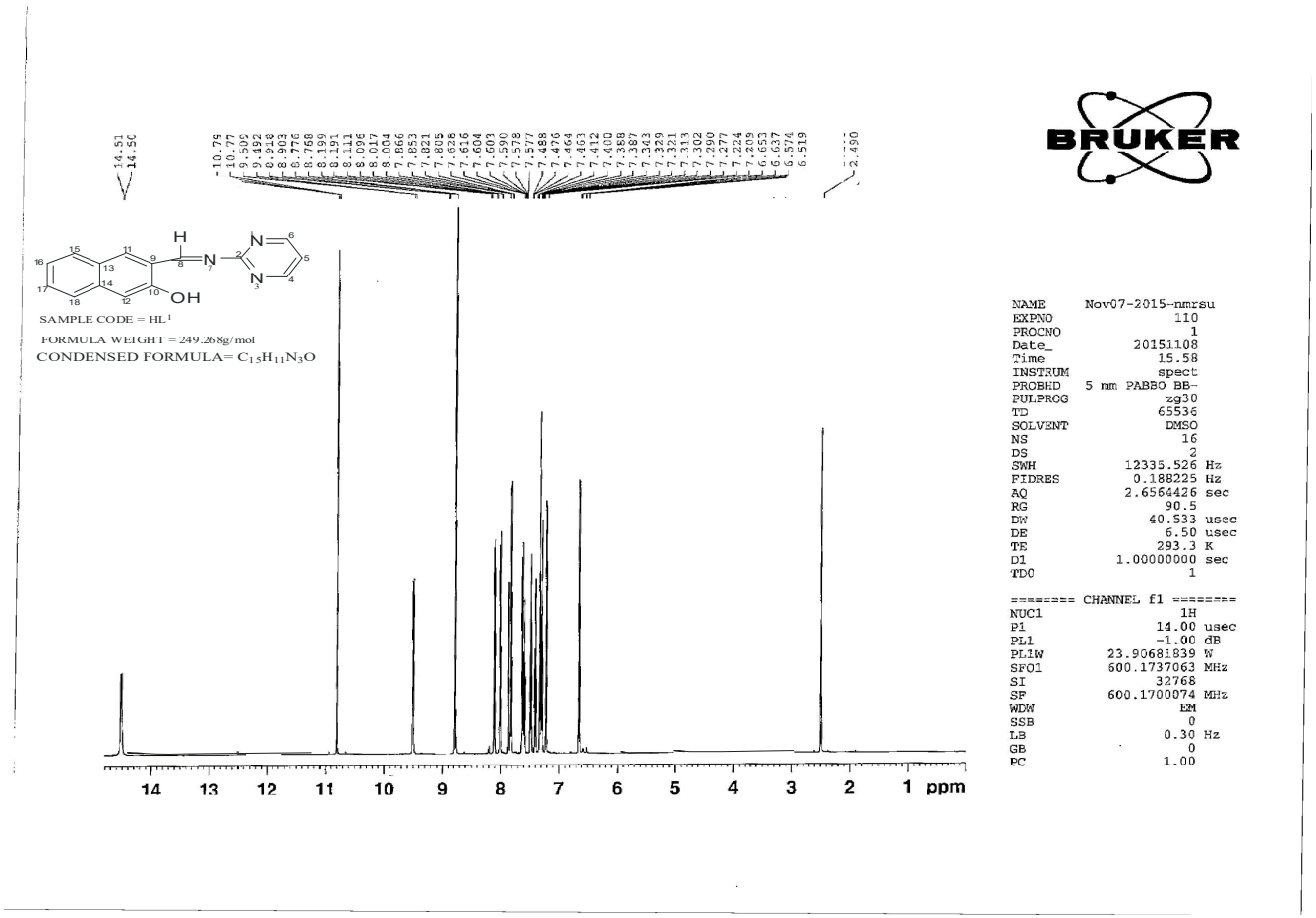

Figure 4.4.1. ^{13}Cnmr spectrum of 3-{[-(pyrimidin-2-yl)imino]methyl} napthalen-2-ol (HL^1) ligand

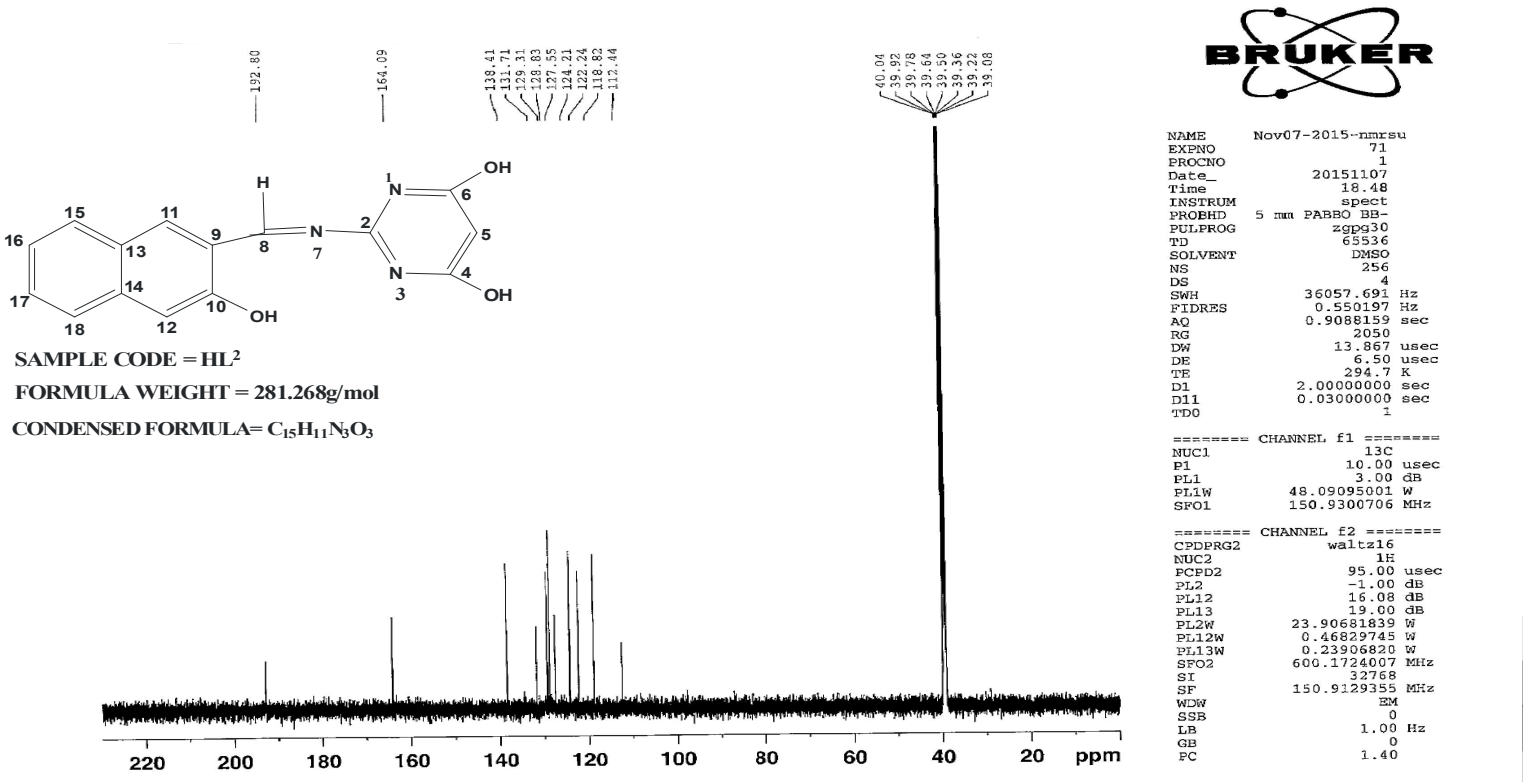

Figure 4.4.2. ^{13}Cnmr spectrum of 3-{[(4,6-dihydroxypyrimidin-2-yl)imino]methyl}napthalen-2-ol (HL^2) ligand

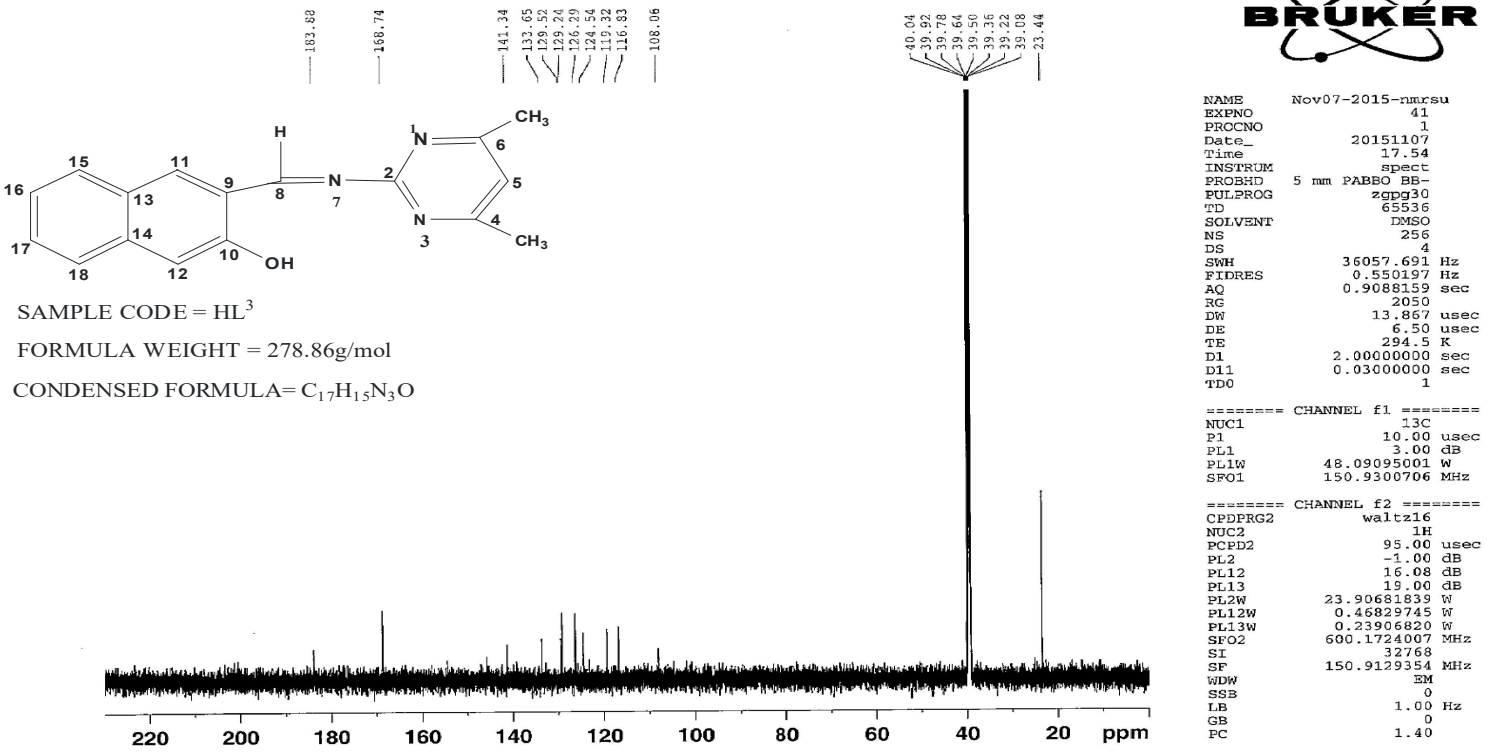


```
NAME          Nov07-2015-nmrsu
EXPNO                       41
PROCNO                       1
Date_                 20151107
Time                     17.54
INSTRUM                  spect
PROBHD     5 mm PABBO BB-
PULPROG                 zgpg30
TD                       65536
SOLVENT                   DMSO
NS                          256
DS                            4
SWH                 36057.691 Hz
FIDRES               0.550197 Hz
AQ                   0.9088159 sec
RG                        2050
DW                      13.867 usec
DE                        6.50 usec
TE                       294.5 K
D1                  2.00000000 sec
D11                 0.03000000 sec
TD0                          1

======== CHANNEL f1 ========
NUC1                        13C
P1                        10.00 usec
PL1                        3.00 dB
PL1W               48.09095001 W
SFO1              150.9300706 MHz

======== CHANNEL f2 ========
CPDPRG2                waltz16
NUC2                        1H
PCPD2                     95.00 usec
PL2                       -1.00 dB
PL12                      16.08 dB
PL13                      19.00 dB
PL2W               23.90681839 W
PL12W               0.46829745 W
PL13W               0.23906820 W
SFO2              600.1724007 MHz
SI                        32768
SF                150.9129354 MHz
WDW                         EM
SSB                          0
LB                        1.00 Hz
GB                           0
PC                        1.40
```

Figure 4.4.3. ^{13}Cnmr spectrum of 3-{[(4,6-dimethylpyrimidin -2-yl)imino]methyl}napthalen-2-ol (HL^3) ligand

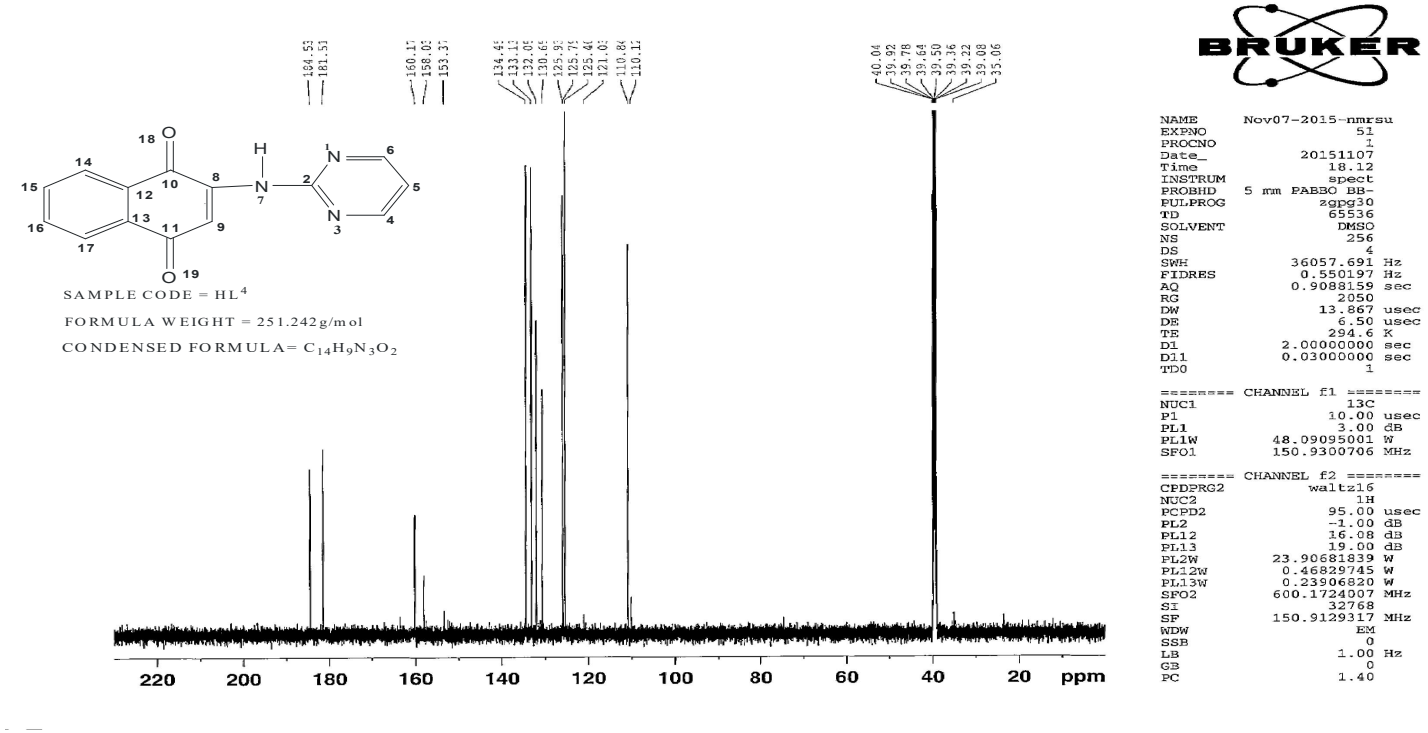

Figure 4.4.4. ^{13}Cnmr spectrum of 2-(pyrimidin-2-ylamino)naphthalene-1,4-dione, (HL^4) ligand

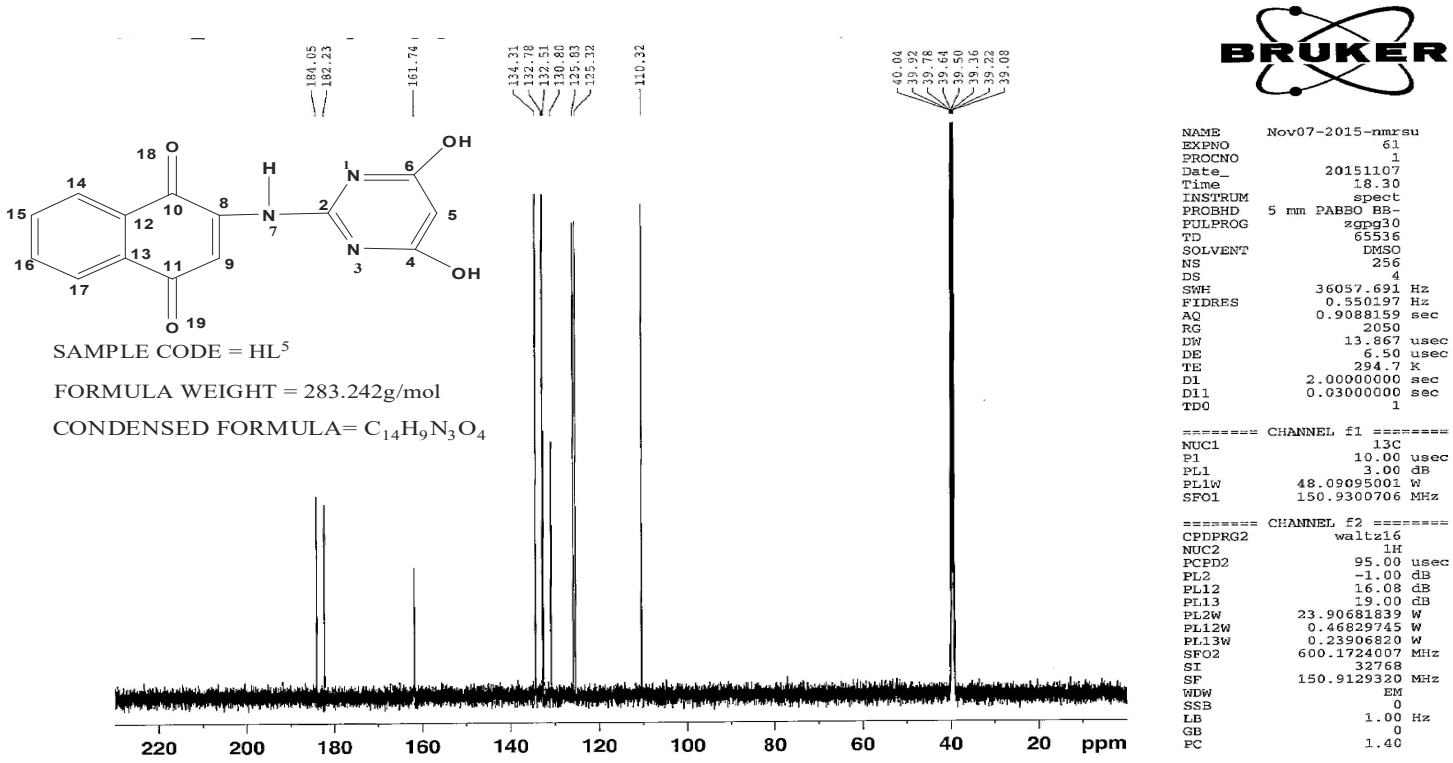

Figure 4.4.5. ^{13}Cnmr spectrum of 2-(4,6-dihydroxypyrimidin-2-ylamino)naphthalene-1,4-dione (HL^5) ligand

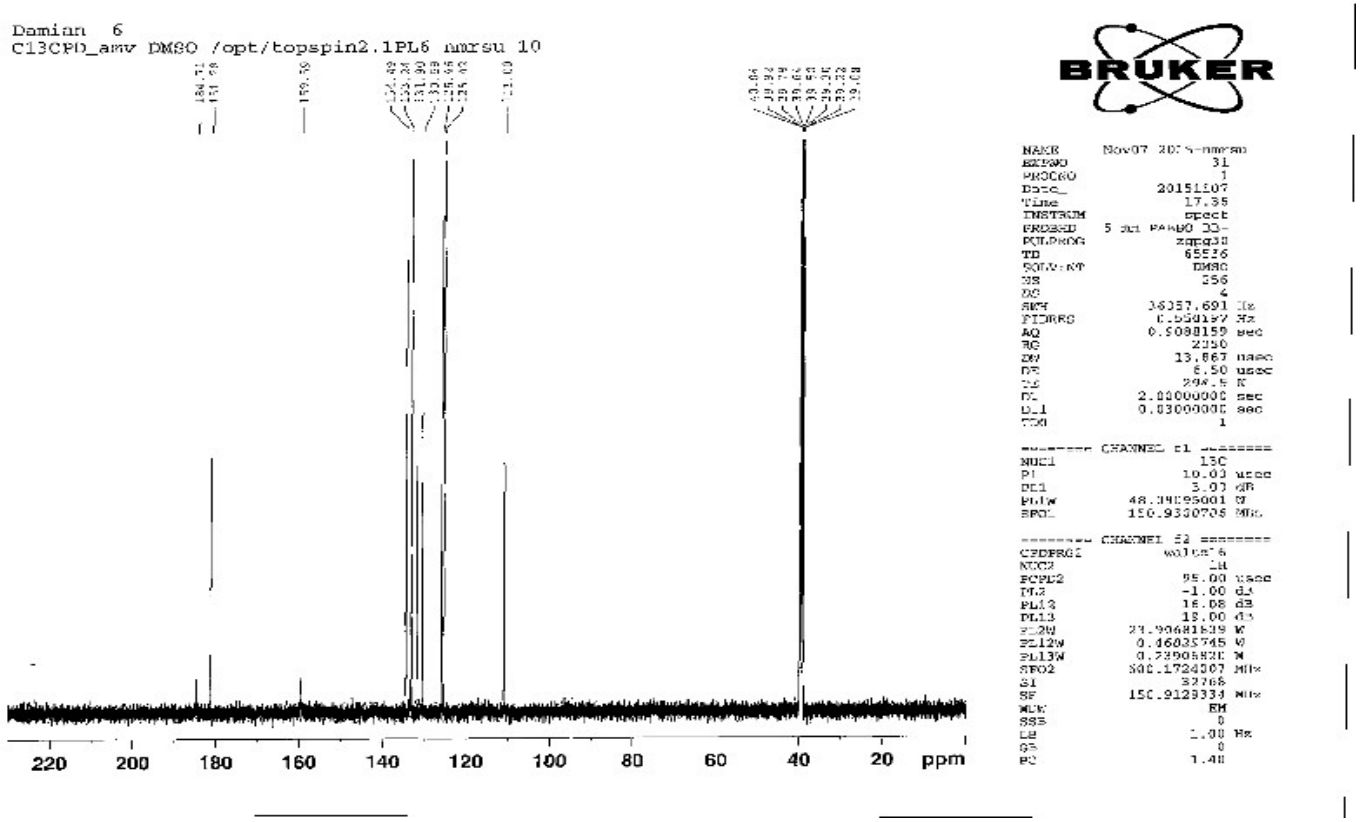

Figure 4.4.6. ^{13}Cnmr spectrum of 2-(4,6-dimethyl pyrimidin-2-ylamino)naphthalene-1,4-dione (HL^6) ligand

Table 4.6.1. Mass spectra result for HL^{1-6} ligands

S/NO	Ligands	Fragmentation	
		m/e	m/z
	HL^1		169 [$-C_{11}H_7NO]^+$
1	$C_{15}H_{11}N_3O$	250.096 [m^+]	229 [$-C_{15}H_{10}N_3]^+$
	[249.268]		173, 175, 251 [EMU]
	HL^2		255.16 [-CO, 28]
2	$C_{15}H_{11}N_3O_3$	281.00	211 [$-C_3H_3O_2$, 71]
	[281.268]		130.13 [$-CN_3$, 26.03]
	HL^3		279.24 [m+1], 280.11 [m+2]
3	$C_{17}H_{15}N_3O$	278.12	276.12 [$-H_2$, 2.016], 250.17$[COH]^+$, 193.66$[NC_2H_2O]^+$,
	[278.86]		142.92$[C_2N_2H]^+$, 125$[OH]^+$
4	HL^4	250.0	225.0 [$-C_2H_2$, 26]$^+$
	$C_{14}H_9N_3O_2$		175.0 [$-C_2N_2$, 53]$^+$
	[251.242]		
5	HL^5		256.96 [CO, 28]
	$C_{14}H_9N_3O_4$	283.0	200 [$-C_2NOH$, 55],
	[283.242]		175 [-CHO, 29]
	HL^6		278.0 [-H], 251 [-CO, 28]
	$C_{16}H_{13}N_3O_2$		236 [$-CH_3$, 15], 175 [$-C_4H_4N_2$, 61]
6	[279.294]	278.0	148 [-CHN, 27]

***Keys*:** EMU=Extra mass unit

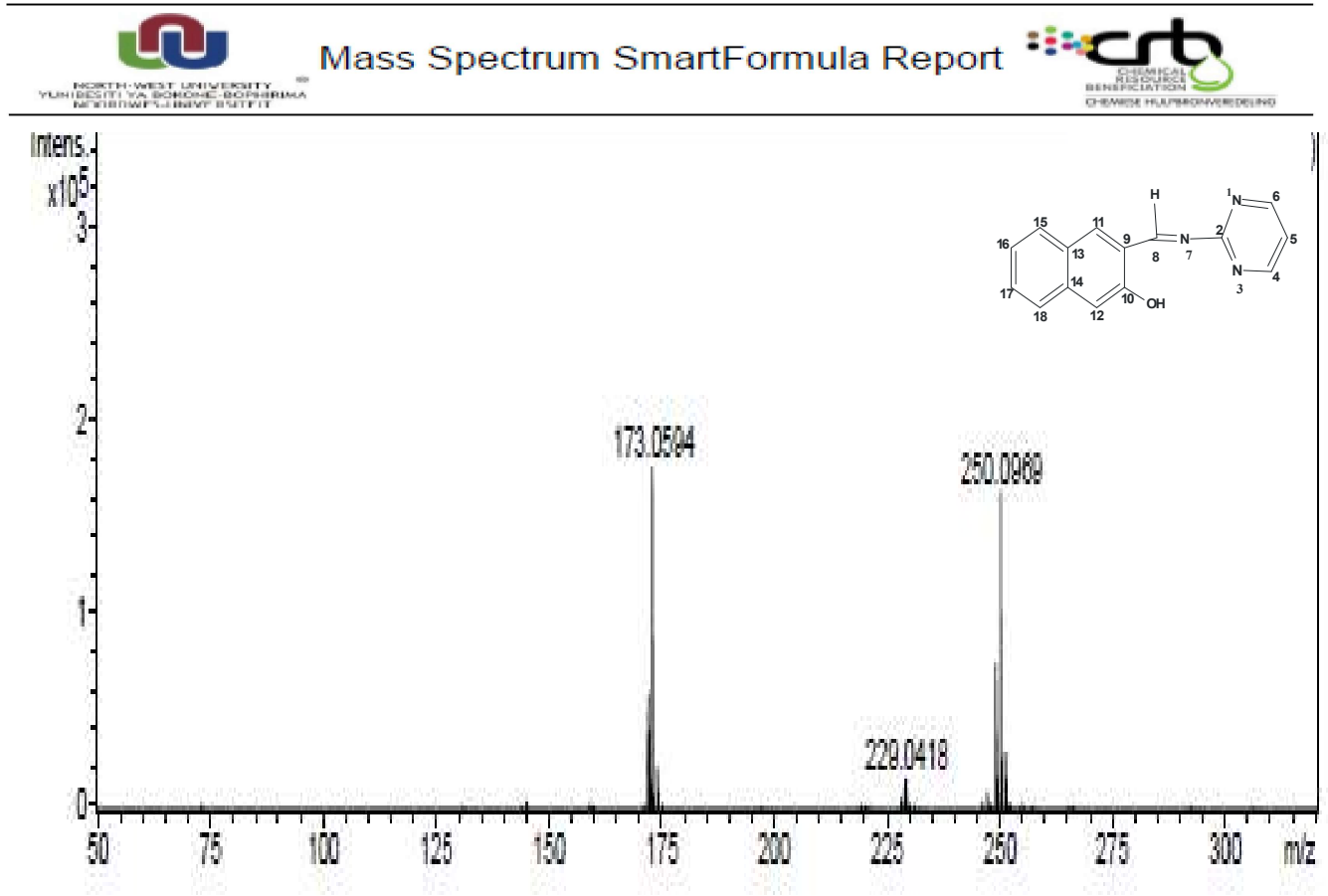

Figure 4.5.1. Mass spectrum of 3-{[-(pyrimidin-2-yl)imino]methyl} napthalen-2-ol (HL^1) ligand

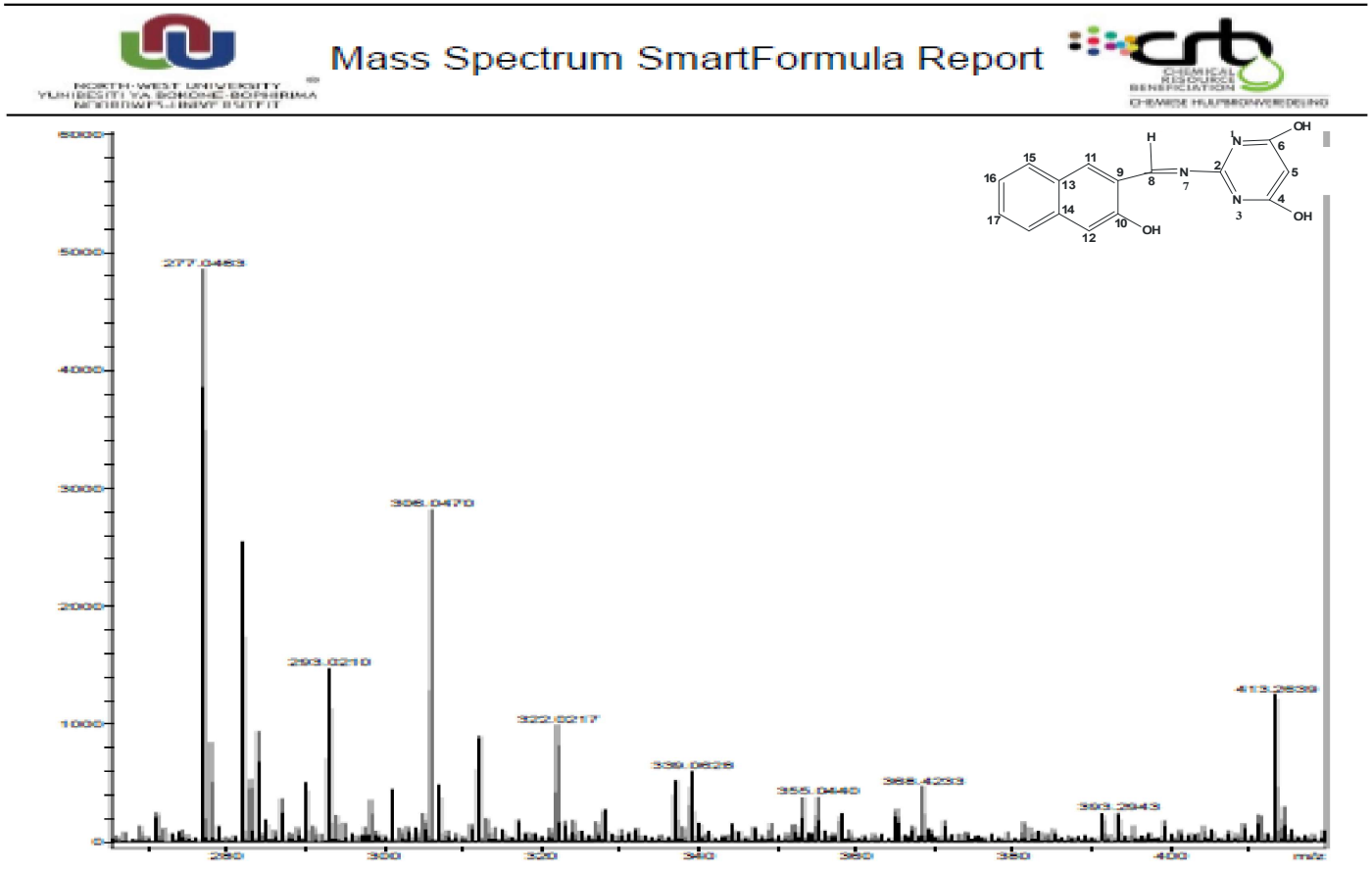

Figure 4.5.2. Mass spectrum of 3-{[(4,6-dihydroxypyrimidin-2-yl)imino]methyl}napthalen-2-ol (HL^2) ligand

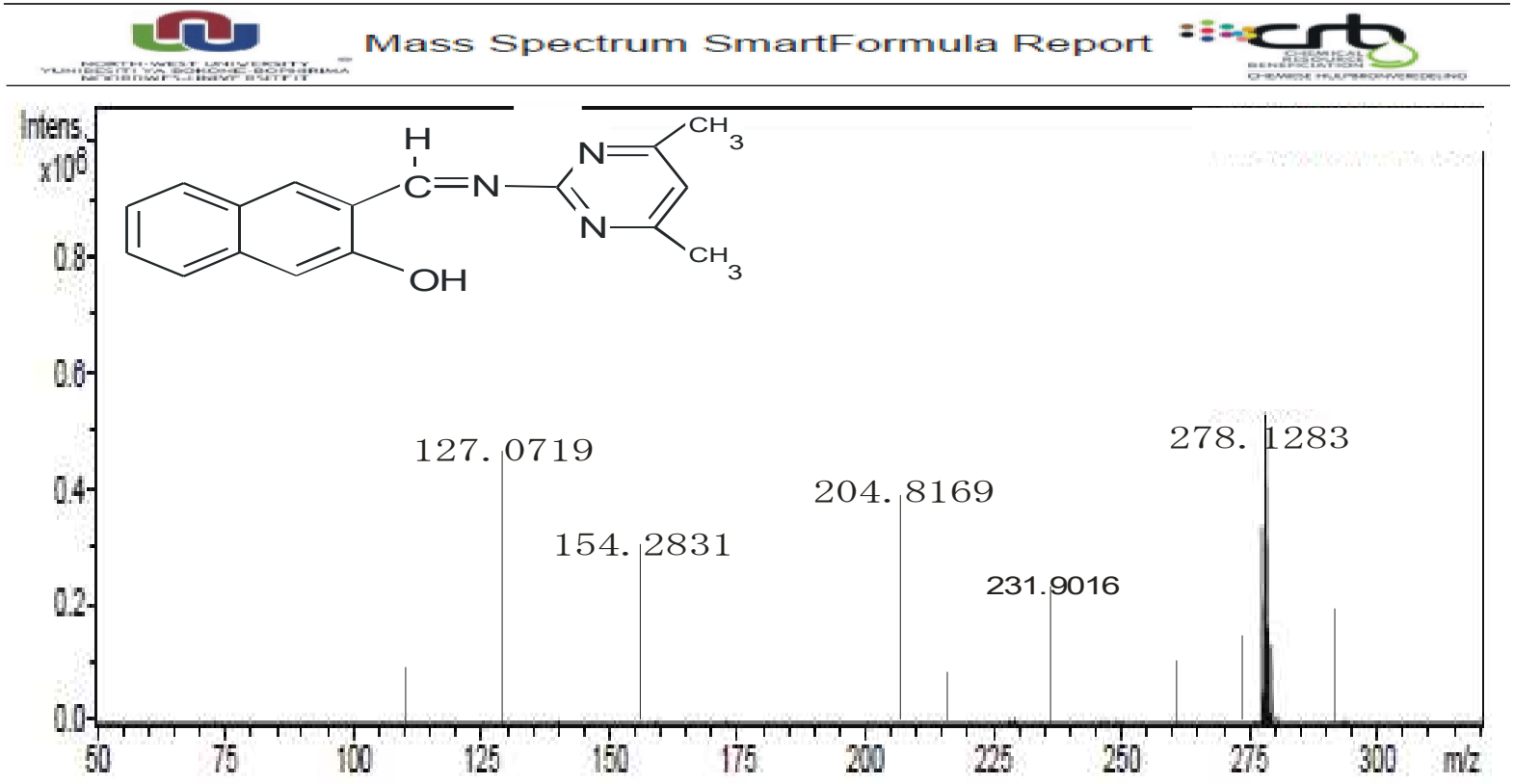

Figure 4.5.3. Mass spectrum of 3-{[(4,6-dimethylpyrimidin -2-yl)imino]methyl}napthalen-2-ol (HL^3) ligand

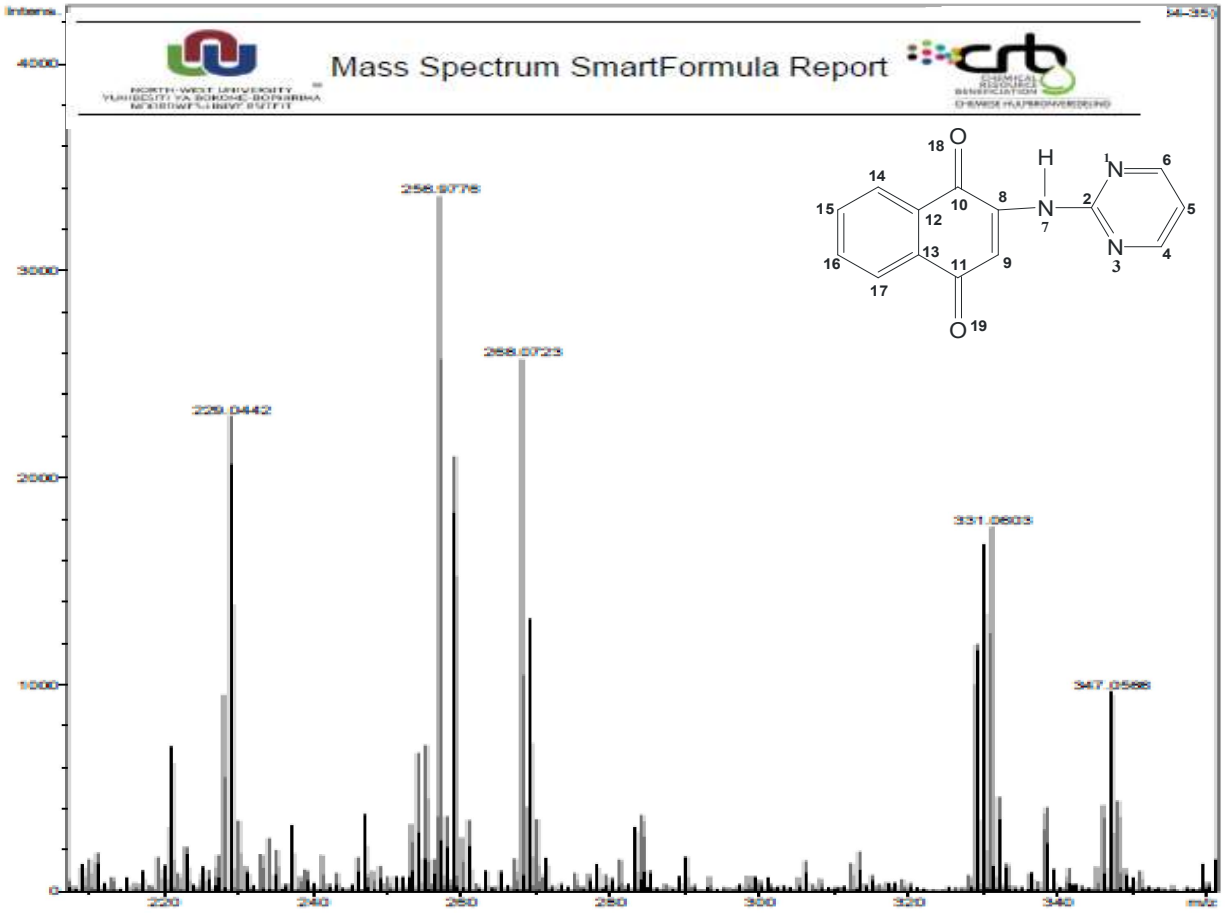

Figure 4.5.4. Mass spectrum of 2-(pyrimidin-2-ylamino)naphthalene-1,4-dione, (HL^4) ligand

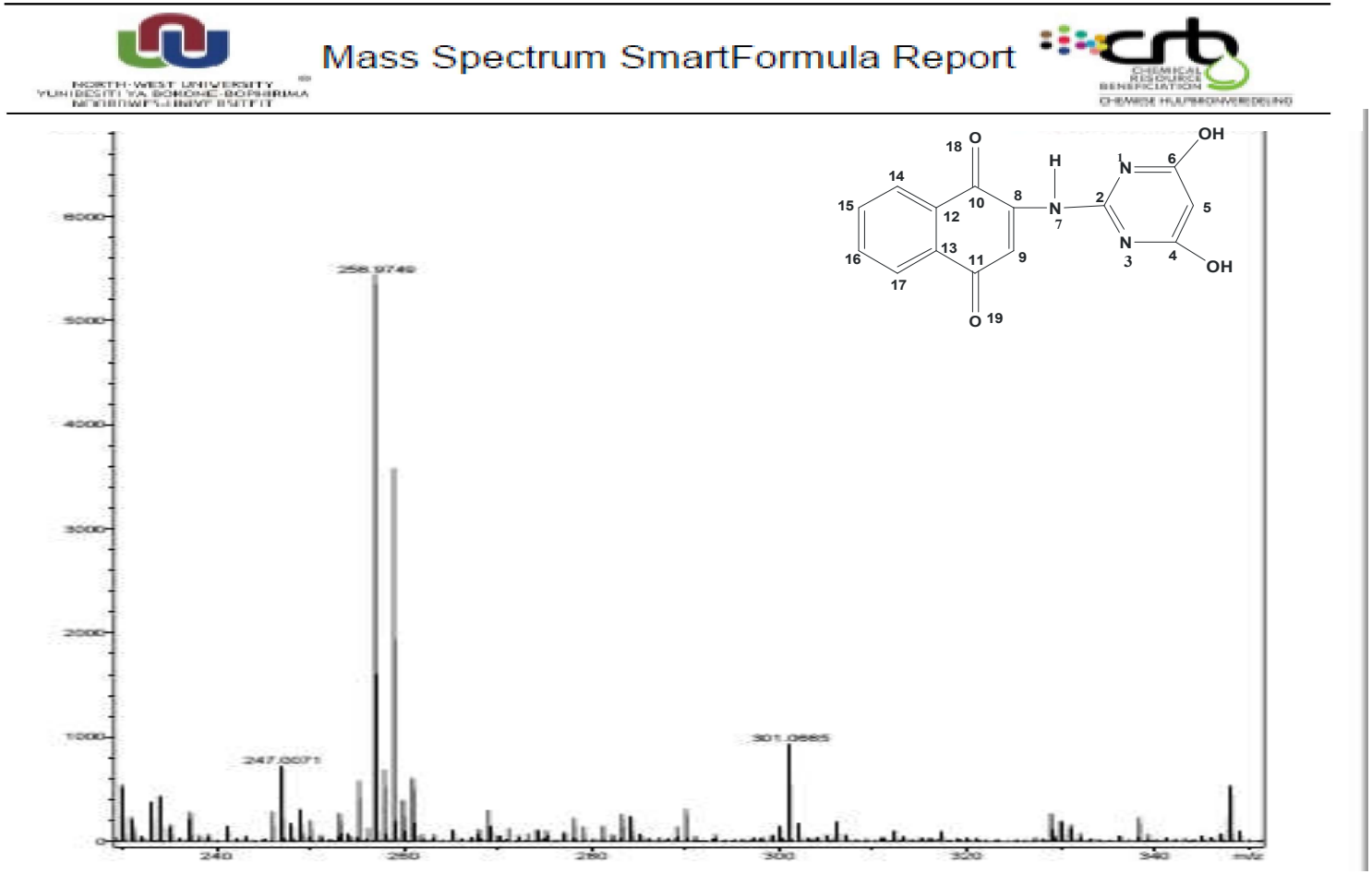

Figure 4.5.5. Mass spectrum of 2-(4,6-dihydroxypyrimidin-2-ylamino)naphthalene-1,4-dione (HL^5) ligand

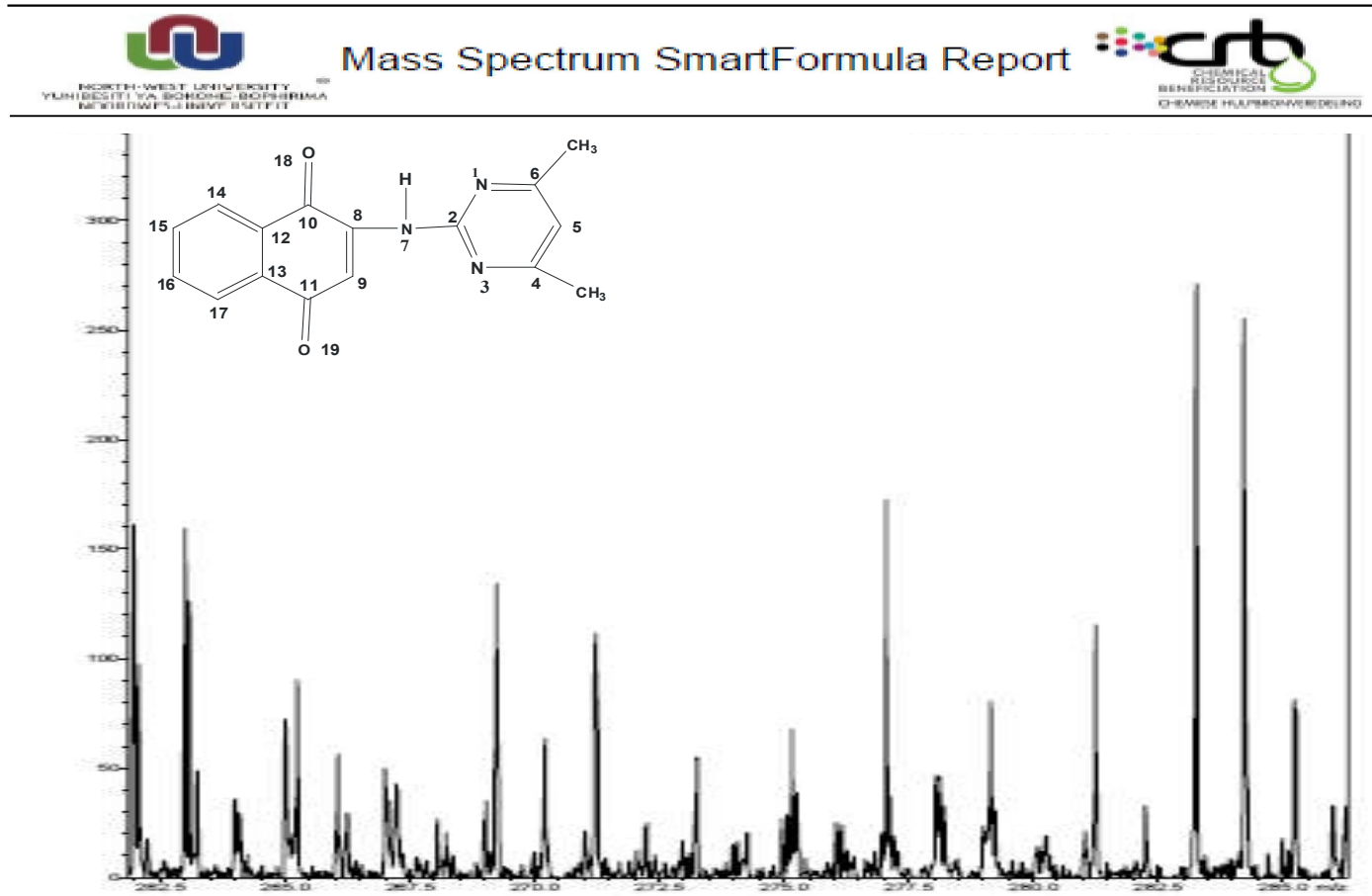

Figure 4.5.6. Mass spectrum of 2-(4,6-dimethyl pyrimidin-2-ylamino)naphthalene-1,4-dione (HL^6) ligand

Table 4.7.1. Antibacterial result for HL^1 ligands and its metal(II) complexes

Compound/ Bacteria	***Bacillus cereus***	***Escherichia coli***	***Klebsillaoxytoca***	***Pseudomonas aeruginosa***	***Staphylococcus aureus***	***Proteus mirabilis***
HL^1	9.0±1.4	0.0±0.0	16.5±1.4	11.0±6.3	16.9±0.4	0.0±0.0
$[Mn(L^1)_2].H_2O$	0.0±0.0	6.5±2.8	18.0±2.8	13.5±0.0	13.0±2.8	21.0±0.7
$[Fe(L^1)_2(H_2O)_2]$	0.0±0.0	0.0±0.0	0.0±0.0	12.5±2.1	0.0±0.0	0.0±0.0
$[Co(L^1)_2].2H_2O$	95.0±0.0	0.0±0.0	14.5±0.7	5.0±0.7	0.0±0.0	0.0±0.0
$[Ni(L^1)_2].H_2O$	0.0±0.0	0.0±0.0	13.0±0.0	13.0±2.1	0.0±0.0	13.0±2.1
$[Cu(L^1)_2]$	12.5±0.0	17.0±2.8	12.0±2.1	0.0±0.0	7.0±2.1	15.0±0.0
$[Zn(L^1)_2]$	17.0±1.4	12.0±2.8	15.0±2.8	17.5±2.1	0.0±0.0	16.0±1.4
$^+$Ciprofloxacin	33.0 ± 3.5	32.0 ± 1.4	36.0 ± 2.8	26.5 ± 0.7	29.0 ± 2.1	23.0 ± 1.4
-DMSO	0.0±0.0	0.0±0.0	0.0±0.0	0.0±0.0	0.0±0.0	0.0±0.0

Table 4.7.2. Antibacterial result for HL^1 ligand and its heteroleptical(II) complexes

Compound/ Bacteria	***Bacillus cereus***	***Escherichia coli***	***Klebsillaoxytoca***	***Pseudomonas aeruginosa***	***Staphylococcus aureus***	***Proteus mirabilis***
HL^1	9.0±1.4	0.0±0.0	16.5±1.4	11.0±6.3	16.9±0.4	0.0±0.0
Bipy	15.5 ± 0.7	12.0 ± 2.8	26.0 ± 2.8	8.5 ± 0.7	17.0 ± 4.2	19.5 ± 2.1
$[Mn(L^1)(Bipy)(OAc)]$	15.0±2.1	0.0±0.0	10.0±0.7	12.0±2.1	9.0±0.0	13.0±0.7
$[Fe(L^1)(Bipy)(SO_4)]$	13.5±2.8	8.0±2.1	11±2.8	10.5±2.8	0.0±0.0	8.0±1.4
$[Co(L^1)(Bipy)(OAc)].H_2O$	10.5±0.0	13.0±1.4	6.5±2.1	9.0±0.0	11.0±0.7	0.0±0.0
$[Ni(L^1)(Bipy)(OAc)].H_2O$	8.0±1.4	5.0±2.8	11.0±02.8	0.0±0.0	12.0±2.1	5.0±2.8
$[Cu(L^1)(Bipy)(OAc)]$	12.0±1.4	15.0±0.0	14.5±2.1	17.0±2.8	13.5±0.7	18.0±2.1
$[Zn(L^1)(Bipy)(OAc)].2H_2O$	7.5±2.8	0.0±0.0	0.0±0.0	8.5±0.7	0.0±0.0	9.0±2.1
$^+$Ciprofloxacin	33.0 ± 3.5	32.0 ± 1.4	36.0 ± 2.8	26.5 ± 0.7	29.0 ± 2.1	23.0 ± 1.4
-DMSO	0.0±0.0	0.0±0.0	0.0±0.0	0.0±0.0	0.0±0.0	0.0±0.0

Table 4.7.3. Antibacterial result for HL^2 ligand and its metal(II) complexes

Compound/ Bacteria	***Bacillus cereus***	***Escherichia coli***	***Klebsillaoxytoca***	***Pseudomonas aeruginosa***	***Staphylococcus aureus***	***Proteus mirabilis***
HL^2	14.5±0.7	5.5±0.7	15.5±3.5	11.5±2.1	20.0±1.4	19.5±2.1
$[Mn(L^2)_2].2H_2O$	14.5±2.1	5.5±2.1	14.0±2.8	12.0±1.4	14.0±0.0	12.5±1.4
$[Fe(L^2)_2].2H_2O$	13.0±1.4	6.5±0.7	12.0±1.4	0.0±0.0	0.0±0.0	5.5±0.7
$[Co(L^2)_2].H_2O$	17.5±0.7	17.0±1.4	16.0±1.4	25.0±1.4	23.0±1.4	16.0±0.0
$[Ni(L^2)_2].H_2O$	17.0±1.4	11.0±1.4	11.5±0.7	15.5±0.7	18.5±3.5	12.0±0.0
$[Cu(L^2)_2]$	18.0±2.8	25.5±2.1	22.5±0.7	19.5±2.1	20.0±0.7	19.5±3.5
$[Zn(L^2)_2]$	13.5±0.7	6.0±1.4	6.5±0.7	7.5±2.1	10.5±.07	0.0±0.0
$^+$Ciprofloxacin	33.0 ± 3.5	32.0 ± 1.4	36.0 ± 2.8	26.5 ± 0.7	29.0 ± 2.1	23.0 ± 1.4
-DMSO	0.0±0.0	0.0±0.0	0.0±0.0	0.0±0.0	0.0±0.0	0.0±0.0

Table 4.7.4: Antibacterial Data of HL^2 Ligands and its Heteroleptic Metal(II) Complexes

Compound/ Bacteria	*Bacillus cereus*	*Escherichia coli*	*Klebsillao xytoca*	*Pseudomona s aeruginosa*	*Staphylococcus aureus*	*Proteus mirabilis*
HL^2	24.5±2.1	5.5±0.7	15.5±3.5	11.5±2.1	20.0±1.4	19.5±2.1
Bipy	15.5 ± 0.7	12.0 ± 2.8	26.0 ± 2.8	8.5 ± 0.7	17.0 ± 4.2	19.5 ± 2.1
$[Mn(L^2)(Bipy)(OAc)].H_2O$	15.0±1.4	20.5±0.7	22.0±0.0	16.0±1.4	21.0±0.0	24.5±0.7
$[Fe(L^2)(Bipy)(SO_4)].H_2O$	18.5±3.5	13.5±2.1	23.5±2.8	14.0±2.8	15.5±0.7	16.0±0.0
$[Co(L^2)(Bipy)(OAc)]$.	15.5±0.7	14.0±2.8	17.5±0.7	18.5±2.1	16.5±2.1	23.0±2.8
$[Ni(L^2)(Bipy)(OAc)].H_2O$	18.0±0.0	17.5±3.5	25.5±2.1	20.0±1.4	18.0±2.8	20.0±2.8
$[Cu(L^2)(Bipy)(OAc)].H_2O$	20.0±0.0	26.5±2.1	23.5±3.5	8.5±0.7	19.0±2.1	22.0±2.8
$[Zn(L^2)(Bipy)(OAc)]$	14.0±0.0	15.5±0.7	20.5±3.5	17.5±0.7	15.0±0.0	20.5±0.7
$^+$Ciprofloxacin	33.0 ± 3.5	32.0 ± 1.4	36.0 ± 2.8	26.5 ± 0.7	29.0 ± 2.1	23.0 ± 1.4
-DMSO	0.0±0.0	0.0±0.0	0.0±0.0	0.0±0.0	0.0±0.0	0.0±0.0

Table 4.7.5. Antibacterial data of HL^3 ligand and its heteroleptic metal(II) complexes

Compound/ Bacteria	***Bacillus cereus***	***Escherichia coli***	***Klebsillaoxytoca***	***Pseudomonas aeruginosa***	***Staphylococcus aureus***	***Proteus mirabilis***
HL^3	5.5±2.1	17.0±2.8	15.0±0.0	12.0±2.8	16.0±1.4	14.0±2.8
Bipy	15.5 ± 0.7	12.0 ± 2.8	26.0 ± 2.8	8.5 ± 0.7	17.0 ± 4.2	19.5 ± 2.1
$[Mn(L^3)(Bipy)(OAc)]$	15.0±1.4	10.0±1.4	15.5±2.1	21.0±2.8	9.5±0.7	13.5±2.1
$[Fe(L^3)(Bipy)(SO_4)].H_2O$	18.5±3.5	15.5±0.7	18.0±1.4	9.0±1.4	16.0±2.8	19.5±2.1
$[Co(L^3)(Bipy)(OAc)]$	16.0±0.0	20.0±1.4	21.5±3.5	16.0±2.8	18.0±2.8	11.0±2.8
$[Ni(L^3)(Bipy)(OAc)]$	12.5±2.1	14.0±2.8	17.5±3.5	18.5±1.7	9.5±2.1	16.0±2.8
$[Cu(L^3)(Bipy)(OAc)]$	25.0±1.4	21.0±2.8	24.5±2.1	19.5±2.1	21.0±2.8	22.5±0.7
$[Zn(L^3)(Bipy)(OAc)].H_2O$	16.0±0.7	14.0±2.8	8.5±0.7	12.0±1.4	5.5±0.7	13.5±0.7
$^+$Ciprofloxacin	33.0 ± 3.5	32.0 ± 1.4	36.0 ± 2.8	26.5 ± 0.7	29.0 ± 2.1	23.0 ± 1.4
-DMSO	0.0±0.0	0.0±0.0	0.0±0.0	0.0±0.0	0.0±0.0	0.0±0.0

Table 4.7.6. Antibacterial result of HL^4 ligand and its metal(II) complexes

Compound/ Bacteria	***Bacillus cereus***	***Escherichia coli***	***Klebsillaoxytoca***	***Pseudomonas aeruginosa***	***Staphylococcus aureus***	***Proteus mirabilis***
HL^4	15.0 ±1.4	21.0±2.8	17.0±1.4	16.5±0.7	21.0±0.7	16.5±3.5
$[Mn(L^4)_2].H_2O$	17.5±2.8	22.0±2.8	19.02.1	18.0±1.4	11.5±3.5	20.5±3.5
$[Fe(L^4)_2].H_2O$	0.0±0.0	0.0±0.0	19.5±3.5	18.0±1.4	24.0±2.8	18.5±0.7
$[Co(L^4)_2].H_2O$	21.0±2.8	22.6±0.7	20.5±0.7	21.0±0.0	29.0±2.1	25.0±4.2
$[Ni(L^4)_2].H_2O$	23.0±2.1	0.0±0.0	0.0±0.0	21.0±2.1	0.0±0.0	0.0±0.0
$[Cu(L^4)_2]$	16.5±2.8	22.0±1.4	19.0±2.3	23.5±2.5	21.5±0.7	15.0±0.7
$[Zn(L^4)_2].H_2O$	20.0±1.4	16.5±0.7	23.0±1.4	19.5±0.3	18.0±0.0	20.3±1.4
$^+$Ciprofloxacin	33.0 ± 3.5	32.0 ± 1.4	36.0 ± 2.8	26.5 ± 0.7	29.0 ± 2.1	23.0 ± 1.4
-DMSO	0.0±0.0	0.0±0.0	0.0±0.0	0.0±0.0	0.0±0.0	0.0±0.0

Table 4.7.7. Antibacterial data of HL^4 ligand and its heteroleptic metal(II) complexes

Compound/ Bacteria	***Bacillus cereus***	***Escherichia coli***	***Klebsillaoxytoca***	***Pseudomonas aeruginosa***	***Staphylococcus aureus***	***Proteus mirabilis***
HL^4	15.0	21	17	16.5	21	16.5
Bipy	15.5 ± 0.7	12.0 ± 2.8	26.0 ± 2.8	8.5 ± 0.7	17.0 ± 4.2	19.5 ± 2.1
$[Mn(L^4)(Bipy)(OAc)].H_2O$	23.0±2.1	0.0±0.0	24.0±2.8	20.5±3.5	22.0±2.8	15.5±3.5
$[Fe(L^4)(Bipy)(SO_4)].H_2O$	22.5±2.1	13.5±2.8	18.0±2.8	16.5±0.7	13.0±2.8	19.0±3.5
$[Co(L^4)(Bipy)(OAc)]$	19.0±2.1	23,0±3.5	24.5±2.8	20.0±3.5	22.0±2.1	15.5±0.7
$[Ni(L^4)(Bipy)(OAc)].H_2O$	15.0±0.7	16.0±3.5	0.0±0.0	16.5±2.1	10.0±2.8	18.0±0.7
$[Cu(L^4)(Bipy)(OAc)].H_2O$	19.0±0.7	27.5±0.7	24.5±2.1	28.5±0.7	22.5±2.8	16.0±2.8
$[Zn(L^4)(Bipy)(OAc)]$	21.0±2.8	15.0±0.7	0.0±0.0	16.5±0.7	9.0±0.7	19.0±2.1
$^+$Ciprofloxacin	33.0 ± 3.5	32.0 ± 1.4	36.0 ± 2.8	26.5 ± 0.7	29.0 ± 2.1	23.0 ± 1.4
-DMSO	0.0±0.0	0.0±0.0	0.0±0.0	0.0±0.0	0.0±0.0	0.0±0.0

Table 4.7.8. Antibacterial data of HL^5 ligand and its metal(II) complexes

Compound/ Bacteria	***Bacillus cereus***	***Escherichia coli***	***Klebsillaoxytoca***	***Pseudomonas aeruginosa***	***Staphylococcus aureus***	***Proteus mirabilis***
HL^5	13.5±1.7	9.0±2.8	15.0±2.4	19.0±0.6	0.0±0.0	12.5±1.4
$[Mn(L^5)_2(H_2O)_2]$	19.0±0.0	12.0±0.7	16.0±3.5	0.0±0.0	0.0±0.0	11.0±0.7
$[Fe(L^5)_2(H_2O)_2]$	15.5±2.1	18.5±0.0	14.0±0.0	0.0±0.0	0.0±0.0	25.0±0.0
$[Co(L^5)_2(H_2O)_2].H_2O$	24.0±0.0	23.0±1.4	21.0±2.1	29.0±0.0	22.5±0.7	26.0±0.0
$[Ni(L^5)_2(H_2O)_2].H_2O$	0.0±0.0	0.0±0.0	9.5±1.4	0.0±0.0	0.0±0.0	0.0±0.0
$[Cu(L^5)_2]$	12.0±1.7	19.0±2.8	18.0±2.4	16.5±0.6	11.5±0.7	20.0±1.4
$[Zn(L^5)_2(H_2O)_2]$	0.0±0.0	21.0±0.1	16.0±1.4	14.5±2.1	20.0±1.7	15.0±0.7
$^+$Ciprofloxacin	33.0 ± 3.5	32.0 ± 1.4	36.0 ± 2.8	26.5 ± 0.7	29.0 ± 2.1	23.0 ± 1.4
-DMSO	0.0±0.0	0.0±0.0	0.0±0.0	0.0±0.0	0.0±0.0	0.0±0.0

Table 4.7.9. Antibacterial data of HL^5 ligand and its heteroleptic metal(II) complexes

Compound/ Bacteria	***Bacillus cereus***	***Escherichia coli***	***Klebsillaoxytoca***	***Pseudomonas aeruginosa***	***Staphylococcus aureus***	***Proteus mirabilis***
HL^5	13.5±1.7	9.0±2.8	15.0±2.4	19.0±0.6	0.0±0.0	12.5±1.4
Bipy	15.5 ± 0.7	12.0 ± 2.8	26.0 ± 2.8	8.5 ± 0.7	17.0 ± 4.2	19.5 ± 2.1
$[Mn(L^5)(Bipy)(OAc)].H_2O$	21.5 ±0.7	23.5 ±0.7	20.0 ±2.1	18.0 ±0.7	24.5 ±2.8	0.0 ±0.0
$[Fe(L^5)(Bipy)(SO_4)]$	24.5 ±1.4	17.5 ±1.4	28.5 ±2.1	19.5 ±2.8	14.5 ±0.7	20.0 ±2.1
$[Co(L^5)(Bipy)(OAc)].2H_2O$	27.0 ±2.8	30.0 ±0.0	22.5 ±0.0	23.5 ±0.7	27.0 ±0.0	29.0 ±2.1
$[Ni(L^5)(Bipy)(OAc)].H_2O$	19.5 ±2.1	24.5 ±0.0	19.5 ±0.0	16.0 ±2.1	0.0 ±0.0	0.0 ±0.0
$[Cu(L^5)(Bipy)(OAc)]$	26.0 ±1.4	21.5 ±0.7	29.0 ±1.4	21.3 ±0.0	22.5 ±0.0	24.0 ±0.7
$[Zn(L^5)(Bipy)(OAc)].H_2O$	21.0 ±1.4	18.0 ±2.8	20.0 ±2.1	17.0 ±2.1	14.5 ±2.8	22.0 ±0.7
$^+$Ciprofloxacin	33.0 ± 3.5	32.0 ± 1.4	36.0 ± 2.8	26.5 ± 0.7	29.0 ± 2.1	23.0 ± 1.4
-DMSO	0.0±0.0	0.0±0.0	0.0±0.0	0.0±0.0	0.0±0.0	0.0±0.0

Table 4.7.10.

Compound/	*Bacillus*	*Escherichia*	*Klebsillaoxytoca*	*Pseudomonas*	*Staphylococcus*	*Proteus*

Antibacterial data of HL^6 and ligand and its heteroleptic metal(II) complexes

Bacteria	***cereus***	***coli***		***aeruginosa***	***aureus***	***mirabilis***
HL^6	24.5±1.7	16.0±2.8	26.0±2.4	18.0±0.6	11.5.0±0.7	16.0±1.4
Bipy	15.5 ± 0.7	12.0 ± 2.8	26.0 ± 2.8	8.5 ± 0.7	17.0 ± 4.2	19.5 ± 2.1
$[Mn(L^6)(Bipy)(OAc)]$	31.0±2.5	18.7±0.1	23±0.8	16.5±0.7	20.0±1.6	28.0±2.2
$[Fe(L^6)(Bipy)(SO_4)]$	15.5±0.7	23.5±0.1	19.0±1.4	21.0±2.1	28.0±1.7	25.0±0.7
$[Co(L^6)(Bipy)(OAc)]$	29.0±3.5	21.0±2.8	27.0±0.7	32.0±0.1	23.0±0.7	26.0±2.1
$[Ni(L^6)(Bipy)(OAc)]$	21.0±0.7	28.5±2.1	0.0±0.0	0.0±0.0	26.0±0.7	18.5±2.8
$[Cu(L^6)(Bipy)(OAc)].H_2O$	29.0±0.7	22.0±0.7	24.6±2.8	31.0±1.4	34.0±1.7	27.0±2.4
$[Zn(L^6)(Bipy)(OAc)]$	16.0±0.6	24.5±1.7	21.0±2.1	31.0±0.0	20.0±1.4	28.0±0.0
$^+$Ciprofloxacin	33.0 ± 3.5	32.0 ± 1.4	36.0 ± 2.8	26.5 ± 0.7	29.0 ± 2.1	23.0 ± 1.4
-DMSO	0.0±0.0	0.0±0.0	0.0±0.0	0.0±0.0	0.0±0.0	0.0±0.0

Table 4.8.1. Antifungal result for HL^1 ligands and its metal(II) complexes

Fungal/Compounds	***Aspergillus niger***	***Aspergillus flevus***	***Rhizopus Stolonifer***
HL^1	13±2.8	15±1.4	7±1.0
$[Mn(L^1)_2].H_2O$	11± 0.35	17±0.35	15±1.41
$[Fe(L^1)_2(H_2O)_2]$	-	-	-
$[Co(L^1)_2].2H_2O$	-	-	-
$[Ni(L^1)_2].H_2O$	-	23	19±1.06
$[Cu(L^1)_2]$	-	-	19±0.77
$[Zn(L^1)_2]$	-	19	13±1.06
$^+$ Fluconazole	36±0.35	29±0.77	38±0.33
-DMSO	-	-	-

Table 4.8.2. Antifungal result for HL^1 ligands and its metal(II) complexes

Fungal/Compounds	***Aspergillus niger***	***Aspergillus flevus***	***Rhizopus Stolonifer***
HL^1	13±2.8	15±1.4	7±1.0
Bipy	16±1.6	19±1.4	13±0.7
$[Mn(L^1)(Bipy)(OAc)]$	-	-	11±0.3
$[Fe(L^1)(Bipy)(SO_4)]$	-	8±0.0	-
$[Co(L^1)(Bipy)(OAc)].H_2O$	-	17±1.4	-
$[Ni(L^1)(Bipy)(OAc)].H_2O$	9±0.1	-	-
$[Cu(L^1)(Bipy)(OAc)]$	-	-	16±1.4
$[Zn(L^1)(Bipy)(OAc)].2H_2O$	18±0.6	-	-
$^+$ Fluconazole	36±0.3	29±0.7	38±0.3
-DMSO	-	-	-

Table 4.8.3. Antifungal result for HL^1 ligand and its metal(II) complexes

Fungal/Compounds	***Aspergillus niger***	***Aspergillus flevus***	***Rhizopus Stolonifer***
HL^2	20±0.0	22±2.1	17±0.7
$[Mn(L^2)_2].2H_2O$	-	28±0.1	25±1.4
$[Fe(L^2)_2].2H_2O$	29±1.4	19±2.1	22±1.0
$[Co(L^2)_2].H_2O$	18±0.7	-	21±0.0
$[Ni(L^2)_2].H_2O$	-	21±0.7	20±2.1
$[Cu(L^2)_2]$	10±1.4	27±1.4	-
$[Zn(L^2)_2]$	-	29±1.6	21±2.8
$^+$ Fluconazole	36±0.3	29±0.7	38±0.3
-DMSO	-	-	-

Table 4.8.4. Antifungal result for HL^2 ligand and its metal(II) complexes

Fungal/Compounds	***Aspergillus niger***	***Aspergillus flevus***	***Rhizopus Stolonifer***
HL^2	20±0.0	22±2.1	17±0.7
Bipy	16±1.6	19±1.4	13±0.7
$[Mn(L^2)(Bipy)(OAc)].H_2O$	30±1.4	29±0.0	27±0.7
$[Fe(L^2)(Bipy)(SO_4)].H_2O$	22±2.1	17±0.7	22±0.6
$[Co(L^2)(Bipy)(OAc)]$.	21±0.0	29±0.0	16±1.4
$[Ni(L^2)(Bipy)(OAc)].H_2O$	33±0.0	23±1.4	24±0.3
$[Cu(L^2)(Bipy)(OAc)].H_2O$	17±1.4	25±0.7	29±0.0
$[Zn(L^2)(Bipy)(OAc)]$	26±0.0	21±0.0	18±2.1
$^+$ Fluconazole	36±0.3	29±0.7	38±0.3
-DMSO	-	-	-

Table 4.8.5. Antifungal result for HL^3 ligand and its heteroleptic metal(II) complexes

Fungal/Compounds	***Aspergillus niger***	***Aspergillus flevus***	***Rhizopus Stolonifer***
HL^3	19±1.4	21±0.7	-
Bipy	16±1.6	19±1.4	13±0.7
$[Mn(L^3)(Bipy)(OAc)]$	39±0.0	49±2.8	39±0.7
$[Fe(L^3)(Bipy)(SO_4)].H_2O$	15±1.4	17±0.0	-
$[Co(L^3)(Bipy)(OAc)]$	-	21±0.7	27±0.0
$[Ni(L^3)(Bipy)(OAc)]$	15±0.0	-	29±1.0
$[Cu(L^3)(Bipy)(OAc)]$	-	-	-
$[Zn(L^3)(Bipy)(OAc)].H_2O$	17±2.1	21±0.0	-
$^+$ Fluconazole	36±0.3	29±0.7	38±0.3
-DMSO	-	-	-

Table 4.8.6. Antifungal result for HL^4 ligands and its metal(II) complexes

Fungal/Compounds	***Aspergillus niger***	***Aspergillus flevus***	***Rhizopus Stolonifer***
HL^4	23±0.0	27±2.1	19±1.4
$[Mn(L^4)_2].H_2O$	29±0.7	19±2.5	25±0.0
$[Fe(L^4)_2(H_2O)_2]$	11±2.1	15±0.0	13±1.4
$[Co(L^4)_2(H_2O)_2].H_2O$	11±1.4	33±2.1	15±0.0
$[Ni(L^4)_2(H_2O)_2].H_2O$	13±0.0	-	-
$[Cu(L^4)_2(H_2O)_2]$	11±0.0	25±0.0	17±0.7
$[Zn(L^4)_2].H_2O$	19±0.7	23±1.4	19±0.0
$^+$ Fluconazole	36±0.3	29±0.7	38±0.3
-DMSO	-	-	-

Table 4.8.7. Antifungal result for HL^4 ligand and its heteroleptic metal(II) complexes

Fungal/Compounds	*Aspergillus niger*	*Aspergillus flevus*	*Rhizopus Stolonifer*
HL^4	23±0.0	27±2.1	19±1.4
Bipy	16±1.6	19±1.4	13±0.7
$[Mn(L^4)(Bipy)(OAc)].H_2O$	29±2.1	31±0.0	-
$[Fe(L^4)(Bipy)(SO_4)].H_2O$	-	-	-
$[Co(L^4)(Bipy)(OAc)]$	13±1.4	17±0.7	-
$[Ni(L^4)(Bipy)(OAc)].H_2O$	13±0.0	15±1.4	17±2.1
$[Cu(L^4)(Bipy)(OAc)].H_2O$	-	-	23±0.0
$[Zn(L^4)(Bipy)(OAc)]$	19±1.4	19±0.0	17±0.7
$^+$ Fluconazole	36±0.3	29±0.7	38±0.3
-DMSO	-	-	-

Table 4.8.8. Antifungal result for HL^5 ligand and its metal(II) complexes

Fungal/Compounds	***Aspergillus niger***	***Aspergillus flevus***	***Rhizopus Stolonifer***
HL^5	15±1.4	39±0.7	40±2.1
$[Mn(L^5)_2(H_2O)_2]$	11±0.0	21±0.7	11±1.4
$[Fe(L^5)_2(H_2O)_2]$	-	13±0.0	-
$[Co(L^5)_2(H_2O)_2].H_2O$	11±1.2	17±1.4	13±0.0
$[Ni(L^5)_2(H_2O)_2].H_2O$	-	-	-
$[Cu(L^5)_2]$	15±0.0	-	17±1.4
$[Zn(L^5)_2(H_2O)_2]$	11±1.4	-	13±0.1
$^+$ Fluconazole	36±0.3	29±0.7	38±0.3
-DMSO	-	-	-

Table 4.8.9. Antifungal result for HL^5 ligands and its heteroleptic metal(II) complexes

Fungal/Compounds	***Aspergillus niger***	***Aspergillus flevus***	***Rhizopus Stolonifer***
HL^5	15±1.4	39±0.7	40±2.1
Bipy	16±1.6	19±1.4	13±0.7
$[Mn(L^5)(Bipy)(OAc)].H_2O$	14±1.7	-	17±0.1
$[Fe(L^5)(Bipy)(SO_4)]$	-	-	-
$[Co(L^5)(Bipy)(OAc)].2H_2O$	-	14±0.0	-
$[Ni(L^5)(Bipy)(OAc)].H_2O$	-	24±1.4	-
$[Cu(L^5)(Bipy)(OAc)]$	13±1.4	19±0.7	-
$[Zn(L^5)(Bipy)(OAc)].H_2O$	19±0.7	23±0.1	33±2.1
$^+$ Fluconazole	36±0.3	29±0.7	38±0.3
-DMSO	-	-	-

Table 4.8.10. Antifungal result for HL^6 ligand and its heteroleptic metal(II) complexes

Fungal/Compounds	***Aspergillus niger***	***Aspergillus flevus***	***Rhizopus Stolonifer***
HL^6	23±0.3	29±1.4	27±0.7
Bipy	16±1.6	19±1.4	13±0.7
$[Mn(L^6)(Bipy)(OAc)]$	13±0.6	21±0.1	-
$[Fe(L^6)(Bipy)(SO_4)]$	11±1.4	17±0.7	13±0.0
$[Co(L^6)(Bipy)(OAc)]$	23±0.7	21±0.6	25±0.7
$[Ni(L^6)(Bipy)(OAc)]$	13±0.0	23±0.0	-
$[Cu(L^6)(Bipy)(OAc)].H_2O$	-	-	-
$[Zn(L^6)(Bipy)(OAc)]$	11±1.4	19±2.1	-
$^+$ Fluconazole	36±0.3	29±0.7	38±0.3
-DMSO	-	-	-

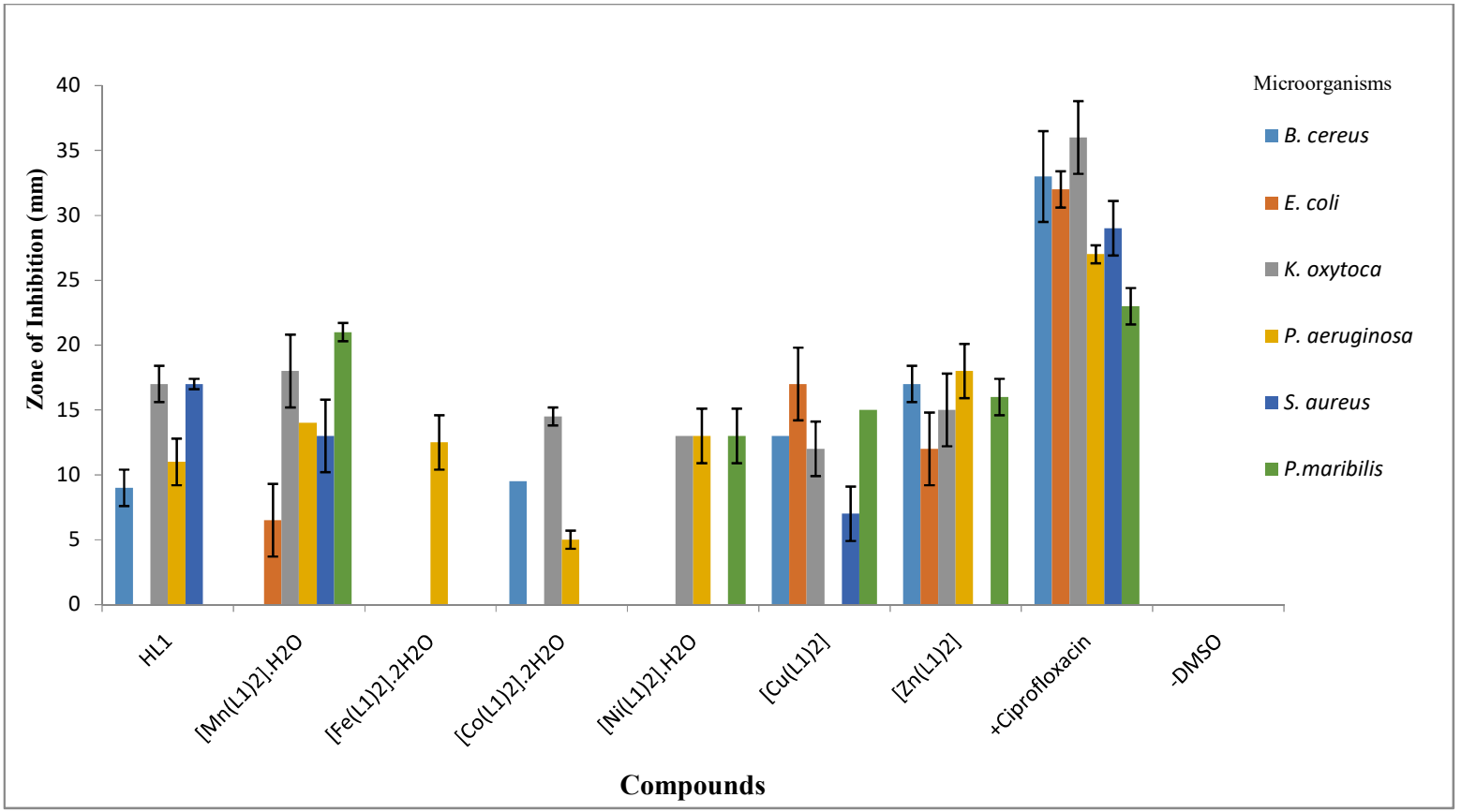

Figure 4.6.1. Histogram of the antibacterial activities of HL^1 ligand and its metal(II) complexes

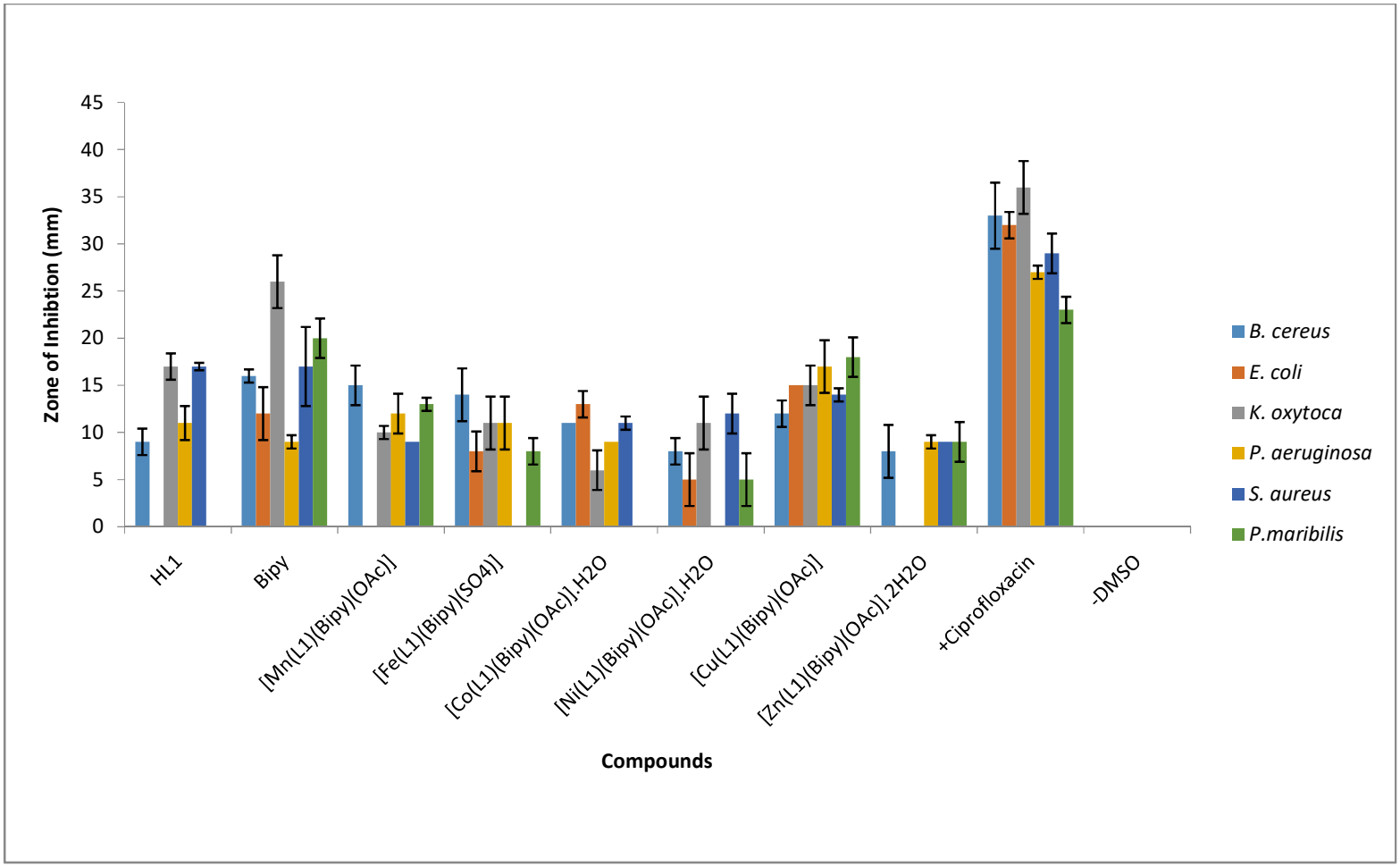

Figure 4.6.2. Histogram of theAntibacterial activities of HL^1 ligand and its heteroleptic metal(II) complexes

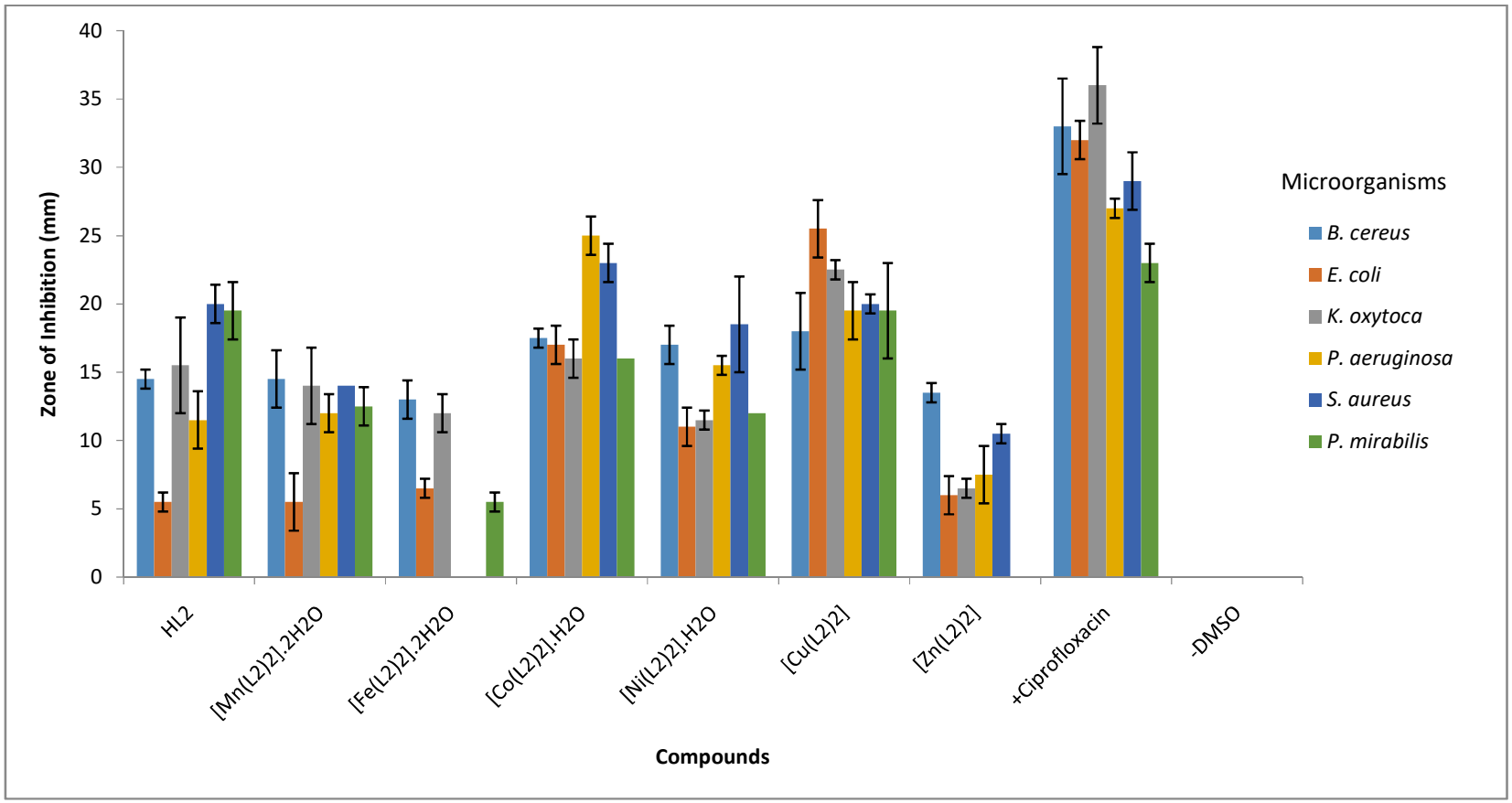

Figure 4.6.3. Histogram of theantibacterial activities of HL^2 ligand and its metal(II) complexes

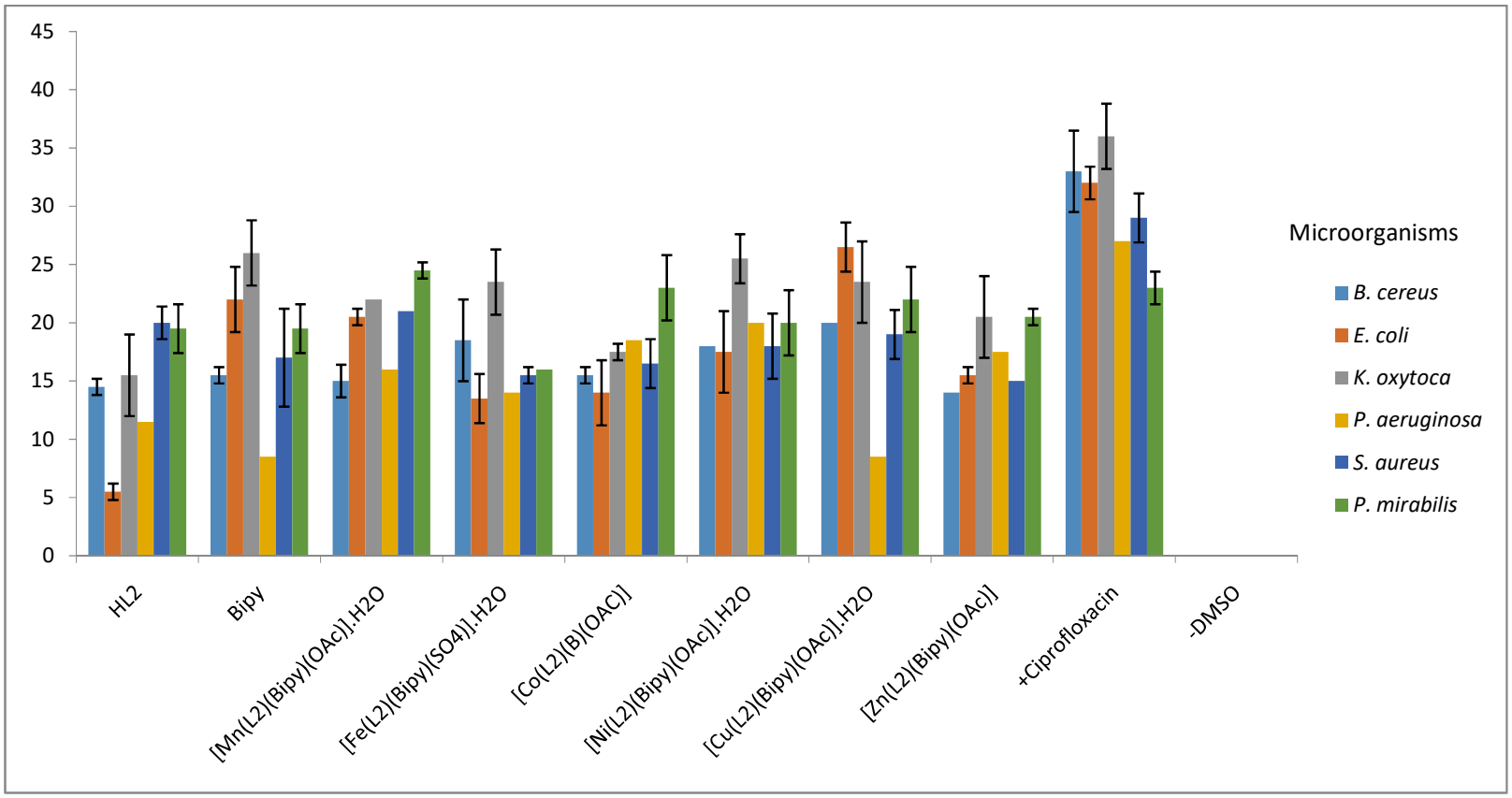

Figure 4.6.4. Histogram of the antibacterial activities of HL^2 ligand and its heteroleptic metal(II) complexes

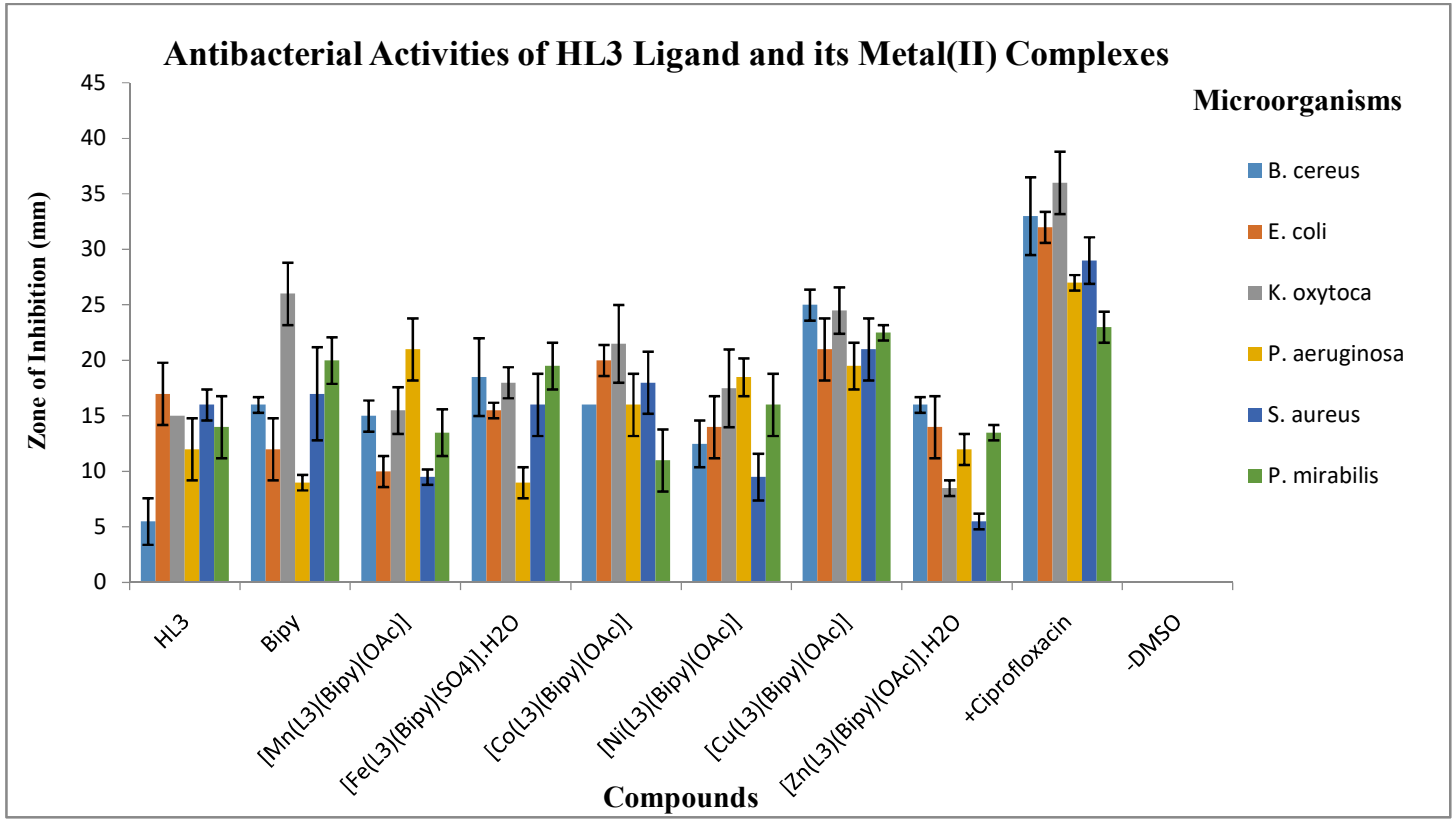

Figure 4.6.5. Histogram of the antibacterial activities of HL^3 ligand and its heteroleptic metal(II) complexes

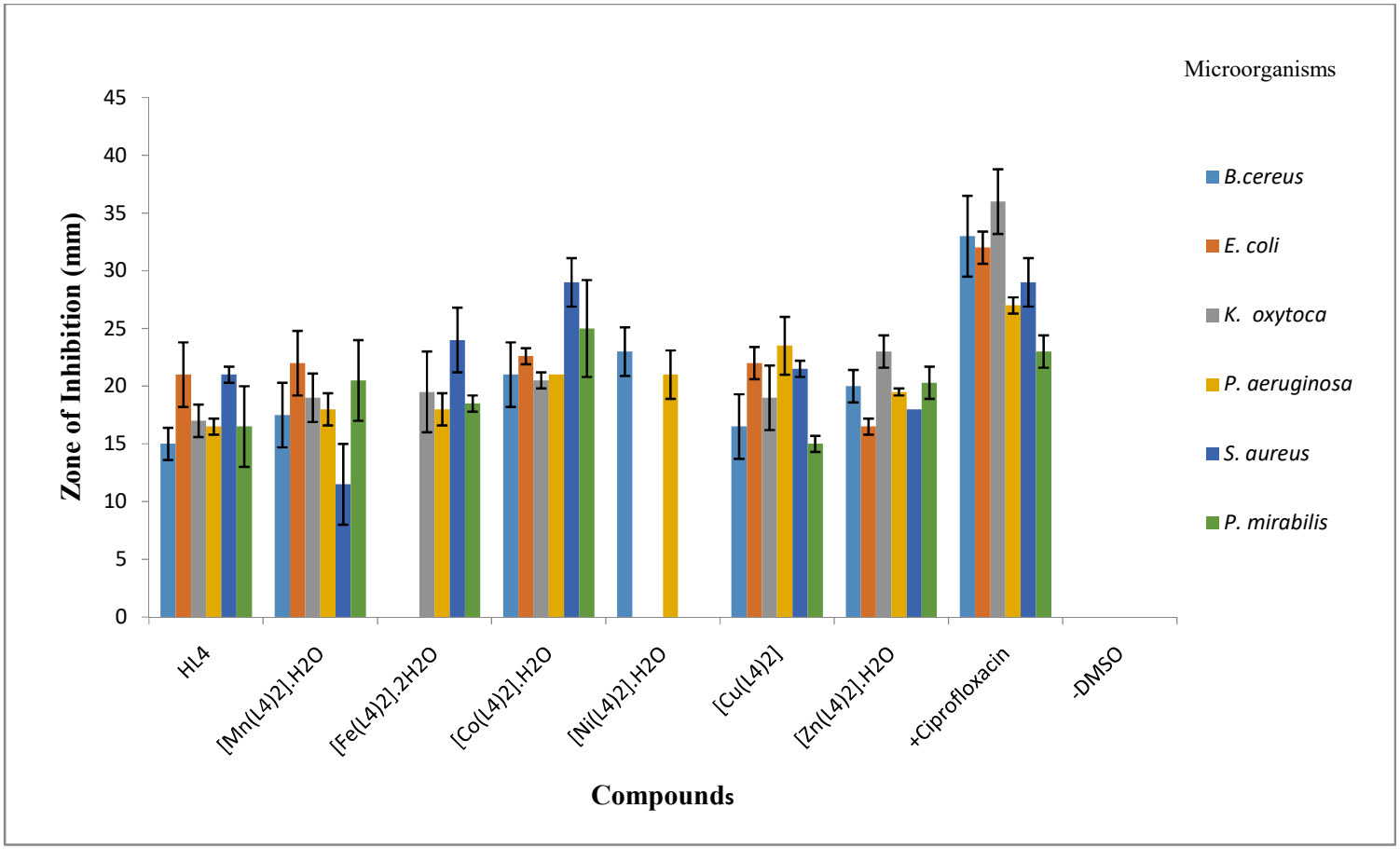

Figure 4.6.6. Histogram of theantibacterial activities of HL^4 ligand and its metal(II) complexes

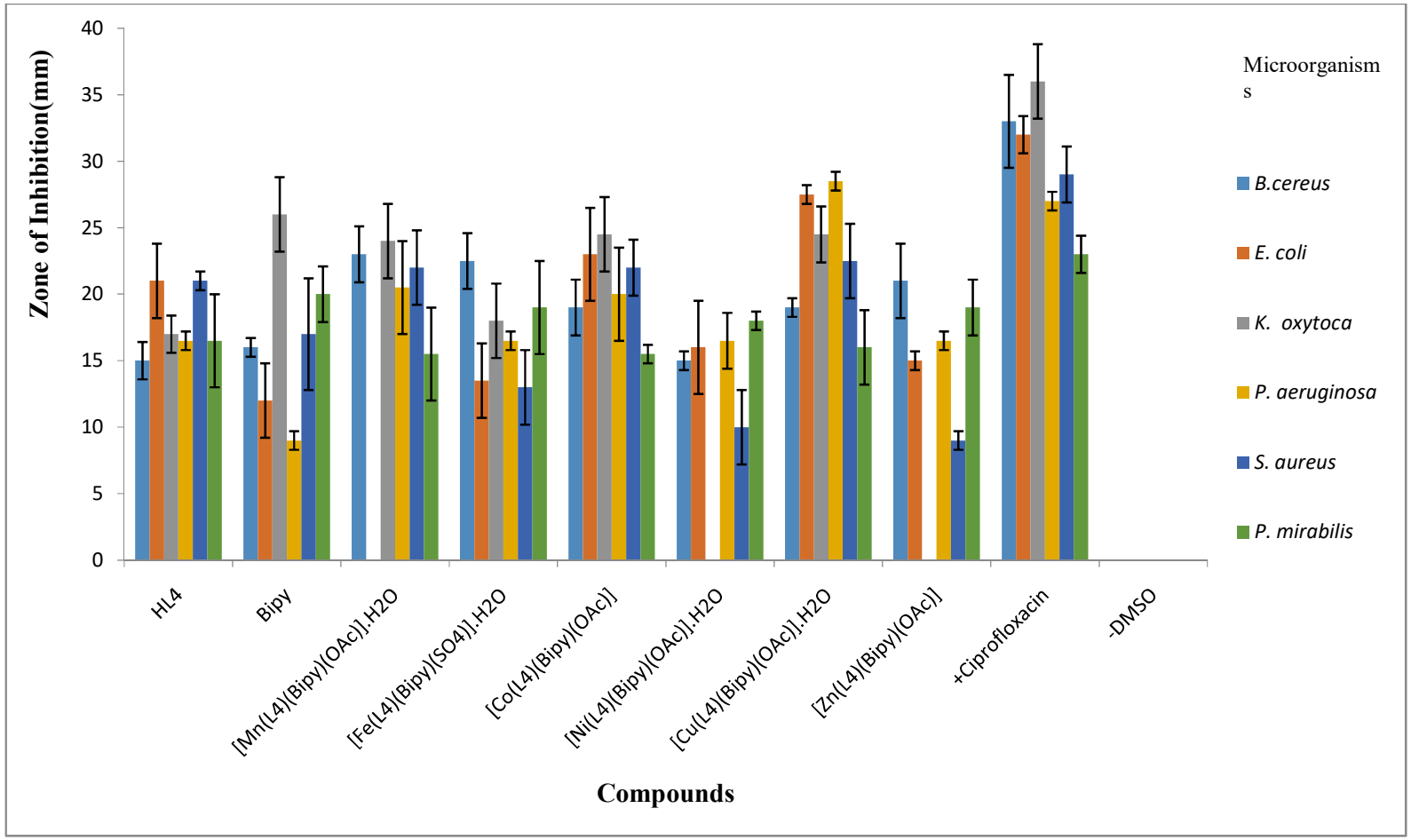

Figure 4.6.7. Histogram of the antibacterial activities of HL^4 ligand and its heteroleptic metal(II) complexes

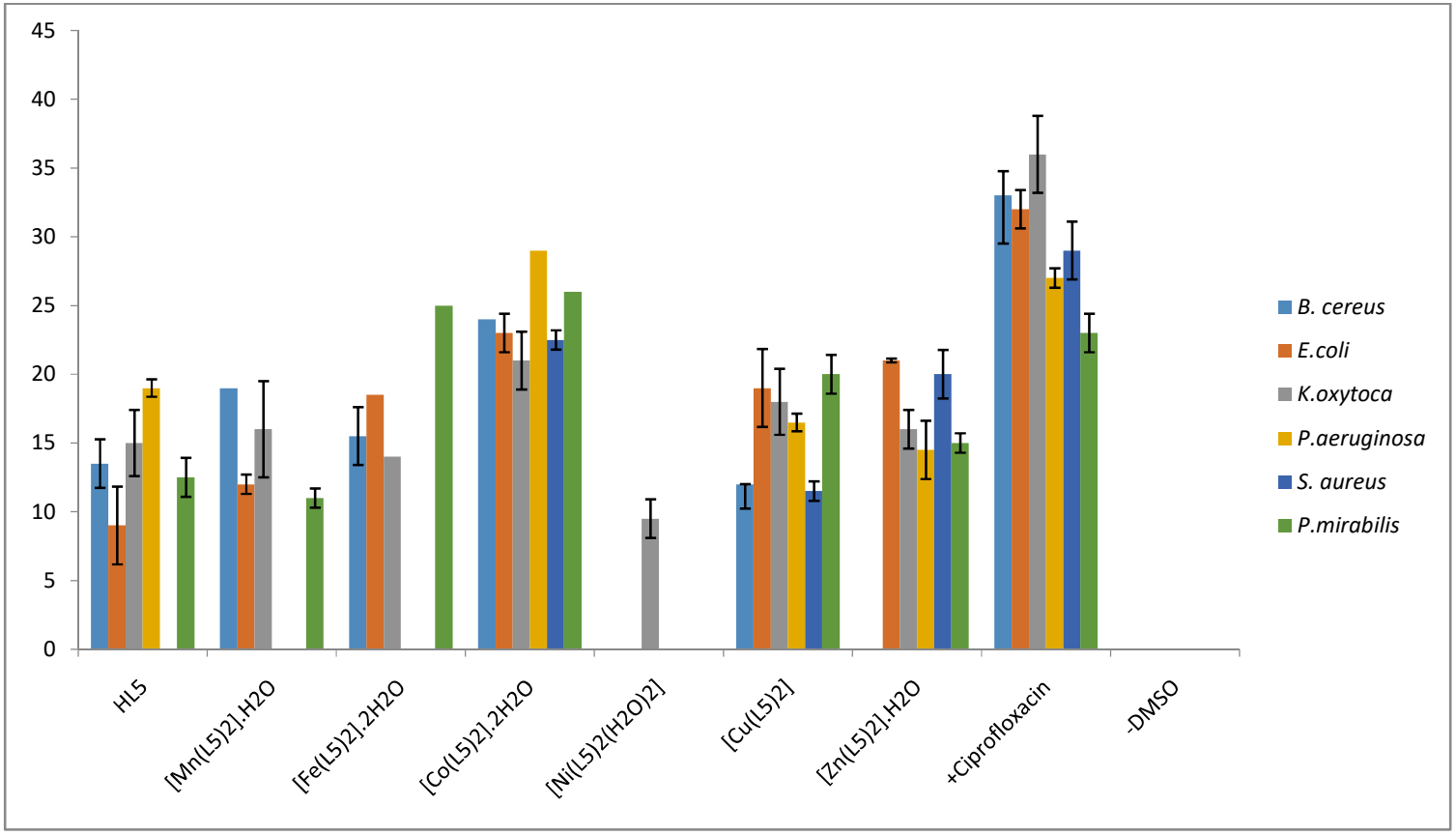

Figure 4.6.8. Histogram of the antibacterial activities of HL^5 ligand and its metal(II) complexes

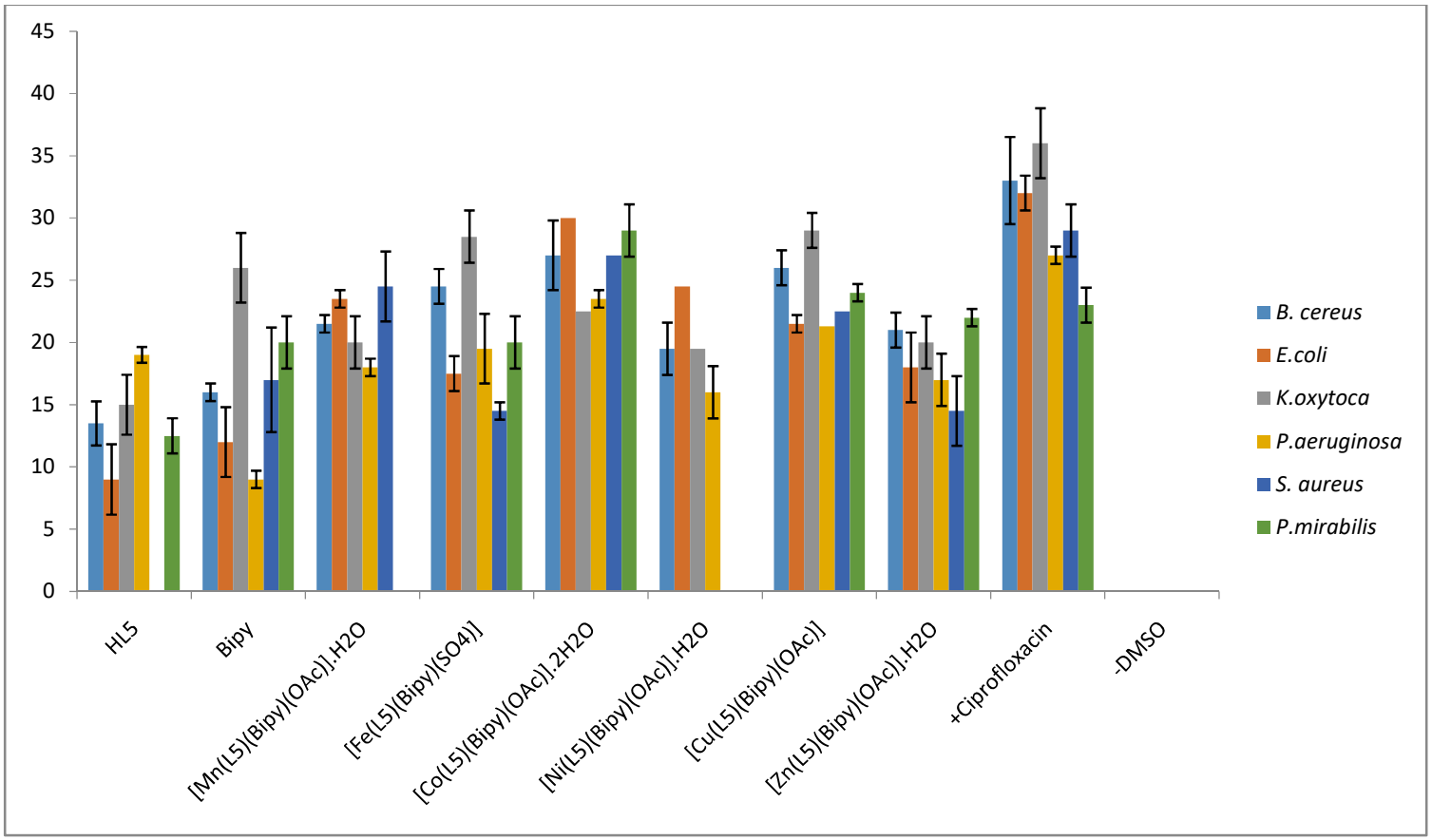

Figure 4.6.9. Histogram of the antibacterial activities of HL^5 ligand and its heteroleptic metal(II) complexes

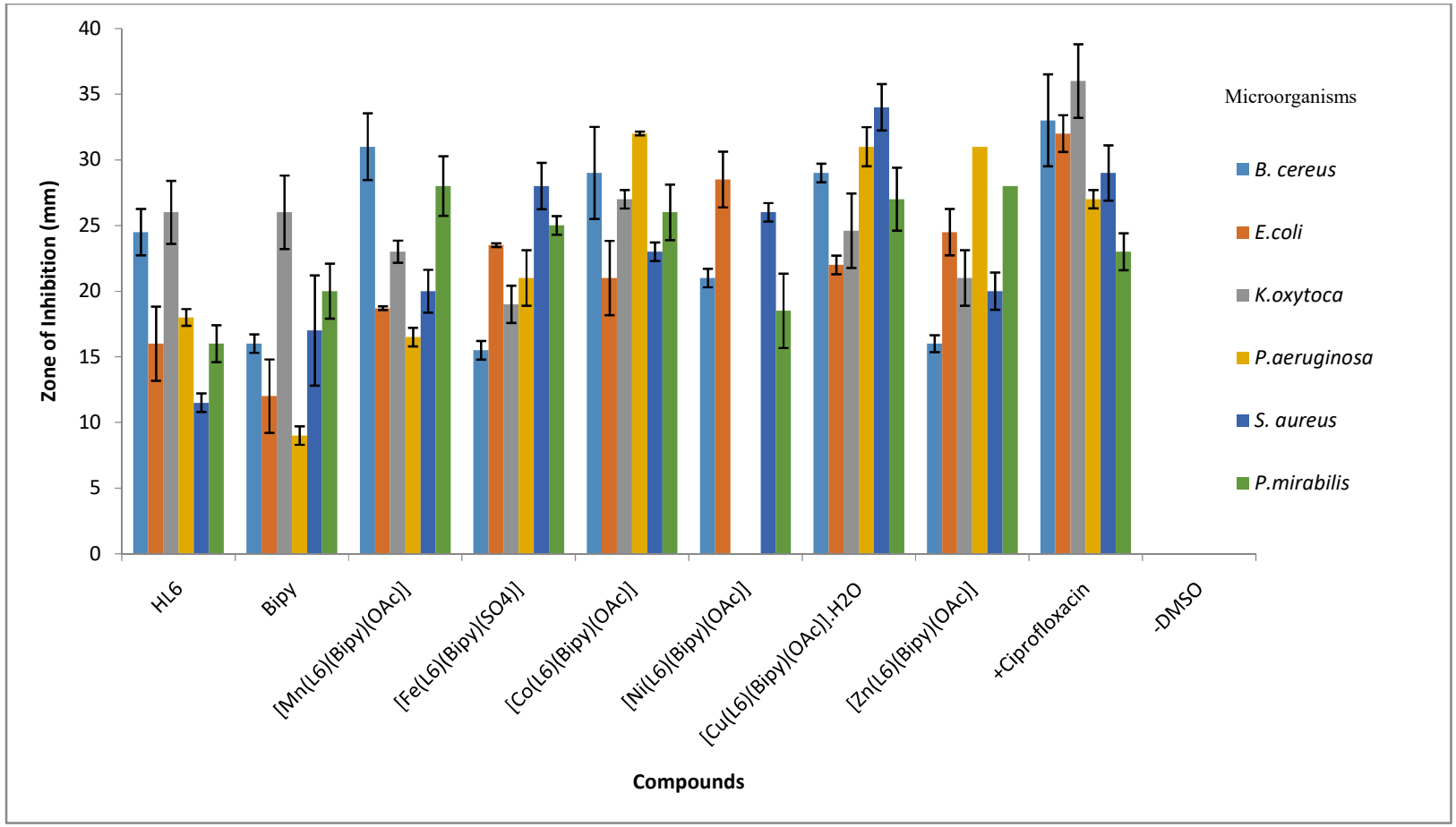

Figure 4.6.10. Histogram of the antibacterial activities of HL^6 ligand and its heteroleptic metal(II) complexes

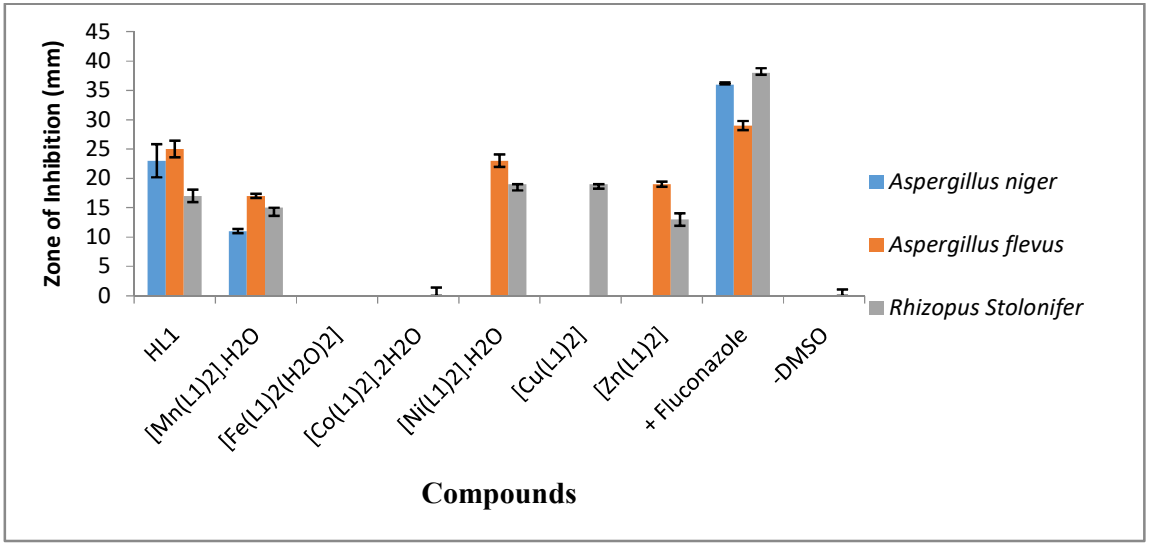

Figure 4.7.1. Histogram of the antifungal activities of HL^1 ligand and its metal(II) complexes

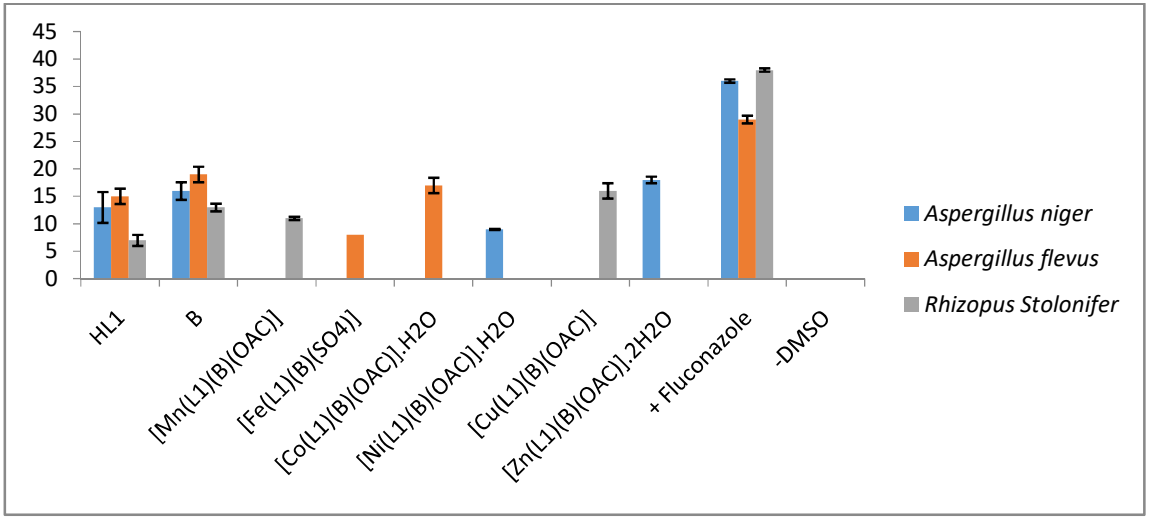

Figure 4.7.2. Histogram of the antifungal activities of HL^1 ligand and its heteroleptic metal(II) complexes

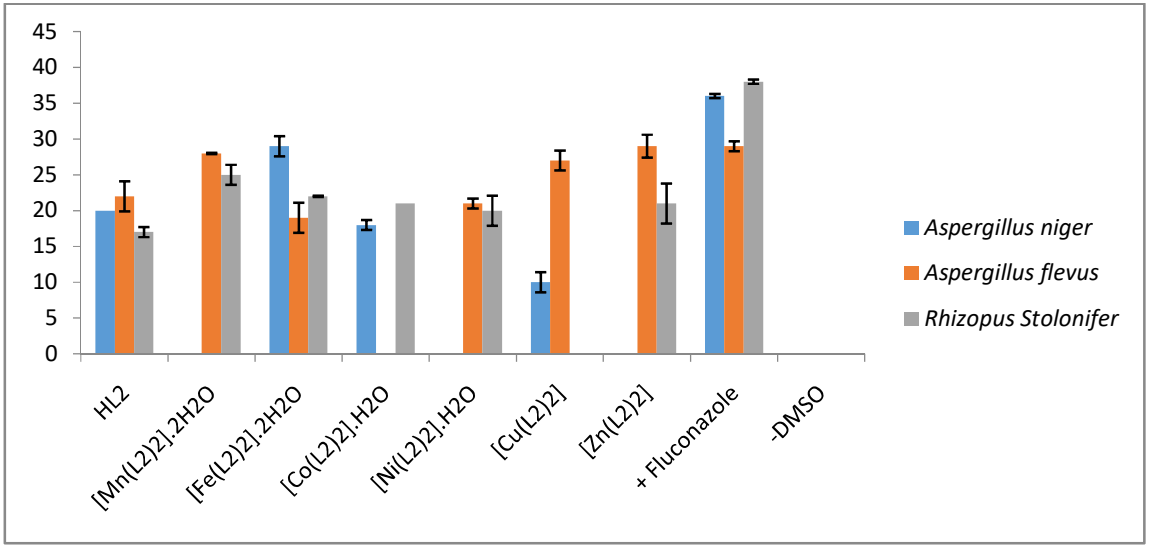

Figure 4.7.3. Histogram of the antifungal activities of HL^2 ligand and its metal(II) complexes

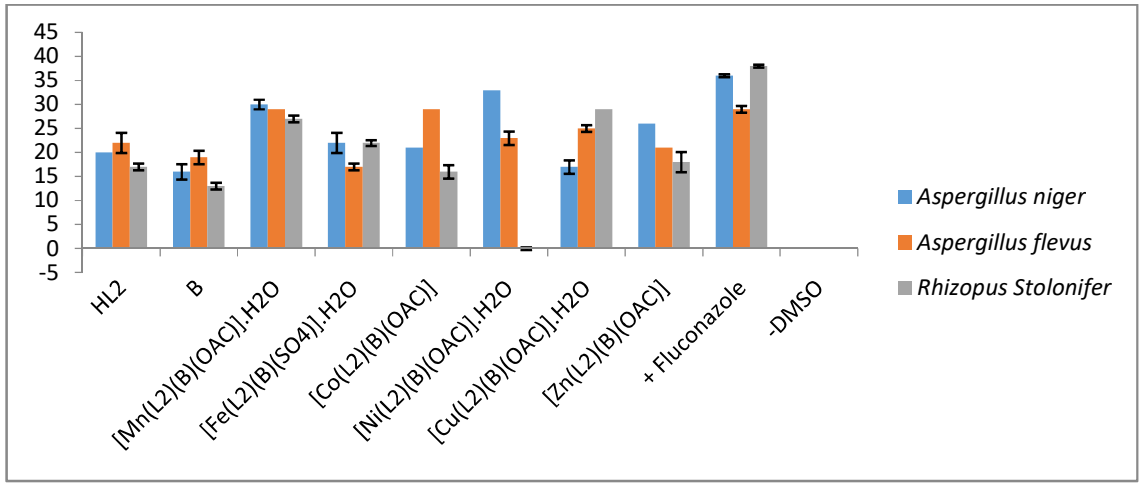

Figure 4.7.4. Histogram of the antifungal activities of HL^2 ligand and its heteroleptic metal(II) complexes

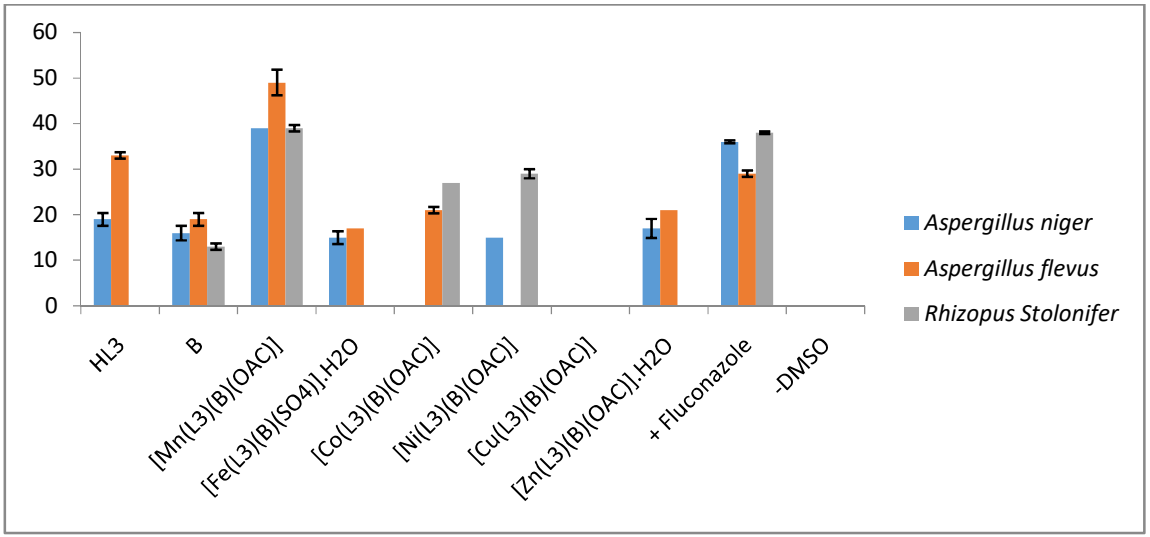

Figure 4.7.5. Histogram of the antifungal activities of HL^3 ligand and its heteroleptic metal(II) complexes

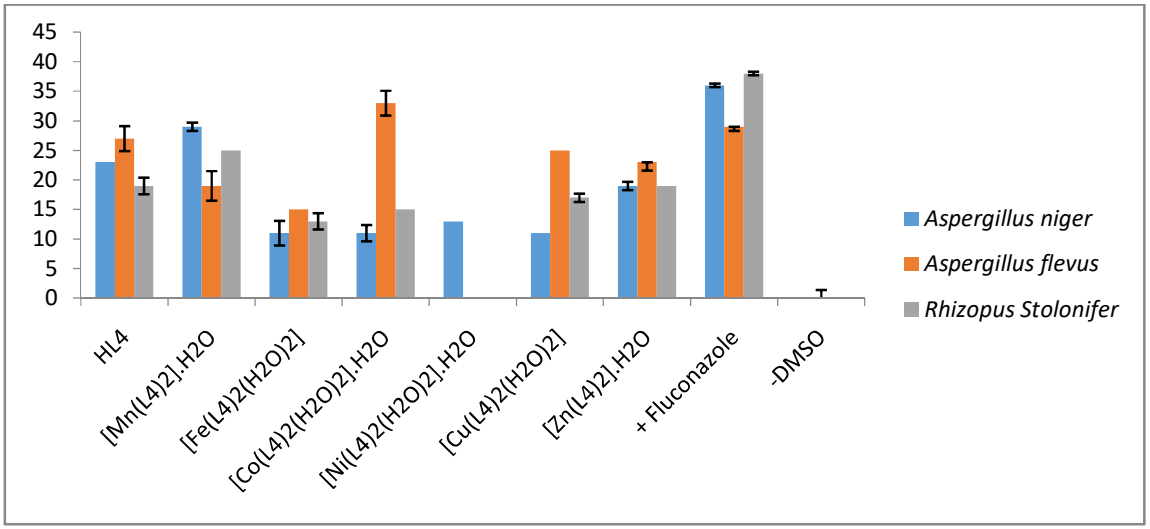

Figure 4.7.6. Histogram of the antifungal activities of HL^4 ligand and its metal(II) complexes

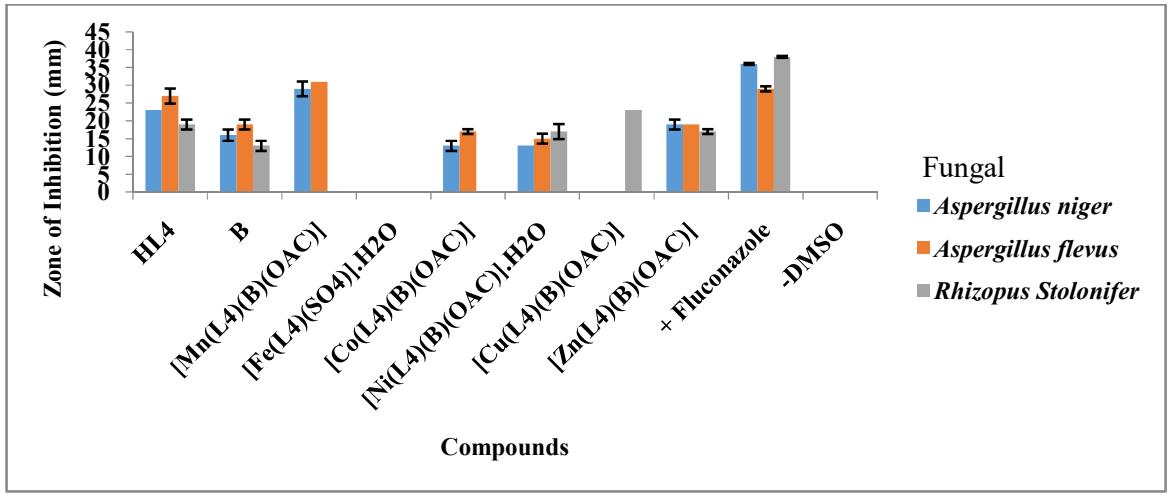

Figure 4.7.7. Histogram of the antifungal activities of HL^4 ligand and its heteroleptic metal(II) complexes

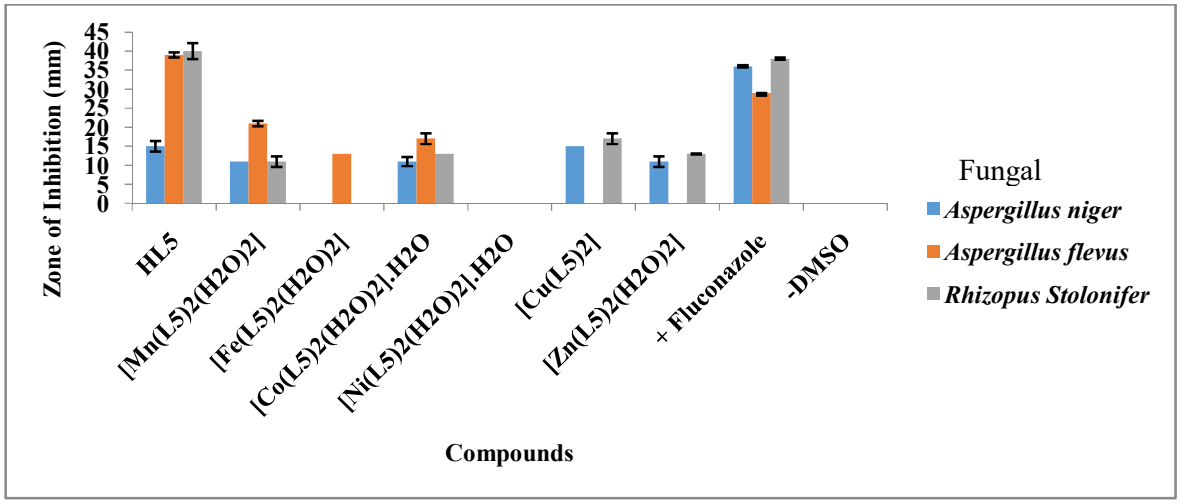

Figure 4.7.8. Histogram of the antifungal activities of HL^5 ligand and its metal(II) complexes

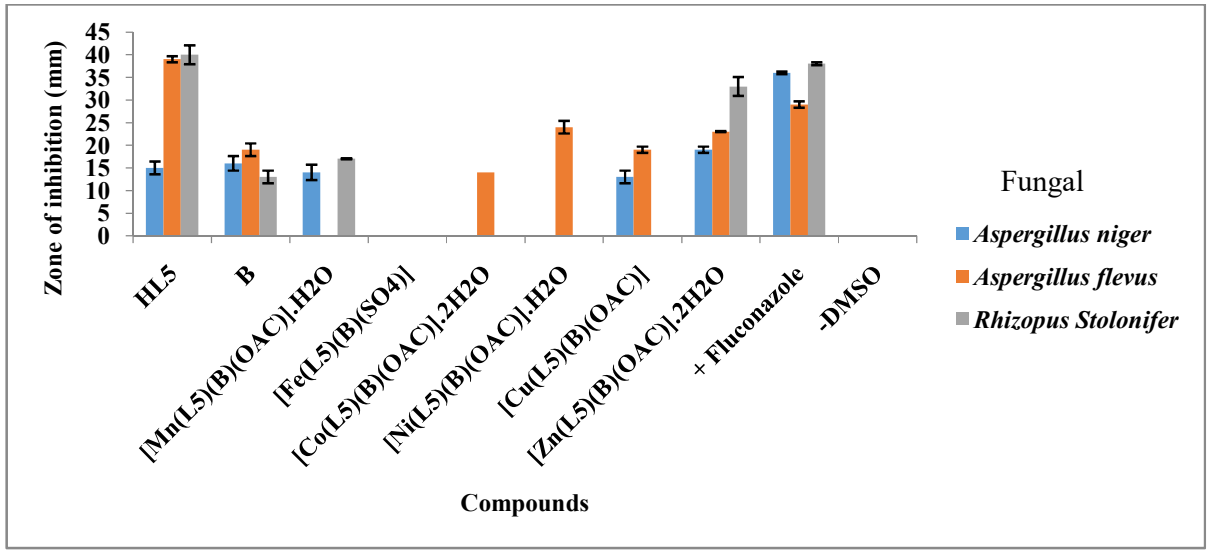

Figure 4.7.9. Histogram of the antifungal activities of HL^5 ligand and its heteroleptic metal(II) complexes

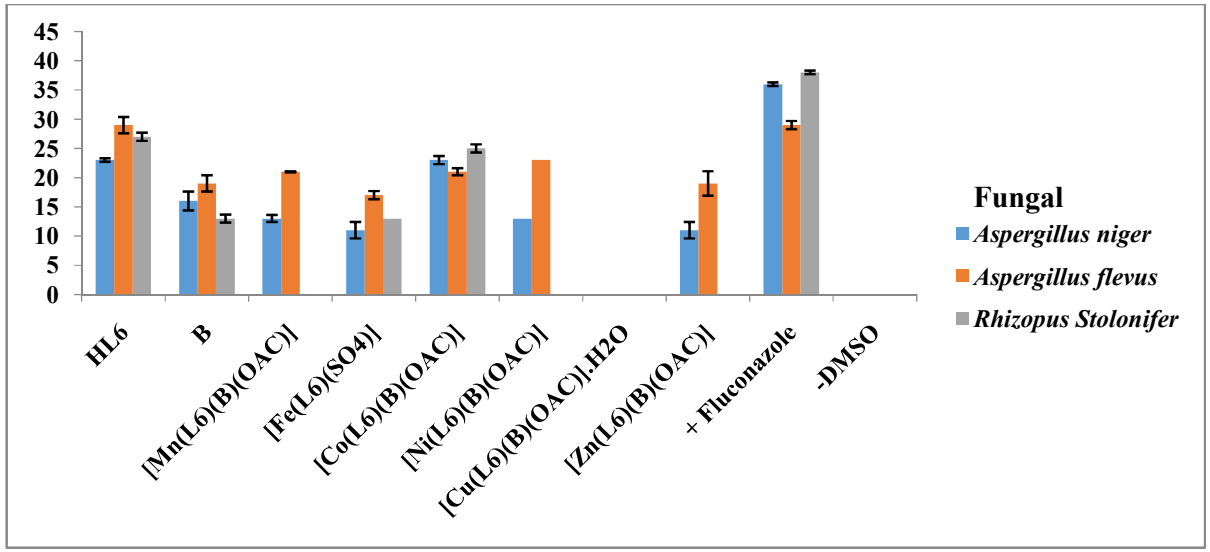

Figure 4.7.10. Histogram of the antifungal activities of HL^6 ligand and its heteroleptic metal(II) complexes

Table 4.9.1. DPPH radical scavenging data of HL^1 ligand and its metal (II) complexes

Compounds	Concentration	Absorbance			Mean(Error)	% Inhibition (Error)
		1	2	3		
Blank	-	0.77	0.78	0.78	-	-
HL^1	Ic_{50}	0.017	0.020	0.022	0.757(±0.003)	97.47 (±0.30)
	Ic_{100}	0.013	0.014	0.014	0.763(±0.005)	98.23 (±0.07)
	Ic_{200}	0.002	0.003	0.003	0.774(±0.005)	99.63(±0.07)
$[Mn(L^1)_2].H_2O$	Ic_{50}	0.012	0.012	0.011	0.765(±0.006)	98.50(±0.10)
	Ic_{100}	0.009	0.008	0.009	0.768(±0.006)	98.86(±0.12)
	Ic_{200}	0.006	.006	0.005	0.771(±0.006)	99.26(±0.12)
$[Fe(L^1)_2(H_2O)_2]$	Ic_{50}	0.123	0.123	0.129	0.652(±0.005)	83.90(±0.36)
	Ic_{100}	0.69	0.62	0.64	0.715(±0.003)	92.00(±0.25)
	Ic_{200}	0.009	0.009	0.010	0.767(±0.006)	98.76(±0.07)
$[Co(L^1)_2].2H_2O$	Ic_{50}	0.032	0.032	0.030	0.745(±0.006)	95.96 (±0.21)
	Ic_{100}	0.030	0.030	0.030	0.747(±0.006)	96.16(±0.07)
	Ic_{200}	0.027	0.029	0.029	0.748(±0.004)	96.36(±0.12)
$[Ni(L^1)_2].H_2O$	Ic_{50}	0.058	0.062	0.064	0.715(±0.003)	92.13(±0.35)
	Ic_{100}	0.030	0.030	0.032	0.746(±0.005)	96.06(±0.15)
	Ic_{200}	0.024	0.026	0.024	0.752(±0.007)	96.80(±0.17)
$[Cu(L^1)_2]$	Ic_{50}	0.025	0.025	0.025	0.752(±0.006)	96.80(±0.00)
	Ic_{100}	0.019	0.019	0.019	0.758(±0.006)	97.5(±0.07)
	Ic_{200}	0.000	0.002	0.005	0.774(±0.004)	99.7(±0.30)
$[Zn(L^1)_2]$	Ic_{50}	0.021	0.020	0.020	0.756(±0.006)	97.36(±0.07)
	Ic_{100}	0.005	0.004	0.004	0.772(±0.006)	99.46(±0.07)
	Ic_{200}	0.002	0.000	0.001	0.773(±0.006)	99.52(±0.07)
Standard Ascorbic Acid	Ic_{50}	0.093	0.089	0.094	0.578(±0.002)	86.26(±0.38)
	Ic_{100}	0.085	0.081	0.082	0.587(±0.002)	87.66(±0.32)
	Ic_{200}	0.078	0.074	0.076	0.594(±0.002)	88.67(±0.35)

Table 4.9.2. DPPH radical scavenging data of HL^1 ligand and its heteroleptic metal complexes

Compounds	Concentration	Absorbance			Mean(Error)	% Inhibition (Error)
		1	2	3		
Blank	-	0.77	0.78	0.78	-	-
HL^1	Ic_{50}	0.017	0.020	0.022	0.757(±0.003)	97.47 (±0.308)
	Ic_{100}	0.013	0.014	0.014	0.763(±0.005)	98.23 (±0.070)
	Ic_{200}	0.002	0.003	0.003	0.774(±0.005)	99.63(±0.070)
Bipy	Ic_{50}	0.172	0.170	0.168	0.501(±0.004)	74.76(±0.570)
	Ic_{100}	0.160	0.160	0.158	0.510(±0.002)	76.23(±0.234)
	Ic_{200}	0.152	0.152	0.150	0.518(±0.002)	77.40(±0.173)
$[Mn(L^1)(Bipy)(OAc)]$	Ic_{50}	0.082	0.082	0.083	0.694(±0.005)	89.43(±0.070)
	Ic_{100}	0.080	0.078	0.078	0.698(±0.007)	89.96(±0.234)
	Ic_{200}	0.057	0.058	0.058	0.719(±0.005)	92.60(±0.000)
$[Fe(L^1)(Bipy)(SO_4)]$	Ic_{50}	0.132	0.132	0.132	0.645(±0.006)	83.03(±0.122)
	Ic_{100}	0.105	0.106	0.107	0.671(±0.005)	86.36(±0.070)
	Ic_{200}	0.045	0.044	0.045	0.732(±0.006)	94.26(±0.122)
$[Co(L^1)(Bipy)(OAc)].H_2O$	Ic_{50}	0.016	0.017	0.019	0.759(±0.004)	97.76(±0.158)
	Ic_{100}	0.001	0.008	0.006	0.769(±0.007)	98.96(±0.254)
	Ic_{200}	0.004	0.007	0.006	0.771(±0.004)	99.26(±0.212)
$[Ni(L^1)(Bipy)(OAc)].H_2O$	Ic_{50}	0.014	0.015	0.016	0.762(±0.005)	98.10(±0.10)
	Ic_{100}	0.008	0.009	0.009	0.768(±0.005)	98.86(±0.122)
	Ic_{200}	0.006	0.006	0.007	0.770(±0.005)	99.16(±0.070)
$[Cu(L^1)(Bipy)(OAc)]$	Ic_{50}	0.005	0.005	0.005	0.577(±0.256)	74.36(±0.332)
	Ic_{100}	0.008	0.008	0.008	0.697(±0.006)	89.70(±0.10)
	Ic_{200}	0.043	0.045	0.044	0.733(±0.005)	94.33(±0.122)
$[Zn(L^1)(Bipy)(OAc)].2H_2O$	Ic_{50}	0.036	0.037	0.036	0.740(±0.005)	95.33(±0.070)
	Ic_{100}	0.052	0.051	0.051	0.730(±0.000)	93.40(±0.173)
	Ic_{200}	0.019	0.018	0.019	0.758(±0.005)	97.63(±0.070)
Standard Ascorbic Acid	Ic_{50}	0.093	0.089	0.094	0.578(±0.002)	86.26(±0.38)
	Ic_{100}	0.085	0.081	0.082	0.587(±0.002)	87.66(±0.32)
	Ic_{200}	0.078	0.074	0.076	0.594(±0.002)	88.67(±0.35)

Table 4.9.3. DPPH radical scavenging data of HL^2 ligand and its metal(II) complexes

Compounds	Concentration	Absorbance			Mean(Error)	% Inhibition (Error)
		1	2	3		
Blank	-	0.669	0.670	0.671	-	-
HL^2	Ic_{50}	0.095	0.097	0.097	0.573(±0.000)	85.60(±0.173)
	Ic_{100}	0.095	0.095	0.095	0.575(±0.001)	85.80(±0.000)
	Ic_{200}	0.103	0.103	0.103	0.567(±0.001)	84.60(±0.000)
$[Mn(L^2)_2].2H_2O$	Ic_{50}	0.018	0.018	0.018	0.652(±0.001)	97.30(±0.000)
	Ic_{100}	0.006	0.006	0.006	0.610(±0.001)	91.03(±0.070)
	Ic_{200}	0.005	0.005	0.005	0.665(±0.001)	99.30(±0.000)
$[Fe(L^2)_2].2H_2O$	Ic_{50}	0.111	0.112	0.112	0.558(±0.000)	83.33(±0.070)
	Ic_{100}	0.164	0.164	0.164	0.506(±0.001)	75.53(±0.070)
	Ic_{200}	0.611	0.611	0.609	0.610(±0.001)	91.10(±0.264)
$[Co(L^2)_2].H_2O$	Ic_{50}	0.023	0.024	0.024	0.646(±0.000)	96.46(±0.122)
	Ic_{100}	0.034	0.033	0.033	0.636(±0.001)	95.03(±0.122)
	Ic_{200}	0.062	0.059	0.059	0.610(±0.002)	91.03(±0.291)
$[Ni(L^2)_2].H_2O$	Ic_{50}	0.021	0.023	0.021	0.648(±0.001)	96.80(±0.173)
	Ic_{100}	0.023	0.023	0.023	0.647(±0.001)	96.60(±0.000)
	Ic_{200}	0.036	0.036	0.036	0.634(±0.001)	94.60(±0.000)
$[Cu(L^2)_2]$	Ic_{50}	0.047	0.046	0.045	0.624(±0.002)	93.13(±0.158)
	Ic_{100}	0.023	0.021	0.022	0.648(±0.001)	96.73(±0.158)
	Ic_{200}	0.001	0.002	0.001	0.668(±0.001)	99.8(±0.122)
$[Zn(L^2)_2]$	Ic_{50}	0.023	0.025	0.025	0.645(±0.000)	96.40(±0.173)
	Ic_{100}	0.031	0.031	0.031	0.693(±0.001)	95.40(±0.000)
	Ic_{200}	0.008	0.008	0.007	0.662(±0.001)	98.87(±0.122)
Standard Ascorbic Acid	Ic_{50}	0.093	0.089	0.094	0.578(±0.002)	86.26(±0.38)
	Ic_{100}	0.085	0.081	0.082	0.587(±0.002)	87.66(±0.32)
	Ic_{200}	0.078	0.074	0.076	0.594(±0.002)	88.67(±0.35)

Table 4.9.4.DPPH radical scavenging data of HL^2 ligand and its heteroleptic metal complexes

Compounds	Concentration	Absorbance			Mean(Error)	% Inhibition (Error)
		1	2	3		
Blank	-	0.669	0.670	0.671	-	-
HL^2	Ic_{50}	0.095	0.097	0.097	0.573(±0.000)	85.60(±0.173)
	Ic_{100}	0.095	0.095	0.095	0.575(±0.001)	85.80(±0.000)
	Ic_{200}	0.103	0.103	0.103	0.567(±0.001)	84.60(±0.000)
Bipy	Ic_{50}	0.172	0.170	0.168	0.501(±0.004)	74.76(±0.570)
	Ic_{100}	0.160	0.160	0.158	0.510(±0.002)	76.23(±0.234)
	Ic_{200}	0.152	0.152	0.150	0.518(±0.002)	77.40(±0.173)
$[Mn(L^2)(Bipy)(OAc)].H_2O$	Ic_{50}	0.046	0.045	0.045	0.624(±0.001)	93.23(±0.122)
	Ic_{100}	0.013	0.011	0.013	0.657(±0.001)	98.2(±0.173)
	Ic_{200}	0.008	0.008	0.008	0.662(±0.001)	98.80(±0.000)
$[Fe(L^2)(Bipy)(SO_4)].H_2O$	Ic_{50}	0.109	0.109	0.109	0.561(±0.001)	83.73(±0.070)
	Ic_{100}	0.101	0.102	0.104	0.567(±0.000)	84.73(±0.212)
	Ic_{200}	0.002	0.000	0.000	0.669(±0.002)	99.9(±0.173)
$[Co(L^2)(Bipy)(OAc)]$	Ic_{50}	0.010	0.001	0.002	0.335(±0.577)	50.03(±0.861)
	Ic_{100}	0.009	0.009	0.009	0.661(±0.001)	98.70(±0.000)
	Ic_{200}	0.003	0.000	0.000	0.669(±0.002)	99.86(±0.234)
$[Ni(L^2)(Bipy)(OAc)].H_2O$	Ic_{50}	0.009	0.009	0.009	0.661(±0.001)	98.7(±0.000)
	Ic_{100}	0.011	0.011	0.011	0.659(±0.001)	98.4(±0.000)
	Ic_{200}	0.019	0.020	0.019	0.650(±0.001)	97.1(±0.122)
$[Cu(L^2)(Bipy)(OAc)].H_2O$	Ic_{50}	0.012	0.012	0.012	0.658(±0.001)	98.20(±0.000)
	Ic_{100}	0.001	0.001	0.001	0.669(±0.001)	99.9(±0.000)
	Ic_{200}	0.003	0.002	0.003	0.667(±0.001)	99.63(±0.070)
$Zn(L^2)(Bipy)(OAc)]$	Ic_{50}	0.001	0.002	0.003	0.668(±0.000)	99.73(±0.158)
	Ic_{100}	0.012	0.011	0.011	0.658(±0.001)	98.33(±0.122)
	Ic_{200}	0.024	0.024	0.024	0.646(±0.001)	96.4(±0.000)
Standard Ascorbic Acid	Ic_{50}	0.093	0.089	0.094	0.578(±0.002)	86.26(±0.38)
	Ic_{100}	0.085	0.081	0.082	0.587(±0.002)	87.66(±0.32)
	Ic_{200}	0.078	0.074	0.076	0.594(±0.002)	88.67(±0.35)

Table 4.9.5. DPPH radical

Compounds	Concentration	Absorbance			Mean(Error)	% Inhibition (Error)
		1	2	3		
Blank	-	0.77	0.78	0.78	-	-
HL^3	Ic_{50}	0.09	0.09	0.09	0.58(±0.001)	86.56(±0.07)
	Ic_{100}	0.088	0.083	0.083	0.585(±0.003)	87.33(±0.46)
	Ic_{200}	0.082	0.078	0.079	0.590(±0.002)	88.1(±0.36)
Bipy	Ic_{50}	0.172	0.170	0.168	0.501(±0.004)	74.76(±0.570)
	Ic_{100}	0.160	0.160	0.158	0.510(±0.002)	76.23(±0.234)
	Ic_{200}	0.152	0.152	0.150	0.518(±0.002)	77.40(±0.173)
$[Mn(L^3)(Bipy)(OAc)]$	Ic_{50}	0.018	0.017	0.017	0.652(±0.001)	97.43(±0.12)
	Ic_{100}	0.01	0.01	0.01	0.66(±0.001)	98.5(±0.00)
	Ic_{200}	0.008	0.008	0.008	0.662(±0.001)	98.8(±0.00)
$[Fe(L^3)(Bipy)(SO_4)].H_20$	Ic_{50}	0.167	0.167	0.168	0.502(±0.001)	75.03(±0.07)
	Ic_{100}	0.092	0.092	0.092	0.578(±0.001)	86.26(±0.07)
	Ic_{200}	0.050	0.057	0.050	0.617(±0.004)	92.16(±0.57)
$[Co(L^3)(Bipy)(OAc)]$	Ic_{50}	0.028	0.028	0.029	0.641(±0.001)	95.76(±0.07)
	Ic_{100}	0.028	0.028	0.028	0.642(±0.001)	95.8(±0.00)
	Ic_{200}	0.064	0.064	0.064	0.606(±0.001)	90.43(±0.07)
$[Ni(L^3)(Bipy)(OAc)]$	Ic_{50}	0.034	0.033	0.033	0.636(±0.001)	95.03(±0.12)
	Ic_{100}	0.033	0.032	0.033	0.637(±0.001)	95.13(±0.07)
	Ic_{200}	0.031	0.032	0.032	0.638(±0.000)	95.26(±0.12)
$[CuL^3)(Bipy)(OAc)].H_2O$	Ic_{50}	0.655	0.653	0.652	0.016(±0.000)	2.466(±0.35)
	Ic_{100}	0.500	0.500	0.500	0.170(±0.001)	25.4(±0.10)
	Ic_{200}	0.211	0.209	0.209	0.460(±0.002)	68.73(±0.21)
$[Zn(L^3)(Bipy)(OAc)].H_2O$	Ic_{50}	0.024	0.018	0.019	0.649(±0.004)	96.96(±0.49)
	Ic_{100}	0.005	0.011	0.014	0.66(±0.003)	98.53(±0.71)
	Ic_{200}	0.006	0.004	0.002	0.666(±0.003)	99.4(±0.30)
Standard Ascorbic Acid	Ic_{50}	0.093	0.089	0.094	0.578(±0.002)	86.26(±0.38)
	Ic_{100}	0.085	0.081	0.082	0.587(±0.002)	87.66(±0.32)
	Ic_{200}	0.078	0.074	0.076	0.594(±0.002)	88.67(±0.35)

scavenging data of HL^3 ligand and its heteroleptic metal complexes

Table 4.9.6. DPPH radical scavenging data of HL^4 ligand and its metal(II) complexes

Compounds	Concentration	Absorbance			Mean(Error)	% Inhibition (Error)
		1	2	3		
Blank	-	0.669	0.670	0.671	-	-
HL^4	Ic_{50}	0.214	0.214	0.214	0.456(±0.001)	68.08(±0.07)
	Ic_{100}	0.212	0.212	0.212	0.458(±0.001)	68.36(0.07)
	Ic_{200}	0.208	0.209	0.209	0.461(±0.000)	68.86(±0.07)
	Ic_{50}	0.247	0.247	0.247	0.423(±0.001)	63.13(±0.07)

	Ic_{100}	0.182	0.182	0.182	0.488(±0.001)	72.83(±0.07)
$[Mn(L^4)_2].H_2O$	Ic_{200}	0.127	0.127	0.127	0.543(±0.001)	81.03(±0.07)
	Ic_{50}	0.169	0.166	0.167	0.502(±0.002)	75.00(±0.07)
	Ic_{100}	0.158	0.159	0.159	0.511(±0.000)	76.33(±0.07)
$[Fe(L^4)_2].2H_2O$	Ic_{200}	0.105	0.103	0.103	0.566(±0.002)	84.50(±0.17)
	Ic_{50}	0.138	0.138	0.139	0.531(±0.000)	79.36(±0.07)
$[Co(L^4)_2].H_2O$	Ic_{100}	0.119	0.118	0.119	0.551(±0.000)	82.3(0.10)
	Ic_{200}	0.079	0.079	0.079	0.591(0.001)	88.2(±0.00)
	Ic_{50}	0.051	0.052	0.051	0.618(±0.001)	92.33(±0.12)
$[Ni(L^4)_2].H_2O$	Ic_{100}	0.023	0.023	0.023	0.647(±0.001)	96.6(±0.00)
	Ic_{200}	0.006	0.006	0.006	0.664(±0.001)	99.1(±0.00)
	Ic_{50}	0.073	0.073	0.073	0.597(±0.001)	89.1(±0.00)
$[Cu(L^4)_2]$	Ic_{100}	0.086	0.087	0.086	0.583(±0.001)	87.1(±0.10)
	Ic_{200}	0.050	0.048	0.049	0.621(±0.002)	92.66(±0.15)
	Ic_{50}	0.110	0.108	0.108	0.561(±0.002)	83.8(±0.17)
$[Zn(L^4)_2].H_2O$	Ic_{100}	0.068	0.068	0.069	0.601(±0.001)	89.8(±0.10)
	Ic_{200}	0.013	0.013	0.013	0.657(±0.001)	98.1(±0.00)
	Ic_{50}	0.093	0.089	0.094	0.578(±0.002)	86.26(±0.38)
Standard	Ic_{100}	0.085	0.081	0.082	0.587(±0.002)	87.66(±0.32)
Ascorbic Acid	Ic_{200}	0.078	0.074	0.076	0.594(±0.002)	88.67(±0.35)

Table 4.9.7. DPPH radical scavenging data of HL^4 ligand and its heteroleptic metal(II) complexes

Compounds	**Concentration**	**Absorbance**			**Mean(Error)**	**% Inhibition (Error)**
		1	**2**	**3**		
Blank	-	0.669	0.670	0.671	-	-
	Ic_{50}	0.214	0.214	0.214	0.456(±0.001)	68.08(±0.07)
HL^4	Ic_{100}	0.212	0.212	0.212	0.458(±0.001)	68.36(0.07)
	Ic_{200}	0.208	0.209	0.209	0.461(±0.000)	68.86(±0.07)
	Ic_{50}	0.172	0.170	0.168	0.501(±0.004)	74.76(±0.570)
Bipy	Ic_{100}	0.160	0.160	0.158	0.510(±0.002)	76.23(±0.234)

	Ic_{200}	0.152	0.152	0.150	0.518(±0.002)	77.40(±0.173)
	Ic_{50}	0.170	0.170	0.170	0.50(±0.001)	74.63(±0.07)
$[Mn(L^4)(Bipy)(OAc)]$	Ic_{100}	0.176	0.176	0.176	0.494(±0.000)	73.76(±0.07)
	Ic_{200}	0.297	0.297	0.297	0.373(±0.001)	55.66(±0.07)
	Ic_{50}	0.026	0.025	0.025	0.644(±0.001)	96.23(±0.12)
$[Fe(L^4)(Bipy)(SO_4)].H_2O$	Ic_{100}	0.024	0.025	0.026	0.645(±0.000)	96.26(±0.15)
	Ic_{200}	0.014	0.014	0.014	0.656(±0.001)	97.9(±0.00)
	Ic_{50}	0.155	0.157	0.155	0.514(±0.001)	76.76(±0.15)
$[Co(L^4)(Bipy)(OAc)]$	Ic_{100}	0.095	0.094	0.094	0.575(±0.001)	85.93(±0.12)
	Ic_{200}	0.08	0.081	0.083	0.588(±0.000)	87.83(±0.21)
$[Ni(L^4)(Bipy)(OAc)].H_2O$	Ic_{50}	0.207	0.207	0.206	0.463(±0.001)	69.16(±0.12)
	Ic_{100}	0.109	0.109	0.109	0.561(±0.001)	83.73(±0.07)
	Ic_{200}	0.095	0.094	0.095	0.575(±0.001)	85.86(±0.12)
	Ic_{50}	0.183	0.183	0.183	0.487(±0.001)	72.66(±0.07)
$[Cu(L^4)(Bipy)(OAc)]$	Ic_{100}	0.076	0.077	0.078	0.593(±0.000)	88.5(±0.10)
	Ic_{200}	0.009	0.006	0.007	0.662(±0.002)	98.93(±0.21)
	Ic_{50}	0.108	0.108	0.108	0.562(±0.001)	83.9(±0.00)
$[Zn(L^4)(Bipy)(OAc)]$	Ic_{100}	0.059	0.059	0.061	0.610(±0.000)	91.1(±0.17)
	Ic_{200}	0.051	0.049	0.048	0.620(±0.002)	92.63(±0.21)
	Ic_{50}	0.093	0.089	0.094	0.578(±0.002)	86.26(±0.38)
Standard	Ic_{100}	0.085	0.081	0.082	0.587(±0.002)	87.66(±0.32)
Ascorbic Acid	Ic_{200}	0.078	0.074	0.076	0.594(±0.002)	88.67(±0.35)

Table 4.9.8. DPPH radical scavenging data of HL^5 ligand and its metal(II) complexes

Compounds	**Concentration**	**Absorbance**			**Mean(Error)**	**% Inhibition (Error)**
		1	**2**	**3**		
Blank	-	0.669	0.670	0.671	-	-
	Ic_{50}	0.241	0.241	0.241	0.429(±0.001)	64.03(±0.07)
	Ic_{100}	0.175	0.177	0.174	0.494(±0.002)	73.83(±0.25)
HL^5	Ic_{200}	0.177	0.170	0.168	0.498(±0.005)	74.36(±0.77)
	Ic_{50}	0.105	0.105	0.105	0.565(±0.001)	84.33(±0.07)

$[Mn(L^5)_2].H_2O$	Ic_{100}	0.057	0.057	0.057	0.613(±0.001)	91.5(±0.000)
	Ic_{200}	0.015	0.019	0.020	0.652(±0.001)	97.33(±0.000)
	Ic_{50}	0.231	0.231	0.231	0.439(±0.001)	65.53(±0.07)
	Ic_{100}	0.231	0.230	0.231	0.439(±0.001)	65.6(±0.10)
$[Fe(L^5)_2].2H_2O$	Ic_{200}	0.218	0.219	0.220	0.451(±0.000)	67.3(±0.1)
	Ic_{50}	0.130	0.126	0.126	0.542(±0.003)	81.0(±0.34)
	Ic_{100}	0.061	0.067	0.068	0.604(±0.002)	90.26(±0.55)
$[Co(L^5)_2].2H_2O$	Ic_{200}	0.025	0.029	0.030	0.642(±0.001)	95.83(±0.41)
	Ic_{50}	0.073	0.075	0.072	0.596(±0.002)	89.06(±0.25)
	Ic_{100}	0.049	0.048	0.047	0.622(±0.002)	92.83(±0.15)
$[Ni(L^5)_2(H_2O)_2]$	Ic_{200}	0.01	0.01	0.01	0.66(±0.001)	98.5(±0.00)
	Ic_{50}	0.091	0.091	0.091	0.579(±0.001)	86.4(±0.00)
	Ic_{100}	0.079	0.079	0.079	0.591(±0.001)	88.2(±0.00)
$[Cu(L^5)_2]$	Ic_{200}	0.037	0.037	0.037	0.633(±0.001)	94.5(±0.00)
	Ic_{50}	0.037	0.036	0.035	0.634(±0.002)	94.63(±0.15)
	Ic_{100}	0.028	0.028	0.029	0.641(±0.000)	95.76(±0.07)
$[Zn(L^5)_2].H_2O$	Ic_{200}	0.000	0.003	0.002	0.668(±0.001)	99.76(±0.21)
	Ic_{50}	0.093	0.089	0.094	0.578(±0.002)	86.26(±0.38)
Standard	Ic_{100}	0.085	0.081	0.082	0.587(±0.002)	87.66(±0.32)
Ascorbic Acid	Ic_{200}	0.078	0.074	0.076	0.594(±0.002)	88.67(±0.35)

Table 4.9.9. DPPH radical scavenging data of HL^5 ligand and its heteroleptic metal(II) complexes

Compounds	**Concentration**	**Absorbance**			**Mean(Error)**	**% Inhibition (Error)**
		1	**2**	**3**		
Blank	-	0.669	0.670	0.671	-	-
	Ic_{50}	0.241	0.241	0.241	0.429(±0.001)	64.03(±0.07)
HL^5	Ic_{100}	0.175	0.177	0.174	0.494(±0.002)	73.83(±0.25)
	Ic_{200}	0.177	0.170	0.168	0.498(±0.005)	74.36(±0.77)
	Ic_{50}	0.172	0.170	0.168	0.501(±0.004)	74.76(±0.570)
Bipy	Ic_{100}	0.160	0.160	0.158	0.510(±0.002)	76.23(±0.234)
	Ic_{200}	0.152	0.152	0.150	0.518(±0.002)	77.40(±0.173)

	Ic_{50}	0.097	0.098	0.099	0.572(±0.000)	85.36(±0.15)
$[Mn(L^5)(Bipy)(OAc)].H_2O$	Ic_{100}	0.065	0.068	0.070	0.602(±0.001)	89.93(±0.35)
	Ic_{200}	0.005	0.004	0.003	0.666(±0.002)	99.43(±0.15)
	Ic_{50}	0.225	0.223	0.224	0.446(±0.001)	66.56(±0.15)
$[Fe(L^5)(Bipy)(SO_4)]$	Ic_{100}	0.222	0.221	0.220	0.449(±0.002)	67.0(±0.20)
	Ic_{200}	0.192	0.193	0.194	0.477(±0.000)	71.2(±0.10)
	Ic_{50}	0.139	0.140	0.141	0.53(±0.000)	79.1(±0.10)
$[Co(L^5)(Bipy)(OAc)].2H_2O$	Ic_{100}	0.117	0.118	0.116	0.553(±0.001)	82.53(±0.15)
	Ic_{200}	0.088	0.089	0.087	0.582(±0.001)	86.83(±0.15)
	Ic_{50}	0.152	0.153	0.152	0.517(±0.001)	77.23(±0.12)
$[Ni(L^5)(Bipy)(OAc)].H_2O$	Ic_{100}	0.141	0.141	0.141	0.529(±0.001)	78.96(±0.07)
	Ic_{200}	0.085	0.085	0.085	0.585(±0.001)	87.3(±0.000)
	Ic_{50}	0.124	0.124	0.120	0.547(±0.003)	81.7(±0.34)
$[Cu(L^5)(Bipy)(OAc)]$	Ic_{100}	0.093	0.092	0.093	0.577(±0.001)	86.16(±0.12)
	Ic_{200}	0.092	0.092	0.092	0.578(±0.001)	86.26(±0.07)
	Ic_{50}	0.142	0.141	0.143	0.528(±0.001)	78.83(±0.15)
$[Zn(L^5)(Bipy)(OAc)].2H_2O$	Ic_{100}	0.058	0.057	0.056	0.613(±0.002)	91.5(±0.2)
	Ic_{200}	0.009	0.01	0.012	0.659(±0.000)	98.46(±0.25)
	Ic_{50}	0.093	0.089	0.094	0.578(±0.002)	86.26(±0.38)
Standard	Ic_{100}	0.085	0.081	0.082	0.587(±0.002)	87.66(±0.32)
Ascorbic Acid	Ic_{200}	0.078	0.074	0.076	0.594(±0.002)	88.67(±0.35)

Table 4.9.10. DPPH radical scavenging data of HL^6 ligand and its heteroleptic metal(II) complexes

Compounds	**Concentration**	**Absorbance**			**Mean(Error)**	**% Inhibition (Error)**
		1	**2**	**3**		
Blank	-	0.669	0.670	0.671	-	-
	Ic_{50}	0.281	0.283	0.281	0.388(±0.001)	57.96(±0.15)
HL^6	Ic_{100}	0.131	0.131	0.126	0.540(±0.003)	80.66(±0.46)
	Ic_{200}	0.111	0.111	0.113	0.557(±0.000)	83.23(±0.15)
	Ic_{50}	0.172	0.170	0.168	0.501(±0.004)	74.76(±0.570)
Bipy	Ic_{100}	0.160	0.160	0.158	0.510(±0.002)	76.23(±0.234)

	Ic_{200}	0.152	0.152	0.150	0.518(±0.002)	77.40(±0.173)
	Ic_{50}	0.089	0.086	0.087	0.582(±0.002)	86.96(±0.25)
$[Mn(L^6)(Bipy)(OAc)]$	Ic_{100}	0.69	0.071	0.072	0.392(±0.35)	58.53(±0.53)
	Ic_{200}	0.045	0.045	0.046	0.624(±0.000)	93.23(±0.12)
	Ic_{50}	0.025	0.026	0.027	0.644(±0.000)	96.13(±0.15)
$[Fe(L^6)(Bipy)(SO_4)]$	Ic_{100}	0.01	0.011	0.01	0.659(±0.001)	98.46(±0.07)
	Ic_{200}	0.001	0.002	0.003	0.668(±0.000)	99.73(±0.15)
	Ic_{50}	0.119	0.119	0.118	0.551(±0.001)	82.26(±0.12)
$[Co(L^6)(Bipy)(OAc)]$	Ic_{100}	0.105	0.05	0.105	0.583(±0.031)	87.06(±0.47)
	Ic_{200}	0.041	0.04	0.043	0.628(±0.001)	93.83(±0.21)
	Ic_{50}	0.279	0.277	0.281	0.391(±0.001)	58.36(±0.30)
$[Ni(L^6)(Bipy)(OAc)]$	Ic_{100}	0.177	0.179	0.182	0.490(±0.001)	73.23(±0.30)
	Ic_{200}	0.162	0.164	0.161	0.507(±0.002)	75.76(±0.25)
	Ic_{50}	0.119	0.119	0.118	0.551(±0.001)	82.26(±0.12)
$[Cu(L^6)(Bipy)(OAc)].H_2O$	Ic_{100}	0.105	0.105	0.106	0.564(±0.000)	84.26(±0.07)
	Ic_{200}	0.041	0.040	0.043	0.628(±0.001)	93.83(±0.21)
	Ic_{50}	0.205	0.206	0.207	0.464(±0.000)	69.30(±0.10)
$[Zn(L^6)(Bipy)(OAc)]$	Ic_{100}	0.089	0.091	0.092	0.579(±0.000)	86.46(±0.21)
	Ic_{200}	0.074	0.075	0.073	0.596(±0.001)	88.93(±0.15)
	Ic_{50}	0.093	0.089	0.094	0.578(±0.002)	86.26(±0.38)
Standard	Ic_{100}	0.085	0.081	0.082	0.587(±0.002)	87.66(±0.32)
Ascorbic Acid	Ic_{200}	0.078	0.074	0.076	0.594(±0.002)	88.67(±0.35)

Table 4.10. Ferrous chelating data of the ligands (HL^1 – HL^6)

Compounds	**Concentration**	**Absorbance**			**Mean(Error)**	**% Inhibition (Error)**
		1	**2**	**3**		
Blank	-	0.169	0.170	0.168	-	-
	Ic_{50}	0.017	0.020	0.022	0.065(±0.005)	76.8(±3.40)
HL^1	Ic_{100}	0.013	0.014	0.014	0.071(±0.004)	83.86(±1.25)
	Ic_{200}	0.003	0.002	0.003	0.082(±0.004)	96.83(±0.75)

	Ic_{50}	0.029	0.029	0.034	0.054(±0.002)	63.96(±2.45)
HL^2	Ic_{100}	0.026	0.027	0.026	0.060(±0.006)	71.3(±5.04)
	Ic_{200}	0.013	0.012	0.013	0.072(±0.003)	85.1(±0.17)
	Ic_{50}	0.038	0.038	0.038	0.047(±0.003)	55.23(±1.91)
HL^3	Ic_{100}	0.039	0.040	0.040	0.045(±0.004)	53.26(±2.55)
	Ic_{200}	0.028	0.027	0.022	0.059(±0.005)	69.74(±4.08)
	Ic_{50}	0.027	0.030	0.028	0.056(±0.005)	66.56(±3.23)
HL^4	Ic_{100}	0.040	0.039	0.039	0.045(±0.002)	53.33(±1.40)
	Ic_{200}	0.027	0.029	0.028	0.057(±0.004)	66.96(±2.57)
	Ic_{50}	0.059	0.056	0.056	0.028(±0.002)	32.93(±2.00)
HL^5	Ic_{100}	0.035	0.035	0.040	0.048(±0.004)	56.83(±3.35)
	Ic_{200}	0.028	0.029	0.028	0.056(±0.004)	66.6(±2.11)
	Ic_{50}	0.029	0.030	0.029	0.056(±0.004)	65.8(±2.43)
HL^6	Ic_{100}	0.022	0.021	0.022	0.063(±0.003)	74.5(±0.45)
	Ic_{200}	0.017	0.019	0.018	0.067(±0.004)	78.76(±2.12)
Standard	Ic_{50}	0.039	0.038	0.039	0.046(±0.003)	53.96(±1.86)
Ascorbic Acid	Ic_{100}	0.035	0.036	0.037	0.049(±0.004)	57.33(±2.41)
	Ic_{200}	0.027	0.029	0.030	0.056(±0.004)	66.2(±2.72)

CHAPTER FIVE

DISCUSSIONS OF RESULTS

5.1 Synthesis

Six novel ligands, 3-{[-(pyrimidin-2-yl)imino]methyl}napthalen-2-ol (HL^1), 3-{[(4,6-dihydroxypyrimidin-2-yl)imino]methyl}napthalen-2-ol (HL^2), 3-{[(4,6-dimethylpyrimidin -2-yl)imino]methyl}napthalen-2-ol (HL^3), 2-(pyrimidin-2-ylamino)naphthalene-1,4-dione, (HL^4), 2-(4,6-dihydroxypyrimidin-2-ylamino)naphthalene-1,4-dione (HL^5) and 2-(4,6-dimethylpyrimidin-2-ylamino)naphthalene-1,4-dione (HL^6) were synthesised in 1:1 stoichiometry from various pyrimidines (2-amino-pyrimidine, 2-amino-4,6-dihydroxypyrimidine and 2-amino-4,6-dimethylpyrimidine); and 2-hydroxyl-1-napthaldehyde/2-hydroxy-1,4-naphthoquinone. The metal(II) (Mn, Fe, Co, Ni, Cu and Zn) complexes of the above novel ligands were prepared. Additionally, heteroleptic Mn(II), Fe(II), Co(II), Ni(II), Cu(II) and Zn(II) complexes of the synthesised HL^1, HL^2, HL^3, HL^4, HL^5 and HL^6 ligands were also synthesised with 2,2'-bipyridine. All the synthesised compounds were characterized using elemental analysis; infrared and UV-Vis spectroscopies. The metal(II) complexes were further characterized by room temperature magnetic susceptibilities, percentage metal and molar conductance measurements while the ligands were further characterized by ^{1}H NMR and ^{13}C NMR spectroscopy and mass spectrometry

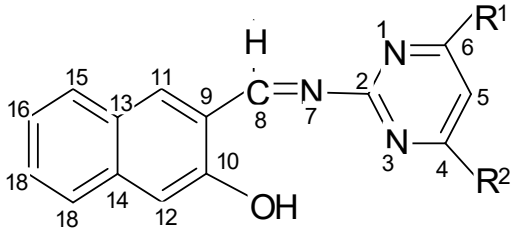

$HL^1 = R^1 = R^2 = H$

$HL^2 = R^1 = R^2 = OH$

$HL^3 = R^1 = R^2 = CH_3$

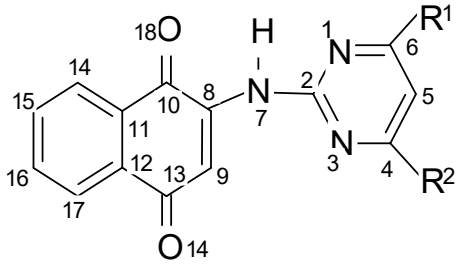

$HL^4 = R^1 = R^2 = H$

$HL^5 = R^1 = R^2 = OH$

$HL^6 = R^1 = R^2 = CH_3$

5.2 Physical measurements

5.2.1 Colour

The synthesised complexes with their Schiff base ligands exhibited various shades of colour. Most of the compounds displayed different shades of brown, i.e. HL^2, HL^6, $[Mn(L^1)_2].H_2O$, $[Mn(L^2)(Bipy)(OAc)].H_2O$, $[Mn(L^3)(Bipy)(OAc)]$, $[Mn(L^4)_2].H_2O$, $[Mn(L^5)_2].H_2O$, $[Mn(L^5)(Bipy)(OAc)].H_2O$, $[Fe(L^1)_2(H_2O)_2]$, $[Fe(L^1)_2(Bipy)(SO_4)]$, $[Fe(L^2)_2].2H_2O$, $[Fe(L^3)(Bipy)(SO_4)].H_2O$, $[Fe(L^4)_2].2H_2O$, $[Fe(L^2)(Bipy)(SO_4)].H_2O$, $[Fe(L^4)(Bipy)(SO_4)].H_2O$, $[Fe(L^6)(Bipy)SO_4]$, $[Fe(L^5)_2].2H_2O$, $[Ni(L^1)_2(Bipy)(OAc)].H_2O$, $[Ni(L^4)_2].H_2O$, $[Ni(L^2)_2].H_2O$, $[Ni(L^2)(Bipy)(OAc)].H_2O$, $[Ni(L^3)(Bipy)(OAc)]$, $[Ni(L^5)_2(H_2O)_2]$, $[Co(L^5)(Bipy)(OAc)].2H_2O$, $[Co(L^2)_2].H_2O$, $[Co(L^2)(Bipy)(OAc)]$, $[Co(L^4)(Bipy)(OAc)]$, $[Cu(L^1)_2]$, $[Cu(L^2)(Bipy)(OAc)].H_2O$, $[Cu(L^3)(Bipy)(OAc)]$, $[Cu(L^2)_2]$, $[Cu(L^4)(Bipy)(OAc)].H_2O$ and $[Cu(L^6)(Bipy)(OAc)].H_2O$), while different shades of red were observed for $[Co(L^1)_2].2H_2O$, $[Co(L^1)(Bipy)(OAc)].H_2O$, $[Co(L^4)_2].H_2O$, $[Cu(L^4)_2]$, $[Zn(L^4)_2].H_2O$, $[Cu(L^5)_2]$, $[Mn(L^4)(Bipy)(OAc)].H_2O$, $[Ni(L^4)(Bipy)(OAc)].H_2O$, $[Zn(L^4)(Bipy)(OAc)]$, $[Zn(L^5)_2].H_2O$, $[Fe(L^5)(Bipy)(SO_4)]$, $[Ni(L^5)(Bipy)(OAc)].H_2O$, $[Co(L^6)(Bipy)(OAc)]$, $[Ni(L^6)(Bipy)(OAc)]$ and $[Zn(L^6)(Bipy)(OAc)]$ complexes.

Similarly, HL^1, HL^3 and $[Zn(L^3)(Bipy)(OAc)].H_2O$; and $[Co(L^3)(Bipy)(OAc)]$ and $[Zn(L^5)(Bipy)(OAc)].H_2O$ compounds were generally of various shades of yellow and pink respectively, while $[Zn(L^1)(Bipy)(OAc)].2H_2O$ and $[Cu(L^5)(Bipy)(OAc)]$ complexes exhibited different coffee shades.

Additionally, $[Mn(L^2)_2].2H_2O$, $[Zn(L^2)_2]$ and $[Zn(L^2)(Bipy)(OAc)]$ displayed different gray shades. The $[Ni(L^1)_2].H_2O$, $[Zn(L^1)_2]$ and $[Cu(L^1)(Bipy)(OAc)]$ complexes had shades of green while various orange shades were observed for $[Mn(L^1)(Bipy)(OAc)]$, HL^4, HL^5 and $[Co(L^5)_2(H_2O)_2].H_2O$ compounds.

5.2.2 Melting points

All the synthesised ligands, HL^1, HL^2, HL^3, HL^4, HL^5 and HL^6 displayed melting points in the range 110-222 ^oC which were different from their starting materials. Similarly, the

metal(II) complexes had good melting points greater than the ligands except [Mn(L^3)(Bipy)(OAc)] and [Zn(L^4)$_2$].H_2O and [Cu(L^4)$_2$] complexes with melting points in the ranges 216-218 and 209-211^oC, while [Ni(L^1)$_2$].H_2O and [Zn(L^2)(Bipy)(OAc)] complexes decomposed at 250-252 and 156-158 ^oC respectively.

5.2.3 Percentage metal compositions of the complexes

The percentage metal compositions of the complexes have been determined through complexometric titration method and results obtained. There were good agreements between the experimental and theoretical (calculated) values in percentage of the metals.

5.2.4 Molar conductance measurement

The molar conductance measurement of the metallic compounds and their heteroleptic analogues with 2,2'-bipyridine were obtained in dimethylsulphoxide (DMSO). Generally, the obtained values were below 40.0 $Ohm^{-1}mol^{-1}cm^2$ which indicates non-ionic nature for all the soluble compounds synthesised, since a value of 45-90 $Ohm^{-1}mol^{-1}cm^2$ and 90-120 $Ohm^{-1}mol^{-1}cm^2$ are expected for 1:1 and 1:2 electrolyte(s) (Geary, 1971). The molar conductance results were effectively validated by the mirco-(CHN) and quantitative analyses data where anions were not noticed.

5.2.5 Solubility results of the synthesised ligands and their metal(II) complexes

The solubility tests of the ligands, metal(II) complexes and their heteroleptic analogues in both polar and non-polar organic solvents have been determined. Generally, the synthesised compounds exhibited varied solubilities in the solvents used but were majorly or slightly insoluble in water and nitromethane. Additionally, the ligands with their metallic compounds had good solubilities in the solvents; chloroform, dimethyl sulfoxide and dimethyl formamide but were sparingly soluble in ethanol, methanol and dichloromethane. The solubility tests for the heteroleptic complexes followed the same trend as their symmetrical analogues.

5.2.6 Percentage yields

All the synthesised compounds (ligands and complexes) exhibited good to moderate (45-100%) yields, since reaction yields of 90-100%, 70-80% and 50-60% of the theoretical are often considered excellent, good and adequate. However, $[Co(L^1)_2(H_2O)_2]$, $[Zn(L^5)_2(H_2O)_2]$, $[Cu(L^5)_2]$ and $[Cu(L^1)_2]$ had percent yields that were below 40% and could be attributed to experimental errors.

5.3 Analytical results

The elemental analysis, C, H, S, N data for the synthesised ligands (HL^1, HL^2, HL^3, HL^4, HL^5 and HL^6) and their complexes (symmetrical and heteroleptic) have been obtained on an Elementar, Vario EL Cube setup. The obtained values were consistent with the calculated (theoretical) results and corroborates 2L:1M and 1L:1M:1Bipy stiochiometries for the symmetrical and heteroleptic complexes (where L=synthesised ligands, M=Fe(II), Mn(II), Co(II), Ni(II), Cu(II) and Zn(II) and Bipy = 2,2'-bipyridine) and conforms with the empirical formula proposed for each compound.

5.4 Spectroscopic studies

5.4.1 Infrared (IR) spectra data of synthesised compounds

The relevant infrared spectral bands of the pyrimidinyl ligands and their divalent metal complexes (symmetrical and non-symmetrical) were observed between 350 and 4000 cm^{-1}.The observed spectral bands were tentatively apportioned by associating the spectra of the synthesised compounds with documented literature on related systems (Atmaram and Kirian, 2011; Ramana *et al.,* 2012 and Suparan, 2013). The ligands did not display bands corroborative of the amino groups as were observed in the spectra of the amines used for syntheses indicating condensation via the amino groups with the aldehydes/ketones (Valarmathy and Subbalakshmi, 2014). The ligands, HL^1, HL^2 and HL^3, in their respective IR spectrum exhibited broad to medium absorption bands at 3389, 3341 and 3441 cm^{-1} and were apportioned as intra molecular H-bonding vibrations (νO-H….N) of an enol tautomer which is often observed in Schiff bases containing hydroxyl (-OH) groups (Pyle *et al.,* 1989). These bands remained absent in the spectra of the metal(II) complexes and corroborates complexation through the naphthol oxygen atom of

the ligand. However, observed medium to broad bands at the range 3348-3447 cm^{-1} in all the HL^1-HL^3 metallic compounds were attributed to *ν*OH of coordinated/hydrated water molecules. On the other hand, the infrared spectra of HL^4, HL^5 and HL^6 ligands had strong bands at 3439, 3584 and 3536 cm^{-1} respectively which were assigned to ν(NH) of a secondary amide. The broadening of these bands in the ligands may be attributed to intramolecular hydrogen bonding (Dixit and Patel, 1979). The sharp to medium hydrogen stretching bands of the aromatic rings, ν(Ar–H), appeared between 3013 and 3001 cm^{-1}in the complexes while the methyl substituted HL^3 and HL^6 ligands and their complexes exhibited medium asymmetric and symmetric stretching vibrations for the alkyl substituents within the region 2929-2913 cm^{-1}. The absorption bands at 1669 cm^{-1}, 1688 cm^{-1} and 1628 cm^{-1} due to the imine moiety in the ligands HL^1, HL^2 and HL^3, moved to lower/higher wavenumbers in the complexes to the range 1614-1667 cm^{-1}, corroborating participation of the imine nitrogen atom in complexation with the metallic ions.

The absorption bands of the C=N and C=C vibrations were of almost equal intensity in the ligands (exception of HL^4, HL^5 and HL^6) in the regions 1688-1669 cm^{-1} and 1651-1625 cm^{-1} but moved to lower/higher wavenumbers by 60–48 cm^{-1}in all the complexes. The former indicates participation of the imine nitrogen atom in interaction with the metallic ions while the latter supports aromatic conjugations and effect of complexation (Jayabalakrishnan and Natarajan, 2002). The *ν*(C=N) which appeared as a lone band in the ligands still remained as single bands in the spectra of the metallic compounds indicative of Fermi resonance in most of the heteroleptic complexes (Kalsi, 2004). The ligands, HL^4, HL^5 and HL^6 underwent keto-enol tuatomerism in solution to form C=N during complexation (Laxmi *et al.,* 2014). Similarly, the uncoordinated ν(C=O) stretching vibrations observed as sharp bands in HL^4, HL^5 and HL^6ligands at 1672, 1682 and 1678 cm^{-1}moved to lower/higher wavenumbers in the metallic compounds corroborating the participation of ketonic *O* atom in complexation. The sharp absorption bands at 1537-1579 cm^{-1}, 1366-1491 cm^{-1} and 981-991 cm^{-1} were allocated to *ν*(C-N) of the aromatic rings, *ν*(C-C) and *δ*(C-H) vibrations. Further confirmation of the enol *O* and imine *N* atoms in coordination to the metallic ions were proved by the presence of novel bands around 400-

470 cm^{-1} and 500-590 cm^{-1} due to ν(M-O) and ν(M-N) in the spectra of the metallic compounds (Valarmathy and Subbalakshmi, 2014).

5.4.1.1 3-{[-(pyrimidin-2-yl)imino]methyl}napthalen-2-ol and its metal(II) complexes

The *ν*OH of the HL^1 ligand was observed as a broad band centred at 3389 cm^{-1} and allocated to the phenolic hydroxyl moiety. This band was not seen in the spectra of the metal(II) compounds and corroborates coordination through the naphthol oxygen atom of the ligand. However, observed medium-broad bands at the range 3332--3435 cm^{-1} in all the HL^1 metallic compounds were attributed to *ν*OH of coordinated/hydrated water molecules. TheC=N stretching vibration of the azomethine group occurred as a lone sharp band at 1669 cm^{-1} in the non-coordinated ligand (HL^1). It remained same in the metallic compounds but moved to lower wavenumber with ±25 cm^{-1}, indicating involvement of the imine nitrogen atom in the complex formation. Furthermore, the observance of a lone sharp *ν*C=N band confirms cis-isomeric forms of geometric isomerism in the metal(II) complexes. Research reports have it that complexes of cis-isomeric forms often display single *ν*C=N bands while trans-isomeric complexes exhibit two/split *ν*C=N bands (Najo *et al.,* 2009a and Najo *et al.,* 2009b). The C=C stretching frequency which occurred at 1625 cm^{-1} in the spectrum of the HL^1 ligand shifted to higher frequencies by ± 89-36 cm^{-1} in the spectra of the complexes. The corresponding *ν*(C-O) bond appeared as a sharp band at 1161 cm^1 in the ligand but shifted to higher frequency after coordination and corroborates deprotonation and complexation of the napthol oxygen atom of the ligand to the metal(II) ions, except $[Zn(L^1)(Bipy)(OAc)].2H_2O$ complex which had a shift to lower frequency. Contrarily, the C-N bands for the compounds were detected within the range 1567-1423 cm^{-1}. The C-N high frequency value is due to resonance with the conjugated benzene rings (Kalsi, 2004). The aromatic *δ*C-H vibrations of the compounds were observed at the range 1022-976 cm^{-1}. The appearance of novel bands in the metallic compounds at 655-519 cm^{-1} and 497-446 cm^{-1} attributed to *ν*M-N and *ν*M-O further confirms coordination of the metallic ions to the Schiff base.

5.4.1.2 3-{[(4,6-dihydroxypyrimidin-2-yl)imino]methyl}napthalen-2-ol and its metal(II) complexes

The spectra of the free ligands (HL^2 and 2,2'-bipyridine) displayed strong bands in the region 1639-1688 cm^{-1} and were allotted to the C=N vibration. The lowering of the ν(C=N) frequencies by ± 21–68 cm^{-1}as observed in the complexes indicates reduction in the C=N bond stretching force constant owing to the participation of the imine *N* atom in bonding to the metallic ions. The uncoordinated phenolic C−O stretching vibration was observed as a sharp lone band at 1268 cm^{-1}in the spectrum of the ligand (HL^2) but exhibited slight shifts in the metal(II) complexes corroborating deprotonation and involvement of naphthol *O* atom in coordination.The latter was also used to identify primary alcohols in compounds as in the case of HL^2 ligand. The metal ions bond linkage with the napthol oxygen and imine nitrogen atoms of the ligand were observed in the regions 486-446 cm^{-1} and 564-529 cm^{-1} and were apportioned to *ν*M-O and *ν*M-N bands separately. The *ν*M-O and *ν*M-N bands were noticed only in the spectra of the metallic compound.

5.4.1.3 3-{[(4,6-dimethylpyrimidin-2-yl)imino]methyl}napthalen-2-ol and its metal(II) complexes

The ligand, 3-{[(4,6-dimethylpyrimidin-2-yl)imino]methyl}napthalen-2-ol showed characteristic C=N and C=C stretching vibrations as sharp bands at 1628 and 1639 cm^{-1}; and 1593 and 1580 cm^{-1}, which eventually moved to lesser/greater wavenumbers by ±10-30 cm^{-1} on coordination to the metal ions. The former was indicative of the participation of imine N donor atom of C=N in coordination to the metallic ions, whereas the latter was suggestive of cyclic ring conjugation. On the other hand, the band at 1290 cm^{-1} in the spectrum of the HL^3 ligand was accredited to *ν*(C-O). This band displayed significant shifts to higher/lower wavenumbers in the spectra of the metallic compounds owing to coordination. The sharp band in the ligand spectrum detected at 981 cm^{-1} was attributed to *δ*CH. The *δ*CH band still appeared prominent in the spectra of the complexes nonetheless moved to greater wavenumbers (977-830 cm^{-1}). The M-N and M-O bands were detected at 594-533 as well as 499-452 cm^{-1} separately, confirming coordination through the imine N and enol O atoms.

5.4.1.42-(pyrimidin-2-ylamino)naphthalene-1,4-dione and its metal(II) complexes

The infrared spectrum of the HL^4 ligand, bearing napthoquinone functional group displayed strong and sharp bands at 3494 and 1554 cm^{-1} assignable to secondary amide N-H stretching as well as C-N bending vibrations. The NH band was not observed in the spectra of the complexes (Halli *et al.,* 2004) confirming involvement of amide N atom in complexation with the metallic atoms. The free C=O stretching bands of the napthoquinone in the keto forms appeared as sharp bands at 1672 cm^{-1} (position 1) and 1651 (position 4) cm^{-1}, while significant shifts in ν(C=O) were noticed in the spectra of the complexes corroborating a decrease in the C=O stretching force constants as a consequence of complexation through the ketonic-oxygen (position 4) atom and effect of complexation of the free base to the metallic ions. Consequently, the stretching vibrations owing to ν(C=O) at position 4 was not seen in the spectra of the complexes rather C-O stretching bands were observed.The new bands observed in the complexes in the region 559-502 cm^{-1} and 486-422 cm^{-1} were allocated to ν(M-N) and ν(M-O) separately.

5.4.1.5 2-(4,6-dihydroxypyrimidin-2-ylamino)naphthalene-1,4-dione and its metal(II) complexes

The infrared spectrum of HL^5 ligandexhibited moderate to sharp bands at 3584, 1485 and 1556 cm^{-1} owing to amide N-H stretching, N-H bending and C-N stretching vibrations respectively.The band corresponding to ν(C=O) at 1682 cm^{-1} in the spectrum of the ligand shifted to a lesser/higher wavenumber in the complexes, corroborative of complexation of the carbonyl oxygen to the metallic ions. The uncomplexed C-O stretching vibration of the ligand which occurred as a sharp band at 1268 cm^{-1}, still remained as a sharp band in the complexes but exhibited slight shifts. The non-significant shift of ν(C-O) in the complexes was attributed to the C-O stretching vibrations of the pyrimidinyl hydroxyl moieties. The bands within the ranges 564–530 and 495–445 $cm^{-1}$are ascribed to ν(M-N) and ν(M–O) vibrations separately.

5.4.1.6 2-(4,6-dimethylpyrimidin-2-ylamino)naphthalene-1,4-dione and its metal(II) complexes

The imine ν(C=N) band of the ligand was not observed rather the C=N and C-N vibrational frequencies of the pyrimidinyl moiety appeared at 1641 and 1579 cm^{-1}. These bands moved to lesser/higher frequencies in the metallic compounds due to complexation effect. Similarly, the band at 1678 cm^{-1} in the spectrum of the ligand consistent of ν(C=O) underwent lower/higher frequency shifts in the metallic compounds, corroborating the participation of the carbonyl oxygen in coordination to the metallic ions. The novel bands noticed in the metallic compounds in the regions 501−551 and 493−421 cm^{-1} were allocated to ν(M-N) and ν(M-O) vibrations respectively.

5.5 Electronic spectra studies of the ligands and their metal(II) complexes

The assignment of stereochemetries to the synthesised metallic compounds were made on the basis of electronic absorption band points as well as the number of *d-d* transition bands by reference to literature on similar systems (Chohan, 2001; Atmaram and Kirian, 2011; Osowole *et al.,* 2013; Osowole *et al.,* 2017). Generally, the ligands; HL^1, HL^2, HL^3, HL^4, HL^5 and HL^6 displayed absorption bands at the range of 26247-28653 cm^{-1} which had significant shifts in the metal(II) complexes and were assigned to n→$\pi*$transition of the C=N moieties. Additionally, the transition $\pi \rightarrow \pi*$ of the ligands were observed around 30030-38759 cm^{-1} and nearly remained unshifted in the spectra of the metallic compounds. These two bands were observed at different wavelengths in the hydroxyl and methyl substituted analogues but shifted to lower/higher energies upon chelations, indicating complexation of the ligands with the metallic ions.

5.5.1 Electronic spectra and magnetic moment data of the manganese(II) complexes

The ultraviolet spectra of the synthesised manganese(II) complexes displayed three absorptions around 26315-28011 cm^{-1}, 30487-38910 cm^{-1} and 40485-50505 cm^{-1} allocated to $\pi^* \leftarrow$ n, $\pi^* \leftarrow \pi$ and charge transfer transitions separately. Manganese(II) complexes are mostly high spin, and are characterized by weak spin and parity prohibited absorption transitions. These transitions are ascribed to the existence of a ^6S ground term as well as an upper quartet (^4G) state. In the octahedral field, three weak absorption bands assigned

to $^6A_{1g}\rightarrow{}^4T_{1g}$, $^6A_{1g}\rightarrow{}^4E_{g(}G)$, and $^6A_{1g}\rightarrow{}^4T_{2g}(G)$ transitions (Abu-el and Issa, 1989) are used to characterized manganese(II) complexes. The electronic spectra of $[Mn(L^1)_2].H_2O$, $[Mn(L^2)_2].2H_2O$ and $[Mn(L^5)_2].H_2O$ complexes displayed two bands each in the 11920-13550 cm^{-1} and 17065-23980 cm^{-1} regions, with the exception of $[Mn(L^4)_2].H_2O$ which had a single band consistent of tetrahedral structure and were attributed to $^6A_1\rightarrow{}^4E_1(\nu_1)$ and $^6A_1\rightarrow{}^4A_1(\nu_2)$ transitions (Lever, 1980; Singh *et al.,* 2001; Durot *et al.,* 2003; Osowole, 2008). However, the electronic spectra of the studied heteroleptic manganese(II) complexes were comparable to one another and displayed three weak absorption bands within the regions 11480-12658 cm^{-1}, 14430-16077 cm^{-1} and 18018-23809 cm^{-1}, assignable to $^6A_{1g}\rightarrow{}^4T_{1g}(\nu_1)$, $^6A_{1g}\rightarrow{}^4T_{2g}(G)$ (ν_2), and $^6A_{1g}\rightarrow{}^4E_g(G)$ (ν_3) transitions respectively of octahedral geometry (Figgis, 1966; Lever, 1968; Osowole*et al.,* 2012a; Abdou *et al.,* 2015).

Divalent manganese possesses $3d^5$ electron configuration and exhibits magnetic moment of a five unpaired electrons (5.92 B.M) regardless of stereochemistry. The latter is largely attributed to orbital contribution of zero, since the ground term for manganese(II) complexes is an A term with no corresponding higher T term of similar multiplicity. All the complexes exhibited effective magnetic moments in the range of 5.54-6.02 B.M indicative of high spin geometries (Osowole *et al.,* 2012c). With the exemption of $[Mn(L^1)_2].H_2O$ compound which exhibited magnetic moment value of 4.39 B.M suggestive of equilibrium amongst low spin and high spin tetrahedral geometry around the manganese ion (Cotton *et al.,* 1999).

5.5.2 Electronic spectra and magnetic moment data of iron(II) complexes

The ultraviolet spectra of the synthesised iron(II) complexes were characterized by two bands attributed to$\pi^*\leftarrow n/\pi^*\leftarrow\pi$ and charge transfer (CT) transitions, expect the hydroxyl substituted $[Fe(L^2)(Bipy)(SO_4)].H_2O$ and $[Fe(L^5)_2].2H_2O$ complexes which had only one absorption band each. Four coordinate tetrahedral iron(II) complexes are often accompanied with a lone high spin allowable transition, $^5E\rightarrow{}^5T_2$ frequently intense and broad owing to electronic wave function and Jahn Teller effect, while square planar iron complexes are rare. d^6 systems usually exhibit crossover phenomena involving $^5T_{2g}$ $(t_2^4e^2)$

and $^{1}A_{1g}$ (t_2^6) states principally with Fe(II) compounds containing nitrogen donor atom ligands (Cotton and Wilkinson, 1978; Jeremiah *et al.,* 2016). The visible spectra of all the iron(II) complexes with the exception of $[Fe(L^2)_2].2H_2O$, $[Fe(L^4)_2].2H_2O$ and $[Fe(L^5)].2H_2O$ showed two characteristic bands around 12578-17762 cm^{-1} and 18832-24252 cm^{-1} with respect to $^{5}T_{2g} \rightarrow {}^{5}A_{1g}$, and $^{5}T_{2g} \rightarrow {}^{5}B_{1g}$ transitions of an octahedral geometry (Kumar and Arabinda, 1994). However, three characteristic bands were observed for $[Fe(L^1)_2(H_2O)_2]$ and $[Fe(L^6)(Bipy)(SO_4)]$ complexes, consistent of $^{5}T_{2g} \rightarrow {}^{5}A_{1g}$, $^{5}T_{2g} \rightarrow {}^{5}B_{1g}$ and $^{5}T_{2g} \rightarrow {}^{5}B_{2g}$ transitions typical of an octahedral geometry (Kumar and Arabinda, 1994). Furthermore, $[Fe(L^2)_2].2H_2O$, $[Fe(L^4)_2].2H_2O$ and $[Fe(L^5)].2H_2O$ complexes had a lone absorption band each at 18116 cm^{-1}, 20161 cm^{-1} and 20325 cm^{-1} respectively attributable to $^{5}E \rightarrow {}^{5}T_2$transition. The latter corroborates tetrahedral structure and the noticed broadness of the bands was assignable to Jahn Teller influence in the excited state (Cotton and Wilkinson, 1978; Cesar *et al.,* 2008).

An observed magnetic moment of 5.0-5.2 B.M is often reported for magnetically dilute iron(II) complexes regardless of stereochemistry with exceptions often observed in spin crossover environments (Cotton and Wilkinson, 1978; Lever, 1980). The synthesised iron(II) complexes exhibited magnetic moments within the array of 4.97-5.25 B.M. which were in agreement with the assigned geometries (Salmon *et al.,* 2009). Furthermore, the obtained moments of 3.91 B.M and 3.74 B.M for $[Fe(L^2)(Bipy)(SO_4)].H_2O$ and $[Fe(L^5)(Bipy)(SO_4)]$ complexes were complementary of spin-crossover from high spin octahedral to low spin octahedral geometries (Lever, 1980; Salmon *et al.,* 2009).

5.5.3 Electronic spectra and magnetic moment data of cobalt(II) complexes

The electronic spectra of the synthesised cobalt(II) complexes displayed three absorptions in the ultraviolet region around 26316-30675, 31348-38023 and 40161-51813 cm^{-1} assignable to $\pi^* \leftarrow n$, $\pi^* \leftarrow \pi$ and charge transfer (CT) transitions separately. The visible spectra of divalent cobalt ($3d^7$) complexes in both octahedral and tetrahedral environments with $^{4}T$and^{4}A ground terms are expected to display three transitions each, with the absorption bands of the latter appearing at lower frequencies and more intense (Blake and Cotton, 1964; Cotton and Wilkinson, 1972). In the ligand field spectra of $[Co(L^1)_2].2H_2O$,

$[Co(L^2)_2].H_2O$, $[Co(L^4)_2].H_2O$ and $[Co(L^5)_2].2H_2O$ complexes studied, characteristic absorptions within 13263-14388 cm^{-1} and 17544-21008 cm^{-1} were obtained. The observed bands above corroborates four coordinate tetrahedral geometry with $^4A_2 \rightarrow {}^4T_1$ (υ_2) and $^4A_2 \rightarrow {}^4T_1(P)$ (υ_3) transitions respectively (Osowole and Akpan, 2012). Similarly, the absorption bands around 5000–7000 cm^{-1} in the six coordinate heteroleptic Co(II) complexes were not seen, but two absorption bands at the ranges 19841-15015 cm^{-1} and 12903-12195 cm^{-1} were observed and ascribed to $^4T_{1g} \rightarrow {}^4A_{2g}$ (υ_2) and $^4T_{1g} \rightarrow {}^4T_{1g}(P)$ (υ_3) transitions correspondingly (Earnshew,1980;Purell and Kotz, 1997; Cotton *et al.,* 1999). Though, $[Co(L^1)(Bipy)(OAc)].H_2O$ and $[Co(L^6)(Bipy)(OAc)]$ complexes displayed three absorption bands each at 23474 and 18382; 17699 and 12642; and 12804 and 11080 cm^{-1} apportioned to $^4T_{1g} \rightarrow {}^4T_{2g}$, $^4T_{1g} \rightarrow {}^4A_{2g}$ and $^4T_{1g} \rightarrow {}^4T_{1g}(P)$ transitions consistent with octahedral geometry.

Magnetic moments ranged from 4.20 B.M to 4.60 B.M are expectedly observed for un-distorted tetrahedral d^7 cobalt complexes (Sonmez and Sekerci*,* 2004). Apparently, high spin six coordinate cobalt(II) complexes possess three unpaired electrons and exhibits magnetic moments close to that of high spin tetrahedral divalent complexes but are often distinguished by the magnitude of the effective magnetic moment deviations from the spin only value of 4.7-5.2 B.M (Yamada, 1966). Furthermore, several cobalt(II) complexes exhibits low-high spin equilibrium behaviour in which the complex becomes more diamagnetic in a low spin state and more paramagnetic in a high spin state (Cotton and Wilkinson, 1972). The effective magnetic moments of the synthesised cobalt(II) complexes were in the range 4.65-5.14 B.M corroborating three unpaired electrons for high spin octahedral geometry around d^7 cobalt(II) complexes (Earnshaw, 1980; Kuruba and Nabiya, 2014; Abd El-Wahed *et al.,* 2008). Conversely, $[Co(L^2)(Bipy)(OAc)]$ and $[Co(L^5)(Bipy)(OAc)].2H_2O$ complexes had observed magnetic moments of 3.92 B.M and 3.81 B.M indicative of equilibrium between low-high spin six coordinate octahedral geometry. Additionally, magnetic susceptibility values of 4.41, 4.53, 4.37 and 4.29 B.M were observed for $[Co(L^1)_2].2H_2O$, $[Co(L^2)_2].H_2O$, $[Co(L^4)_2].H_2O$ and $[Co(L^5)_2].2H_2O$ complexes and were consistent with tetrahedral geometry (Osowole *et al.,* 2012b)

5.5.4 Electronic spectra and magnetic moment data of nickel(II) complexes

Three different absorptions were detected in the UV spectra of the nickel(II) complexes which corroborates $\pi^* \leftarrow n$, $\pi^* \leftarrow \pi$ and charge transfer transitions. These absorptions varied significantly in the hydroxyl substituted analogues. Nickel complexes containing configurations of $3d^8$ electron and having $3F$ and $3P$ terms experience stereo-chemical shifts from four-coordinate square planar to tetrahedral or to six-coordinate octahedral (Bassett *et al.,* 1978) geometry. Furthermore, nickel(II) complexes in octahedral field with a $^3A_{2g}$ ground term are expected to display three transitions in the ranges 9000-13000 cm^{-1}, 14000-20000 cm^{-1} and 21000-24000 cm^{-1} assignable to $^3A_{2g} \rightarrow {}^3T_{2g}$, $^3A_{2g} \rightarrow {}^3T_{1g}$ and $^3A_{2g} \rightarrow {}^3T_{1g}(P)$ respectively. On the other hand, $^3T_1$ ground term nickel(II) complexes of tetrahedral geometry exhibits absorptions around 12000 cm^{-1}, 17500 cm^{-1} and 21000 cm^{-1} often attributed to $^3T_1(F) \rightarrow {}^3T_2(F)$, $^3T_1(F) \rightarrow {}^3A_2(F)$ and $^3T_1(F) \rightarrow {}^3T_1(P)$ transitions, while square planar divalent nickel complexes are expected only to display a single characteristic band around 20000 cm^{-1} due to $^1A_{1g}(D) \rightarrow {}^1A_{2g}(D)$ transition (Lashanizadeganand Boghaei, 2001). The visible spectra of the synthesised nickel(II) complexes with the exception of $[Ni(L^1)_2].H_2O$, $[Ni(L^2)_2].H_2O$ and $[Ni(L^4)_2].H_2O$ exhibited typical absorption bands around 11962-12315 cm^{-1}, 13280-18083 cm^{-1} and 19268-24038 cm^{-1} due to $^3A_{2g} \rightarrow {}^3T_{2g}$, $^3A_{2g} \rightarrow {}^3T_{1g}$ and $^3A_{2g} \rightarrow {}^3T_{1g}(P)$ transitions. The latter corroborates well-defined six coordinate octahedral geometry for the studied nickel(II) complexes (Geary, 1971; Mohamed *et al.,* 2005). However, three characteristic absorption bands around 10072-13316 cm^{-1}, 14027-18116 cm^{-1} and 20920-2364 cm^{-1} were detected in the ligand field spectra of $[Ni(L^1)_2].H_2O$, $[Ni(L^2)_2].H_2O$ and $[Ni(L^4)_2].H_2O$ complexes, assigned to $^3T_1(F) \rightarrow {}^3T_2(F)$, $^3T_1(F) \rightarrow {}^3A_2(F)$ and $^3T_1(F) \rightarrow {}^3T_1(P)$ transitions typical of a four coordinate tetrahedral geometry (Osowole *et al.,* 2008; Ajibade and Zulu, 2011).

Square planar d^8 divalent nickel compounds are mostly diamagnetic, while $3d^8$ tetrahedral nickel complexes are estimated to display magnetic moments within 3.4-4.2 B.M due two unpaired electrons. Nickel(II) complexes in the octahedral field exhibits 2.8-3.3 B.M magnetic moment values. The high magnetic moment values of 2.8 B.M could be

attributed to orbital influence. The synthesised nickel(II) complexes had magnetic moments between 2.77-3.39 B.M suggestive of six coordinate geometry (El-Tabl, 2002; Sallam, 2005), while magnetic moment values of 3.49-3.80 B.M were observed for $[Ni(L^1)_2].H_2O$, $[Ni(L^2)_2].H_2O$ and $[Ni(L^4)_2].H_2O$ corroborating tetrahedral geometry (Day and Selbin, 1969; Gaber *et al.,* 2001).

5.6.5 Electronic spectra and magnetic moment data of copper(II) complexes

The ultraviolet spectra of the synthesised divalent copper compounds displayed three absorptions at the ranges 25100-29219 cm^{-1}, 30300-37964 cm^{-1} and 44843-47619 cm^{-1} arising from $\pi^* \leftarrow n$, $\pi^* \leftarrow \pi$ and charge transfer transitions. Copper(II) ligand field spectra are more complicated to interpret due to unsymmetrical overlapping bands resulting from distortions (Graddon and Schulz, 1965). Octahedral d^9 copper(II) complexes with a ground term of ^2D are expected to display a single absorption band due to $^2E_g \rightarrow {}^2T_{2g}$ transition. Moreover, six coordinate divalent copper complexes are often subjected to Jahn Teller distortion, a consequence of uneven distribution of electrons in the e_g set of the 3*d* orbitals (Nejo *et al.,* 2010). The latter which operate on d^9electronic ground state results into tetragonally distorted octahedral geometry (Figgis, 1966). Square planar Cu(II) complexes exhibits bands around 13000-20000 cm^{-1} region, while regular tetrahedral d^9 copper(II) complexes show single absorption band below 10000 cm^{-1} (Lever, 1986). Consequently, a pair of absorption bands around 17182-18807 cm^{-1} and 19342-23585 cm^{-1} in $[Cu(L^1)_2]$, $[Cu(L^2)_2]$, $[Cu(L^4)_2]$ and $[Cu(L^5)_2]$ complexes were indicative of the transitions $^2B_{1g} \rightarrow {}^2A_{1g}$ and $^2B_{1g} \rightarrow {}^2E_{1g}$ in a square planar environment (Abd El-Wahab, 2008). Furthermore, the visible spectra of ($[Cu(L^1)(Bipy)(OAc)]$, $[Cu(L^2)(Bipy)(OAc)].H_2O$, $[Cu(L^3)(Bipy)(OAc)]$, $[Cu(L^4)(Bipy)(OAc)].H_2O$, $[Cu(L^5)(Bipy)(OAc)]$ and $[Cu(L^6)(Bipy)(OAc)].H_2O$) complexes exhibited a lone broad to medium bands observed at 16807-21413 cm^{-1} ranges consistent with $^2E \rightarrow {}^2T_2$transition of a six coordinate geometry about the Cu(II) ion (Osowole and Akpan, 2012).

Owing to orbital contributions and spin-orbit coupling, the magnetic moments of copper(II) complexes at room temperature are usually greater than the spin-only value of 1.73 B.M. Accordingly, the magnetic moment values of copper(II) are often not employed

for geometry prediction but give information on the number of metal centres in a complex. Mononuclear bivalent copper compounds are projected to exhibit moment values of 1.9–2.2 B.M regardless of stereochemistry. While dinuclear copper complexes may have higher values (Khalil *et al.,* 2002). The studied copper(II) complexes had magnetic moments between 1.75-2.21 B.M validating their mononuclear natures (Ceyhan *et al.,* 2011).

5.5.6 Electronic spectra and magnetic moment data of zinc(II) complexes

The electronic spectra of the zinc(II) complexes expectedly showed lone charge transfer transitions from M→L at 12953 cm^{-1} and 18083 cm^{-1} for $[Zn(L^1)_2]$, 19157 cm^{-1} and 23094 cm^{-1} for $[Zn(L^1)(Bipy)(OAc)].2H_2O$, 13175 cm^{-1} and 20121 cm^{-1} for $[Zn(L^2)_2]$, 13072 cm^{-1} and 17452 cm^{-1} for $[Zn(L^2)(Bipy)(OAc)]$, 13123 cm^{-1} and 23419 cm^{-1} for $[Zn(L^3)(Bipy)(OAc)].H_2O$, 12970 cm^{-1} and 17575 cm^{-1} for $[Zn(L^4)_2].H_2O$, 20450 cm^{-1} for $[Zn(L^4)(Bipy)(OAc)]$, 19880 cm^{-1} for $[Zn(L^5)_2].H_2O$, 19960 cm^{-1} for $[Zn(L^5)(Bipy)(OAc)].H_2O$ and 20040 cm^{-1} for $[Zn(L^6)(Bipy)(OAc)]$, as no *d-d* transition was predictable for d^{10} zinc(II) ions (Atmaran and Kirian, 2011). Observed bands at the 26881-26455 cm^{-1} and 30864-36232 cm^{-1} region are intraligand bands. Divalent zinc possesses $3d^{10}$ electron configuration and exhibits magnetic moments corresponding to zero unpaired electrons. Observed magnetic moments of 0.09-0.43 B.M. was indicative of diamagnetism for the synthesised zinc(II) complexes and corroborates their geometry (Raman *et al.,* 2008).

5.6 ^{1}H nmr and ^{13}c nmr spectra

The NMR spectra of the ligands have been studied. The chemical shifts were reported in parts per million (ppm) with respect to the standard (TMS). All the proton as well as carbon-13 atoms were observed in their expected regions. The prominent resonance signals of these ligands were compared with those reported in literature (Raziyeh and Saeid, 2012; Shubhangi and Harjeet *et al.,*, 2013; Joshi *et al.,* 2014; Valarmathy and Subbalakshmi, 2014 and Tarek *et al.,* 2015).

The Schiff base ligand, HL^1 displayed chemical shifts due to napthalene phenyl protons; H_{12}, H_{11}, H_{15}, $H_{18,}$ H_{17} and H_{16} as singlet at 6.51 ppm, as singlet at 8.903 ppm, multiplet at 8.004-8.199 ppm, multiplet at 7.805-7.866 ppm, multiplet at 7.577-7.590 ppm and multiplet at 7.209-7.488 ppm separately. Likewise, the cyclic protons peaks of the pyrimidine ring were observed as multiplet at 7.603-7.628 ppm and singlet at 10.77 ppm for H_5 and $H_{4,6}$ atoms. The peak arising from O-H group common of 2-hydroxy-1,4-napthaldehyde was identified in the ligand spectrum at 14.52 ppm while the azomethine proton peak was displayed at 9.49 ppm. The ^{13}C NMR spectrum of 3-{[-(pyrimidin-2-yl)imino]methyl}napthalen-2-ol ligand showed resonance signals consistent of the napthalene carbon atoms (C_9, C_{12}, C_{16}, C_{18}, C_{15} C_{11} C_{13} C_{14} C_{10}) at 108.36, 112.41, 124.61, 126.10-128.81, 129.20-131.69, 133.55, 138.40, 141.43 ppm and 157.07 ppm. The signal at 163.98 was typical of the azomethine carbon atom (C_8). Also, observed resonance signals at 183.72 ppm, 159.23 ppm and 118.07-119.47 ppm were attributed to C_2, $C_{4,6}$ and C_5 atoms respectively of the pyrimidine moiety.

The NMR spectra of 3-{[(4,6-dihydroxypyrimidin-2-yl)imino]methyl}napthalen-2-ol were shown in Figures 4.3.2 and 4.4.2. The ligand's ^{1}HNMR spectrum exhibited a sharp lone peak at10.80 ppm owing to the phenolic (O-H) protons and another singlet at 8.92 ppm attributed to azomethine (H-C=N) proton. Nevertheless, doublet-multiplet peaks observed at 8.22, 8.07, 7.85, 7.76, 7.56 and 7.33 ppm were ascribed to the cyclic ring protons of naphthalene moiety. Similarly, the appearance of the resonance signal at 6.40 ppm indicates the presence of pyrimidine proton at C_5. Observed signals at 138.4, 129.3, 128.8, 127.5, 124.2, 122.2 and 118.8 ppm in the ^{13}CNMR spectrum of the Schiff base ligand, HL^2 were credited to C_{10}, C_{14}, $C_{11\&13}$, C_{15}, $C_{17\&18}$, C_{16} and C_{12} separately of the napthaldehyde ring. The pyrimidine moiety carbon ($C_{4\&6}$, C_2, C_5) atoms resonated at 192.8, 131.7 ppm and 98.1 ppm. Additionally, the sharp peak observed at 164.1 ppm was typical of imine carbon atom and was assigned same.

Figure 4.3.3explains the ^{1}H-NMR spectrum of 3-{[(4,6-dimethylpyrimidin-2-yl)imino] methyl}napthalen-2-ol, HL^3. The sharp lone peak around 3.34 ppm was apportioned to the methyl protons on the pyrimidine ring, though the hydrogen atom on C_5 vibrated at 6.65-

6.66 ppm. Also, the napthalene cyclic protons (H_{15}, H_{16}, H_{17} and H_{18}) were detected as doublets within 7.83-7.84, 7.10-7.29, 7.50-7.53 and 7.64-7.66 ppm and singlets (H_{11} and H_{12}) at 8.03 ppm and 7.31 ppm separately. The presence of resonance peaks at 14.42 ppm owing to phenolic hydrogen atom as well as at 9.55 ppm arising from imine functional group proton in the ligand spectrum substantiates the existence of an OH moiety and formation of the ligand. The ligand ^{13}CNMR spectrum displayed resonance peaks characteristic of the naphthalene ring C_{11}-C_{20} atoms at 108.06, 133.7, 129.2, 129.5, 126.3, 124.5 ppm and 119.3 ppm separately. The peak at 141.3 was typical of the azomethine carbon atom (C_{10}), whereas the detected resonance peaks around 183.8 ppm, 168.7 ppm as well as at 116.8 ppm were correspondingly apportioned to C_2, $C_{4,6}$ and C_5 atoms of the pyrimidine moiety. Consequently, $C_{7,8}$ resonated as a lone peak at 23.44 ppm.

The HL^4 ligand has been subjected to NMR (^{1}H and ^{13}C) studies. The napthoquinone phenyl protons (H_9, $H_{15,16}$ and $H_{14,17}$) were detected as lone peaks around 6.52 ppm, doublets at 7.33 ppm, and doublet within 7.75-7.77 ppm separately. Likewise, the cyclic protons peaks of the pyrimidine ring were observed as doublet within 6.06-6.12 ppm and triplet around 7.80-7.99 ppm for H_5 and $H_{4,6}$ atoms. The resonance signals arising from O-H moiety characteristic of 2-hydroxy-1,4-naphthoquinone was absent in the ligand's spectrum rather a broad-like signal centred at 4.79 ppm typical of aromatic C-NH (s, N_7H) functional group was noticed. The N-H signal substantiates the suggested ketoamine tautomeric arrangement for the HL^4 ligand in solution other than its enolimine tautomer. The ^{13}CNMR spectrum displayed resonance signals of the napthoquinone carbonyl atoms (C_{10}, C_{11}) around 181.5 ppm and 184.5 ppm. Additionally, observed resonance signals at 158.0 ppm, 125.4 ppm, 130.6 ppm, 125.9 ppm as well as at 132.1 ppm were credited to C_8, C_9, $C_{12,13}$, $C_{14,17}$ and $C_{15,16}$ atoms separately of the naphthoquinone moiety. However, the resonance signals due to C_2, C_5 and $C_{4,6}$ of the pyrimidine ring were seen at 153.4 ppm, 110.8 ppm and 133.1-134.5 ppm accordingly.

The phenolic protons in the metal free ligand, 2-(4,6-dihydroxypyrimidin-2-ylamino)naphthalene-1,4-dione (HL^5) were observed at 6.04 ppm (s, 2H), while the N-H proton resonated as a broad signal at 4.95 ppm. The HL^5 spectrum showed a set of peaks

in multiples at the range 7.52–7.79 ppm and 7.81-7.95 ppm and were apportioned to naphthalene cyclic ring protons ($H_{16,17}$ and $H_{14,15}$) respectively. The C_9-H proton resonated at 6.96 ppm. Similarly, the proton on C_5 in the pyrimidine ring was centred at 6.61 ppm. The ^{13}CNMR spectrum of the ligand, HL^5 had peaks around 132.5 ppm, 103.7 ppm and 161.7 ppm; and 134.3 ppm, 110.3 ppm, 125.3-125.8 ppm and 130.8-132.8 ppm typical of pyrimidine and naphthalene rings' carbon atoms. The signals within 182.2-184.1 ppm and 161.7 ppm in the ligand's spectrum were attributed to C=O and C-O carbon atoms respectively.

The naphthalene protons in HL^6 ligand were observed at the range 7.76-7.98 ppm as multiplets, 7.35 ppm as singlet, though the pyrimidine ring's proton was also observed as a lone peak around 6.28 ppm. The NH protons resonated as a broad singlet peak at 3.38 ppm while the methyl protons were detected as a sharp lone peak around 2.49 ppm. The ^{13}C NMR spectrum of 2-(4,6-dimethylpyrimidin-2-ylamino)naphthalene-1,4-dione ligand showed resonance signals common of the napthoquinone carbon atoms (C_{10}, C_{11}, C_{12}, C_{13}, C_{14}, C_{15}, $C_{16,17}$, C_{18} and C_{19}) at 159.6, 111.0, 181.3, 184.7, 131.9, 130.6, 125.4-125.9, 133.2 ppm and 134.5 ppm. The signal at 31.8 was typical of the carbon atoms ($C_{7,8}$). Furthermore, resonated peaks around 156.9 ppm, 106.7 ppm and 159.6 ppm were assigned to C_2, C_5 and $C_{4,6}$ atoms respectively of the pyrimidine ring system.

5.7 Electrospray ionization mass spectra (ESI-MS) studies

The electrospray ionization mass spectra (ESI-MS) of the ligands (HL^1-HL^6)were carried out to obtain their molecular weight and to study their patterns of fragmentation.

Mass spectrometry was carried out on the ligand, 3-{[-(pyrimidin-2-yl)imino]methyl} napthalen-2-ol. The molecular ion peak observed at m/e 250.096 due to M+1 corroborates the formula weight (FW) of 249.268 for the proposed HL^1 ligand structure which was in conformity to the calculated m^+ data. The low intensity of the molecular ion with extra mass unit may be attributed to cleaved bonds and consequently presence of ^{13}carbon isotope. The HL^1 ligand's mass spectrum also displayed (m/z) peaks at 169 and 229 corresponding to $[C_{11}H_7NO]^+$ and $[C_{15}N_3H_{10}]^+$ fragments respectively. The peaks

observed at m/z 173, 175 and 251 were attributed to extra mass units peaks of m/z 169 and 249 due to the natural presence of ^{13}carbon isotope.

The mass spectrum of HL^2 ligand exhibited the molecular ion peak at m/z281 (Figure 4.5.2). This on loss of carbonyl (CO, m/z = 28.0) and $C_3O_2H_3$ (m/z = 71) fragments gave peaks at m/z255.16 and 211.03 respectively which were equivalent to the calculated molecular weights of the fragments (M.W.=253.258 and 210.216). The molecular ion underwent further fragmentation by loss of CN_3molecule which gave an M+2 fragment ion peak at m/z 130.13.

The ESI-mass spectrum of 3-{(*E*)-[(4,6-dimethylpyrimidin-2-yl)imino]methyl}naphthalen-2-ol ligand displayed dual fragmentation pathways with an m/e+ base peak around 278.12 compatible with the obtained formula weight (278.85) for the prepared ligand. This validates the combination of 2-hydroxy-1-napthaldehyde and 2-amino-4,6-dimethylpyrimdine to give HL Schiff base. The peaks around m/z 250.17, 193.66 and 142.92 were arising from the loss of COH, NC_2H_2O and C_2N_2H groups whereas the peak around m/z 124.81 was possibly owing to the loss of OH singly. Additionally, the spectrum presented L+1 peak at m/z 279.24, a very small intensity peak around m/z 280.11 which might be ascribed to additional mass units, an out fall of carbon-13 existence and an extra average peak at 276.12 arising from lose of hydrogen atoms. Figure 3 and 4 contains the mass spectrum as well as the fragmentation arrangements separately for 3-{[(4,6-dimethylpyrimidin-2-yl)imino] methyl}napthalen-2-ol.

Similarly, the ESI-mass spectrum of 2-(pyrimidin-2-ylamino)naphthalene-1,4-dione ligand was recorded to establish stoichiometric configuration and fragmentation arrangement of the ligand. The spectrum showed peaks arising from the loss of [C_2H_3, m/z = 27.0]$^+$ at m/z 225 and lose of [C_2N_2, m/z = 53] $^+$ at m/z 175 respectively. The former increased due to carbon-13 presence. However, the base peak was observed at m/z 250 corroborating the observed formula of the ligand.

The spectrum of HL^5 ligand showed molecular ion peaks in conformity with the obtained microanalysis values and corroborates the empirical formula for the ligand. The peak around m/z 283 corroborates the formula weight whereas the base peak was detected around m/z 256.97 owing to lose of carbonyl (CO, m/z = 28). The ligand experienced additional disintegrations to produce peaks at m/z 200 and 175 assigned to lose of $[C_2NOH, m/z = 55]^+$ and $[CHO, m/z = 29]^+$ separately. The latter had enhanced value owing to existence of ^{13}carbon. The peak around m/z 301 arose from extra mass unit.

HL^6 ligand ($C_{16}H_{13}N_3O_2$)'s mass spectrum exhibited a molecular ion peak (m^+.) around m/z 278 due to $(L)^+$. (on loss of H) that corresponds to the molecular weight of the ligand. Besides this peak, the ligand displayed fragment ion peaks at m/z 251, 237, 175 and 149 that corresponds to [CO; m/z = 28], $[CH_3; m/z = 15]^+$, $[C_4H_4N_2; m/z = 61]^+$ and [CHN; $m/z = 27]^+$ separately.

5.8 Biological studies

5.8.1.1 Antibacterial activities

The synthesised ligands (HL^1-HL^6) with their corresponding divalent metallic compounds were screened against *Staphylococcus aureus, Pseudomonas aeruginosa, Escherichia coli, Bacillus cereus, Proteus mirabilis* and *Klebsiellaoxytoca* to assess their potentials as antibacterial agents. Using the zone of growth inhibition diameter as a criterion for measurement (Agwara *et al.,* 2010), the antibacterial actions of the compounds were determined asshown in 'Tables 4.8.1-4.8.10 and Figures 4.7.1-4.7.10. Careful analysis of the Tables discloses that most of the ligands and complexes largely had zones of growth inhibition within 12.0-21.0 mm (Table 4.7.1), 11.0-18.0 mm (Table 4.7.2), 12.0-26.0 mm (Table 4.7.3), 15.0-27.0 mm (Table 4.7.4), 14.0-25.0 mm (Table 4.7.5), 11.0-29.0 mm (Table 4.7.6), 10.0-29.0 mm (Table 4.7.7), 9.0-29.0 mm (Table 4.7.8), 14.5-30.0 mm (Table 4.7.9) and 11.5-34.0 mm (Table 4.7.10) respectively.

HL^1 ligand, 3-{[-(pyrimidin-2-yl)imino]methyl}napthalen-2-ol, exhibited activity against the tested bacterial organisms; *Staphylococcus aureus, P. aeruginosa, B. cereus* and *K.oxytoca* excluding *E. coli* and *P. mirabilis* with zones of inhibition in the range 9.0-16.5. The complexes; Mn(II), Cu(II) and Zn(II) were significantly active towards five microbes viz.; *S. aureus, P. aeruginosa, E. coli, P. mirabilis* and *K.oxytoca; S. aureus, E. coli, B. cereus, P. mirabilis* and *K. oxytoca; and P. aeruginosa, E. coli, B. cereus, P. mirabilis* and *K. oxytoca* with zones of growth inhibition within 6.5-21.0 mm; 7.0-17.0 mm and 12.0-17.5 mm respectively. Similarly, bivalent cobalt and nickel complexes showedactivity towards *B. cereus, P. aerugenosa* and *K.oxytoca;* and *P. aeruginosa, P. mirabilis* and *K.oxytoca* with zones of growth inhibition 5.0-14.5 mm and 13.0 mm ranges separately. The bivalent iron complex was only weakly active against *P. aeruginosa* with 12.5 mm iinhibitory zone. The inactivity of bivalent iron, cobalt and nickel compounds against most of the tested bacterial organisms may be attributed to production of potent protein toxins by the bacterial organisms to activate their cell surface proteins which in turn prevents adequate permeation of the metal complexes into the bacterial cells, and lower lipophilicity of the complexes which also decreases their penetration through the lipid membrane (Cater *et al.,* 2000 and Thangadurai and Nataranja , 2001).

Generally, the bivalent metallic compounds were more active towards the tested organisms compared to the ligand, attributable to chelation (Mittal and Uma, 2010), with the exception of the bivalent copper and zinc complexes whose activities towards *K. oxytocaand S. aureus*; and *K. oxytoca* with zones of inhibition around 12.0 mm and 7.0 mm; and 15.0 mm respectively were lower than that of the HL^1 ligand. Moreover, bivalent manganese, cobalt and nickel complexes' activities of 13.0 mm; 14.5 mm and 5.0 mm; and 13.0 mm against *S. aureus; K. oxytoca* and *P. aeruginosa*; and *K. oxytoca* were less than the inhibitory zones of the ligand against the same organisms. However, Mn(II), Cu(II) and Zn(II) complexes exhibited strong antibacterial actions against *P. mirabilis, K. oxytoca, E. coli, B. cereus, P. aeruginosa,* thus verifying their effectiveness as possible broad-spectrum antibacterial agents.

The antimicrobial data presented in Table 4.8.2 for the heteroleptic metal(II) complexes of HL^1 ligand indicates that the synthesised compounds were active against all the tested microorganisms. Conversely, *E. coli, P. mirabilis and S. aureus* showed resistance to the antibacterial activities of HL^1, Mn(II) and Zn(II); HL^1 and Co(II); and Fe(II) and Zn(II).

Similarly, Ni(II) and Zn(II) complexes were not active against*P. aeruginosa and K. oxytoca*. Cu(II) complex was active towards all the species with higher zones of inhibition than that of the ligand, except against *K. oxytoca* and *S. aureus,* where 14.5 mm and 13.5 mm zones of inhibition were lower than that of the ligand. The Mn(II) and Fe(II) complexes exhibited improved activity against *B. cereus* (15.0), *P. mirabilis* (13.0) and *P. aeruginosa* (12.0 mm); and *B. cereus* (13.5), *E. coli* (8.0) and *P. mirabilis* (8.0 mm) when compared with HL^1 ligand's activity (9.0 mm), (0.0 mm) and (11.0 mm) respectively. Furthermore, Co(II) and Zn(II) complexes were effectively active towards *B. cereus* and *E. coli*; and *P. mirabilis* than the ligand, HL^1. Interestingly, Mn(II), Co(II) and Cu(II) complexes were exceptional with higher antibacterial activities greater than that of both HL^1 and 2,2'-bipyridine ligands against *P. aeruginosa* (12.0 mm); *E. coli* (13.0 mm); and *E. coli* (15.0 mm) and *P aeruginosa* (17.0 mm).

The antibacterial results of the Schiff base, (HL^2) with its divalent metallic compounds presented in Table 4.8.3 showed that they were generally active against all the bacteria organisms screened, except the divalent complexes of iron and zinc which were inactive against *P. aeruginosa* and *S. aureus;* and *P. mirabilis.* Consequently, the Schiff base, $HL^2$was mostly more active than the complexes of zinc, manganese and iron against all the microorganisms tested with zones of inhibition from 5.5 mm to 20.0 mm. This may be attributed to hydrogen bonding between the cellular constituents of the microbial cell and imine nitrogen and napthanenol oxygen atoms of the Schiff base, hence causing the death of the bacteria with higher inhibitory zones (Atmaram and Kirian, 2011). With *B. cereus* and *P. aeruginosa*, Co(II), Ni(II) and Cu(II) complexes displayed higher antibacterial activities than the Schiff base ligand with zones of inhibition at 17.5 mm and 25.0 mm; 17.0 mm and 15.5 mm; and 18.0 mm and 19.5 mm. Co(II) and Cu(II) complexes showed greater growths compared to that of HL^2 ligand against *E. coli*, *K. oxytoca* and *S. aureus* with zones of

inhibition at 17.0 mm, 16.0 mm and 23.0 mm; and 25.5 mm, 22.5 mm and 20.0 mm separately. The increased antibacterial actions of the metallic compounds against the tested microorganisms were attributed to chelation, which increased the lipophilic character of the metal(II) complexes and favoured their penetration through the lipid layer of the bacterial membranes (Ahmed *et al.,* 2002).

The ligands; HL^2 and 2,2'-bipyridine with their heteroleptic metal(II) complexes were significantly active against all the screened organisms exhibiting variable levels of inhibitory influences (Spinu *et al.,* 2008). Generally, the complexes had better activities in one form or the other higher than the ligands, except with *B. cereus* (24.5 mm) and *S. aureus* (20.0 mm) where the HL^2 ligand had greater antibacterial activities as against the heteroleptic metallic compounds on the individual growth of the tested microorganisms. Consequently, Mn(II) and Cu(II) complexes exhibited high actions against *E. coli* (20.5 mm), *K. oxytoca* (22.0 mm), *S. aureus* (21.0 mm) and *P. mirabilis* (24.5 mm); and *B. cereus* (20.0 mm), *E. coli* (26.5 mm), *K. oxytoca* (23.5 mm) and *P. mirabilis* (22.0 mm) greater than that of the ligands and comparable to but not greater than the values displayed by the standard drug, ciprofloxacin. Similarly, the complexes; Fe(II), Co(II), Ni(II) and Zn(II) were more active than the HL^2 ligand against one/two of the tested bacterial organism(s), i.e. *K. oxytoca* (23.5 mm); *P. mirabilis* (23.0 mm); *K. oxytoca* (25.5 mm) and *P. aeruginosa* (20.0 mm); and *K. oxytoca* (20.5 mm) and *P. mirabilis* (20.5 mm) respectively. Interestingly, Mn(II) and Co(II) complexes had greater/comparable actions to that of the standard drug, ciprofloxacin thus indicating their significance as potential broad-spectrum antibacterial agents in-vitro (Osowole and Ott, 2012; Ajibade and Zulu, 2011).

The heteroleptic metal(II) complexes of HL^3 ligand were generally active and displayed varying levels of inhibitory influences on the growing rate of the screened organisms when likened to that of the ligands. However, the general inhibition of the microorganisms by the HL^3 ligand with zones of inhibition ranged from 8.5 mm to 26.0 mm may be due to the presence of the phenol and the imine groups often reported to enhance antibacterial activities (Nogrady, 1988; Osowole and Fagade, 2007). Similarly, the heteroleptic Cu(II)

complex was more effective than the ligands (HL^3 and 2,2'-bipyridine) against *B. cereus, E. coli, K. oxytoca, P. aeruginosa* and *S. aureus* displaying zones of inhibition from 19.5-25.0 mm. Co(II) complex had zones of inhibition within 16.0-21.5 mm against all the screened organisms, excluding *P. mirabilis.* Furthermore, Mn(II), Fe(II) and Ni(II) complexes exhibited inhibitory effects higher than that of the ligands against only *P. aeruginosa* (21.0 mm); *B. cereus* (18.5 mm); and *P. aeruginosa* (18.5 mm) respectively. Comparing the activities of the complexes, Cu(II) complex presented superlative antibacterial actions indicating its potential significance in new antibacterial drug designs.

The antibacterial activity of HL^4, 2-(pyrimidin-2-ylamino)naphthalene-1,4-dione and its metallic compounds tested in-vitro against Gram-positive bacteria "*S. aureus, and B. cereus";* and Gram-negative bacteria "*P. mirabilis*, *K. oxytoca, "E. coli,* and "*P. aeruginosa*" are presented in Table 4.7.6. The compounds generally were active against all the microorganisms with exception of Ni(II) and Fe(II) complexes which were inactive against *E. coli*, *K. oxytoca*, *S. aureus* and *P. mirabilis*; and *B. cereus* and *E. coli*. The lipophobic nature of Ni(II) and Fe(II) complexes could be responsible to their inactivity against the screened microbes. Accordingly, the divalent zinc complex exhibited greater actions compared to that of the ligand (HL^4) against *B. cereus* (20.0 mm), *K. oxytoca* (23.0 mm), *P. aeruginosa* (19.5 mm) and *P. mirabilis* (20.3 mm). Likewise, Mn(II) and Cu(II) complexes showed greater actions more than the ligand against *B. cereus*, E. coli, *K. oxytoca, P. aeruginosa,S. aureus* and *P. mirabilis* with zones of inhibition at 17.5 mm and 20.0 mm; 22.0 mm and 22.0 mm; 19.0 mm and 19.0 mm; 18.0 mm and 23.5 mm; 21.5 mm; and 20.5 mm separately. Remarkably, the divalent cobalt complex displayed substantial and enhanced broad spectrum action than that of the ligand against the entire verified microbial organisms and greater than of the standard antibiotics against *P. mirabilis* (25.0 mm).

The antibacterial activity depicted histogram (Figure 4.7.7) for the heteroleptic metal(II) complexes of HL^4 ligand confirmed that the ligands with their metallic compounds were active against all the microbial organisms. However, *E. coli and K. oxytoca* displayed resistance to the antibacterial actions of Mn(II), Ni(II) and Zn(II)complexes.On the other

hand, divalent cobalt and copper compounds were active entirely against the microbial species with higher zones of inhibition compared to the ligands, except against *P. mirabilis* where inhibitory zones of 15.5 mm and 16.0 mm were lower than that of the ligands. Additionally, Mn(II), Zn(II) and Fe(II) complexes displayed better activities against *B. cereus* (23.0), *P. aeruginosa* (20.5 mm) and *S. aureus* (22.0 mm); *B. cereus* (21.0 mm); and *B. cereus* (22.5) when compared with HL^4 and 2,2'-bipyridine ligands' activities (15.0-15.5 mm), (8.5-16.5 mm) and (17.0-21.0 mm) respectively. Additionally, the Ni(II) complex was active towards screened organisms entirely with lower inhibitory zone effects than the ligands. If the bacterial actions of the compounds against each microbe were graded and the grading added, an action sequence could be inferred in the order, Ni(II) < Zn(II) < 2,2'-Bipy < Fe(II) < Mn(II) < HL^4<< Cu((II) > Co(II)

The ligand, HL^5 was entirely active towards the tested microbeswith zones of inhibition within 9.0-19.0 mm nonetheless it was not active against *S. aureus*. As anticipated, the divalent metallic compounds were more susceptible to *K. oxytoca* and *E. coli* excluding divalent nickel complex which was non-vulnerable to the latter. This was predictable arising from the tinny peptidoglycan layer of the gram negative microbes which makes it easier for the divalent metallic compounds to gain penetrability into the cell walls with zones of inhibition ranged from 9.5 mm to 21.0 mm and 12.0-23.0 mm (Thangadurai and Natarajan, 2001). Additionally, all the metal(II) complexes were active against *E. coli* and *P. mirabilis* with zones of inhibition within 12.0-23.0 mm and 11.0-26.0 mm separately, except for divalent nickel complex which displayed no activity. The bacteria species; *P. aeruginosa* and *S. aureus* showed no activity to the divalent manganese, iron and nickel complexes, while the inactivity of *B. cereus* to the Ni(II) and Zn(II) complexes were ascribed to the production of extended-spectrum beta-lactamases (ESBL) by these microbes, resulting in the deactivation of the compounds (Kamalakannan and Venkappayya, 2002; Vitkauskiene *et al.,* 2006). The poor microbial actions exhibited by Mn(II), Fe(II), Ni(II), Cu(II) and Zn(II) complexes comparative to the HL^5 ligand against *P. mirabilis* (11.0 mm), *K. oxytoca* (14.0 mm), *K. oxytoca* (9.5 mm), *B. cereus* (12.0 mm) and *P. aeruginosa* (14.5 mm)could be ascribed to low level of penetrability of the microbial cells (Rafique *et al.,* 2010). Surprisingly, Fe(II) and Co(II) complexes exhibited

exceptional actions higher than that of the HL^5 ligand and the standard drug, ciprofloxacin against *P. mirabilis* (25.0 mm); and *P. aeruginosa* (29.0 mm) and *P. mirabilis* (26.0 mm) respectively.

HL^5 ligand and its heteroleptic divalent metal complexes displayed variable levels of inhibitory effects on the growing rate of the screened microbial organisms. Generally, the complexes displayed good activities higher than that the ligands (HL^5 and 2,2'-bipyridine) against the microorganisms due to chelation (Neelakantan *et al.,* 2010). The ligand, HL^5 exhibited better antibacterial actions than Mn(II), Ni(II) and Zn(II) complexes against *P. aureginosa*. This may be attributed to better permeability and lipophilic nature of the ligand through the bacteria cells compared to Mn(II), Ni(II) and Zn(II) complexes. Ni(II) complex was inactive against *S. aureus* and *P. mirabilis* while Mn(II) complex showed no activity against *P. mirabilis* only. This could be attributed to the bacteria's secretion of β-lactamases, an enzyme which claves to the β-lactam ring (imine moiety) thereby rendering the complexes inactive (Jacoby and Sutton, 1991). Additive ranking of the growth inhibition by the compounds against the micro-organisms shows the order as *K. oxytoca* > *B. cereus* >*E. coli* >*P. aeruginosa* >*P. mirabilis* > *S. aureus*. *K. oxytoca, B. cereus and E. coli* were most generally inhibited by all the synthesised compounds. However, the entire heteroleptic divalent metallic compounds exhibited broad spectrum action towards the entirely tested microbial species, excluding the complexes of Mn(II) and Ni(II); showing their effectiveness as probable broad-spectrum antibacterial agents.

The antibacterial result of HL^6 ligand and its heteroleptic divalent metallic compounds indicate that the compounds generally had activity against all the microorganisms, except of Ni(II) complex which indicated no activity towards *K. oxytoca* and *P. aureginosa.* As expected, the metallic compounds significantly were more active when compared to the ligands (HL^6 and 2,2'-bipyridine). e.g. all the metallic compounds displayed excellent activity than that of the ligands against the bacteria *E. coli*and *P. mirabilis* with zones of inhibition within 18.0-28.0 mm and 18.5-28.0 mm. Furthermore, Co(II), Cu(II), and Mn(II) complexes unexpectedly were more susceptible than the ligands against *B. cereus* with zones of inhibition at 31.0 mm, 29.0 mm and 29.0 mm separately. Similarly, Cu(II),

Zn(II), Co(II), Fe(II) and Mn(II) complexes displayed broad-spectrum activities greater than that of both the ligands and the standard drug, ciprofloxacin against *P. aeruginosa* (31.0 mm), *S. aureus* (34.0 mm) and *P. mirabilis* (27.0 mm); *P. aeruginosa* (31.0 mm) and *P. mirabilis* (28.0 mm); *P. aeruginosa* (32.0 mm) and *P. mirabilis* (26.0 mm); *S. aureus* (28.0 mm) and *P. mirabilis* (25.0 mm); and *P. mirabilis* (28.0 mm) verifying their possible practicality as broad-spectrum antibacterial agents.

5.8.1.2 Antifungal studies

The antifungal activities of HL^1, HL^2 and HL^3 Schiff bases, and their symmetrical and non-symmetrical complexes against *A. niger, A. flevus and R. Stolonifer*are presented in Tables 4.9.1-4.9.5. The 3-{[-(pyrimidin-2-yl)imino]methyl}napthalen-2-ol, HL^1 ligand showed activity against all the tested organisms; *A. niger, A. flevus and R. Stolonifer*with zones of inhibition in the range 7.0-15.0. The Mn(II), Ni(II) and Zn(II) complexes were meaningfully active against *A. flevus and R. Stolonifer* onlywith zones of inhibition within 13.0 - 23.0 mm. Similarly, Cu(II) complex displayed activity only against *R. Stolonifer*with inhibitory zone of 19.0 mm. Contrarily, the heteroleptic complexes generally had low activity against the fungal organisms compared to symmetrical complexes and HL^1 ligand. However, the heteroleptic Mn(II), Co(II), Cu(II) and Zn(II) complexes exhibited activity against *R. Stolonifer, A. flevus, R. Stolonifer*and *A. niger* with inhibitory zones of 11.0 mm, 17.0 mm, 16.0 mm and 18.0 mm respectively. The HL^2 ligand with its divalent metallic compounds displayed significant activities against all the organisms screened, with the exception of symmetrical Mn(II), Ni(II) Cu(II) and Zn(II) complexes which were inactive against *A. niger, A. niger*, *R. Stolonifer*and *A. flevus* respectively. Consequently, the heteroleptic metal(II) complexes of HL^2 ligand were generally more active toward the entire microorganisms tested with inhibitory zone ranges of 16.0-30.0 mm. The methyl substituted HL^3 Schiff base and its heteroleptic complexes had adequate to excellent antifungal activity towards the screened microbes with the exception Cu(II) complex which exhibited no activity towards the evaluated microorganisms. Nevertheless, *R. Stolonifer* was resistance to HL^3 ligand and Zn(II) complex, whereas Ni(II) complex was inactive against *A. flevus*.

The results of the antifungal actions of the synthesised HL^4, HL^5 andHL^6 ligands with their metallic compounds against *A. niger, A. flevus and R. Stolonifer*indicates that they had average to good inhibitory zones. The entire fungal microbes were inhibited by the ligands (HL^4-HL^6) with higher zones of inhibition ranged 15.0 mm to 27.0 mm. The activities of the ligands towards the screened organisms were unexpectedly higher than that of the metal complexes (Nogrady, 1988). However, $[Mn(L^4)_2].H_2O$, $[Co(L^4)_2].H_2O$, $[Mn(L^4)(Bipy)(OAc)].H_2O$, $[Cu(L^4)(Bipy)(OAc)].H_2O$, $[Ni(L^5)(Bipy)(OAc)].H_2O$ and $[Zn(L^5)(Bipy)(OAc)].H_2O$ exhibited activities greater than that of their starting ligands against *A. niger* (29.0 mm), *R. Stolonifer*(25.0 mm), *A. flevus* (33.0 mm), *A. niger* (29.0 mm), *A. flevus* (31.0 mm), *A. flevus* (21.0 mm), *A. flevus* (24.0 mm), *A. niger* (17.0 mm) and *A. flevus* (23.0 mm) respectively. Generally, the metal(II) complexes of HL^4, HL^5 andHL^6 ligands had moderate zones of inhibition within 11.0 – 33.0 mm unexpectedly less susceptible than the metal free ligands. $Zn(L^5)(Bipy)(OAc)].2H_2O$ displayed higher activity compared to those of the ligands, a consequence of the well absorption of Zn(II) ions on the surface of the fungal cell walls.

5.8.2 Antioxidant studies

Antioxidants are vital substances which prevent the free radical damage of reactive oxygen species (ROS) and other unstable molecules (generally called free radicals) in the cells of living organisms. Free radicals (hydroxyl ion, superoxide anion and hydrogen peroxide) formed during bodily biochemical processes are very reactive and damaging to living cells causing various ailments such as cancer, heart disease, atherosclerosis and even aging (Indira, 2005 and Resat *et al.,* 2008).The synthesised compounds (ligands and complexes) were examined for antioxidant potentials using two different antioxidant assays; ferrous ion chelating ability and DPPH radical scavenging assays. While the metal(II) complexes were evaluated using only the DPPH radical scavenging assay, the ligands were studied using the two assays.

5.8.2.1 Ferrous ion-chelating ability

The antioxidant capacities of the synthesised ligands were investigated by ferrous ion-chelating assay (FICA). The FICA values obtained were generally stated as an equivalent

of the standard antioxidant agent (ascorbic acid). The values presented in Table 4.10 show that all the ligands possess good chelating ability towards the ferrous ion. At all concentrations of measurement, 3-{[-(pyrimidin-2-yl)imino]methyl}napthalen-2-ol (HL^1) displayed the best ferrous ion chelating antioxidant ability. Furthermore, HL^2, HL^6 and HL^3 had FICA values of 85.1 and 71.3%; 78.76 and 74.5% and 69.74% respectively at concentrations of 200 and 100 mg/mL higher than that of the standard ascorbic acid, while HL^4 and HL^5 ligands at 200 mg/mL concentration exhibited comparable antioxidant activities to the standard. The ligands, HL^3, HL^4 and HL^5 showed relatively less antioxidant power at Ic_{100}. The ferrous ion chelating abilities of HL^5 was less significant at Ic_{50}.

5.8.2.2DPPH radical scavenging studies

The use of DPPH (1,1-diphenyl-2-picryl-hydrazyl) radical scavenging assay for the antioxidant studies of synthesised compounds is considered dependable as well as standard assay in antioxidant evaluative studies. The ligands and their divalent metallic compounds were evaluated for free radical scavenging effects with DPPH radical at different concentrations (200, 100 and 50μg/mL) in 1mL DMSO. The data of DPPH radical scavenging actions for the compounds on the grounds of percent inhibition are contained in Tables 4.9.1-4.9.10. A careful look at the Tables shows that the compounds mostly exhibited radical scavenging actions in DPPH assay. Inhibitory data usually reflect extent of radical scavenging actions. The ligands (HL^1-HL^6) significantly demonstrated percentage inhibitory values lower or comparable to that of the standard (ascorbic acid) indicating their antioxidant possibilities. The antioxidant abilities of the latter enhanced significantly on complexation with divalent metal ions. However, $[Fe(L^1)(Bipy)(SO_4)]$, $[Fe(L^2)_2].2H_2O$, $[Fe(L^2)(Bipy)(SO_4)].H_2O$, $[Fe(L^3)(Bipy)(SO_4)].H_2O$, $[Fe(L^4)_2)].2H_2O$, $[Mn(L^4)(Bipy)(OAc)].H_2O$, $[Fe(L^5)_2)].2H_2O$, $[Fe(L^5)(Bipy)(SO_4)]$, $[Ni(L^5)(Bipy)(OAc)].H_2O$ and $[Ni(L^6)(Bipy)(OAc)]$ showed comparable percentage inhibitory values to those of the ligands but lower than ascorbic acid (Vitamin C). Generally, the divalent metallic compounds showed improved DPPH radical scavenging actions. Consequently, the results of the DPPH antioxidant activities proved that the

compounds can be used for design and syntheses of drugs for the management of pathological ailments due to oxidative stress.

Figure 5.1. Structures of 3-{[-(pyrimidin-2-yl)imino]methyl}napthalen-2-ol (HL^1) ligand and its metal(II) complexes

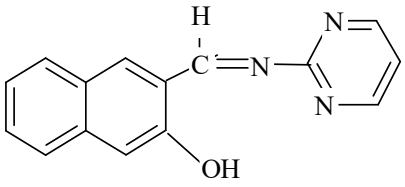

H L^1 Ligand

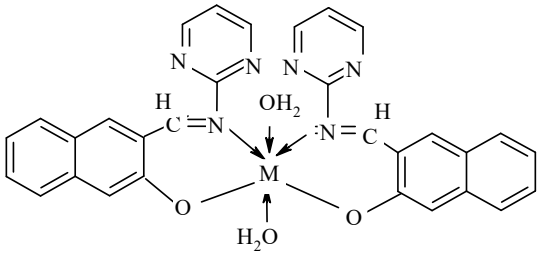

$[Fe(L^1)_2(H_2O)_2]$ = Octahedral

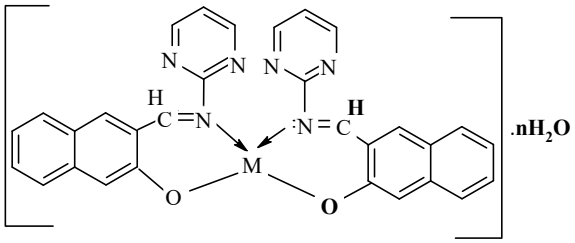

$[Mn(L^1)_2].H_2O$ = Tetrahedral
$[Co(L_1)_2].2H_2O$ = Tetrahedral
$[Ni(L^1)_2].H_2O$ = Tetrahedral
$[Cu(L^1)_2]$ = Square Planar
$[Zn(L^1)_2]$ = Tetrahedral

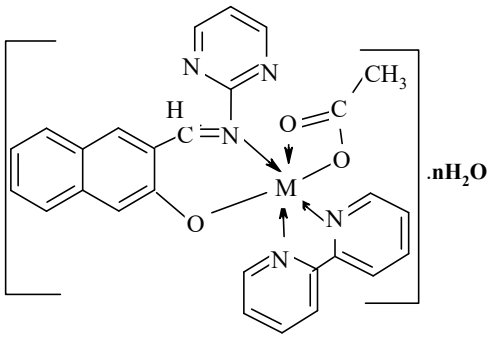

$[Mn(L^1)(Bipy)(OAc)]$ = Octahedral
$[Co(L^1)(Bipy)(OAc)].H_2O$ = Octahedral
$[Ni(L^1)(Bipy)(OAc)].H_2O$ = Octahedral
$[Cu(L^1)(Bipy)(OAc)]$ = Tetrahedral
$[Zn(L^1)(Bipy)(OAc)].2H_2O$ = Octahedral

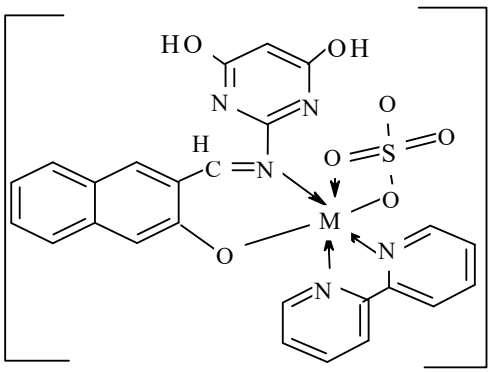

[Fe(L^1)(Bipy)(SO$_4$)] = Octahedral

Figure 5.2. Sturctures of 3-{[(4,6-dihydroxypyrimidin-2-yl)imino]methyl}napthalen 2-ol (HL^2) ligand and its divalent metallic complexes

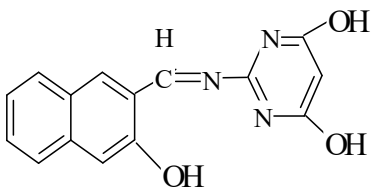

H L^2 Ligand

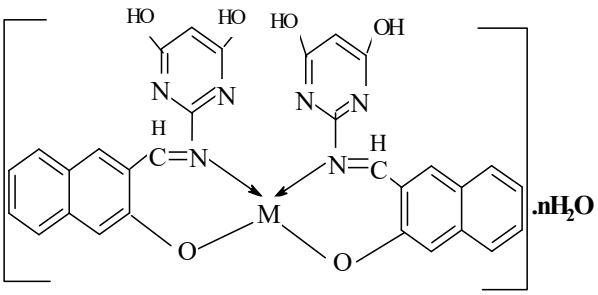

$[Mn(L^2)_2].2H_2O$ = Tetrahedral **$[Cu(L^2)_2]$ = Square Planar**

$[Fe(L^2)_2].2H_2O$ = Tetrahedral

$[Co(L^2)_2].H_2O$ = Tetrahedral

$[Ni(L^2)_2].H_2O$ = Tetrahedral

$[Zn(L^2)_2]$ = Tetrahedral

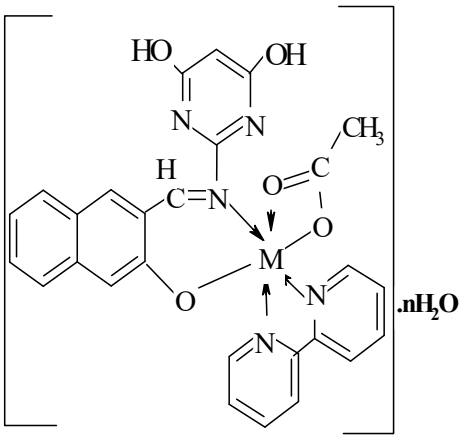

$[Mn(L^2)(Bipy)(OAc)].H_2O$ = Octahedral

$[Co(L^2)(Bipy)(OAc)]$ = Octahedral

$[Ni(L^2)(Bipy)(OAc)].H_2O$ = Octahedral

$[Cu(L^2)(Bipy)(OAc)].H_2O$ = Tetrahedral

$[Zn(L^2)(Bipy)(OAc)]$ = Octahedral

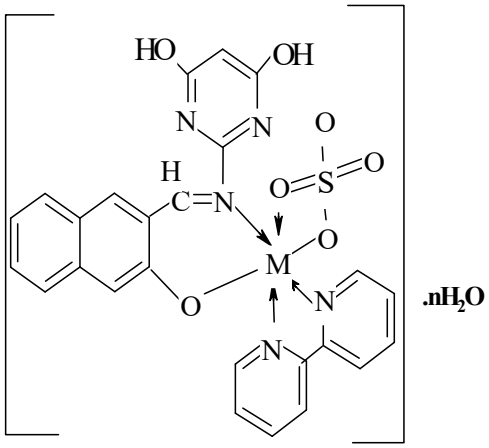

$[Fe(L^2)(Bipy)(SO_4)].H_2O$ = Octahedral

Figure 5.3. Structures of 3-{[(4,6-dimethylpyrimidin-2-yl)imino]methyl}napthalen-2-ol (HL^3) and its heteroleptic divalent metallic compounds

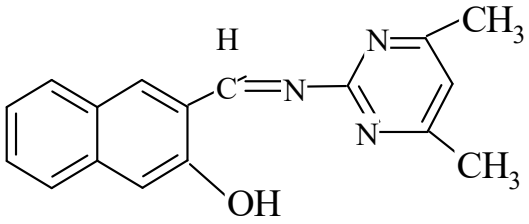

H L^3 Ligand

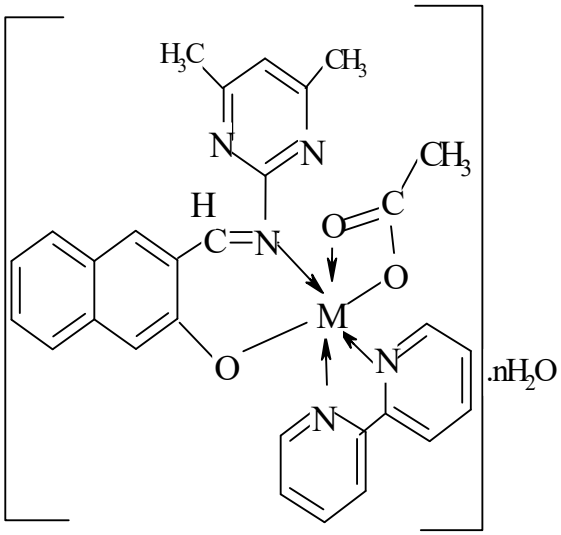

[Mn(L^3)(Bipy)(OAc)] = Octahedral

[Co(L^3)(Bipy)(OAc)] = Octahedral

[Ni(L^3)(Bipy)(OAc)] = Octahedral

[Cu(L^3)(Bipy)(OAc)] = Tetrahedral

[Zn(L^3)(Bipy)(OAc)].H_2O = Octahedral

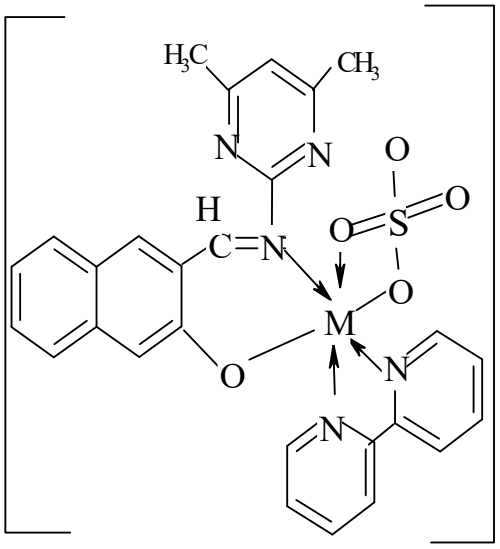

[Fe(L^3)(Bipy)(SO_4)].H_2O = Octahedral

Figure 5.4. Structures of 2-(pyrimidin-2-ylamino)naphthalene-1,4-dione (HL^4) ligand and its metal(II) complexes

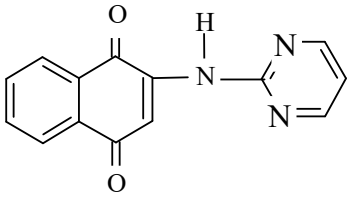

HL^4 Ligand

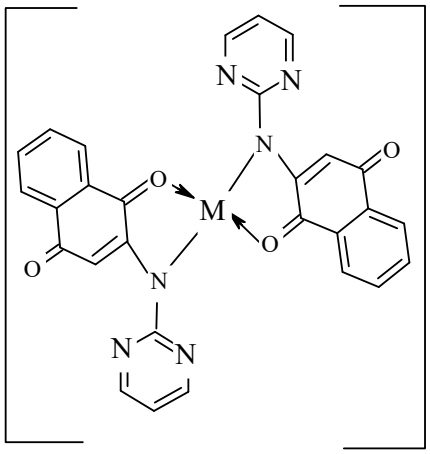

$[Mn(L^4)_2].H_2O$ = Tetrahedral

$[Fe(L^4)_2].2H_2O$ = Tetrahedral

$[Co(L^4)_2].H_2O$ = Tetrahedral

$[Ni(L^4)_2].H_2O$ = Tetrahedral

$[Cu(L^4)_2]$ = Tetrahedral

$[Zn(L^4)_2].H_2O$ = Tetrahedral

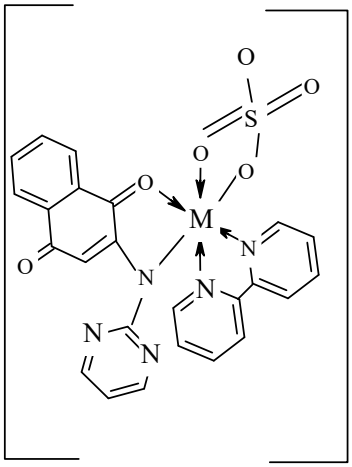

$[Fe(L^4)(Bipy)(SO_4].H_2O$ = Octahedral

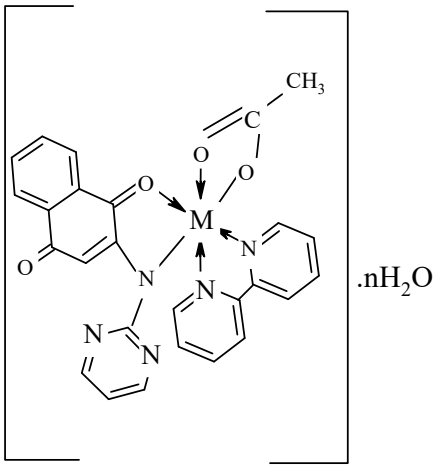

$[Mn(L^4)(Bipy)(OAc)].H_2O$ = Octahedral

$[Co(L^4)(Bipy)(OAc)]$ = Octahedral

$[Ni(L^4)(Bipy)(OAc)].H_2O$ = Octahedral

$[Cu(L^4)(Bipy)(OAc)].H_2O$ = Octahedral

$[Zn(L^4)(Bipy)(OAc)]$ = Octahedral

Figure 5.5. Structures of 2-(4,6-dihydroxypyrimidin-2-ylamino)naphthalene-1,4-dione (HL^5) ligand and its divalent metallic complexes

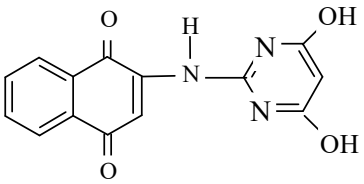

HL^5 Ligand

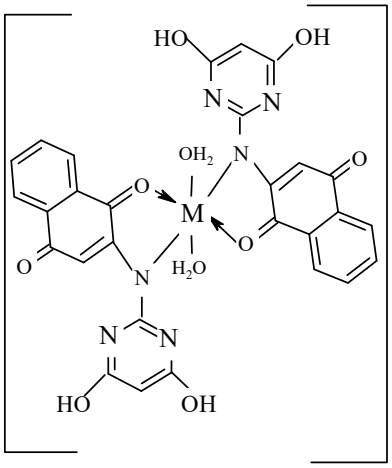

$[Ni(L^5)_2(H_2O)_2]$ = Octahedral

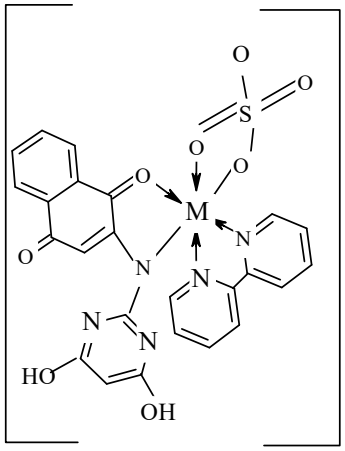

$[Fe(L^5)(Bipy)(SO_4]$ = Octahedral

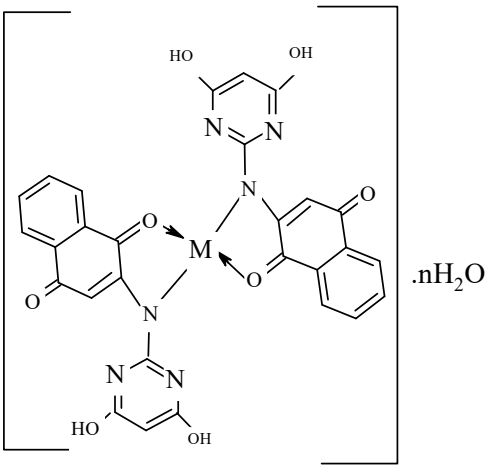

$[Mn(L^5)_2].H_2O$ = Tetrahedral

$[Fe(L^5)_2].2H_2O$ = Tetrahedral

$[Co(L^5)_2].2H_2O$ = Tetrahedral

$[Cu(L^5)_2]$ = Square Planar

$[Zn(L^5)_2].H_2O$ = Tetrahedral

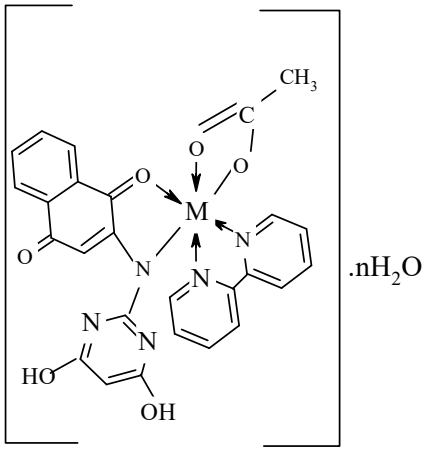

$[Mn(L^5)(Bipy)(OAc)].H_2O$ = Octahedral

$[Co(L^5)(Bipy)(OAc)].2H_2O$ = Octahedral

$[Ni(L^5)(Bipy)(OAc)].H_2O$ = Octahedral

$[Cu(L^5)(Bipy)(OAc)]$ = Octahedral

$[Zn(L^5)(Bipy)(OAc)].H_2O$ = Octahedral

Figure 5.6. Structures of 2-(4,6-dimethylpyrimidin-2-ylamino)naphthalene-1,4-dione (HL^6) and its heteroleptic metal(II) complexes

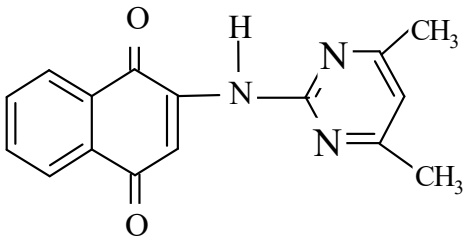

HL^6 Ligand

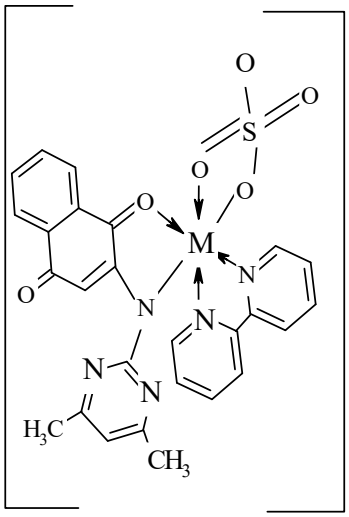

$[Fe(L^6)(Bipy)(SO_4]$ = Octahedral

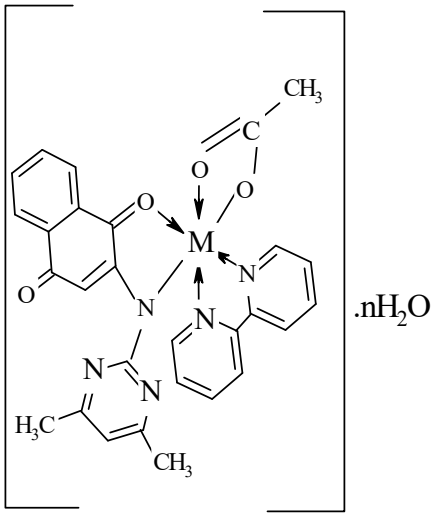

$[Mn(L^6)(Bipy)(OAc)]$ = Octahedral

$[Co(L^6)(Bipy)(OAc)]$ = Octahedral

$[Ni(L^6)(Bipy)(OAc)]$ = Octahedral

$[Cu(L^6)(Bipy)(OAc)].H_2O$ = Octahedral

$[Zn(L^6)(Bipy)(OAc)]$ = Octahedral

CHAPTER SIX

SUMMARY AND RECOMMENDATIONS

6.1 Summary

Six different pyrimidinyl Schiff bases, 3-{[-(pyrimidin-2-yl)imino]methyl} napthalen-2-ol, 3-{[(4,6-dihydroxypyrimidin-2-yl)imino]methyl}napthalen-2-ol, 3-{[(4,6-dimethylpyrimidin-2-yl)imino]methyl}napthalen-2-ol, 2-(pyrimidin-2-ylamino)naphth alene-1,4-dione, 2-(4,6-dihydroxypyrimidin-2-ylamino)naphthalene-1,4-dione and 2-(4,6-dimethylpyrimidin-2-ylamino)naphthalene-1,4-dione were synthesised by the condensation reactions of 2-amino-pyrimidine, 2-amino-4,6-dihydroxypyrimidine and 2-amino-4,6-dimethylpyrimidine with 2-hydroxyl-1-napthaldehyde or 2-hydroxy-1,4-naphthoquinone. The reaction of the synthesised ligands with $FeSO_4.7H_2O$, $Mn(OAc)_2.4H_2O$, $Co(OAc)_2.4H_2O$, $Ni(OAc)_2.4H_2O$, $Cu(OAc)_2.H_2O$ and $Zn(OAc)_2.2H_2O$ salts gave corresponding twenty-four (24) metal(II) complexes and thirty-six (36) heteroleptic metal(II) complexes on further reaction with 2,2'-bipyridine. The synthesised compounds were characterized by elemental (CHN), and percentage metal-analysis, infrared, electronic and ^{1}H- and ^{13}C-nmr spectroscopies, mass spectrometry, magnetic susceptibility and molar conductivity measurements. Additionally, the compounds were assessed for biological possibilities. The antibacterial and antifungal screening of the compounds were carried out against *S. aureus, P. aeruginosa, E. coli, B. cereus, P. mirabilis, K. oxytoca;* and*A. niger, A. flevus* and *R. Stolonifer* respectively. The antioxidant activities of the complexes and their ligands were assessed using ferrous ion chelating and DPPH scavenging assays.

The synthesised compounds on physicochemical basis, were generally non-hygroscopic, stable at room temperature, insoluble in water, fairly soluble in MeOH, EtOH, nitromethane and methylenechloride but reasonably soluble in dimethylformamide and dimethylsulphoxide. The compounds generally exhibited varied melting points distinct from the starting materials confirming coordination of the reactants and purity of the products. The molar conductance values obtained in DMSO were very low (5.03–15.02 $ohm^{-1}cm^2mol^{-1}$) to accommodate dissociation of

the complexes and verifies the electrolytically dilute nature of the metallic compounds. Quantitative analyses further corroborate the molar conductivity values obtained. The complexes with their ligands exhibited various shades of colour (i.e. brown, red, yellow, pink, grey, green and orange) quite different from their precursors. The mass spectra of the Schiff bases gave disintegration pathways, stoichiometric compositions as well as molecular weight of the ligands. The molecular ion signals were in conformity with the microanalysis values and corroborates the proposed empirical formulation for the ligands. The microanalysis further confirmed the formation of the ligands and their corresponding divalent metallic compounds on the basis of relative percentage of carbon, hydrogen, nitrogen and sulfur. Apparently, the elemental analyses results and the percentage metal compositions of the metal(II) complexes indicate good agreement between the experimental and theoretical values obtained and were consistent with the suggested molecular formulas for the metallic compounds.

The NMR spectra of the Schiff bases (HL^1-HL^3) exhibited diagnostic peaks which further affirmed the formation of the ligands. The peak(s) arising from O-H group common of 2-hydroxy-1-napthaldehyde was/were detected in the spectra of the Schiff bases at 10.80-14.52 ppm range while the azomethine proton peak was seen within 8.92-9.55 ppm. On the other hand, the peak(s) arising from O-H group typical of 2-hydroxy-1,4-naphthoquinone was entirely absent in the spectra of HL^4, HL^5 and HL^6 ligands rather a broad-like peak centred at 3.38-4.95 ppm consistent of cyclic C-NH (s, NH) functional group was observed. The N-H signal indicates the ketoimine tautomeric arrangement for the ligands in solution and not its enolimine structure. The naphthalene phenyl protons resonated within the ranges 6.51-8.22 ppm, 7.31-8.903 ppm, 7.83-8.199 ppm, 7.64-7.866 ppm, 7.33-7.590 ppm and 7.209-7.488 ppm while the protons due to naphthoquinone ring were observed at the ranges 6.52-6.77 ppm, 7.33-7.79 ppm and 7.75-7.95 ppm. Likewise, the cyclic hydrogen atoms peaks of the pyrimidine ring were observed around 6.28-7.628 ppm. However, HL^3 and HL^6 ligands with electron donating groups (methyl) showed peaks that were less desheilded than HL^2 and HL^5 ligands bearing the hydroxyl groups (OH). The ^{13}C spectra of the Schiff base ligands displayed peaks that gave credence to the assignment of the proton peaks. The azomethine carbon peak was observed within 141.3-164.1 ppm. The resonance signals consistent of the naphthalene and pyrimidine carbon atoms were

observed at the expected ranges and corroborates assigned structures of the Schiff bases.

The Schiff bases (HL^1, HL^2 and HL^3) in their respective infrared spectrum exhibited characteristic absorption bands at 3389, 3341 and 3441 cm^{-1} due to intra-molecular H-bonding vibrations (νO-H….N) of an enol tautomer which is often observed in Schiff bases containing hydroxyl moieties. The absence of these bands in the spectra of the divalent metallic compounds corroborated coordination of the Schiff bases to the metallic ions through the naphthol oxygen atom. Similarly, the infrared spectra of HL^4, HL^5 and HL^6 ligands had strong bands at 3439, 3584 and 3536 cm^{-1} respectively and were assigned to ν(NH) of a secondary amide. The broadness of the bands in the ligands (HL^4, HL^5 and HL^6) were attributed to intramolecular hydrogen bonding. Furthermore, the sharp to medium hydrogen stretching bands of the aromatic rings, ν(Ar–H), appeared between 3013 and 3001 cm^{-1}in the complexes while the methyl substituted HL^3 and HL^6 ligands and their complexes exhibited medium asymmetric and symmetric stretching vibrations for the alkyl moieties in the region 2929-2913 cm^{-1}. The absorption bands at 1669 cm^{-1}, 1688 cm^{-1} and 1628 cm^{-1} due to the imine moiety in the Schiff bases (HL^1, HL^2 and HL^3) moved to lesser/higher wavenumbers in the metallic compounds to the range 1614-1667 cm^{-1}, confirming participation of the imine nitrogen atom in complexation with the metallic ions. The absorption bands due to C=N and C=C vibrations detected in the Schiff bases were of almost equal intensity in the regions 1688-1669 cm^{-1} and 1651-1625 cm^{-1} but moved to lower/greater wavenumbers by 60–48 cm^{-1}in all the divalent metal compounds. The former indicates involvement of the imine nitrogen atom in coordination with the metallic ions while the latter supports aromatic conjugations and effect of complexation. The C=N stretching vibration appeared as a single band in the spectra of the ligands and remained same in the spectra of the heteroleptic complexes corroborating Fermi resonance in most of the complexes. The ligands, HL^4, HL^5 and HL^6 underwent keto-enol tuatomerism in solution to form C=N during complexation. Similarly, the uncoordinated ν(C=O) stretching vibrations were observed as sharp bands in HL^4-HL^6ligands at 1672, 1682 and 1678 cm^{-1}but moved to lower/higher wavenumbers in the metal(II) complexes corroborating deprotonation and involvement of naphthol *O* atom in coordination. The sharp absorption bands at 1537-1579 cm^{-1}, 1366-1491 cm^{-1} 981-991 cm^{-1} were assigned to ν(C-N) of the aromatic rings, ν(C-C) and δ(C-H)

vibrations. Further confirmation of the enol *O* and imine *N* atoms in complexation to the metallic ions were proved by the presence of novel bands within 400-470 cm^{-1} and 500-590 cm^{-1} due to ν(M-O) and ν(M-N) in the spectra of the metallic compounds. Additionally, geometric isomerism types (cis- and trans-) and pseudo-aromatic nature were confirmed in the symmetrical complexes by the observation of a single or double *ν*C=N bands and a shift of *δ*C-H vibration to higher frequency.

The electronic spectra of the ligands displayed no absorption bands at the visible region but showed two bands at the ranges 26247-28653 and 30030-38759 cm^{-1} arising from n→π∗and π→π∗ transitions. The former band had significant shifts, while the latter nearly persisted unshifted in the spectra of the divalent metallic compounds. These two bands were observed at different wavelengths in the hydroxyl and methyl substituted analogues but shifted to lower/higher energies upon chelations, indicating coordination of the ligands with the metallic ions. Apparently, the electronic spectra of the divalent metallic compounds exhibited various characteristic bands in the visible region and were attributed to *d-d* transitions. On the account of the *d-d* transitions of electrons, four coordinate tetrahedral stereochemistry were entirely attributed to all the symmetrical divalent metallic compounds except $[Cu(L^1)_2]$, $[Cu(L^2)_2]$, $[Cu(L^4)_2]$ and $[Cu(L^5)_2]$; and $[Fe(L^1)_2(H_2O)_2]$ and $[Ni(L^5)_2(H_2O)_2]$ which assumed square planar and octahedral geometries respectively. Similarly, octahedral geometry was also suggested for all the heteroleptic complexes. The ultraviolet spectra of the synthesised complexes displayed two to three bands around 25000-29000 cm^{-1}, 30000-39000 cm^{-1} and 40000-50000 cm^{-1} due to n→π∗,π→π∗ and charge transfer transitions separately.

The geometries assigned to the metal(II) complexes were corroborated by the values acquired from magnetic susceptibility determinations. The obtained magnetic moments of 3.92 B.M and 3.81; 3.91 B.M and 3.74 B.M; and 4.39 B.Mwere corroborative of equilibrium amid low-high spin within six coordinate geometry for $[Co(L^2)(Bipy)(OAc)]$ and $[Co(L^5)(Bipy)(OAc)].2H_2O$ complexes; spin-crossover from high spin to low spin state for $[Fe(L^2)(Bipy)(SO_4)].H_2O$ and $[Fe(L^5)(Bipy)(SO_4)]$ complexes in an octahedral environment; and equilibrium between low spin and high spin of a tetrahedral geometry for $[Mn(L^1)_2].H_2O$ respectively. Similarly, magnetic susceptibility values of 4.41, 4.53, 4.37, 4.29, 3.49, 3.59 and 3.80 B.M were observed for $[Co(L^1)_2].2H_2O$, $[Co(L^2)_2].H_2O$, $[Co(L^4)_2].H_2O$, $[Co(L^5)_2].2H_2O$, $[Ni(L^1)_2].H_2O$,

$[Ni(L^2)_2].H_2O$ and $[Ni(L^4)_2].H_2O$ complexes and were consistent with tetrahedral geometry. The complexes of Mn(II), Fe(II), Co(II) and Ni(II) were generally paramagnetic with effective magnetic moments in the ranges 5.54-6.02, 4.97-5.25, 4.65-5.14 and 2.77-3.39 B.M. The synthesised divalent copper complexes exhibited mononuclearity having magnetic moment data of 1.75-2.21 B.M, while the Zn(II) complexes were diamagnetic in nature. Observed magnetic moments of 0.09-0.43 B.M. were indicative of diamagnetism for the synthesised zinc(II) complexes and corroborates their geometry.

The results of the antimicrobial actions against *S. aureus, P. aeruginosa, E. coli, B. cereus, P. mirabilis, K. oxytocaA. niger, A. flevus and R. Stolonifer* indicate that the synthesised compounds had adequate to excellent inhibitory zones. All the microorganisms were inhibited by the ligands (HL^1-HL^6) with zones of inhibition ranged from 5.5mm to 26.0 mm, exception of *E. coli* and *P. mirabilis*; *P. aeruginosa* and *Rhizopus stolonifer* which showed resistance to HL^1, HL^5 and HL^3 ligands. The activities of the ligands against the tested organisms may be ascribed to the presence of the heteroatoms and –C=N- moiety which are known to enhance antimicrobial activities. The divalent metallic compounds with inhibitory zones in 6.5–9.0 mm range were expectedly more susceptible than the ligands. Additionally, the heteroleptic divalent metallic compounds were more effective and active than their precursor complexes. An explanation to the increased actions of the divalent metallic compounds could be credited to enhanced lipophilicity, a consequence of chelation which accounts for reduction in the polarity of metallic ions as well as increases delocalization of pii-electron over the entire chelate ring. The positive standard drug, ciprofloxacin and fluconazole were active against all the organisms. It is important to note here that the compounds studied were structurally different from the standard drugs; nevertheless, most of them exhibited higher/comparable activities to the standard drugs, verifying their potential effectiveness as broad-spectrum antimicrobial agents. Similarly, the obtained values for the antioxidant actions of the ligands and the corresponding divalent metallic compounds were generally comparable/higher to that of the standard, ascorbic acid suggesting a similar pathway for their antioxidant activities and proving their potentials as probable anticancer agents.

6.2 Recommendations for further research work

The six novel chelating ligands, twenty-four symmetrical metal(II) complexes and thirty-six heteroleptic complexes were successfully synthesised and studied. However, research is always a frontier of knowledge; hence the need to suggest the following in continuation to the research works.

1. Variable temperature magnetic susceptibility determinations should be carried out on the metallic compounds to establish their true high- low spin equilibria.
2. Complexes of 4*d*, 5*d* and 6*d* metal ions should be synthesised and characterised.
3. Isolation of single crystals of the compounds should be carried out.
4. Electrochemical and corrosion behavior studies of the complexes should be carried out.
5. The metal complexes should be applied/studied as electrochemical sensors, chromatographic instruments and optical devices.
6. X-ray determination of the complexes should be done to confirm their structures.

REFERENCES

Abbas, K. A. Salman, S. R. Kana'n, S.M. and Fatafteh, Z.A. 1996. *Can. J. Appl. Chem. Spectrosc.* 41.5: 119.

Abdel-Nasser, M. A. A. and Hoda, A. B. 2013. Synthesis, spectral properties and potentiometric studies on some metal Schiff base complexes derived from 4-chlorophenyl-2-aminothiazole. *International Journal Electrochem. Science* 8: 11860-11876.

Abd El-Wahed, M. G., Refat, M. S. and El-Megharbel, S. M. 2008. "Metal complexes of antiuralethic drug: Synthesis, spectroscopic characterization and thermal study on allopurinol complexes," *Journal of Molecular Structure* 888.1–3:416–429.

Abd El-Wahab, Z. H. 2008. "Complexation of 4-amino-1,3dimethyl-2,6 pyrimidine-dione derivatives with cobalt(II) and nickel(II) ions: synthesis, spectral, thermal and antimicrobial studies," *Journal of Coordination Chemistry* 61.11:1696–1709.

Abdou, S. E., Moshira, M. A., El-Waheed, M. A. W. and Nahla, A. E. A. 2015. Synthesis, characterization, and anticancer activity of new metal complexes derived from 2-hydroxy-3-(hydroxyimino)-4-oxopentan-2-ylidene)benzohydrazide.*Bioinorganic Chemistry and Applications* 2015.

Abdullah, M. A. and Salman, A. K. 2010. Synthesis of a novel Schiff base from 5-amino-3,4-dimethyl isoxazole and 2-hydroxy-1-naphthaldehyde. Ph.D Thesis. Department of Chemistry, University of Ibadan viii+23

Abdullah, M. A.and Khadija, O. B. 2007. Synthesis of some new anils: Reaction of 2-hydroxy-benzaldehyde and 2-hydroxynaphthaldehyde with 2-aminopyridene and 2-aminopyrazine *Molecules* 12:1796-1804.

Abdul, R. 2005. Synthesis and biological studies of Schiff base compounds and their transition metal complexes. Ph.D thesis submitted to the Behuadd in Zakrya University, Multan Pakiastan (unpublished).

Abu-el, S. M. W. and Issa, R. M. 1989. "The preparation of a series of Mn(II) complexes of the type [Mn(SB)SO_2]," *Bulletin de la Soci′et′e Chimique de France* 5:595–598.

Abuo–Melha, K. S. and Faruk, H. 2008. Bimetallic complexes of Schiff base bis-[4-hydroxy coumarin-3-yl]-$^{1}N_{1}{}^{5}N$ thiocarbohydrazone as a potentially diabasic pentadendate ligand: synthesis, spectral, and antimicrobial properties. *J. Iran. Chem. Soc.* 5.1:122-134.

Agwara, M. O., Ndifon, P. T., Ndosiri, N. B., Paboudam, A. G., Yufanyi, D. M., and Mohamadou, A. 2010 "Synthesis, characterization and antimicrobial Activities

of cobalt(II), copper(II) and zinc(II) mixed-ligand complexes containing 1,10-phenanthroline and 2,2'-bipyridine" Bull. Chem. Soc. Ethiop., 24 (3): 383-389.

Agarwal, N. L. and Mital, R. L. 1976. Synthesis of 6-anilino-12H-benzo[a]phenothia zin-5-ols. *Ind. J. Chem*. 14:381-382.

Ahmed, S. A., Ali, O. M., Adnan, A. H., AL-juboori, I. K. and Emad, M. O. 2009. Synthesis and characterization of some Schiff bases (derived from thiazole) and their complexes with Co(II), Ni(II) and Cu(II). *Journal of Kirkuk University – Scientific Studies* 4.2:2009.

Ahmed, A. A., Yasmien, K. A., Heba, H. I. and Ali. A. A. 2002. Antioxidant, antimicrobial, and theoretical studies of the thiosemicarbazone derivative Schiff base 2-(2-imino-1-methyl imidazolidin-4-ylidene) hydrazine carbothioamide (IMHC). *Org Med ChemLett* 2.4.

Ajibade, P. A. and Zulu, N.H. 2011. Metal complexes of diisopropylthiourea: Synthesis, characterization and antibacterial studies. *International Journal of Molecular Science* 12:7186-7198.

Ajibade, P. A. and Idemudia, O. G. 2013. Synthesis, characterization and antibacterial studies of Pd(II) and Pt(II) complexes of some diaminopyrimidine derivatives. *Bioinorg. Chem. Appl.* 2013:1–8.

Alam, M. S. and Lee, D. U. 2012. Synthesis, molecular structure and antioxidant activity of (E)-4-[Benzylideneamino]-1,5-dimethyl-2-phenyl-1H-pyrazol-3(2H)-one, a Schiff base ligand of 4-aminoantipyrine. *J. Chem. Crystallogr.* 42:93–102.

Ali, A. K; Kamellia, N. and Zolfaghar, R. 2005. Synthesis, characterization and study of the use of cobalt(II) Schiff base complexes as catalysts for the oxidation of styrene by molecular oxygen. *Molecules;* 10:302-311.

Aliyu, H. N., Kurawa, M. A. and Sani, U. 2013a. Characterization of Schiff base derived from 2-hydroxo-1-naphthaldehyde and Ethylenediammine and its Copper (II) Complex by Potentiometric and Spectrophotometric Methods. *ChemSearch Journal.* 5.1:12-20, June, 2014

Aliyu, H. N. and Zayyan, R. S. 2013. Synthesis, characterization of biologically active N, N^{I}-bis(4Benzeneazosalicylidene)-o-phenylenediiaminattocobalt(II) complex. *Bayero Journal of Pure and Applied Sciences.* 6.2:127-131.

Al-Amiery, A. A., Kadhum, A. A. H. and Mohammed, A. B. 2012. "Antifungal and antioxidant activities of pyrolidone thiosemicarbazone complexes," *Bioinorganic Chemistry and Applications*, 6.2012.

Al-Masoudi, W. A., Mohammed, T. and Hama, A. A. 2015. Synthesis, characterization and pharmacological study of new Schiff base derived from amoxicillin drug. *International Research Journal of Pharmac.* 6:6.

Anouar, E., Calliste, C., Kosinova, P., di-Meo, F., Duroux, J., Champavier, Y., Marakchi, K. and Trouillas, P. 2009. Free radical scavenging properties of

guaiacol oligomers: A combined experimental and quantum study of the guaiacyl-moiety role. *J. Phys. Chem.* 113:13881–13891.

Anacona, J. R., Johan, C. and Ovidio, A. A. 2013. Synthesis, spectroscopic, and magnetic studies of mono- and polynuclear Schiff base metal complexes containing salicylidene-cefotaxime ligand. *International Journal of Inorganic Chemistry* 2013.

Antonov, L., Fabian, W. M. F., Nedeltcheva, D. and Kamounah, F. S. 2000. *J. Chem. Soc., Perkin Trans.* 2.6:1173-1175.

Apak, R., Kubilay, G. O., Zyu¨rek, M. and Saliha, E. C. 2008. Mechanism of antioxidant capacity assays and the CUPRAC (cupric ion reducing antioxidant capacity) assay. *Microchim Acta* 160:413–419.

Atmaram, K. M. and Kirian, V. M. 2011. Synthesis, characterization and antimicrobial activity of mixed Schiff base ligand complexes of transition metal(II) ions. *Intl. J. ChemTech Research* 3.1:477-482.

Aysel, G. and Nilgun, K. 2003. Synthesis, characterisation and primary antituberculosis activity evaluation of 4-(3-coumarinyl)-3-benzyl-4-thiazolin-2-one benzylidenehydrazones. *Turk. J. Chem.* 27:545-551.

Bagihalli, G. B., Patil, S. A. and Badami, P. S. 2009. Synthesis, physicochemical investigation and biological studies of Zinc(II) complexes with 1,2,4-triazole Schiff bases. *Journal of the Iranian Chemical Society* 6.2:259-270.

Bassett, J., Denney, R. C., Jeffery, G. H. and Mendham, J. 1978. *Vogel's textbook of quantitative inorganic analysis*. 4th Ed, ELBS: London.

Befta, 1985. Unsymmetrical 1:2 chromium complex dyes, Fabio (to Ciba Geigy AG). *Eur Chem Abstr,* 103:216910.

Bernadette, S. C., Denise, A. E., Kevin, K. M. M., Mary, M. A., Bhumika, T. and Maureen, W. 2007. Synthesis, characterization and antimicrobial activity of Cu(II) and Mn(II) complexes of coumarin-6,7-dioxyacetic acid ($cdoaH_2$) and 4-methylcoumarin-6,7-dioxyacetic acid (4-$MecdoaH_2$). *J. Inorg. Chem.*101.8:1108-1119.

Berners, S. J. 2007. Metals in medicine. Keynote Lectures.: the mitochondrial cell death pathway as a target for gold and other metalbased antitumor compounds. *J Biol Inorg Chem*. 12:S7–S52.

Birsen, T., Mevlut, E., Pelinkelicen, D. and Rumeysa, D. 1999. *Farmaco II,* 54.9:588-593.

Blake, A. B. and Cotton, F. A.(1964). "Octahedral and tetrahedral complexes of Co(II)" *Inorganic Chemistry* 3:5-6.

Brown, D. J., Evans, R. F., Cowden, W. B. and Fenn, M. D. 1990. *The pyrimidines*. New York: John Wiley and Sons.

Brown, D. J., Evans, R. F., Cowden, W. B. and Fenn, M. D. 1994. *The pyrimidines*. New York: John Wiley and Sons.

Brown, W. and Smith, D. H. 1990. *Enzyme chemistry: impact and applications*. Chapmann and Hall: London.

Cater, A. P., Clemons, W. M., Brodersen, D. E., Morgan-Warren, R. I., Wimberly, B. T. and Ramakrishnan, V. 2000. Functional insights from the structure of the 30S ribosomal subunit and its interactions with antibiotics. *Nature* 407.6802:340-348.

Cesar, G. F. 2005. Relevance, essentiality and toxicity of trace elements in human health. *Molecular Aspects of Medicine* 26:235-244.

Cesar, S., Maria, P. and Cristian. T. 2008. Biologically active transition metal chelates with a 2-thiophenecarboxaldehyde-derived Schiff base: Synthesis, characterization and antibacterial properties. *Turkish Journal of Chemistry* 32:487-493.

Ceyhan, G., Çelik, C., Urus, S., Demirtas, M., Elmastas, M. and Tümer, M. 2011. antioxidant, electrochemical, thermal, antimicrobial and alkane oxidation properties of tridentate Schiff base ligands and their metal complexes. *Spectrochim. Acta A Mol. Biomol.Spectr*. 81:184-198.

Chakraborty, H., Paul, N. and Rahman, M. L. 1994. Catalytic activities of Schiff bases aquo complexes of Cu(II) in the hydrolysis of aminoacid esters, *Trans Met Chem (Lond)* 19:524-526.

Chakraborty, A. K., Bhagat, S. and Rudrawar, S. (2004). Magnesium perchlorate as an efficient catalyst for the synthesis of imines and phenylhydrazones. *Tetrahedron Letters* 45.41:7641–7644.

Cheng, L., Tang, J., Luo, H., Jin, X., Dai, F., Yang, J., Qian, Y., Li, X. and Zhou, B. 2010. Antioxidant and antiproliferative activities of hydroxyl-substituted Schiff bases, *Bioorg. Med. Chem. Lett.* 20:2417-2420.

Chew, K. B., Tarafder, T. H., Crouse, K. A., Ali, A. M., Yamm, B. and Fun, H. K. 2004. *Polyhedron* 23:1385.

Chohan, Z. H. 2001. Synthesis, characterization and biological properties of bivalent transition metal complexes of Co(II), Cu(II), Ni(II), and Zn(II) with some acylhydrazine derived from furanyl and thienyl ONO and SNO donor Schiff base ligands. *Synth. React. Inorg. Met.-org. Chem.* 31.1:1-6.

Clark, J., Shahhet, M. J., Korakas, D. and Varvounis, G. 1993. Synthesis of thieno[2,3-*d*]pyrimidines from 4,6-dichloropyrimidine-5-carbaldehydes. *J. Heterocyclic Chem.* 30:1065-1072.

Cotton, F. A. and Wilkinson, G. 1966. *Advanced Inorganic Chemistry: A comprehensive text*. 2nd Ed. Wilet Eastern Limited: New Delhi.

Cotton, F. A. and Wlkinson, G. 1972. *Advanced Inorganic Chemistry: A comprehensive text.* 3rd ed. Wilet Eastern Limited: New Delhi.

Cotton, F. A. and Wilkinson, G. 1978. *Advanced Inorganic Chemistry.* Wiley Eastern Limited: New Delhi.

Cotton, F. A., Wlkinson, G., Murillo, C. A. and Bochmann, M. 1999. *Advanced Inorganic Chemistry*. 6th.Ed. John wiley: New York.

Crystal, Y. W., Sathiyanarayanan, V., Sundar, M. and Easwaramoorthy, D. 2015. B-Tolyl alanine derived Schiff base complexes: Synthesis, characterization and antimicrobial assessment. *Journal of Pharmacy, Sciences and Research.* 7.1:25-32.

Day, M. C.(jr) and Selbin, J. (1969). *Theoretical Inorganic Chemistry*. 2nd Ed. Litton Educational publishing.

Dekkers, J., Van-Doornen, L. and Kemper, H. 1996. "The role of antioxidant vitamins and enzymes in the prevention of exercise-induced muscle damage". *Sports Med*21.3:213–38.

Desiree, C. S., Sabrina, B. F., Laura, N. C., David, R. R., Miriam, S. M., Myna, N., Philip, J. R., Vitor, F. F. and Celia, R. S. G. 2013. Biological evaluation of hydroxynaphthoquinones as anti-malarials. *Malaria Journal* 12:234-239.

Dressman, J. B. and Reppas, C. 2000. *In vitro-in vivo* correlations for lipophilic, poorly water-soluble drugs. *European Journal of Pharmaceutical Sciences.* 11.2:73–80.

Dixit, N. S. and Patel, C. C. 1979. Amine exchange reactions of mixed ligand nickel(II) complexes of Isonitroso-β-ketoimines. *Indian Journal of Chemistry* 17.2:1789-191.

Durot, S., Policar, C., Pelosi, G., Bisceglie, F., Mallah, T. and Mahyt, J. P. 2003. "Structural and magnetic properties of carboxylatobridged manganese(II) complexes involving tetradentate ligands: Discrete complex and 1D polymers. Dependence of J on the nature of the carboxylato bridge," *Inorganic Chemistry*, 42.24:8072–8080.

Earnshew, A. 1980. *Introduction to Magnetochemistry*. Academic Press, London: UK.

Efimova, G. A. and Efros, L. S. 1967. Heterocyclic derivatives of substituted 1,4-naphtho-quinones IV Condensation of 2,3-diamino-1,4-naphthoquinone and its monomethyl derivative with 1,3-diketones. *Zhurnal Organicheskoi Khim* 3:162-8.

Ejidike, I. P. and Ajibade, P. A. 2015. "Transition metal complexes of symmetrical and asymmetrical Schiff bases as antibacterial, antifungal, antioxidant, and

anticancer agents: progress and prospects," *Reviews in Inorganic Chemistry* 35.4:191–224

Elham, S. A. 2010. Synthesis and characterization of mono-and binuclear metal complexes of a new fluorescent dye derived from 2-hydroxyl-I-naphthaldehyde and 7-amino-4-methylcoumarin. *JKAU Sci.* 22.2:101-116.

El-Hossini, M. S., Fadda, A. A. and Khodeir, M. N. 1991. Synthesis, therapeutic and pharmacological activitiesof pyrimidine and its derivatives. *Cheminform 22.12:25-27.*

El-Tabl, A. S. 2002. Synthesis and physico-chemical studies on cobalt(II), nickel(II) and copper(II) complexes of benzidine diacetyloxime. *Transition Met. Chem.* 27:166-170.

Elzahany, E. A., Khaled, H. H., Safaa, K. H., Khalil, M and Nabil, S. Y. 2008. Synthesis, characterization and biological activity of some transition metal complexes with Schiff bases derived 2-fromylindole, sahcylialdehyde and N-amino-Rhodanime. *Austrlian Journal of Basic and Applied Science* 2.2:210-220.

Figgis, B. N. and Lewis, J. 1964. Transition metal complexes. *Prog. Inorg. Chem.*6:207.

Figgis, B. N. 1966. *Introduction to ligand fields*. Interscience Publishers, New York: USA.

Gaber, M. Mabrouk , H. E. Al-Shihry, S. 2001. Complexing behaviour of naphthylidenesulfa methazine Schiff base ligand towards some metal ions. *Egyptian J. Chem*. 44:191-200.

Geary, W. J. 1971. The use of conductivity measurements in organic solvents for the characterization of coordination compounds. *Coord. Chem. Rev.* 7:81.

Gladiola, T., Mihai, N. and Lenuta, P. 2013. Synthesis and biological evaluation of some new Schiff bases and their Cu(II) and Mg(II) complexes. *African Journal of Pharmacy and Pharmacology* 7.20:1225-1230.

Gomathi, V., Selvameena, R., Subbalakshmi, R. and Valarmathy, G. 2013. Synthesis, spectral characterization and antimicrobial screening of Mn(II) and Zn(II) complexes derived from (E)-1-((*p*-tolylimino)methyl)naphthalene-2-ol. *Oriental Journal of Chemistry.* 29.2:533-538.

Gopalakrishnan, M., Sureshkumar, P., Kanagarajan, V. and Thanusu, J. 2007. New environmentally-friendly solvent-free synthesis of imines using calcium oxide under microwave irradiation. *Research Chemistry Intermed.* 33.6:541–548.

Grace E. I., Isaac T. I. and Samson, O. O. 2015. Antimicrobial studies of synthesised Zinc(II) Schiff base complexes of L-arginine-2-hydroxy-1-naphthaldehyde and glycine-2-hydroxy-1-naphthaldehyde. *International Journal of Scientific & Technology Research* 4:8.

Halli, M. B., Shashidhar, S. and Quresi, Z. S. 2004. Synthesis, spectral studies and biological activity of metal complexes of benzofuran thiosemicarazides'. *Synthesis and Reactivity in Inorganic and metal-organic Chemistry.* 34.10:1755-1768.

Hoffman, R. V. 2004. *Organic Chemistry: an Intermediate Text*. 2nd Edition, John Wiley and Sons Inc.

Hatice, G. S., Tugba, T. T., Feyza, Y., Ismet, B. and Mehmet, S. 2015. Synthesis, characterization, biological studies, and molecular modeling of mixed ligand bivalent metal complexes of Schiff bases based on *N*-aminopyrimidine-2-one/2-thione. *Turkish Journal of Chemistry* 39:497-509.

Houghton, M. 2009. *The American Heritage Dictionary of the English Language*. 4th Ed. Houghton Mifflin Company.

Huang, Z. Qu, S. and Feng, Y. 1998. The antibacterial activity of o-vanilline glucosamine Schiff base Zn complex. *Huaxue Yanjiu Yu Yingyong* 10:595-599.

Hughes, L., Covian, R., Gribble, G. and Trumpower, B. 2010. Probing binding determinants in center P of the cytochrome bc(1) complex using novel hydroxy-naphthoquinones. *Biochim Biophys Acta* 1797:38–43.

Ibrahim, F., Nassar, A. and El assaly, S. 2011. Synthesis, reactivity and antitumor activity of some new pyrazolo[3,4-d] pyrimidine and their triazole derivatives *Der pharma Chemica* 3.1:229-238.

Idemudia, O. G. and Ajibade, P. A. 2010. Antibacterial activity of metal complexes of antifolate drug pyrimethamine. *Afr. J. Biotechnol*. 9:4885-4889.

Indira, K. P. 2005. Molecular mechanisms involving free radical reactions of antioxidants and radioprotectors. *Founder's day special issue* 1-6.

Iniama, G. E., Iorkpiligh, I. T. and Olanrele, S. O. 2015. Antimicrobial studies of synthesised Zinc(II) Schiff base complexes of L-arginine-2-hydroxy-1-naphthaldehyde and glycine-2-hydroxy-1-naphthaldehyde. *International Journal of Scientific and Technology Research.* 4.8:24-27.

Ikechukwu, P. E. and Peter, A. A. 2015. Synthesis, characterization, antioxidant, and antibacterial studies of some metal(II) complexes of tetradentate Schiff base ligand:(4E)-4-[(2-{(E)-[1-(2,4-Dihydroxyphenyl)ethylidene]amino}ethyl) imino] pentan-2-one.*Bioinorganic Chemistry and Applications* 1-9.

Jachak, M; Mittelbach, M. and Junek, H. 1993. Cyanoacetaldehyde-New synthetic applications of an old compound syntheses with nitriles, XCI. *Heterocyclic*, 124.2:199–207

Jayabalakrishnan, C. and Natarajan, K. 2002. "Ruthenium(II) carbonyl complexes with tridentate Schiff bases and their antibacterial activity," *Transition Metal Chemistry* 27.1: 75–79.

Jencks, W.P. 1964. Mechanism and catalysis of simple carbonyl group reactions. *Prog. Phys.Org. Chem*. 2: 63.

Jeremiah, J. S., David, H. T., Carola, S. V., Jorg, S., Karsten, M. and Jeremy, M. S. Spin crossover in a four-coordinate iron(II) complex. *Journal of American Chemical Society* 1-4.

Jignesh, H. P., Rajendra, N. J. and Kalpesh, J. G. 2014. Spectral characterization and biological evaluation of Schiff bases and their mixed ligand metal complexes derived from 4,6-diacetylresorcinol. *Journal of Saudi Chemical Society* 18:190-199.

Joshi, K. R., Rojivadiya, A. J. and Pandya, J. H. 2014. Synthesis and spectroscopic and antimicrobial studies of Schiff base metal complexes derived from 2-hydroxy-3-methoxy-5-nitrobenzaldehyde. *International Journal of Inorganic Chemistry* 2014.

Ju´ lio, C. C. F., Andre, L. F. S., Amanda, B, B., Angelina, M. F., Jaqueline, R. B., Caio, M. P. S., Rose, M. C., Paulo, C. V., Joa˜o, B. F. and Ma´ rcia, R. C. 2014. Copper(II) and 2,2[I]-bipyridinecomplexation improves chemopreventive effects of naringenin against breast tumor cells. www.plosone.org. 9:9.

Julija, M. S., Marijana, V. and Dra`en, V. T. 2006. NMR spectroscopy of 2-hydroxy-1-naphthylidene Schiff bases with chloro and hydroxy substituted aniline moiety. *Croatica Chemica Acta Ccacaa*79.3:489-495.

Kamalakannan, P. and Venkappayya, D. 2002. Spectral, thermal, and antimicrobial studies on the copper(II), zinc(II), cadmium(II), and mercury(II) chelates of a new antimetabolite–5-dimethylaminomethyl-2-thiouracil. *Russian Journal of Coordination Chemistry.* 28:423–433.

Kalsi, P. S. 2004. *Spectroscopy of organic compounds*. 6th Edition. New age International publishers: India 71-7249.

Ketan S. P., Jiten, C. P., Hitesh, R. D., Vishal, K. P. and Kanuprasad, D. P. 2012. Synthesis of Cu(II), Ni(II), Co(II), and Mn(II) complexes with ciprofloxacin and their evaluation of antimicrobial, antioxidant and anti-tubercular activity. *Open Journal of Metal* 2:49-59

Khalil, S. M. E., Seleem, H. S., El-Shetary, B. A. and Shebl, M. 2002. "Mono- and bi-nuclear metal complexes of schiff-base hydrazone (ONN) derived from o-hydroxyacetophenone and 2-amino-4-hydrazino-6-methyl pyrimidine," *Journal of Coordination Chemistry*, 55.8: 883–899.

Kiran, S., Yogender, K., Parvesh, P., Chetan, S. and Kamal, R. A. 2012. Thermal, spectral, fluorescence, and antimicrobial studies of cobalt, nickel, and zinc

complexes derived from 4-[(5-bromo-thiophen-2-ylmethylene)-amino]-3-mercapto-6-methyl-5-oxo-[1,2,4]triazine. *International Journal of Inorganic Chemistry* 2012.

Koch, A. 2003. Bacterial wall as target for attack, past, present and future research. *Clin. Microbial Rev.* 16.14:673-68.

Kolawole, G. A. 1979. Synthesis and characterization of Schiff base complexes of oxovanadium (IV). Ph.D Thesis. Department of Chemistry, University of Ibadan xii+42.

Kuruba, S. and Nabiya, S. M. 2014. Synthesis, spectroscopic characterization, and biological evaluation studies of 5-bromo-3-(((hydroxy-2-methylquinolin-7-yl)methylene)hydrazono)indolin-2-one and its metal(II) complexes. *Bioinorganic Chemistry and Applications* 2014.

Kumar, M. and Arabinda, K. S. 1994. Synthesis and characterization of Mn^{2+}, Fe^{2+}, Co^{2+} and Ni^{2+} complexes of Schiff bases derived from phenylene diamines and 3-carboxaldehyde. *Asian J. Chem.* 6.4:782-788.

Kumar, S. S. L., Oblennavar, K., Mohammedshafi, A. P. and Jagannath, C. K. 2009. Synthesis, characterization and antimicrobial properties of Schiff bases derived from condensation of 8-formly-7-hydroxy-4-methyl coumarin and substituted triazole derivatives. *E-Journal of Chem.* 6.S1:239-246.

Kumar, K. S., Kanth, A. V., Reddy, K. T. and Omprakash, G. 2011. Synthesis and characterization of some novel pyrimidines via aldol condensation. *J. Chem. Pharm. Res*. 3.5: 234-252.

Kumar, S. T. 2012. Biological applications of Schiff base and its metal complexes-A Review. *International Journal of Science and Research* 3:9.

Kumbhar, A. S., Padhye, S. B. and Jitender, K. R. K. 1997. Naturally occurring hydroxy napthquinones and their iron complexes as modulators of radiation induced lipid peroxidation in synaptosomes. *Metal-Based Drugs* 4: 279-285.

Laxmi, K., Pranya, V. J., Tapan, K. D., Sanjima, P., Milind, N., Thomas, W., Vedavati, G.P., Badireenath, V.K. and Sunita, S. 2014. Reaction between lawsone and aminophenol derivatives: synthesis, characterization, molecular structures and antiproliferative activity. *J. Mol. Struct*. 1075:397–405.

Lashanizadegan, M. and Boghaei, D. M. 2001. Template synthesis and x-ray structure determination of unsymmetrical tetradentate schiff base complexes of nickel(II) and copper(II). Synthesis and Reactivity in Inorganic and Metal-Organic Chemistry. 31.8:1519-1529

Lee, J. D. 1999. *Concise Inorganic Chemistry*: 5th Ed. Blackwell Science Ltd, Oxford: London.

Leopoldini, M., Russo, N. and Toscano, M. 2011. The molecular basis of working mechanism of natural polyphenolic antioxidants. *Food Chem.* 125:288–306.

Lever, A. B. P. 1984. *Inorganic Electronic Spectroscopy.* Elsevier publishers, Amsterdam: The Netherlands.

Lever, A. B. P. 1968. "Editorial note," *Coordination Chemistry Reviews* 3.1:1.

Lever, A. B. P**.** 1980. *Inorganic Electronic spectroscopy*. 4th Ed. Elsevier publishing, Amsterdam: The Netherlands.

Lever, A. B. P. 1986. *Inorganic Electronic spectroscopy*. Elsevier publishing, London: New York.

Liu, Y. and Yang, Z. 2009. Crystal structures, antioxidation and DNA binding properties of Eu(II) complexes with Schiff base ligands derived from 8-hydroxyquinoline-2-carboxyaldehyde and three aroylhyrazines. *J. Inorg. Bio. Chem.* 103:1014-1022.

Look, G. C., Murphy, M. M., Campbell, D. A. and Gallop, M. A. 1995. Trimethylorthoformate: A mild and effective dehydrating reagent for solution and solid phase imine formation. *Tetrahedron Letters.* 36.17: 2937–2940.

Lopes, J. N. C., Johnson, A. W., Grove, J. F. and Bulhoes, M. S. 1977. Synthesis of 2-amino-1,4-napthoquinone derivatives and the evaluation of their larvicidal and molluscidal activities. *Ciencia e Cultura* 29:1145-1149.

Love, B. E. and Ren, J. 1993. Synthesis of sterically hindered imines. *Journal of Organic Chemistry* 58.20: 5556–5557.

Lucumi, E., Darling, C., Jo, H., Napper, A. D., Chandramohanadas, R. and Fisher, N. 2010. Discovery of potent small-molecule inhibitors of multidrug-resistant Plasmodium falciparum using a novel miniaturized highthroughput luciferase-based assay. *Antimicrobial Agents Chemother* 54:3597-604.

Mahasin, A., Sahar, I. and Abd Mousa, S. 2015. Synthesis, characterization and theoretical study of some mixed-ligand complexes of 2-quinoline carboxylic acid and 4,4′ -dimethyl,2,2′-bipyridyl with some transition metal ions. *Journal of Al-Nahrain University* 18: 28-38.

Marjan, E., Shohreh, M., Behnam, D. B., Salimeh, A., Ali, G., Seyed, A. A.and Farzad, K. 2015. Synthesis and antiplatelet aggregation activity evaluation of some 2-aminopyrimidine and 2-substituted-4,6-diaminopyrimidine derivatives. *Iranian Journal of Pharmaceutical Research* 14.2: 417-424.

Masuda, K. 1987. Isolation of antimicrobial 5,8-dihydroxy-2,3-dimethoxy-6,7-methylenedioxy-1,4-napthoquinone and its isomers from Tritonia crocosmaeflora (Iridaceae). *Eur Pat Appl.* 13.

Mehabaw, G. D., Raju, V. J. T. and Negussie, R. 2002. Synthesis and characterization of some metal complexes of a Schiff base derived from ninhydrin and ,l-alanine. *Bull. Chem. Soc. Ethiop*. 16: 53-64.

Melaku, U., Clive, E. W. and Habtamon, F. 2005. Content of zinc, iron, calcium and their absorption inhibitors in foods commonly consumed in Enthiopia. *J. Food composite Anal.* 18:803-817.

Mendu, P., Pragathi, J. and Kumari. G. C. 2011. Synthesis, spectral characterization, molecular modeling and biological activity of first row transition metal complexes with Schiff base ligand derived from chromone-3-carbaldehyde and o-amino benzoic acid. *J. Chem. Pharm. Res.* 3.4:602-613

Mennicke, W, and Westphal. *Mixtures of 1:2 chromium complex dyes. Inorganic Chemistry*. 2nd Ed. Sunders College Publishing: Indian.

Michael, H. C. 2011. Bacteria: Encyclopedia of earth .Eds. Sidney, D. and Devland, C. J. National Council for Science and the Environment. Washington DC.

Mishra, A. P. and Monika, S. 2008. "Synthesis, structural and biological studies of Schiff bases and their metal complexes. *Hindawi publishing corporation metal based drugs* 2008.

Mittal, P. and Uma, V. 2010. Synthesis, spectroscopic and cytotoxic studies of biologically active new Co(II), Ni (II), Cu (II) and Mn (II) complexes of Schiff base hydrazones. *Pelagia Research Library*:*Der Chemica Sinica* 1.3: 124-137

Moamen, S. R., El-Deen, I, M., Mohamed, A. Z., Abdel, M. A, A. and Mohamed, I. K. 2013. Spectroscopic, structural and electrical conductivity studies of Co(II), Ni(II) and Cu(II) complexes derived from 4-acetylpyridine with thiosemicarbazide. *Int. J. Electrochem. Sci.* 8: 9894–9917.

Mohammed, N. I. and Salah, E. A. S. 2007. Synthesis, characterization and use of Schiff bases as fluorimetric analytical reagents. 4.4:531-535.

Mohamed, G. G., Omar, M. M. and Hindy, A. M. M. 2005. "Synthesis, characterization and biological activity of some transition metals with Schiff base derived from 2-thiophene carboxaldehyde and aminobenzoic acid," *Spectrochimica Acta Part A:Molecular and Biomolecular Spectroscopy* 62:1140–1150.

Mohammed, K. K., Shah, Z., Uddin, A. V., Khan, M., Taha, M., Rahim, F., Ali, S., Ambreen, N., Perveen, S. and Iqbal, Choudhary, M. 2012. 2,4,6-Trichlorophenylhydrazine Schiff bases as DPPH radical and super oxide anion scavengers. *Med. Chem.* 8:452–461.

Nejo, A. A., Kolawole, G. A., Opoku, A. R., Wolowska, J. and Brien, P. O. 2009a. Synthesis, characterization and preliminary Insulin-enhancing studies of symmetrical tetradentate Schiff base complexes of oxovanadium(IV). *Inorganica Chimica Acta.*362:3993-4001.

Nejo, A. A., Kolawole, G. A., Opoku, A., Muller, C. and Wolowska, J. 2009b. Synthesis, characterization and insulin-enhancing studies of unsymmetrical tetradentate Schiff base complexes of oxovanadium(IV). *Journal of Coordination Chemistry* 62.21:3411-3424.

Nakamoto, K. 1986. Infrared and raman spectra of inorganic and coordination compounds. Part A and B, John Wiley and sons, New York, USA.

Nasser, M. A. O. 2003. Studies on nitrogen heterocyclic systems: A Ph.D thesis submitted to the Department of Chemistry, Zagazig University.

Neelakantan, M. A., Esakkiammal, M., Mariappan, S. S., Dharmaraja,J. and Jeyakumar, T. 2010. Synthesis, characterization and biocidal activities of some Schiff base metal complexes. *Indian J. Pharm Sci.* 72.2: 216–222.

Ngoc-Chau, T., Minh-Tri, L., Dinh-Nga, N. and Thanh-Dao, T. 2009. Synthesis and biological evaluation of halogen substituted 1,4-naphthoquinones as potent antifungal agents. *Proceedings of 1st international electronic conference on synthetic organic chemistry*. 1st-30th November 2009.

Nogrady, T. 1988. *Medical Chemistry: A biochemistry approach*. Oxford University Press: New York.

O'Kennedy, R. and Thornes, R. D. 1997. *Coumarins: biology, applications and mode of action*. Wiley & sons: Chichester.

Ogawa, H., Harada, J., Fujiwara, T. and Yoshida, S. 2001. *J. Phys.Chem. A* 105: 3425–3427.

Olugbade, T. A., Usifoh, C. O., Oluwadiya, J. O. and Reisch, J. 1990. *J. Heterocyclic Chem*. 6.27:1727.

Omar, H. A. 2012.Synthesis, characterization and antimicrobial screening of mixed-ligand Cu(II) and Zn(II) complexes: DNA binding studies on Cu(II) complex. *Open Journal of Inorganic Non-metallic Materials*. 2: 59-64.

Osowole, A. A., Kolawole, G. A., Fagade, O. E. 2005. Synthesis, physicochemical and biological properties of Nickel(II), Copper(II) and Zinc(II) complexes of an unsymmetrical tetradentate Schiff base and their adducts. *Synth. React. Inorg. Met. Org. Chem. & Nano-Met. Chem.* 35:829-836.

Osowole, A. A. and Fagade, O. E. 2007. "Synthesis, characterization and biopotency of some metal(II) *β*-ketoiminates and their mixed-ligand complexes," *Polish Journal of Chemistry*. 81.12 2039–2048.

Osowole, A. A., Kolawole, G. A. and Fagade, O. E. 2008a. Synthesis, characterization and biological studies of unsymmetrical Schiff base Ni(II), Cu(II), and Zn(II) complexes and adducts with 2, 2^1-dipyridyl and 1,10-Phenanthroline. *J. Coord. Chem.* 23:193-196.

Osowole, A. A. 2008b. Synthesis and characterization of tetradendate Schiff base complexes and their heteroleptic analogues. *Euro. Journal of Chemistry* 5: 130-135.

Osowole, A. A., Kolawole, G. A., Kempe, R. and Fagade, O. E. 2009. Spectroscopic, magnetic and biological studies on some metal(II) complexes of 3-(4,6-dimethyl-2-pyrimidinylamino)-l-phenyl-2-butenone and their adducts with 2,2^{I}-bipyridine and 1,10-phenanthroline'. *Synth. React. Inorg. Met. Org. Chem & Nano-Met. Chem.* 39:165-174.

Osowole, A. A., Kempe, R., Schobert, R. and Effenberger, K. 2011. Synthesis, spectroscopic, thermal and *in-vitro* anticancer properties of some metal(II) complexes of 3-(-1-(4,6-dimethyl-2-pyrimidinylimino)methyl-2- napthol. *Synth. React. Inorg. Met. Org. Chem & Nano-Met. Chem*. 41.7: 825-833.

Osowole, A. A., Kempe , R. and Schobert, R. 2012a. Synthesis, spectral, thermal, *In-vitro* antibacterial and anticancer activities of some metal (II) complexes of 3-(-1-(4-methoxy-6-methyl)-2-pyrimidinylimino)methyl-2-napthol. *International Research Journal of Pure andApplied Chemistry* 2.2: 105-129.

Osowole, A. A., Oni, A. A., Onyegbula, K. and Hassan. A. T. 2012b."Synthesis, spectral, magnetic and *in-vitro* anticancer properties of some metal(II) complexes of 3-[2,4-dihydro-1H-inden-4-ylimino) methyl] napthalene-2-ol," *International Research Journal of Pure and Applied Chemistry*, 2.3: 211–220.

Osowole, A.A. and Ott, I. 2012c. Synthesis, characterization, *in-vitro* anticancer and antimicrobial properties of some metal (II) complexes of 4-[(2,3-dihydro-1*H*-inden-4- ylimino) methyl] benzene-2,4-diol. *International Research Journal of Pure and Applied Chemistry* 2:156-169.

Osowole, A. A. 2012d. Synthesis, spectroscopic characterization, in-vitro antibacterial and antiproliferative activities of some metal(II) complexes of 3,4-dihydronaphthalen-1(2h)-one schiff base. *Excli journal* 11:338-345.

Osowole, A. A. and Akpan, E. J. 2012e. Synthesis, spectroscopic characterisation, in-vitro anticancer and antimicrobial activities of some metal(II) complexes of 3-{4, 6-dimethoxy pyrimidinyl) Iminomethyl naphthalen-2-ol. *Eur. J. Appl. Sci.* 4.1:14-20.

Osowole, A. A., Anthony, C. E., Benedict, O. A. and Godwin, H. E. 2013. Synthesis, spectroscopic characterisation and structure related antibacterial activities of some metal(II) complexes of substituted triflurobutenol. *Elixir International Journal.* 59 :15848-15852.

Osowole, A. A., Anthony, C. E., and Austin, E. O. 2013. Synthesis, spectroscopic and antibacterial properties of some metal (ii) mixed ligand complexes of riboflavin and 2,2^{I}-bipyridine. *Research and Reviews: Journal of Chemistry* 3.1: 32-37.

Osowole , A. A. and Reuben, O. Y. 2014. Synthesis, characterization and biopotency of some mixed ligand metal(II) complexes of 4-amino-6-hydroxy-2-mercaptopyrimidine and 2,2^{I}-bipyridine. *Excli Journal.* 11: 338-345.

Osowole, A. A.,Ekennia, A. C., Olubiyi, O. O., Olagunju, M. 2017.Synthesis, spectral, thermal, antibacterial and molecular docking studies of some metal(II) complexes of 2-(1,3-benzothiazol-2-ylamino)naphthalene-1,4-dione. Research on Chemical Intermediates 43(4):2565-2585.

Otunla, E. O. 2008. Synthesis and characterization of metal complexes of Schiff bases derived from 3-nitroaniline with benzoylacetone and 2-hydroxyl-1-naphthaldehyde. M.Sc Thesis submitted to Inorganic unit, Chemistry Department, University of Ibadan (unpublished).

Owolabi, S. A. 2005. Synthesis and characterization of metal(II) chelate adducts of two Schiff bases and adducts. M.Sc Thesis submitted to Inorganic unit, Chemistry Department, University of Ibadan (unpublished).

Panneerselvam, P; Rather, B. A; Reddy, D. R. S and Kimar, N. R. 2010. Synthesis and antimicrobial screening of some Schiff bases of 3-amino-8-dibromo-2-phyenlquinzolin-4(*3H*)-ones. *Eur.J. Med. Chem.* 44. 2328-2333.

Papageorgiou, V. P., Assimopoulou, A. N., Couladouros, E. A., Hepworth, D. and Nicolaou, K. C. 1999. The chemistry and biology of alkannin, shikonin, and related naphthazarin natural products. *Angewandte Chemie International*, 38: 270-300.

Patel, S. K., Raval, N. K., Patel, P. S., Patel, G. A. and Patel, V. S. 2012. A review on the synthesis and biological activities of pyrimidine derivatives. *International Journal of Pharmacy and Biological Sciences.* 2.3: 170-182.

Pfeiffer, P., Buhholz, E. B. and Bauer, O. 1931. *J. Prakt. Chem.* 129:163.

Pinner, A. 1884. Ueber dieEinwirkung von Acetessigether auf die Amidine. *Berichte der Deutschen Chemischen Gesellschaft* A17:2519-2520.

Poterfield, W. W. 1984. *Inorganic Chemistry: A Unified Approach*. 2nd Ed. Academic press INC: USA.

Purell, K. F. and Kotz, J. C. 1997. *Inorganic Chemistry.* Holt-Saunders International Ed. W.B. Saunders Company: Philadelphia-London.

Pyle, A. M., Rehmann, J. P., Meshoyrer, R., Kumar, C. V., Turro, N. J. and Barton, J. K.1989. "Mixed-ligand complexes of ruthenium(II):factors governing binding to DNA," *Journal of the American Chemical Society* 111. 8: 3051–3058.

Rabab, L. Z., Haider, A. M. and Al-Mowali, A. H. 2015. Synthesis, charactrization and antioxidant activity of some new Schiff bases derived from 2-hydroxy-1-naphthaldehyde. *Journal of Natural Sciences Research.* 5.5:78.

Rakesh, S. and Anuja, C. 2014. An overview of biological importance of Pyrimidines. *World Journal of Pharmacy and Pharmaceutical Sciences*. 3.12: 574-597.

Ramana, K., Kumar, A., Raghavendra, G. P., Srilalitha, V., Narayana, G. and Sravindranath, L. K. 2012. Synthesis and characterization of Iron complexes of resacetophenone salicyloyl hydrazone. *Chem. Bull. "POLITEHNICA" Univ. (Timisoara)*57:7-14.

Raman, N., Raja, Y. P. and Kulandaisamy, A. 2001. Synthesis and characterization of Cu(II), Ni(II), Mn(II), Zn(II) and (IV) Schiff base complexes derived from o-phenylenediamine and acetoacetanilide. *Proc. Indian Acad. Sci. (Chem. Sci.)* 113.3:183-189.

Raman, N., Ravichandran, S. and Thangaraja, C. 2004."Copper(II), cobalt(II), nickel(II) and zinc(II) complexes of Schiff base derived from benzil-2,4-dinitrophenylhydrazone with aniline," *Journal of Chemical Sciences* 116.4: 215–219.

Raman, N., Dhaveethu, J., Raja and Sakthivel, A. 2007. Synthesis and spectral characterization of Schiff base transition metal complexes. DNA cleavage and antimicrobial studies. *J. Chem. Sci.* 119.4:303-310.

Raman, K. R. K.,Suneetha, P., Karigar, C. S.,Manjnath, N. H. and Mahendra, K. N. 2008. Co (II), Ni(II), Cu (II), Zn (II), Cd (II), Hg (II), UO2 (VI) and Th (IV) complexes from ONNN Schiff base ligand. *Journal of the Chilean Chem. Soc.* 53:4

Raziyeh, A. A. and Saeid, A. 2012. Synthesis, spectroscopy, thermal analysis, magnetic properties and biological activity studies of Cu(II) and Co(II) complexes with Schiff base dye ligands. *Molecules.* 17:6434-6448.

Reddy, B. N., Avaji, P. G., Badami, P. S. and Patil, S. A. 2007. "Synthesis, spectral and biological studies of Co(II), Ni(II) and Cu(II) complexes with 1,5-bis(thiophenylidene) thiocarbohydrazone. *Journal of Saudi Chemical Society.* 11.2: 253–268.

Reddy, N. S., Shankara, B. S., Krishana, P. M., Basavaraj, C. and Mahesh, B. 2013. Synthesis, characterization and antibacterial activity of Co(II), Ni(II), Cu(II), Zn(II), Cd(II) and Hg(II) complexes of Schiff's base type ligands containing benzofuran moiety. *International Journal of Inorganic Chemistry.* 2013:11.

Redha, I. H., AL-Bayati, M. F. R. and Ahmed, A. A. 2010. Synthesis, spectroscopic and antimicrobial studies of transition metal complexes of N-amino quinolone derivatives. *14th International Electronic Conference on synthetic Organic Chemistry* 1-30.

Rekha, S. H., Basavaraj, R. P., Dayananda, S. B., Ramesh, S. V., Kalagouda, B. G., Chandrashekhar, V. M. and Iranna, S. M. 2010. A study of anti-inflammatory and analgesic activity of new 2,3-disubstituted 1,2-dihydroquinazolin-4(3h)-one derivative and its transition metal complexes. *Eur J Med Chem.*2010:6-9.

Renata, G., Katarina, K. and Margita, L. 2009. Reactions of 4-hydroxycoumarin with heterocyclic aldehydes. *Nova Biotechnologica* 9:3.

Resat, A., Kubilay, G., Mustafa, O., Zyu¨rek, S. and Esin, C. 2008. Mechanism of antioxidant capacity assays and the CUPRAC (cupric ion reducing antioxidant capacity) assay. *Microchim Acta.* 160: 413–419.

Revanasiddappa, M., Suresh, T., Syed, K., Raghavendray, S. C., Basavaraja, C. and Angadi, S. D. 2008. Transition metal complexes of 1, 4(2'-hydroxyphenyl-1-yl) di-imino azine: synthesis, characterization and antimicrobial studies. *E-Journal of Chemistry* 5.2: 395-403.

Rice, R., Brew, B., Sidtis, J., Rosenblum, M., Scheck, A. and Cleary, P. 1988. *Science* 239:586-592.

Riffel, A., Medina, L. F., Stefani, V., Santos, R.C., Bizani, D. and Brandelli, A. 2002. *In vitro* antimicrobial activity of a new series of 1,4-naphthoquinones.*BArnatzimiliiacnro Jboiuarl naacl tiovfi tMy eodf incaalp ahnthdo Bquioinloogniceasl Research* 35: 811-818.

Saadiyah, A. D., Nask, M. A. and Shaimaa, R. B. 2012. Synthesis, characterization and antimicrobial studies of complexes of some metal ions with 2-[2-amino-5-(3,4,5-trimethoxy-benzyl)-pyrimidinyl-4-azo]-4-bromo-phenol. *Int.l Journal of Basic and Applied Sciences.* 126:58-67.

Saidul, M. I., Akhter, M. F., Bodruddoza, M. A. K. and Shahidul, M. A. 2001. Antimicrobial and toxicological studies of mixed ligand transition metal complexes of Schiff bases. *Online journal of biological sciences* 1.8:711-713.

Saleh, A. A., Ali, O.M., Adnan, A. H.,Ihmood, K. A. and Emad, M. O. 2009. Synthesis and characterization of Some Schiff bases (derived from thiazole) and their complexes with Co(II),Ni(II) and Cu(II). *Journal of Kirkuk University–Scientific Studies,* 4.2.

Salman, S. R. and Saleh-Nai'l, A. I. 1998. *Spectrosc. Lett.* 31.6: 1179.

Salman, S. R., Farrant, R. D., and Lindon, J. C. 1991. *Spectrosc. Lett.* 24:1071.

Salman, S. R., Lindon, J. C., Farrant, R. D., and Carpenter, T. A. 1993. *Mag. Res. Chem.* 31: 991.

Salman, S. R., Shawkat, S. H. and Al-Obaidi, G. M. 1999. *Canadian Journal of Spectroscopy* 35:25

Sallam, S. A. 2005. Synthesis, characterization and thermal decomposition of copper(II), nickel(II) and cobalt(II) complexes of 3-amino-5-methylpyrazole Schiff-bases. *Transition Met. Chem*.30:341-351.

Salmon, L., Molnar, G., Cobo, S., Oulié, P., Etienne, M., Mahfoud, T., Demont, P., Eguchi, A., Watanabe, H., Tanaka, K. and Bousseksou, A. 2009. Reinvestigation of the spin crossover phenomenon in the ferrous complex $[Fe(HB(pz)_3)_2]$. *New Journal of Chemistry* 33.6: 1283-1289.

Sajjad, H. S., Muhammad, I., Sabahat, A., Muhammad, I., Muhammad, D. and Fouzia, S. R. 2014. Synthesis, spectral characterization and biological evaluation of transition metal complexes of bidentate N, O donor Schiff bases. *Bioinorganic Chemistry and Applications* 2014.

Satyl, P., Tuli, G. D., Basu, S. K. and Madan, R. D. 2004. *Advanced Inorganic Chemistry*. Vol: II. S.Chand and company Ltd. Ram Nagar: New Delhi.

Schmeyers, J., Toda, F., Boy, J. and Kaupp, G. 1998. Quantitative solid–solid synthesis of azomethines. *Journal of Chemical Society of Perkin Trans.* 2: 989–93

Sobola, A. O. 2005. Synthesis characterization of metal(II) chelate adductss of two Schiff bases and adducts. M.Sc Thesis, Chemistry Department, University of Ibadan (unpublished)

Spinu, C. and Kriza, A. 2000. Co(II), Ni(II) and Cu(II) complexes of bidendate Schiff base. *Acta Chimica. Slovenica* 47:179-185.

Shalin, K., Durga, N. D. and Saxena, P. N. 2009. Application of metal complexes of Schiff bases: A Review. *Journal of Scientific and Industrial Research* 68:181-187.

Shubhangi, N. K. and Harjeet, D. J. 2013. Synthesis, characterization and antimicrobial studies of N, O Donor Schiff base polymeric complexes. *Journal of Chemistry* 2013.

Singh, K. N., Singh, D. K. and Singh, S. B. 2001. Synthesis, characterization and biological studies on Co(II), Ni(II), Cu(II), and Zn(II) complexes with N-picolinoyl-N-thiobenzoyl hydrazine. *Synth. React. Inorg .Met.-Org Chem.* 32.4: 703-720.

Singh, R. and Chouhan, A. 2014. An overview of bioliogical important of pyrimidines. *World Journal of Pharmacy and pharmaceutical Sciences* 3.12: 574-597.

Smal, M., Cheung, H. T. A. and Davies, P. E. 1986. *J. Chem. Soc. Perkin Trans*, 1:747.

Smaill, J. B., Rawcastle, G. W., Loo, J. A., Greis, K. D., Chan, O. H., Reyner, E. L., Lipka, E., Holliss Showalter, H. D., Vincent, P. W., Elliott, W. L., and Denny, W.A., 2000. *J. Med. Chem*. 43.7:1380-1397.

Soenmez, M. and Sekerci, M. 2004. A new heterocyclic Schiff base and its metal complexes. *Synth. React. Inorg. Met. Org. Chem*. 34.3: 489-502.

Sonmez, M., Levent, A. and Sekerci, M. 2004. “Synthesis, characterization, and thermal investigation of some metal complexes containing polydentate ONO-donor heterocyclic Schiff base ligand,” *Russian Journal of Coordination Chemistry* 30.9: 655–660.

Spinu, C., Pleniceanu, M. and Tigae, C. 2008. Biologically active transition metal chelates with a 2-thiophenecarboxaldehyde-derived Schiff base: synthesis, characterization, and antibacterial properties. *Turk. J. Chem.,* 32:487-493

Sreekala, R., Yusuff, K. K. and Mohammed, K. 1999. Catalytic activity of mixed ligand five coordinate Co(II) complexes of a polymer bound Schiff base. *Catal (Pap Natl Symp), Chem Abstr.* 130:507-510.

Srivastava, V. K., Kaushik, N. K. and Khera, B. 1987. Phthiocol chelates of bis(cyclopentadienyl titanium(IV). *Synth React Inorg Met Org Chem.* 17:15-24.

Steward, J. E. 1970. ‘*Infrared Spectroscopy’.* 1st Edition, Marcel Dekker, INC: USA

Stuart, B., George, B. and Mclntyre, P. 1986. *Modern Infrared Spectroscopy*. 1st Ed, Wiley Publications Ltd.

Subbaraj, P., Ramu, A., Raman, N. and Dharmaraja, J. 2015. Synthesis, characterization, DNA interaction and pharmacological studies of substituted benzophenone derived Schiff base metal(II) complexes. *Journal of Saudi Chemical Society.* 19: 207-216.

Suparna, G. 2013. Synthesis and pharmacological studies of some bivalent metal complexes with Schiff based ligand derived from xipamide. *Der Pharma Chemica* 5.3: 232-235.

Taguchi, K. and Westheimer, F. H. 1971. Catalysis by molecular sieves in the preparation of ketimines and enamines. *Journal of Organic Chemistry* 36.11:1570–1572.

Tarek, M. I., El-Ghamry, M. A., Abu-El-Wafa, S. M. and Sallam, D. F. 2015. Synthesis, characterization, 3D-modelling, biological activities of some metal complexes of novel sulpha drug Schiff base ligand and its nano Cu complex. *Modern Chemistry: Science publishing group* 3.2: 18-30.

Taylor, R. T., Flood, L. A. 1983. "Polystyrene-Bound Phenylseleninic Acid: Catalytic oxidations of olefins, ketones, and aromatic systems". *The Journal of Organic Chemistry*48. 26: 5160–5164.

Thangadurai, T. D. and Natarajan, K. 2001. Mixed ligand complexes of ruthenium(II) containing α, β unsaturated-β-ketoamines and their antibacterial activity. *Trans Met Chem.* 26:500–504.

Thomson, R. H. 1971. Naturally occurring quinones. Academic Press, London, England.

Touraire, C., Caupole, R., Payard, M., Commenges, G., Bessieres, M. H., Bories, C., Loiseal, P. M. and Gayral, P. 1996. Synthesis and protozoocidal activities of quinones. *European Journal of Medicinal Chemistry*. 31: 507-511.

Tozkoparan, B., Ertan, M., Kelicen, P. and Demirdamar, R. 1999. Synthesis and anti-inflammatory activities of some thiazolo[3,2-a]pyrimidine derivatives. *Farmaco*. 54: 588-593.

Tripathi, L., Kumar, P. and Singhai, A. K. 2007. Role of chelates in treatment of cancer. *Indian J. Cancer* 44: 62-71.

Troughton, J. S., Greenfield, M. T., Greenwood, J. M., Dumas, S., Wiethoff, A. J., Wang, J., spiller, M., Mc-Murry, T. J. and Caravan, P. 2004. *Biochem.* 43: 6313.

Vachala, S. D., Bhargavi, B. and Keloth, K. S. 2012. Fused Pyrimidines: The heterocycles of diverse biological and pharmacological significance. *Scholars Research Library* 4.1: 255-265

Valarmathy, G. and Subbalakshmi, R. 2014. Synthesis, spectral characterisation, electrochemical, and fluorescence studies of biologically active novel Schiff base complexes derived from E-4-(2-hydroxy-3-methoxybenzlideneamino)-N-(pyrimidin-2-yl)benzenesulfonamide. *Turkish Journal of Chemistry* 38: 521-530

Vazquez, M. A., Landa, M., Reyes, L., Miranda, R., Tamariz, J. and Delgado, F. 2004. Infrared irradiation: effective promoter in the formation of N-benzylideneanilines in the absence of solvent. *Synth Commun*. 34.15: 2705–2718.

Vitkauskiene, A., Dudzevicius, V., Ryskus, L., Adukauskiene, D. and Sakalauskas, R. 2006. The rate of isolation of Klebsiella pneumoniae producing extended-spectrum beta-lactamases and resistance to antibiotics. (Article in Lithuanian). Medicina (Kaunas) 42:288–293

Vukadin, M. L., Violeta, S. J., Ljiljana, S. J. and Goran A. B. 2005 *J. Serb. Chem. Soc.* 70: 393-422.

Wade, L. G. 1999. *Organic Chemistry*. 4th Ed. Upper saddle River Publishing: New Jersey.

Wikipedia, 2013. The free encyclopedia: Mechanisms of antibiotic resistance. *Retrieved online 2nd Sept., 2013.*

William, W. P. 1993. *Inorganic chemistry: a unified approach*. 2nd Ed. New York: Academy press INC: USA

Xi, Z., Liu, W., Cao, G., Du, W., Huang, J., Cai, K. and Guo, H. 1987. Catalytic oxidation of naphthol by metalloporphyrins. *Chem Abstr.* 106: 140082.

Xue-Qiang, C; Wen-Bin, C; Xiao-Ping, X. and Shun-Jun, J.(2017). Iron Catalysis for Modular Pyrimidine Synthesis through β-Ammoniation/Cyclization of Saturated Carbonyl Compounds with Amidines. *J. Org. Chem.* 82.2:1145-1154.

Yang, H. J., Wen, H. S., Zi, L. L. and Zhi, M. A. 2002. The rapid synthesis of Schiff-base without solvent under microwave irradiation. *Chinese Chem Letters* 13:3-6.

Yang, D. P., Ji, H. F., Tang, G. Y., Ren, W. and Zhang, H. Y. 2007. How many drugs are catecholics? *Molecules* 12:878–884.

Yamada, S. 1966. Recent aspects of the stereochemistry of Schiff base metal complexes, *Coord. Chem. Rev.* 1: 415.

Ye, N., Park, G., Przyborowska, A. M., Sloan, P. E., Clifford, T., Bauer, C. B., Broker, G. A., Rogers, R. D., Ma, R., Torti, S. V., Brechbied, M. N. and Planalp, R. P. 2004. *Dalton Trans.* 1304.

Yildiz, M., Dulger, B., Koyuncu, S. Y. and Yapici, B. M. 2004. Synthesis and antimicrobial activity of bis(imido) Schiff bases derived from thiosemicarbazide with some 2- hydroxyaldehydes and metal complexes. *J. Indian Chem.* Soc. 81: 7.

Yu-Ye, Y., Hui-Duo, X., Jain-Feng, L. and Guo-Liang, Z. 2009. Synthesis, characterization, crystal structure and antibacterial activities of transition metal (II) complexes of the Schiff base 2-[(4-methylphenylimino)methyl]-6-methoxyphenol. *Molecules* 14: 1747-1754.

Zahid, H. C., Praveen, M. and Ghaffar, A. 1997. Structural and biological behaviour of Co(II), Cu(II) and Ni(II) metal complexes of some amino acid derived Schiff bases. *Metal-Based –Drugs J.* 4.5: 267-272.

Zahid, H. C., Arif, M., Muhammad, A. A. and Claudiu T. S. 2006. Metal-based antibacterial and antifungal agents: synthesis, characterization, and *in vitro* biological evaluation of Co(II), Cu(II), Ni(II), and Zn(II) complexes with amino acid-derived compounds. *Bioinorganic Chemistry and Applications* 2006.

Zahid, K., Zahida, T. M., Muhammad, A. K. T., Khalid, M. K., Lubna, I. and Mehreen, L. 2015. Synthesis, characterization, *In-Vitro* antimicrobial and antioxidant activities of Co^{+2}, Ni^{+2}, Cu^{+2} and Zn^{+2} complexes of 3-(2-(2-hydroxy-3-methoxybenzylidene) hydrazono)indolin-2-one. *Journal of Basic and Applied Sciences* 11: 125-130.

Zahid, H. C. and sabuhi M. 2000. Antibacterial cobalt(II) and zinc(II) complexes of pyrazine-derived NNO and NNN donor Schiff-bases. *Pakistan Journal of Pharmaceutical Sciences* 13: 21-27.

Zhaohua, H., Zhaoliang, L. and Junlian. 2001. A novel kind of antitumor drugs using sulfonamide as parent compound. *European journal of medicinal chemistry.*

Zoeb A. F., Sanjay, M. N. and Raju, M. P. 2008. Synthesis of Schiff base from 2,2'-diaminodibenzyl with 2-hydroxy naphthaldehyde and its complexes with Mn(II),VO(II) and UO_2(II). *Asian Journal of Chemistry* 20.4: 3298-3300

Zugir, R. L., Mahdi, H. A. and Al-Mowali A. H. 2015. Synthesis, characterization and antioxidant activity of some new Schiff bases derived from 2-hydroxy-1-naphthaldehyde. *Journal of Natural Sciences Research 5(5): 78-85.*

APPENDICES

Appendice I: Magnetic Susceptibilty Calculation for $[Fe(L^1)(H_2O)_2]$Complex

HL^1 Ligand = $C_{30}H_{20}N_6O_2$

χ_L = 30 C x -6.0	= -180.0	Constitutive Corrections	
= 20 H x -2.93	= - 58.6	2 C=C x 5.5	= 11.0
= 4 N(ring) x -4.61	= - 18.44	6 C=N x 8.2	= 49.2
= 2 N(imine) x -2.11	= - 4.22	20 C (Benzene Ring) x 0.24	= 4.8
= 2 O(alcohol)x-4.61	= - 9.22		**= 65.0**
	= -270.48		

χ_L = -270.48 + 65.0 = -205.48 x 10^{-6}

$[Fe(L^1)(H_2O)_2]$= $[Fe(C_{30}H_{20}N_6O_2)(H_2O)_2]$ = 591.422

$$\chi_g = \frac{2.0 \times 379}{10^{-9} \times 0.0391} = 1.9386189 \times 10^{-5}$$

$\chi_m = \chi_m \times mw = 1.9386189 \times 10^{-5} \times 591.422 = 1.1465\ 10^{-2}$

$\chi_A = \chi_m - \chi_L = 1.1465\ 10^{-2} – (-231.48 \times 10^{-6}) = 1.169648 \times 10^{-2}$

$\mu_{eff} = 2.83\sqrt{1.169648 \times 10^{-2} \times 300}$ = **5.30 B.M**.

Appendice II: Relationship for determination of molarity for standardized solution

$M_{EDTA}. V_{EDTA} = M_{ZnSO_4}. V_{ZnSO_4}$

$M_{EDTA} = M_{ZnSO_4}. V_{ZnSO_4} / V_{EDTA}$

Where M_{EDTA} = Molarity of EDTA solution.

M_{ZnSO_4}= Molarity of Zinc(II) sulphate solution.

V_{EDTA} = Volume of EDTA solution obtained.

V_{ZnSO_4} = Volume of Zinc(II) sulphate solution obtained.

Table 3.2 Titration Table for the Standardization of EDTA solution

	Rough (mL)	Ist (mL)	2nd (mL)
Final titre	19.20	35.60	52.10
Initial titre	0.00	19.20	35.60
Titre value	19.20	16.40	16.50

Average titre value = 16.40 + 16.50 / 2 = 16.45 cm^3

Volume of EDTA (V_A) = 16.45 cm^3

Molarity of EDTA (M_A) = ?

$\underline{M_A x V_A} = \underline{n_A}$

$$M_A = \frac{M_B \times V_B \times n_A}{V_A \times n_B}$$

$$M_A = \frac{0.005\ M \times 25\ cm^3 \times 1}{16.45\ cm^3 \times 1}$$

$$M_A = 7.598 \times 10^{-3}\ M = 0.008\ M \approx 0.01M$$

Appendice III: Calculations steps for the metal analysis of metal complexes

Table 3.3Burette Reading for % Metal Titration

Burette readings in cm^3 (mL)	Rough	1st titre	2nd titre
Final burette reading	0.90	1.40	2.00
Initial burette reading	0.00	0.90	1.40
Volume of EDTA used	0.90	0.50	0.60

Average volume of EDTA used $= \frac{0.50 + 0.60}{2}$

$= \frac{1.10}{2}$

Average volume of EDTA used $= 0.55\ cm^3$

Volume of EDTA $= 0.55\ cm^3$

Number of moles of EDTA used $= \frac{\text{Volume} \times \text{Molarity}}{1000} = \frac{0.55 \times 0.008}{1000} = 4.4 \times 10^{-6}$ moles.

Amount of Ni^{2+} $= \frac{\text{No of moles of EDTA} \times 4 \times \text{atomic mass of element} \times 100}{\text{Amount of complex weighed for digestion}}$, (100/25 = 4)

Amount of Ni^{2+} = $\frac{4.4 \times 10^{-6} \times 4 \times 58.71 \times 100}{0.012\ g}$

Amount of Ni^{2+} = 10.07%

Theoretically, amount of Ni^{2+} = $\frac{\text{Atomic mass of Ni} \times 100}{\text{Molar mass of } NiL^{1} \text{ complex}}$

= $\frac{58.71 \times 100}{558.268}$

= 10.52%

Appendice IV: Petri Dishes of the Antibacterial Activities for some Metal(II) Complexes

Note:*S. a=Staphylococcus aureus, P.a=Pseudomonas aeruginosa, E.c=Escherichia coli, B.c=Bacillus cereus, P.m=Proteus mirabilis and K.o=Klebsilla oxytoca*

Appendice V: Petri Dishes of the Antibacterial Activities for Heteroleptic Complexes

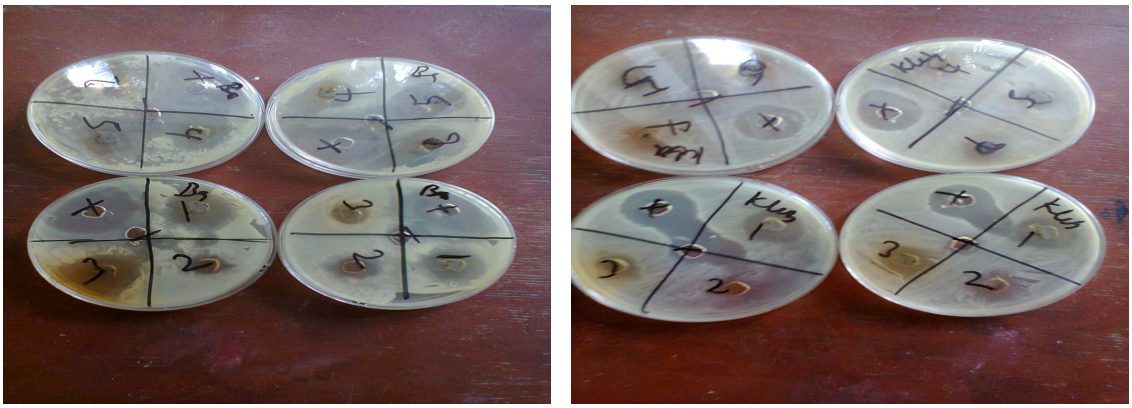

Note:*S. a=Staphylococcus aureus, P.a=Pseudomonas aeruginosa, E.c=Escherichia coli, B.c=Bacillus cereus, P.m=Proteus mirabilis and K.o=Klebsilla oxytoca*